

THESIS

Probing the Early Universe with the CMB Scalar, Vector and Tensor Bispectrum

*A dissertation submitted to Nagoya University
in partial fulfillment of requirements for the degree of
Doctor of Philosophy in Science*

Maresuke Shiraishi

March 2012

Abstract

Although cosmological observations suggest that the fluctuations of seed fields are almost Gaussian, the possibility of a small deviation of their fields from Gaussianity is widely discussed. Theoretically, there exist numerous inflationary scenarios which predict large and characteristic non-Gaussianities in the primordial perturbations. These model-dependent non-Gaussianities act as sources of the Cosmic Microwave Background (CMB) bispectrum; therefore, the analysis of the CMB bispectrum is very important and attractive in order to clarify the nature of the early Universe. Currently, the impacts of the primordial non-Gaussianities in the scalar perturbations, where the rotational and parity invariances are kept, on the CMB bispectrum have been well-studied. However, for a complex treatment, the CMB bispectra generated from the non-Gaussianities, which originate from the vector- and tensor-mode perturbations and include the violation of the rotational or parity invariance, have never been considered in spite of the importance of this information.

On the basis of our current studies [1–7], this thesis provides the general formalism for the CMB bispectrum sourced by the non-Gaussianities not only in the scalar-mode perturbations but also in the vector- and tensor-mode perturbations. Applying this formalism, we calculate the CMB bispectrum from two scalars and a graviton correlation and that from primordial magnetic fields, and we then outline new constraints on these amplitudes. Furthermore, this formalism can be easily extended to the cases where the rotational or parity invariance is broken. We also compute the CMB bispectra from the non-Gaussianities of the curvature perturbations with a preferred direction and the graviton non-Gaussianities induced by the parity-violating Weyl cubic terms. We also present some unique impacts to the violation of these invariances on the CMB bispectrum.

References

- [1] M. Shiraishi, S. Yokoyama, D. Nitta, K. Ichiki, and K. Takahashi, *Analytic formulae of the CMB bispectra generated from non- Gaussianity in the tensor and vector perturbations*, *Phys. Rev.* **D82** (2010) 103505, [[arXiv:1003.2096](#)].
- [2] M. Shiraishi, D. Nitta, S. Yokoyama, K. Ichiki, and K. Takahashi, *CMB Bispectrum from Primordial Scalar, Vector and Tensor non-Gaussianities*, *Prog. Theor. Phys.* **125** (2011) 795–813, [[arXiv:1012.1079](#)].
- [3] M. Shiraishi, D. Nitta, S. Yokoyama, K. Ichiki, and K. Takahashi, *Cosmic microwave background bispectrum of vector modes induced from primordial magnetic fields*, *Phys. Rev.* **D82** (2010) 121302, [[arXiv:1009.3632](#)].
- [4] M. Shiraishi, D. Nitta, S. Yokoyama, K. Ichiki, and K. Takahashi, *Computation approach for CMB bispectrum from primordial magnetic fields*, *Phys. Rev.* **D83** (2011) 123523, [[arXiv:1101.5287](#)].
- [5] M. Shiraishi, D. Nitta, S. Yokoyama, K. Ichiki, and K. Takahashi, *Cosmic microwave background bispectrum of tensor passive modes induced from primordial magnetic fields*, *Phys. Rev.* **D83** (2011) 123003, [[arXiv:1103.4103](#)].
- [6] M. Shiraishi and S. Yokoyama, *Violation of the Rotational Invariance in the CMB Bispectrum*, *Prog.Theor.Phys.* **126** (2011) 923–935, [[arXiv:1107.0682](#)].
- [7] M. Shiraishi, D. Nitta, and S. Yokoyama, *Parity Violation of Gravitons in the CMB Bispectrum*, *Prog.Theor.Phys.* **126** (2011) 937–959, [[arXiv:1108.0175](#)].

Acknowledgements

First, I acknowledge the support of my supervisor, Prof. Naoshi Sugiyama. He backed my studies with much well-directed advice, enhancement of computing resources, and recruitment of high-caliber staff. In addition, owing to his powerful letters of recommendation, I could spend a fulfilling life in academia as a JSPS research fellow with ample opportunities to make presentations about our studies and communicate with top-level researchers in a variety of fields.

The work presented in this thesis is based on seven papers written in collaboration with Shuichiro Yokoyama, Kiyotomo Ichiki, Daisuke Nitta, and Keitaro Takahashi. Shuichiro Yokoyama supported and encouraged me in all seven papers. He mainly provided advice on nature in the inflationary era and on the cosmological perturbation theory. Kiyotomo Ichiki's comments focused mainly on the impacts of the primordial magnetic fields on CMB and on the technical side of numerical calculations. A preface to these works arose from a chat with Shuichiro Yokoyama and Kiyotomo Ichiki. They also corrected my drafts in a tactful way. Daisuke Nitta's main contribution was in telling me about several mathematical skills and fresh ideas necessary for calculating the primordial non-Gaussianities and the CMB bispectrum. Keitaro Takahashi gave me a polite lecture about the CMB scalar-mode bispectrum and discussed an application of our formalism to the primordial magnetic fields and cosmological defects. Owing to these four collaborators, I could gain a better understanding of the primordial non-Gaussianities and the CMB bispectrum.

Financially, these individual works that comprise this thesis were supported in part by a Grant-in-Aid for JSPS Research under Grant No. 22-7477, a Grant-in-Aid for Scientific Research on Priority Areas No. 467 "Probing the Dark Energy through an Extremely Wide and Deep Survey with the Subaru Telescope", and a Grant-in-Aid for the Nagoya University Global COE Program "Quest for Fundamental Principles in the Universe: from Particles to the Solar System and the Cosmos" from the Ministry of Education, Culture, Sports, Science and Technology of Japan.

I also acknowledge the Kobayashi-Maskawa Institute for the Origin of Particles and the Universe, Nagoya University, for providing computing resources useful in conducting the research reported in this thesis.

I was helped by many useful comments from Takahiko Matsubara, Chiaki Hikage, Kenji Kadota, Toyokazu Sekiguchi, and several researchers in other laboratories and institutions. My friends Masanori Sato and Shogo Masaki, my junior fellows Takahiro Inagaki and Yoshitaka Takeuchi, and other students provided advice on not only science and computers but also life. I owed my energy to them. Owing to Shohei Saga's careful reading, I could fix many typos in this thesis.

Finally, I would like to thank my family for their concerns and hopes.

Contents

1	Introduction	12
1.1	Big Bang Universe	12
1.2	Paradigm in the early Universe	13
1.3	Concept of this thesis	14
2	Fluctuations in inflation	17
2.1	Dynamics of the scalar field	17
2.2	Slow-roll inflation	18
2.3	Reheating	20
2.4	Inflation models	21
2.4.1	Single-field slow-roll inflation	21
2.4.2	Beyond the single-field slow-roll inflation	23
2.5	Scalar perturbations	24
2.5.1	Quadratic action	24
2.5.2	Quantization and initial condition	25
2.5.3	Solution in de Sitter space-time	26
2.5.4	Power spectrum of curvature perturbations	26
2.6	Tensor perturbations	27
2.7	Consistency relations in the slow roll limit	28
3	Fluctuations in cosmic microwave background radiation	31
3.1	Einstein equations	32
3.1.1	Homogeneous contribution	33
3.1.2	Perturbed contribution	34
3.2	Boltzmann equations	36
3.3	Stokes parameters	37
3.4	Boltzmann equations for photons	39
3.5	Thomson scattering	40
3.6	Transfer functions	42
3.7	All-sky formulae for the CMB scalar-, vector- and tensor-mode anisotropies	49
3.8	Flat-sky formulae for the CMB scalar-, vector- and tensor-mode anisotropies	54
3.9	CMB power spectrum	57
4	Primordial non-Gaussianities	65
4.1	Bispectrum of the primordial fluctuations	65
4.2	Shape of the non-Gaussianities	66
4.2.1	Local type	67
4.2.2	Equilateral type	67
4.2.3	Orthogonal type	68
4.3	Observational aspects	68
4.4	Beyond the standard scalar-mode non-Gaussianities	69
5	General formalism for the CMB bispectrum from primordial scalar, vector and tensor non-Gaussianities	75

6	CMB bispectrum induced by the two scalars and a graviton correlator	79
6.1	Two scalars and a graviton interaction during inflation	79
6.2	Calculation of the initial bispectrum	80
6.3	Formulation of the CMB bispectrum	81
6.4	Estimation of the signal-to-noise ratio	84
6.5	Summary and discussion	85
7	Violation of the rotational invariance in the CMB bispectrum	88
7.1	Statistically-anisotropic non-Gaussianity in curvature perturbations	88
7.2	CMB statistically-anisotropic bispectrum	91
7.2.1	Formulation	92
7.2.2	Behavior of the CMB statistically-anisotropic bispectrum	94
7.3	Summary and discussion	96
8	Parity violation of gravitons in the CMB bispectrum	100
8.1	Parity-even and -odd non-Gaussianity of gravitons	101
8.1.1	Calculation of the primordial bispectrum	101
8.1.2	Running coupling constant	104
8.2	CMB parity-even and -odd bispectrum	105
8.2.1	Formulation	105
8.2.2	Evaluation of $f_{W^3}^{(r)}$ and $f_{\widetilde{W}W^2}^{(r)}$	109
8.2.3	Results	111
8.3	Summary and discussion	114
9	CMB bispectrum generated from primordial magnetic fields	118
9.1	CMB fluctuation induced from PMFs	118
9.1.1	Setting for the PMFs	119
9.1.2	Scalar and tensor modes	121
9.1.3	Vector mode	123
9.1.4	Expression of $a_{\ell m}$'s	125
9.1.5	CMB power spectrum from PMFs	126
9.2	Formulation for the CMB bispectrum induced from PMFs	131
9.2.1	Bispectrum of the anisotropic stress fluctuations	131
9.2.2	CMB all-mode bispectrum	133
9.3	Treatment for numerical computation	137
9.3.1	Thin LSS approximation	140
9.3.2	Selection rules of the Wigner- $3j$ symbol	141
9.4	Shape of the non-Gaussianity	142
9.5	Analysis	145
9.6	Summary and discussion	149
10	Conclusion	155
A	Spin-weighted spherical harmonic function	156
B	Wigner D-matrix	158

C	Wigner symbols	159
C.1	Wigner-3j symbol	159
C.2	Wigner-6j symbol	160
C.3	Wigner-9j symbol	161
C.4	Analytic expressions of the Wigner symbols	162
D	Polarization vector and tensor	164
E	Calculation of $f_{W^3}^{(a)}$ and $f_{\widetilde{W}W^2}^{(a)}$	167
F	Graviton non-Gaussianity from the Weyl cubic terms	169
F.1	\widetilde{W}^3	169
F.2	$\widetilde{W}W^2$	171

List of Figures

- 1.1 Evolution of the Universe. The events in the Universe are presented as the function of the time and energy scales. In addition, the several cosmological probes, which provide us with information about the structure and evolution of the Universe, are illustrated. *Acronyms:* Big bang nucleosynthesis (BBN), large scale structure (LSS), baryon acoustic oscillations (BAO), quasi-stellar objects = quasars (QSO), Lyman-alpha ($\text{Ly}\alpha$), cosmic microwave background (CMB), Type Ia supernovae (Ia), hydrogen 21cm-transition (21cm). This figure is quoted from Ref. [4] 13
- 1.2 Balance between the scale of the density fluctuation and the comoving horizon. These are functions of the comoving scales $|\tau|$ and the scale factors a . The comoving horizon evolves as $\tau \equiv \int^t dt'/a(t') \propto -a^{-1}$ (at the inflationary epoch), a (at the radiation dominated era), and $a^{1/2}$ (at the matter dominated era). The scales of the density contrasts were larger than the Hubble radius until $a \sim 10^{-5}$. However, before inflation operated, all interest scales of the density contrasts were smaller than the Hubble radius and therefore the physics is described in terms of the quantum mechanics. Similarly, at a very late time, the scales of the cosmological interests re-entered in the Hubble radius. This figure is quoted from Ref. [4] 15
- 2.1 Example of the potential of the inflaton ϕ . An accelerated expansion of the Universe occurs when $V(\phi) \gg \frac{1}{2}(\partial_t \phi)^2$. Inflation ends at $\phi = \phi_{\text{end}}$ when $\frac{1}{2}(\partial_t \phi)^2 \approx V$. The CMB fluctuations are generated from the quantum fluctuations $\delta\phi$ about 60 e -folds before the end of inflation. At reheating, the energy density of the inflaton is converted into radiations. This figure is quoted in Ref. [1] 18
- 2.2 Large-field inflation. This shape of the potential can be realized when $V(\phi) \propto \phi^p$. In cases like this, the inflaton field moves over a super-Planckian range during inflation, namely, $\Delta\phi > M_{\text{pl}}$, and a large amplitude of the gravitational waves is produced. This figure is quoted in Ref. [1]. 21
- 2.3 Small natural inflation. If the periodicity $2\pi f$ is super-Planckian, the model can naturally induce a large amplitude of the gravitational waves. This figure is quoted in Ref. [1]. 23
- 3.1 CMB anisotropy on the last scattering surface. The red (blue) parts correspond to the hot (cold) spots (Copyright 2011 by Daichi Kashino). 31
- 3.2 Interaction between several components in the Universe. 38
- 3.3 Geometry of Thomson scattering. Blue (Red) solid and two dashed arrows denote the incident (scattered) wave number vector and its orthogonal unit vectors, respectively. We set that $\hat{\mathbf{x}}' = \hat{\mathbf{x}}$ 40
- 3.4 Geometry for the line-of-sight direction. 50
- 3.5 The CMB spectra of the II (left top panel), IE (right top one), EE (left bottom one) and BB (right bottom one) modes. Here we consider a power-law flat Λ CDM model and fix the tensor-to-scalar ratio as $r = 0.1$. The other cosmological parameters are fixed to the mean values reported in Ref. [27]. 59
- 3.6 CMB II power spectra sourced from the scalar-mode perturbations in a power-law flat Λ CDM model. The red solid line is plotted with $\omega_c = 0.112, \Omega_\Lambda = 0.728, \omega_b = 0.02249, n_s = 0.967, \kappa = 0.088$ [27]. The green dashed, blue dotted and magenta dot-dashed lines are calculated if ω_c decreases to 0.1, Ω_Λ increases to 0.8, and ω_b increases to 0.028, respectively. 60

- 4.1 Representations of triangles forming the bispectrum, $F^{\lambda_1\lambda_2\lambda_3}(k_1, k_2, k_3)$, with various combinations of the wave numbers satisfying $k_3 \leq k_2 \leq k_1$. This figure is adopted from Ref. [19]. 66
- 4.2 Two dimensional color contour for the shapes of the primordial bispectra. Each panel describes the normalized amplitude of $S(k_1, k_2, k_3)(k_2/k_1)^2(k_3/k_1)^2$ as a function of k_2/k_1 and k_3/k_1 for $k_3 \leq k_2 \leq k_1$. Since the primordial bispectra shown here are nearly scale invariant, the shapes may look similar regardless of the values of k_1 . The amplitude is normalized by a rule that it is unity at the point where $S(k_1, k_2, k_3)(k_2/k_1)^2(k_3/k_1)^2$ takes on the maximum value. The top-left panel is the local form given by Eq. (4.7), which peaks at the squeezed configuration. The bottom-left panel is the equilateral form given by Eq. (4.10), which peaks at the equilateral configuration. The top-right panel is the orthogonal form given by Eq. (4.11), which has a positive peak at the equilateral configuration, and a negative valley along the elongated configurations. Note that all of these shapes are almost orthogonal to each other. This is quoted in Ref. [11]. 69
- 5.1 The CMB *III* (left top panel), *IIE* (right top one), *IEE* (left bottom one), and *EEE* (right bottom one) bispectra induced from the local-type (red solid line), equilateral-type (green dashed one), and orthogonal-type (blue dotted one) non-Gaussianities of curvature perturbations. The three multipoles are fixed as $\ell_1 = \ell_2 = \ell_3 \equiv \ell$. Here we consider a power-law flat Λ CDM model and fix the nonlinear parameters as $f_{\text{NL}}^{\text{local}} = f_{\text{NL}}^{\text{equil}} = f_{\text{NL}}^{\text{orthog}} = 100$. The other cosmological parameters are fixed to the mean values reported in Ref. [9]. 76
- 5.2 The CMB *III* (left top panel), *IIE* (right top one), *IEE* (left bottom one), and *EEE* (right bottom one) bispectra induced from the local-type (red solid line), equilateral-type (green dashed one), and orthogonal-type (blue dotted one) non-Gaussianities of curvature perturbations with $f_{\text{NL}}^{\text{local}} = f_{\text{NL}}^{\text{equil}} = f_{\text{NL}}^{\text{orthog}} = 100$. Here, we fix the two multipoles as $\ell_1 = \ell_2 = 200$, and plot each curve as the function in terms of ℓ_3 . The cosmological parameters are identical to those in Fig. 5.1. 77
- 6.1 Shape of I/k_1 . For the symmetric property and the triangle condition, we limit the plot range as $k_1 \leq k_2 \leq k_3$ and $|k_1 - k_2| \leq k_3 \leq k_1 + k_2$ 81
- 6.2 Absolute values of the CMB reduced bispectra of temperature fluctuation for $\ell_1 = \ell_2 = \ell_3 \equiv \ell$. The lines correspond to the spectra generated from tensor-scalar-scalar correlation given by Eq. (6.22) with $g_{tss} = 5$ (red solid line) and the primordial non-Gaussianity in the scalar curvature perturbations with $f_{\text{NL}}^{\text{local}} = 5$ (green dashed line). The other cosmological parameters are fixed to the mean values limited from WMAP-7yr data reported in Ref. [10]. 84
- 6.3 Absolute values of the CMB reduced bispectra of temperature fluctuation generated from tensor-scalar-scalar correlation given by Eq. (6.22) (*TSS* + *STS* + *SST*) and the primordial non-Gaussianity in the scalar curvature perturbations (*SSS*) as a function of ℓ_3 with ℓ_1 and ℓ_2 fixed to some values as indicated. The parameters are fixed to the same values defined in Fig. 6.2. 85
- 6.4 Signal-to-noise ratio normalized by g_{tss} as a function of the maximum value between ℓ_1, ℓ_2 and ℓ_3 , namely, ℓ . Each parameter is fixed to the same values defined in Fig. 6.2. 86

7.1	Absolute values of the CMB statistically anisotropic bispectrum of the intensity mode given by Eq. (7.29) with $C = 1$ (red solid line) and the statistically isotropic one given by Eq. (7.31) with $f_{\text{NL}} = 5$ (green dashed line) for $\ell_1 = \ell_2 = \ell_3$. The left and right figures are plotted in the configurations $(m_1, m_2, m_3) = (0, 0, 0), (10, 20, -30)$, respectively. The parameters are fixed to the mean values limited from the WMAP-7yr data as reported in Ref. [38].	95
7.2	Absolute values of the CMB statistically anisotropic bispectra of the intensity mode given by Eq. (7.29) for $(m_1, m_2, m_3) = (0, 0, 0)$ (left panel) and $(10, 20, -30)$ (right one) as the function with respect to ℓ_3 . The lines correspond to the spectra for $(\ell_1, \ell_2) = (102 + \ell_3, 100)$ (red solid line), $(100 - \ell_3 - 2, 100)$ (green dashed line) and $(100 + \ell_3, 100)$ (blue dotted line). The parameters are identical to the values defined in Fig. 7.1.	96
8.1	Shape of $k_1^2 k_2^2 k_3^2 S_A$ for $A = -1/2$ (top left panel), 0 (top right one), $1/2$ (bottom left one), and 1 (bottom right one) as the function of k_2/k_1 and k_3/k_1	110
8.2	Absolute values of the CMB III, IIB, IBB , and BBB spectra induced by W^3 and $\widetilde{W}W^2$ for $A = -1/2, 0, 1/2$, and 1 . We set that three multipoles have identical values as $\ell_1 - 2 = \ell_2 - 1 = \ell_3$. The left figures show the spectra not vanishing for $\sum_{n=1}^3 \ell_n = \text{even}$ (parity-even mode) and the right ones present the spectra for $\sum_{n=1}^3 \ell_n = \text{odd}$ (parity-odd mode). Here, we fix the parameters as $\Lambda = 3 \times 10^6 \text{GeV}$, $r = 0.1$, and $\tau_* = -k_*^{-1} = -14 \text{Gpc}$, and other cosmological parameters are fixed as the mean values limited from the WMAP 7-yr data [4].	112
8.3	Absolute value of the CMB III spectra generated from W^3 for $A = -1/2$ (red solid line), 0 (green dashed one) and $1/2$ (blue dotted one), and generated from the equilateral-type non-Gaussianity given by Eq. (8.58) with $f_{\text{NL}}^{\text{equil}} = 300$ (magenta dot-dashed one). We set that three multipoles have identical values as $\ell_1 = \ell_2 = \ell_3 \equiv \ell$. Here, we fix the parameters as the same values mentioned in Fig. 8.2.	114
9.1	Interaction between several components in the Universe if the PMF exists.	119
9.2	Power spectra of the CMB intensity fluctuations. The red solid, green dashed and blue dotted lines correspond to the spectra generated from the tensor, vector and scalar components of the PMF anisotropic stress for $n_B = -2.9$, respectively. The upper (lower) line of the red solid and blue dotted ones are calculated when $\tau_\nu/\tau_B = 10^{17}(10^6)$. The magenta dot-dashed line expresses the spectrum sourced from the primordial curvature perturbations. The strength of PMFs is fixed to $B_{1\text{Mpc}} = 4.7 \text{nG}$ and the other cosmological parameters are fixed to the mean values limited from WMAP-7yr data reported in Ref. [29].	127
9.3	CMB power spectra of the temperature fluctuations. The lines correspond to the spectra generated from vector anisotropic stress of PMFs as Eq. (9.52) (red solid line) and primordial curvature perturbations (blue dotted line). The green dashed line expresses the asymptotic power of the red solid one. The PMF parameters are fixed to $n_B = -2.9$ and $B_{1\text{Mpc}} = 4.7 \text{nG}$, and the other cosmological parameters are fixed to the mean values limited from WMAP-7yr data reported in Ref. [29].	132
9.4	Diagrams with respect to multipoles [35]. The left panel corresponds to Eq. (9.69). Due to the Wigner- $6j$ symbol originated with the sextuplicate dependence on the Gaussian PMFs, the true multipoles ℓ_1, ℓ_2 and ℓ_3 are linked with the dummy ones L, L' , and L'' and the 1-loop structure is realized. The right panel represents the tree-structure diagram, which arises from the CMB bispectrum induced by the four-point function of the Gaussian fields as mentioned in the previous sections.	138

- 9.5 The ratio of the left-hand side (exact solution) to the right-hand side (approximate solution) in Eq. (9.76). The lines correspond to the case for $L_1 = \ell_1 + 2$ (red solid line), for $L_1 = \ell_1$ (green dashed one), and for $L_1 = \ell_1 - 2$ (blue dotted one). 141
- 9.6 Absolute values of the normalized reduced bispectra of temperature fluctuations for a configuration $\ell_1 = \ell_2 = \ell_3 \equiv \ell$. The red solid, green dashed, and blue dotted lines correspond to the spectra generated from the auto-correlations of the PMF tensor, vector, and scalar anisotropic stresses for $n_B = -2.9$, respectively. The upper (lower) lines of the red solid and blue dotted lines are calculated when $\tau_\nu/\tau_B = 10^{17}(10^6)$. The magenta dot-dashed line expresses the spectrum sourced from the primordial non-Gaussianity with $f_{\text{NL}}^{\text{local}} = 5$. The strength of PMFs is fixed to $B_{1\text{Mpc}} = 4.7\text{nG}$ and the other cosmological parameters are fixed to the mean values limited from WMAP-7yr data reported in Ref. [29]. 146
- 9.7 Absolute values of the normalized reduced temperature-temperature-temperature spectra arising from the auto-correlation between the PMF vector anisotropic stresses for a configuration $\ell_1 = \ell_2 = \ell_3 \equiv \ell$. The lines correspond to the spectra generated from vector anisotropic stress for $n_B = -2.9$ (red solid line) and -2.8 (green dashed line), and primordial non-Gaussianity with $f_{\text{NL}}^{\text{local}} = 5$ (blue dotted line). The strength of PMFs is fixed to $B_{1\text{Mpc}} = 4.7\text{nG}$ and the other cosmological parameters are identical to the values used in Fig. 9.6. 147
- 9.8 Absolute values of the normalized reduced temperature-temperature-temperature bispectra induced by the auto-correlation between the PMF vector anisotropic stresses and generated by primordial non-Gaussianity given by Eq. (9.100) as a function of ℓ_3 with ℓ_1 and ℓ_2 fixed to some value as indicated. Each parameter is fixed to the same value defined in Fig. 9.6. 148
- 9.9 Absolute values of the normalized reduced temperature-temperature-temperature bispectra induced by the auto-correlation between the PMF tensor anisotropic stresses and generated from primordial non-Gaussianity in curvature perturbations given by Eq. (9.100) as a function of ℓ_3 with $\ell_1 = \ell_2$. Each parameter is identical to the values defined in Fig. 9.6. 149
- 9.10 Absolute values of the normalized reduced bispectra of temperature fluctuation for a configuration $\ell_1 = \ell_2 = \ell_3 \equiv \ell$. The red solid and green dashed lines represent the exact and approximate spectra arising from the tensor-tensor-tensor correlation of the PMF anisotropic stresses for $B_{1\text{Mpc}} = 4.7\text{nG}$, $n_B = -2.9$ and $\tau_\nu/\tau_B = 10^{17}$, respectively. The cosmological parameters are identical to the values defined in Fig. 9.6. 150

List of Tables

1.1	Major events in the Universe. This is quoted from Ref. [4]	14
3.1	FLRW solutions dominated by radiation, matter, curvature, or a cosmological constant.	34
3.2	Summary of the cosmological parameters of Λ CDM with finite r model from the WMAP 7-year data [27], and the data set combined with the results of the galaxy survey [32] and Hubble constant measurement [33], respectively. Here z_{reion} denotes the redshift at the reionization epoch, t_0 is the present time of the Universe, and $\omega_m \equiv \omega_b + \omega_c$.	61
A.1	Dipole ($l = 1$) harmonics for spin-0 and 1.	157
A.2	Quadrupole ($l = 2$) harmonics for spin-0 and 2.	157

1 Introduction

1.1 Big Bang Universe

The discovery of Hubble's law that light from distant galaxies is systematically shifted toward the red end of the spectrum supported the Friedmann Universe and guided us to the picture of an expanding Universe [1]. Next, the observed abundance of the light elements (H, He, and Li) and the CMB radiation match the predictions of the Big Bang scenario that the hot Universe cools gradually via the spatial expansion [2, 3]. Table 1.1 and Fig. 1.1 show the major events in the thermal history of the Universe as a function of the time and energy scales. At this point, we will give a summary of these milestones in the evolution of the Universe on the basis of Ref. [4].

From 10^{-10} sec to today, the evolution of the Universe is largely-understood by the theories of the particle physics and gravity. Here, we start by discussing the Universe at 100GeV, namely, the epoch of the electroweak phase transition (10^{-10} sec). Above 100GeV, the electroweak symmetry is restored and the Z and W^\pm bosons behave as massless particles. Then, the interactions are strong enough to keep quarks and leptons in the thermal equilibrium. Below this energy scale, since the electroweak symmetry is broken, the Z and W^\pm bosons acquire a finite mass, and the cross section of the weak interactions decreases as the Universe cools down. As a result, at around 1MeV, neutrinos decouple from matters such as electrons. Promptly after, at 1sec, the temperature of the Universe drops below the electron mass and there is efficient annihilation of electrons and positrons. Then, an initial matter-antimatter asymmetry of about 10^{-9} survives and the resulting photon-baryon fluid maintains a thermal equilibrium. Around 0.1MeV, the nuclear binding processes become important, and the light elements (H, He, Li, and Be) are formed from protons and neutrons during the Big Bang nucleosynthesis (~ 200 sec). The consistency with the observational abundances of H, He, and Li backs up the Big Bang theory. The energy density of matter is comparable to that of radiation around 1eV (10^{11} sec). The charged particles, namely protons and electrons, and photons are strongly coupled in the plasma via the Coulomb and Thomson scatterings, and the density contrasts propagate as the cosmic sound waves. Around 0.1eV (380000years), protons and electrons combine into neutral hydrogen (and helium) atoms. Then, photons decouple and become the free-streaming CMB. After 13.7 billion years, these photons are cooled to around 3K ($300\mu\text{eV}$) because of the red shift and reveal the snapshot of the early Universe. The anisotropies in the CMB intensity and polarizations provide the evidence for the fluctuations in the density of the primordial seed fields.

These tiny density contrasts, namely $\delta \equiv [\rho(\mathbf{x}, t) - \bar{\rho}]/\bar{\rho} \sim 10^{-5}$ with ρ and $\bar{\rho}$ being the energy density at an any point and its mean value respectively, grow via gravitational instability to form large-scale structures observed in the late-time Universe. A competition between the pressure of radiation and the gravitational attractive force affects the growth of the structure. During the radiation dominated era, the growth slows down, namely $\delta \propto \ln a$ with $a(t)$ being the scale factor that quantifies the space-time expansion. The clustering becomes more efficient after matter dominates over the background density (and the pressure vanishes), namely $\delta \propto a$. At first, small-scale contrasts become nonlinear as $\delta \gtrsim 1$, and form gravitationally bound objects that decouple from the overall expansion. This explains the hierarchical structure formation; fast, small-scale structures (like stars and galaxies) are formed and then they merge into larger structures (clusters and superclusters of galaxies). Around redshift $z \sim 25$ ($1 + z \equiv a^{-1}$), high energy photons arising from the first stars begin to ionize hydrogen in the intergalactic medium. This process, so called reionization, lasts until $z \approx 6$. Meanwhile, the most massive stars burn up the nuclear fuels and explode as supernovae. In these explosions, the heavy nucleons (C, O, etc) necessary for the

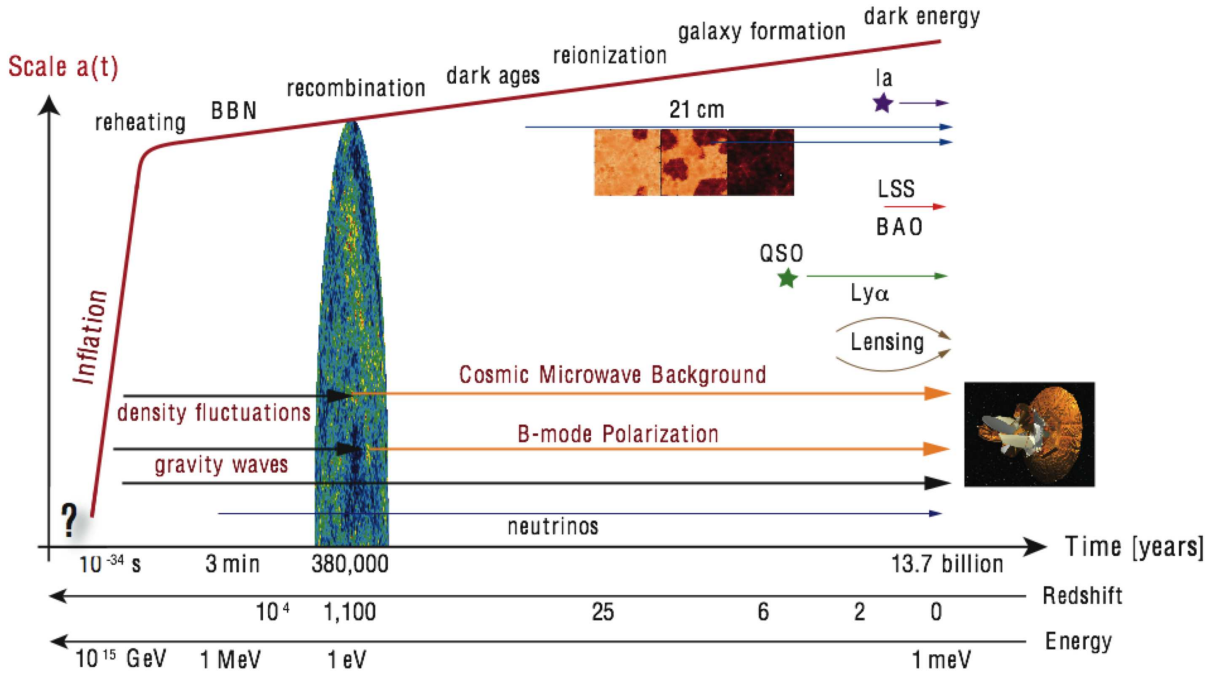


Figure 1.1: Evolution of the Universe. The events in the Universe are presented as the function of the time and energy scales. In addition, the several cosmological probes, which provide us with information about the structure and evolution of the Universe, are illustrated. *Acronyms:* Big bang nucleosynthesis (BBN), large scale structure (LSS), baryon acoustic oscillations (BAO), quasi-stellar objects = quasars (QSO), Lyman-alpha ($\text{Ly}\alpha$), cosmic microwave background (CMB), Type Ia supernovae (Ia), hydrogen 21cm-transition (21cm). This figure is quoted from Ref. [4]

creation of life are generated. At $z \approx 2$, the second accelerated expansion starts. This may be because an unknown energy with negative pressure, the so called “dark energy”, that starts to dominate the Universe. Further, the background space-time is accelerating and the growth of the structure ends as $\delta \sim \text{const.}$

1.2 Paradigm in the early Universe

The evolution of the Universe from 10^{-10}sec (1TeV) after its birth to today as discussed above, is supported by the observational facts and theoretical physics as the standard model of the particle physics and general relativity. Prior to this epoch, the temperature of the Universe exceeded 1TeV and we have not had any direct experimental discoveries so far. Hence, the physics is as speculative as it is fascinating.

To explain the CMB anisotropies, we require an input of the primordial seed fluctuations. We believe that these primordial fluctuations were generated in the very early Universe ($\sim 10^{-34}\text{sec}$) during the inflationary era. We will explain how the microscopic quantum fluctuations of fields get stretched by the inflationary expansion to the macroscopic fluctuations larger than the horizon at that time. After a metric perturbation exits the horizon, no causal physics can affect it, and it remains frozen with constant amplitude until it re-enters the horizon at a later time during the conventional (non-accelerating) Big Bang expansion¹. The fluctuations associated with the cos-

¹This is valid only when there are no anisotropic stress fluctuations.

	Time	Energy	
Planck epoch?	$< 10^{-43}$ sec	10^{18} GeV	
String scale?	$\gtrsim 10^{-43}$ sec	$\lesssim 10^{18}$ GeV	
Grand unification?	$\sim 10^{-36}$ sec	10^{15} GeV	
Inflation?	$\gtrsim 10^{-34}$ sec	$\lesssim 10^{15}$ GeV	
SUSY breaking?	$< 10^{-10}$ sec	> 1 TeV	
Baryogenesis?	$< 10^{-10}$ sec	> 1 TeV	
Electroweak unification	10^{-10} sec	1 TeV	
Quark-hadron transition	10^{-4} sec	10^2 MeV	
Nucleon freeze-out	0.01 sec	10 MeV	
Neutrino decoupling	1 sec	1 MeV	
BBN	3 min	0.1 MeV	
			Redshift
Matter-radiation equality	10^4 yrs	1 eV	10^4
Recombination	10^5 yrs	0.1 eV	$1,100$
Dark ages	$10^5 - 10^8$ yrs		> 25
Reionization	10^8 yrs		$25 - 6$
Galaxy formation	$\sim 6 \times 10^8$ yrs		~ 10
Dark energy	$\sim 10^9$ yrs		~ 2
Solar system	8×10^9 yrs		0.5
We born	14×10^9 yrs	$100 \mu\text{eV}$	0

Table 1.1: Major events in the Universe. This is quoted from Ref. [4]

mological structures re-enter the horizon when the Universe is about 100000 years old, right before the recombination (see Fig. 1.2). Inside the horizon, the perturbation amplitudes are changed by the causal physics, which means the CMB anisotropies, the galaxies, and clusters of galaxies are generated. Since we can calculate the evolution of perturbations after they re-enter the horizon, we can use the late time observations of the CMB and the LSS to infer the input spectrum of the primordial fluctuations. If we assume that this spectrum was produced by inflation, this leads to an observational probe of the physical conditions for the 10^{-34} sec epoch.

1.3 Concept of this thesis

Conventionally, the information of the primordial density fluctuations has been extracted from the two-point functions (power spectra) of the CMB fluctuations. There is a statistical property that although a non-Gaussian variable generates both even and odd-point correlations; a Gaussian variable generates only even-point correlations. Hence, it is hard to discriminate between the Gaussian and non-Gaussian signals in the CMB power spectrum. Theoretically, whether the primordial seed fluctuations are Gaussian depends completely on the inflationary models. Therefore, the check of the non-Gaussianity of the primordial fluctuations will lead to a more precise comprehension of the early Universe. To extract the non-Gaussian signals from the CMB anisotropy, we should focus on the higher order correlations of the CMB fluctuations such as the CMB three-point correlations (bispectra). Owing to the recent precise observation of the Universe, the CMB bispectra are becoming detectable quantities. As a result, the CMB bispectra are good measures of the primordial

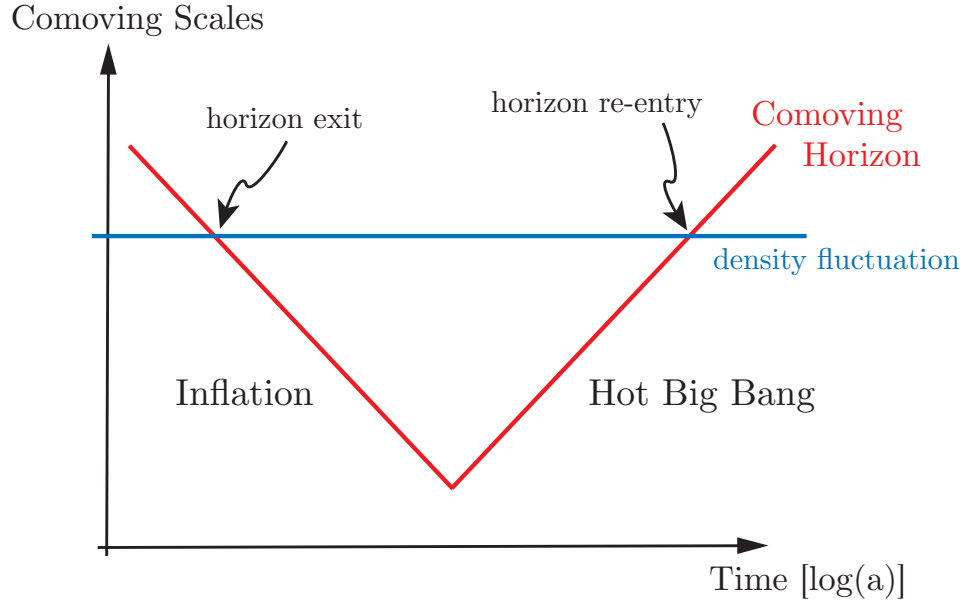


Figure 1.2: Balance between the scale of the density fluctuation and the comoving horizon. These are functions of the comoving scales $|\tau|$ and the scale factors a . The comoving horizon evolves as $\tau \equiv \int^t dt'/a(t') \propto -a^{-1}$ (at the inflationary epoch), a (at the radiation dominated era), and $a^{1/2}$ (at the matter dominated era). The scales of the density contrasts were larger than the Hubble radius until $a \sim 10^{-5}$. However, before inflation operated, all interest scales of the density contrasts were smaller than the Hubble radius and therefore the physics is described in terms of the quantum mechanics. Similarly, at a very late time, the scales of the cosmological interests re-entered in the Hubble radius. This figure is quoted from Ref. [4]

non-Gaussianity.

The primordial non-Gaussianities originating from the scalar components and their effects on the CMB bispectrum have been well-studied (Refs. [5, 6]). However, for some situations the vector components (vorticities) and tensor ones (gravitational waves) also act as non-Gaussian sources. This indicates that unknown signals, unlike the scalar case, may also appear in the CMB bispectra. To study these impacts in detail, we produced the general formulae for the CMB temperature and polarization bispectra from the scalar, vector and tensor non-Gaussianities [7, 8]. Next, utilizing these formulae and computing the practical CMB bispectra, we obtained new constraints on some primordial non-Gaussian sources and learned more about the nature of the early Universe [9–13].

This thesis aims to discuss the CMB bispectra induced by the primordial scalar, vector, and tensor non-Gaussianity on the basis of our recent studies [7–13]. More concrete organization of this thesis is as follows. In Secs. 2 and 3, we demonstrate how to generate the seed fluctuations in the inflationary era on the basis of some review papers and present formulae for the scalar, vector, and tensor modes of the CMB anisotropies as mentioned in Ref. [7]. We also review some observational findings obtained by the analysis of the CMB power spectra. In Secs. 4 and 5, we describe the general formulae of the CMB bispectra generated from the primordial scalar, vector, and tensor non-Gaussianities [8]. We then discuss the applications to the non-Gaussianities in two scalars and a graviton correlator [8] (Sec. 6), involving the violation of the rotational or parity invariance [12, 13] (Secs. 7 and 8), and sourced by the primordial magnetic fields [9–11] (Sec. 9). Finally, summarize this thesis and discuss some future issues (Sec. 10). In the appendices, we describe some mathematical tools and the detailed calculations required for the conduct of our

formalism.

References

- [1] E. Hubble, *A relation between distance and radial velocity among extra-galactic nebulae*, *Proc.Nat.Acad.Sci.* **15** (1929) 168–173.
- [2] R. Alpher, H. Bethe, and G. Gamow, *The origin of chemical elements*, *Phys.Rev.* **73** (1948) 803–804.
- [3] R. Dicke, P. Peebles, P. Roll, and D. Wilkinson, *Cosmic Black-Body Radiation*, *Astrophys.J.* **142** (1965) 414–419.
- [4] D. Baumann, *TASI Lectures on Inflation*, [arXiv:0907.5424](#).
- [5] N. Bartolo, E. Komatsu, S. Matarrese, and A. Riotto, *Non-Gaussianity from inflation: Theory and observations*, *Phys. Rept.* **402** (2004) 103–266, [[astro-ph/0406398](#)].
- [6] E. Komatsu, *Hunting for Primordial Non-Gaussianity in the Cosmic Microwave Background*, *Class. Quant. Grav.* **27** (2010) 124010, [[arXiv:1003.6097](#)].
- [7] M. Shiraishi, S. Yokoyama, D. Nitta, K. Ichiki, and K. Takahashi, *Analytic formulae of the CMB bispectra generated from non- Gaussianity in the tensor and vector perturbations*, *Phys. Rev.* **D82** (2010) 103505, [[arXiv:1003.2096](#)].
- [8] M. Shiraishi, D. Nitta, S. Yokoyama, K. Ichiki, and K. Takahashi, *CMB Bispectrum from Primordial Scalar, Vector and Tensor non-Gaussianities*, *Prog. Theor. Phys.* **125** (2011) 795–813, [[arXiv:1012.1079](#)].
- [9] M. Shiraishi, D. Nitta, S. Yokoyama, K. Ichiki, and K. Takahashi, *Cosmic microwave background bispectrum of vector modes induced from primordial magnetic fields*, *Phys. Rev.* **D82** (2010) 121302, [[arXiv:1009.3632](#)].
- [10] M. Shiraishi, D. Nitta, S. Yokoyama, K. Ichiki, and K. Takahashi, *Computation approach for CMB bispectrum from primordial magnetic fields*, *Phys. Rev.* **D83** (2011) 123523, [[arXiv:1101.5287](#)].
- [11] M. Shiraishi, D. Nitta, S. Yokoyama, K. Ichiki, and K. Takahashi, *Cosmic microwave background bispectrum of tensor passive modes induced from primordial magnetic fields*, *Phys. Rev.* **D83** (2011) 123003, [[arXiv:1103.4103](#)].
- [12] M. Shiraishi and S. Yokoyama, *Violation of the Rotational Invariance in the CMB Bispectrum*, *Prog.Theor.Phys.* **126** (2011) 923–935, [[arXiv:1107.0682](#)].
- [13] M. Shiraishi, D. Nitta, and S. Yokoyama, *Parity Violation of Gravitons in the CMB Bispectrum*, *Prog.Theor.Phys.* **126** (2011) 937–959, [[arXiv:1108.0175](#)].

2 Fluctuations in inflation

Inflation expresses an exponential growth of the scale factor of the Universe in the early time, namely, $a \sim e^{Ht}$. In Einstein gravity, this requires $p \sim -\rho$ with p and ρ being the pressure and energy density, and is often realized by the existence of a enigmatic scalar field, inflaton. We believe that the small fluctuations of this field have created the curvature perturbations and the density contrasts. Moreover, some vorticities and gravitational waves may also have evolved together. In this section, we describe the physical treatment of these fluctuations in the inflationary era in accordance with Ref. [1].

2.1 Dynamics of the scalar field

In the simplest models of inflation, there exists a single scalar field ϕ , the so-called inflaton. The dynamics of a scalar field (minimally) coupled to gravity is derived from the action

$$S = \int d^4x \sqrt{-g} \left[\frac{1}{2} M_{\text{pl}}^2 R + \frac{1}{2} g^{\mu\nu} \partial_\mu \phi \partial_\nu \phi - V(\phi) \right] \equiv S_{\text{EH}} + S_\phi, \quad (2.1)$$

where R denotes the Ricci scalar and $M_{\text{pl}} \equiv (8\pi G)^{-1/2}$ is the reduced Planck mass. This action consists of the gravitational Einstein-Hilbert action, S_{EH} , and the action of a scalar field with canonical kinetic term, S_ϕ . The potential $V(\phi)$ describes the self-interactions of the scalar field. The energy momentum tensor for a scalar field is

$$T_{\mu\nu}^{(\phi)} \equiv -\frac{2}{\sqrt{-g}} \frac{\delta S_\phi}{\delta g^{\mu\nu}} = \partial_\mu \phi \partial_\nu \phi - g_{\mu\nu} \left(\frac{1}{2} \partial^\sigma \phi \partial_\sigma \phi + V(\phi) \right). \quad (2.2)$$

Then, the field equation of ϕ is given by

$$\frac{\delta S_\phi}{\delta \phi} = \frac{1}{\sqrt{-g}} \partial_\mu (\sqrt{-g} \partial^\mu \phi) + V_\phi = 0, \quad (2.3)$$

where $V_\phi = dV/d\phi$. Assuming the FLRW metric as

$$ds^2 = -dt^2 + a^2 dx^2 = a^2 (-d\tau^2 + dx^2) \quad (2.4)$$

with τ being the conformal time and the homogeneity of the inflaton, $\phi(t, \mathbf{x}) \equiv \phi(t)$, its energy momentum tensor takes the form of a perfect fluid with

$$\rho_\phi = \frac{1}{2} (\partial_t \phi)^2 + V(\phi), \quad p_\phi = \frac{1}{2} (\partial_t \phi)^2 - V(\phi). \quad (2.5)$$

Thus, the parameter for the equation of state of ϕ :

$$w_\phi \equiv \frac{p_\phi}{\rho_\phi} = \frac{\frac{1}{2} (\partial_t \phi)^2 - V}{\frac{1}{2} (\partial_t \phi)^2 + V} \quad (2.6)$$

shows that a scalar field can realize the negative pressure ($w_\phi < 0$) and accelerated expansion of the Universe ($w_\phi < -1/3$) when the potential energy V dominates over the kinetic one $(\partial_t \phi)^2/2$. The Friedmann and field equations are written as

$$H^2 = \frac{1}{3M_{\text{pl}}^2} \left[\frac{1}{2} (\partial_t \phi)^2 + V(\phi) \right], \quad (2.7)$$

$$\frac{d^2 \phi}{dt^2} + 3H \frac{d\phi}{dt} + V_\phi = 0,$$

where $H \equiv \partial_t a/a$ is the Hubble parameter. If the potential has large values, ϕ experiences the significant Hubble friction from the term $H \partial_t \phi$.

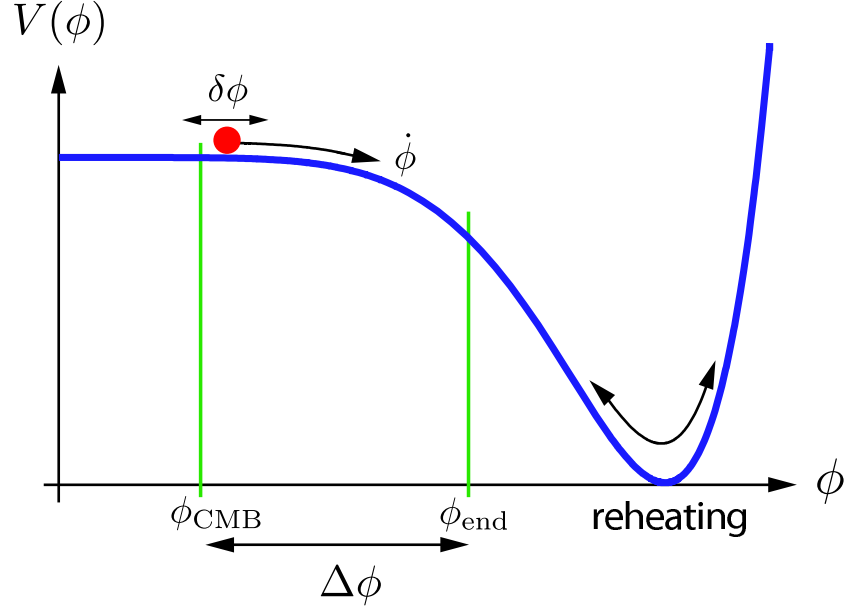


Figure 2.1: Example of the potential of the inflaton ϕ . An accelerated expansion of the Universe occurs when $V(\phi) \gg \frac{1}{2}(\partial_t \phi)^2$. Inflation ends at $\phi = \phi_{\text{end}}$ when $\frac{1}{2}(\partial_t \phi)^2 \approx V$. The CMB fluctuations are generated from the quantum fluctuations $\delta\phi$ about 60 e -folds before the end of inflation. At reheating, the energy density of the inflaton is converted into radiations. This figure is quoted in Ref. [1]

2.2 Slow-roll inflation

The acceleration equation of the Universe dominated by a homogeneous scalar field ϕ is given by

$$a^{-1} \frac{d^2 a}{dt^2} = -\frac{1}{6M_{\text{pl}}^2}(\rho_\phi + 3p_\phi) = H^2(1 - \epsilon_H) , \quad (2.8)$$

where

$$\epsilon_H \equiv \frac{3}{2}(w_\phi + 1) = \frac{1}{2} \left(\frac{\partial_t \phi}{M_{\text{pl}} H} \right)^2 . \quad (2.9)$$

The so-called Hubble slow-roll parameter ϵ_H is defined as

$$\epsilon_H = -\frac{\partial_t H}{H^2} = -\frac{d \ln H}{dN} , \quad (2.10)$$

where $dN = H dt$ with N being the e -folding number. When $\epsilon_H < 1$, an accelerated expansion occurs. For $\epsilon_H \rightarrow 0$, the de Sitter limit, namely, $p_\phi \rightarrow -\rho_\phi$, realizes. Then, the potential energy dominates over the kinetic energy as

$$(\partial_t \phi)^2 \ll V(\phi) . \quad (2.11)$$

Moreover, only if the second time derivative of ϕ is small enough

$$\left| \frac{d^2 \phi}{dt^2} \right| \ll |3H \partial_t \phi|, |V_\phi| , \quad (2.12)$$

an accelerated expansion will be sustained for a sufficiently long period of time. This corresponds to the smallness of a second Hubble slow-roll parameter as

$$\eta_H \equiv -\frac{1}{H\partial_t\phi} \frac{d^2\phi}{dt^2} = \epsilon_H - \frac{1}{2\epsilon_H} \frac{d\epsilon_H}{dN} , \quad (2.13)$$

where owing to $|\eta_H| \ll 1$, the fractional change of ϵ_H per e -fold is small. The slow-roll conditions, $\epsilon_H, |\eta_H| \ll 1$, can be interpreted as the conditions on the shape of the potential as

$$\epsilon(\phi) \equiv \frac{M_{\text{pl}}^2}{2} \left(\frac{V_\phi}{V} \right)^2 , \quad \eta(\phi) \equiv M_{\text{pl}}^2 \frac{V_{\phi\phi}}{V} . \quad (2.14)$$

In the slow-roll regime

$$\epsilon, |\eta| \ll 1 , \quad (2.15)$$

Eq. (2.7) is rewritten as

$$\begin{aligned} H^2 &\approx \frac{V}{3M_{\text{pl}}^2} \approx \text{const.} , \\ \partial_t\phi &\approx -\frac{V_\phi}{3H} , \end{aligned} \quad (2.16)$$

and the former equation leads to the de Sitter space-time as

$$a(t) \sim e^{Ht} . \quad (2.17)$$

The parameters ϵ and η are called the potential slow-roll parameters, and in the slow-roll approximation, the Hubble and potential slow-roll parameters are related as

$$\epsilon_H \approx \epsilon , \quad \eta_H \approx \eta - \epsilon . \quad (2.18)$$

Inflation ends when the slow-roll conditions are broken as

$$\epsilon_H(\phi_{\text{end}}) \equiv 1 , \quad \epsilon(\phi_{\text{end}}) \approx 1 . \quad (2.19)$$

From Eq. (2.16), the e -folding number prior to the end of inflation is evaluated as

$$\begin{aligned} N(\phi) &\equiv \ln \frac{a_{\text{end}}}{a} \\ &= \int_t^{t_{\text{end}}} H dt = \int_\phi^{\phi_{\text{end}}} \frac{H}{\partial_t\phi} d\phi \approx \int_{\phi_{\text{end}}}^\phi \frac{V}{V_\phi} d\phi . \end{aligned} \quad (2.20)$$

Using the slow-roll parameters, this is expressed as

$$N(\phi) = \int_{\phi_{\text{end}}}^\phi \frac{d\phi}{M_{\text{pl}}\sqrt{2\epsilon_H}} \approx \int_{\phi_{\text{end}}}^\phi \frac{d\phi}{M_{\text{pl}}\sqrt{2\epsilon}} . \quad (2.21)$$

To solve the horizon and flatness problems, it is necessary that the total e -folding number exceeds about 60, namely,

$$N_{\text{tot}} \equiv \ln \frac{a_{\text{end}}}{a_{\text{start}}} \gtrsim 60 . \quad (2.22)$$

The precise value depends on the energy scale of inflation and on the nature of reheating after inflation. The initial condition of the observed CMB anisotropies are created at $N_{\text{cmb}} \approx 40 - 60$. Considering an integral constraint

$$\int_{\phi_{\text{end}}}^{\phi_{\text{cmb}}} \frac{d\phi}{M_{\text{pl}}\sqrt{2\epsilon}} = N_{\text{cmb}} \approx 40 - 60 , \quad (2.23)$$

one can calculate the corresponding field value ϕ_{cmb} .

Finally, for an example, let us present the slow-roll analysis of the simplest model of inflation: a single field inflation driven by a mass term as

$$V(\phi) = \frac{1}{2}m^2\phi^2 . \quad (2.24)$$

The slow-roll parameters are

$$\epsilon(\phi) = \eta(\phi) = 2 \left(\frac{M_{\text{pl}}}{\phi} \right)^2 . \quad (2.25)$$

For $\epsilon, |\eta| \ll 1$, we need to consider super-Planckian values for the inflaton as

$$\phi \gg \sqrt{2}M_{\text{pl}} \equiv \phi_{\text{end}} . \quad (2.26)$$

The field value of the inflaton is related with the e -folding number before inflation ends is given by

$$N(\phi) = \frac{\phi^2}{4M_{\text{pl}}^2} - \frac{1}{2} . \quad (2.27)$$

The origins of the observed CMB anisotropies are created at

$$\phi_{\text{cmb}} = 2\sqrt{N_{\text{cmb}}}M_{\text{pl}} \sim 15M_{\text{pl}} . \quad (2.28)$$

2.3 Reheating

After inflation ends, ϕ begins to oscillate around the minimum of the potential as shown in Fig. 2.1. During this phase of the coherent oscillations, ϕ behaves as a pressureless matter:

$$\partial_t \rho_\phi + 3H\rho_\phi = 0 . \quad (2.29)$$

If the coupling of the inflaton field to other particles exists, the inflaton energy decays in accordance with

$$\partial_t \rho_\phi + (3H + \Gamma_\phi)\rho_\phi = 0 , \quad (2.30)$$

where the decay rate Γ_ϕ depends on model-dependent physical processes. Eventually, the inflationary energy density is converted into the relativistic degrees of freedom and the hot Big Bang starts. We can find the detailed review in Ref. [2].

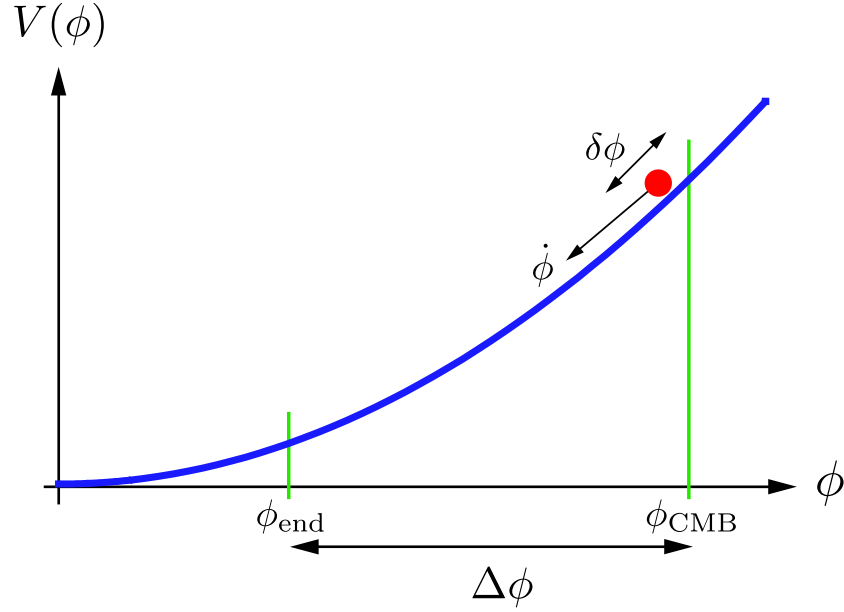


Figure 2.2: Large-field inflation. This shape of the potential can be realized when $V(\phi) \propto \phi^p$. In cases like this, the inflaton field moves over a super-Planckian range during inflation, namely, $\Delta\phi > M_{\text{pl}}$, and a large amplitude of the gravitational waves is produced. This figure is quoted in Ref. [1].

2.4 Inflation models

The nature of inflation is a mystery and there still remain some questions to be answered. However, we believe that inflation has occurred at an enormous energy scale (maybe as high as $\sim 10^{15}$ GeV), far out of reach of the particle accelerators. Hence, any description of the inflationary era requires extrapolations of the known laws of physics, and until recently, a simple phenomenological parametrization of the inflationary dynamics was used. In this approach, a variety of the inflationary potential functions as described in Figs. 2.1 and 2.2 have been discussed and the experimental predictions have been computed. As we will see in the next subsection, the details of the spectra of the primordial perturbations will depend on the precise shape of the inflaton potential.

2.4.1 Single-field slow-roll inflation

The inflationary model selection amounts to a specification of the action of the inflaton and the coupling to the gravity. In the above discussion, we have considered the simplest model, namely, the single-field slow-roll inflation, characterized by the action as

$$S = \int d^4x \sqrt{-g} \left[\frac{1}{2} M_{\text{pl}}^2 R + \frac{1}{2} g^{\mu\nu} \partial_\mu \phi \partial_\nu \phi - V(\phi) \right]. \quad (2.31)$$

From the time when the origins of the CMB fluctuations were generated at ϕ_{cmb} to the end of inflation at ϕ_{end} , the dynamics of the inflaton is determined by the shape of $V(\phi)$. The different properties for $V(\phi)$ are classified by determining whether the change of the inflaton field, which is expressed as $\Delta\phi \equiv \phi_{\text{cmb}} - \phi_{\text{end}}$, is large or small as measured in Planck units.

- *Small-field inflation*

In the small-field models, the change of the field is small (sub-Planckian), namely, $\Delta\phi < M_{\text{pl}}$. This leads to a fact that the amplitude of the gravitational waves produced during inflation is too small to be detected. The potentials realizing such small-field evolution often arise in the mechanisms of the spontaneous symmetry breaking, where the field rolls off an unstable equilibrium toward a displaced vacuum as shown in Fig. 2.1. A simple example is the Higgs-like potential as

$$V(\phi) = V_0 \left[1 - \left(\frac{\phi}{\mu} \right)^2 \right]^2 . \quad (2.32)$$

More generally, the small-field models can be locally approximated by

$$V(\phi) = V_0 \left[1 - \left(\frac{\phi}{\mu} \right)^p \right] + \dots , \quad (2.33)$$

where the dots express the higher-order terms becoming important near the end of inflation and during reheating. A famous inflationary potential is the so-called Coleman-Weinberg potential as [3, 4]

$$V(\phi) = V_0 \left[\left(\frac{\phi}{\mu} \right)^4 \left\{ \ln \left(\frac{\phi}{\mu} \right) - \frac{1}{4} \right\} + \frac{1}{4} \right] , \quad (2.34)$$

which appears from the radiatively-induced symmetry breaking in the electroweak and grand unified theories. Although the original values of the parameters V_0 and μ based on the $SU(5)$ theory are incompatible with the small amplitude of the fluctuations in inflation, this potential remains a popular phenomenological model (e.g. Refs. [5]).

- *Large-field inflation*

In the large-field models, the inflaton shifts from a large field values to a minimum of the potential $\phi = 0$. If the field evolution is super-Planckian, $\Delta\phi > M_{\text{pl}}$, the gravitational waves induced by inflation should be observed in the near future.

The prototypical large-field model is the so-called chaotic inflation where a single monomial term dominates the potential as described in Fig. 2.2:

$$V(\phi) = \lambda_p \phi^p . \quad (2.35)$$

For such a potential, the slow-roll parameters become small for super-Planckian field values, $\phi \gg M_{\text{pl}}$. Note that the slow-roll conditions are independent of the coupling constant λ_p . However, to arrange for a small amplitude of the density fluctuations, the inflaton self-coupling should be very small as $\lambda_p \ll 1$. This condition automatically guarantees that the values of the potential are sub-Planckian as $V \ll M_{\text{pl}}^4$, and the quantum gravity effects are not necessarily important.

The natural inflation, whose potential takes

$$V(\phi) = V_0 \left[\cos \left(\frac{\phi}{f} \right) + 1 \right] , \quad (2.36)$$

is one of the most elegant inflationary models. This potential shown in Fig. 2.3 often appears if the inflaton field is taken to be an axion. Depending on the parameter f , $\delta\phi$ can become small or large. However, it is particularly attractive to consider the natural inflation for the large-field variations, $2\pi f > M_{\text{pl}}$, since for axions a shift symmetry can be employed to protect the potential from the correction terms even over the large field ranges.

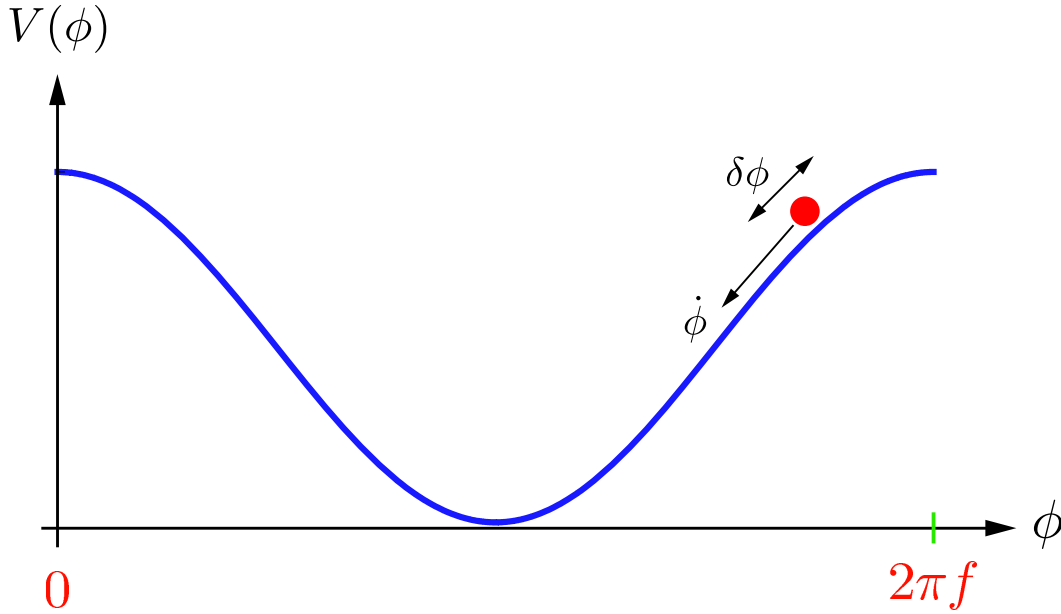


Figure 2.3: Small natural inflation. If the periodicity $2\pi f$ is super-Planckian, the model can naturally induce a large amplitude of the gravitational waves. This figure is quoted in Ref. [1].

2.4.2 Beyond the single-field slow-roll inflation

There are a variety of possibilities for realizing the inflationary expansion. Inflation is often studied as a framework for a theory of the early Universe, but it is not a unique theory. A lot of the phenomenological models have been proposed with the different theoretical motivations and observational predictions. In these models, the simplest inflationary action (2.31) is extended in several ways:

- *Non-minimal coupling to gravity*

The action (2.31) is so-called minimally coupled model in the sense that there is no direct coupling between the inflaton field and the metric. In contrast, we also can imagine a non-minimal coupling between the inflaton and graviton. However, in practice, the non-minimally coupled theories can be transformed to the minimally coupled form by a field redefinition.

- *Modified gravity*

Similarly, the possibilities that the Einstein-Hilbert action is modified at the high energies can be entertained. However, the simplest examples for this UV modification of gravity, so-called $f(R)$ theories, can also be expressed by a minimally coupled scalar field with potential $V(\phi)$.

- *Non-canonical kinetic term*

The action (2.31) has a canonical kinetic term

$$\mathcal{L}_\phi = X - V(\phi), \quad X \equiv \frac{1}{2} g^{\mu\nu} \partial_\mu \phi \partial_\nu \phi. \quad (2.37)$$

Then, inflation can only occur if the potential $V(\phi)$ is very flat. However, we can imagine the high-energy theory with the non-canonical kinetic terms as

$$\mathcal{L}_\phi = F(\phi, X) - V(\phi), \quad (2.38)$$

where $F(\phi, X)$ is the function composed of the inflaton field and its derivatives. For actions like this, inflation can be driven by the kinetic term and occur even in a steep potential. In Sec. 6, we treat the inflationary model with the non-canonical kinetic terms.

- *Multi-field inflation*

If there are two or more fields during inflation, then the possibilities for the inflationary dynamics and evolutions the cosmological perturbations expand dramatically. Several physical properties of the multi-field inflationary models are reviewed in e.g., Ref. [6]. The inflationary model mentioned in Sec. 7 is one of the models of the multi-field inflation.

2.5 Scalar perturbations

Here, we focus on the full computation of the quantum-mechanical scalar fluctuations generated during inflation and their relation to cosmological perturbations. Our calculation follows closely the treatment by Maldacena [7].

We consider the single-field slow-roll inflation defined by

$$S = \frac{1}{2} \int d^4x \sqrt{-g} [M_{\text{pl}}^2 R - (\nabla\phi)^2 - 2V(\phi)] . \quad (2.39)$$

To fix time and spatial reparametrizations, we choose the comoving gauge for the metric g_{ij} and the scalar field ϕ as

$$\delta\phi = 0 , \quad g_{ij} = a^2[(1 + 2\mathcal{R})\delta_{ij} + h_{ij}] , \quad \partial_i h^i_j = h^i_i = 0 . \quad (2.40)$$

In this gauge, the inflaton field is unperturbed and all scalar degrees of freedom are parametrized by the gauge-invariant comoving curvature perturbation $\mathcal{R}(t, \mathbf{x})$. There is an important property that \mathcal{R} remains constant outside the horizon if there exist no extra anisotropic stresses^{1 2}. Hence, we can restrict our computation to the correction functions of \mathcal{R} at horizon crossing.

2.5.1 Quadratic action

One expands the action (2.39) to second order in \mathcal{R} :

$$S^{(2)} = \frac{1}{2} \int d^4x a^3 \left(\frac{\partial_t \phi}{H} \right)^2 \left[(\partial_t \mathcal{R})^2 - \left(\frac{\partial_i \mathcal{R}}{a} \right)^2 \right] . \quad (2.41)$$

Defining the Mukhanov variable

$$v \equiv z\mathcal{R} , \quad z \equiv a \frac{\partial_t \phi}{H} , \quad (2.42)$$

and expressing with the conformal time τ lead to the action for a canonically normalized scalar as

$$S^{(2)} = \frac{1}{2} \int d\tau dx^3 \left[\dot{v}^2 + (\partial_i v)^2 + \frac{\ddot{z}}{z} v^2 \right] , \quad (2.43)$$

¹On superhorizon scales, this \mathcal{R} is consistent with \mathcal{R} in Refs. [8, 9], ζ in Refs. [7, 10], $-\mathcal{R}$ in Refs. [1, 11], and $-\zeta$ in Ref. [12]. In a numerical code CAMB [13, 14], the primordial scalar-mode power spectrum is given by this \mathcal{R} .

²In Sec. 9, we will show that due to the finite anisotropic stresses of the primordial magnetic field, the curvature perturbations (and gravitational waves) do not remain constant even on the superhorizon

where $\dot{} \equiv \partial_\tau$. Performing the Fourier expansion of v as

$$v(\tau, \mathbf{x}) = \int \frac{d^3\mathbf{k}}{(2\pi)^3} v_{\mathbf{k}}(\tau) e^{i\mathbf{k}\cdot\mathbf{x}} , \quad (2.44)$$

we can derive the field equation

$$\ddot{v}_{\mathbf{k}} + \left(k^2 - \frac{\ddot{z}}{z} \right) v_{\mathbf{k}} = 0 . \quad (2.45)$$

The Mukhanov equation (2.45) is hard to solve in full generality because the function z depends on the background dynamics. Then, one may find the numerical solution. However, in the pure de Sitter space-time, we can obtain the analytic solution.

2.5.2 Quantization and initial condition

One can perform the quantization of the field v in completely analogy with the treatment of the quantum harmonic oscillator.

At first, we express the field v and its conjugate momentum \dot{v} with the quantum operator as

$$\begin{aligned} v \rightarrow \hat{v} &= \int \frac{d^3\mathbf{k}}{(2\pi)^3} \left[v_k(\tau) \hat{a}_{\mathbf{k}} e^{i\mathbf{k}\cdot\mathbf{x}} + v_k^*(\tau) \hat{a}_{\mathbf{k}}^\dagger e^{-i\mathbf{k}\cdot\mathbf{x}} \right] \\ &= \int \frac{d^3\mathbf{k}}{(2\pi)^3} \left[v_k(\tau) \hat{a}_{\mathbf{k}} + v_k^*(\tau) \hat{a}_{-\mathbf{k}}^\dagger \right] e^{i\mathbf{k}\cdot\mathbf{x}} . \end{aligned} \quad (2.46)$$

This means that the Fourier component $v_{\mathbf{k}}$ is rewritten as the operator:

$$v_{\mathbf{k}} \rightarrow \hat{v}_{\mathbf{k}} = v_k(\tau) \hat{a}_{\mathbf{k}} + v_k^*(\tau) \hat{a}_{-\mathbf{k}}^\dagger , \quad (2.47)$$

where the creation ($\hat{a}_{\mathbf{k}}^\dagger$) and annihilation ($\hat{a}_{\mathbf{k}}$) operators satisfy the canonical commutation relation as

$$\left[\hat{a}_{\mathbf{k}}, \hat{a}_{\mathbf{k}'}^\dagger \right] = (2\pi)^3 \delta(\mathbf{k} - \mathbf{k}') , \quad (2.48)$$

if the mode functions are normalized as

$$\langle v_k, v_k \rangle \equiv \frac{i}{\hbar} (v_k^* \dot{v}_k - \dot{v}_k^* v_k) = 1 . \quad (2.49)$$

Note that these relations arise from

$$\left[\hat{v}, \dot{\hat{v}} \right] = i\hbar . \quad (2.50)$$

Equation (2.49) is used as one of the boundary conditions on the solutions of Eq. (2.45). The second boundary condition that fixes the mode functions completely comes from the vacuum selection.

We set a vacuum state for the fluctuations:

$$\hat{a}_{\mathbf{k}} |0\rangle = 0 . \quad (2.51)$$

As the vacuum, one often choose the so-called Bunch-Davies Vacuum denoting the Minkowski vacuum of a comoving observer in the far past, when all comoving scales were far inside the Hubble horizon, i.e., $\tau \rightarrow -\infty$ or $|k\tau| \gg 1$. In this limit, the mode equation (2.45) reaches

$$\ddot{v}_k + k^2 v_k = 0 . \quad (2.52)$$

This is identical to the equation of a simple harmonic oscillator with the time-independent frequency. Therefore, we can impose the initial condition as

$$\lim_{\tau \rightarrow -\infty} v_k = \frac{e^{-ik\tau}}{\sqrt{2k}} . \quad (2.53)$$

Owing to the two boundary conditions (2.49) and (2.53), we completely fix the mode functions on all scales.

2.5.3 Solution in de Sitter space-time

Considering the de Sitter limit: $\epsilon \rightarrow 0$ ($H = \text{const.}$) and

$$\frac{\ddot{z}}{z} = \frac{\ddot{a}}{a} = \frac{2}{\tau^2} , \quad (2.54)$$

the mode equation reduces to

$$\ddot{v}_k + \left(k^2 - \frac{2}{\tau^2} \right) v_k = 0 . \quad (2.55)$$

Taking into account the two boundary conditions (2.49) and (2.53), one can gain this solution as

$$v_k = \frac{e^{-ik\tau}}{\sqrt{2k}} \left(1 - \frac{i}{k\tau} \right) . \quad (2.56)$$

Using this, we can express the time evolution of the primordial curvature perturbation as

$$\hat{\mathcal{R}}(\mathbf{k}, \tau) \equiv \frac{H \hat{v}_{\mathbf{k}}}{a \partial_t \phi} = \frac{H}{a \partial_t \phi} [v_k(\tau) \hat{a}_{\mathbf{k}} + v_k^*(\tau) \hat{a}_{-\mathbf{k}}^\dagger] . \quad (2.57)$$

2.5.4 Power spectrum of curvature perturbations

We then compute the power spectrum of curvature perturbations:

$$\begin{aligned} \left\langle \prod_{n=1}^2 \hat{\mathcal{R}}(\mathbf{k}_n, \tau) \right\rangle &= (2\pi)^3 \delta \left(\sum_{n=1}^2 \mathbf{k}_n \right) \left(\frac{H |v_{k_1}(\tau)|}{a \partial_t \phi} \right)^2 \\ &= (2\pi)^3 \delta \left(\sum_{n=1}^2 \mathbf{k}_n \right) \frac{H^2}{2k_1^3} \left(\frac{H}{\partial_t \phi} \right)^2 [1 + (k_1 \tau)^2] . \end{aligned} \quad (2.58)$$

On superhorizon scales, $|k\tau| \ll 1$, this becomes

$$\begin{aligned} \left\langle \prod_{n=1}^2 \mathcal{R}(\mathbf{k}_n) \right\rangle &\equiv (2\pi)^3 P_{\mathcal{R}}(k_1) \delta \left(\sum_{n=1}^2 \mathbf{k}_n \right) , \\ P_{\mathcal{R}}(k) &= \frac{H_*^2}{2k^3} \left(\frac{H_*}{(\partial_t \phi)_*} \right)^2 = \left(\frac{H_*}{M_{\text{pl}}} \right)^2 \frac{1}{4\epsilon_{H_*} k^3} \approx \left(\frac{H_*}{M_{\text{pl}}} \right)^2 \frac{1}{4\epsilon_* k^3} . \end{aligned} \quad (2.59)$$

Here we evaluate all quantities at horizon crossing, namely $\tau_* = -1/k$. Note that since $\mathcal{R} = \text{const.}$ on superhorizon scales, this power spectrum becomes the initial condition for the CMB power spectrum of the scalar mode when a given fluctuation mode re-enters.

2.6 Tensor perturbations

As the quantization of the scalar perturbation have been discussed in detail, the corresponding calculation for tensor perturbations will appear almost trivial.

Expanding the Einstein-Hilbert action, one can obtain the second-order action for tensor fluctuations as

$$S^{(2)} = \frac{M_{\text{pl}}^2}{8} \int d\tau d^3x a^2 \left[\dot{h}_{ij} \dot{h}_{ij} - \partial_l h_{ij} \partial_l h_{ij} \right] . \quad (2.60)$$

Except a normalization factor of $M_{\text{pl}}/2$, this is the same as the action for a massless scalar field in the FLRW Universe. We obey the Fourier expansion as

$$h_{ij} = \int \frac{d^3\mathbf{k}}{(2\pi)^3} \sum_{\lambda=\pm 2} h^{(\lambda)}(\mathbf{k}, \tau) e_{ij}^{(\lambda)}(\hat{\mathbf{k}}) e^{i\mathbf{k}\cdot\mathbf{x}} , \quad (2.61)$$

where $e_{ij}^{(\lambda)}$ is the transverse-traceless polarization tensor which has two circular states $\lambda = \pm 2$. The convention and useful properties of this tensor are described in Appendix D. Taking into account the normalization: $e_{ij}^{(\lambda)}(\hat{\mathbf{k}}) e_{ij}^{(\lambda')}(-\hat{\mathbf{k}}) = 2\delta_{\lambda,\lambda'}$, the tensor quadratic action becomes

$$S^{(2)} = \sum_{\lambda=\pm 2} \int d\tau \left(\frac{M_{\text{pl}} a}{2} \right)^2 \int \frac{d^3\mathbf{k}}{(2\pi)^3} \left[|\dot{h}^{(\lambda)}(\mathbf{k}, \tau)|^2 - k^2 |h^{(\lambda)}(\mathbf{k}, \tau)|^2 \right] . \quad (2.62)$$

Defining the canonically normalized field:

$$v_{\mathbf{k}}^{(\lambda)}(\tau) \equiv \frac{a M_{\text{pl}}}{\sqrt{2}} h^{(\lambda)}(\mathbf{k}, \tau) , \quad (2.63)$$

we have

$$S^{(2)} = \sum_{\lambda=\pm 2} \int d\tau \int \frac{d^3\mathbf{k}}{(2\pi)^3} \frac{1}{2} \left[|\dot{v}_{\mathbf{k}}^{(\lambda)}|^2 - \left(k^2 - \frac{\ddot{a}}{a} \right) |v_{\mathbf{k}}^{(\lambda)}|^2 - \partial_\tau \left(\frac{\dot{a}}{a} |v_{\mathbf{k}}^{(\lambda)}|^2 \right) \right] . \quad (2.64)$$

Here, the third term in the square bracket is the topological term, hence this never affects the equation of motion. Then, through $\delta S / \delta v^{(\lambda)} = 0$, we obtain the mode equation of the gravitational wave:

$$\ddot{v}_{\mathbf{k}}^{(\lambda)} + \left(k^2 - \frac{\ddot{a}}{a} \right) v_{\mathbf{k}}^{(\lambda)} = 0 . \quad (2.65)$$

This is consistent with the equation of the scalar mode (2.55), therefore, the pure de Sitter solution is given by Eq. (2.56). Hence, in the de Sitter limit, the quantized mode function of the gravitational wave becomes

$$\begin{aligned} h^{(\lambda)}(\mathbf{k}, \tau) &= h_k(\tau) \hat{a}_{\mathbf{k}}^{(\lambda)} + h_k^*(\tau) \hat{a}_{-\mathbf{k}}^{(\lambda)\dagger} , \\ h_k(\tau) &= i \frac{H}{M_{\text{pl}}} \frac{e^{-ik\tau}}{\sqrt{k^3}} (1 + ik\tau) , \end{aligned} \quad (2.66)$$

where $\hat{a}^{(\lambda)}$ and $\hat{a}^{(\lambda)\dagger}$ satisfy

$$\begin{aligned} \hat{a}_{\mathbf{k}}^{(\lambda)} |0\rangle &= 0 , \\ [\hat{a}_{\mathbf{k}}^{(\lambda)}, \hat{a}_{\mathbf{k}'}^{(\lambda')\dagger}] &= (2\pi)^3 \delta(\mathbf{k} - \mathbf{k}') \delta_{\lambda,\lambda'} . \end{aligned} \quad (2.67)$$

Then, the power spectrum of primordial gravitational waves on the superhorizon limit, namely, $|k\tau| \ll 1$, is calculated as

$$\begin{aligned} \left\langle \prod_{n=1}^3 h^{(\lambda_n)}(\mathbf{k}_n) \right\rangle &= \left\langle 0 \left| \prod_{n=1}^3 h^{(\lambda_n)}(\mathbf{k}_n, \tau \rightarrow 0) \right| 0 \right\rangle \\ &\equiv (2\pi)^3 \frac{P_h(k_1)}{2} \delta \left(\sum_{n=1}^2 \mathbf{k}_n \right) \delta_{\lambda_1, \lambda_2} , \\ P_h(k) &= \left(\frac{H_*}{M_{\text{pl}}} \right)^2 \frac{2}{k^3} . \end{aligned} \quad (2.68)$$

Note that like the curvature perturbation, the gravitational wave also becomes constant outside the horizon if there are no anisotropic stress fluctuations.

2.7 Consistency relations in the slow roll limit

As a measure of the amplitude of the primordial gravitational wave, one often use the tensor-to-scalar ratio as

$$r \equiv \frac{2P_h(k)}{P_{\mathcal{R}}(k)} . \quad (2.69)$$

Comparing Eq. (2.59) with Eq. (2.68), we find a consistency relation

$$r = 16\epsilon_{H*} \approx 16\epsilon_* . \quad (2.70)$$

Note that using $Hdt = dN$, the tensor-to-scalar ratio r relates directly to the evolution of the inflaton as a function of the e -folding number N

$$r = \frac{8}{M_{\text{pl}}^2} \left(\frac{d\phi}{dN} \right)^2 . \quad (2.71)$$

The total field evolution between N_{cmb} and N_{end} can therefore be written as

$$\frac{\Delta\phi}{M_{\text{pl}}} = \int_{N_{\text{end}}}^{N_{\text{cmb}}} dN \sqrt{\frac{r}{8}} . \quad (2.72)$$

During the slow-roll inflation, $r(N)$ does not evolve much and one may gain the following approximate relation, so called, the Lyth bound [15]:

$$\frac{\Delta\phi}{M_{\text{pl}}} \sim \left(\frac{r}{0.01} \right)^{1/2} . \quad (2.73)$$

Therefore, the large values of the tensor-to-scalar ratio, $r > 0.01$, imply $\Delta\phi > M_{\text{pl}}$, namely, a consequence of the large-field inflation.

The scale dependence of the spectra is quantified by the spectral indices as

$$n_s - 4 \equiv \frac{d \ln P_{\mathcal{R}}}{d \ln k} , \quad n_t - 3 \equiv \frac{d \ln P_h}{d \ln k} . \quad (2.74)$$

From Eqs. (2.59) and (2.68), the right-hand sides are expanded as

$$\begin{aligned}\frac{d \ln P_{\mathcal{R}}}{d \ln k} &= \left(2 \frac{d \ln H_*}{dN} - \frac{d \ln \epsilon_{H_*}}{dN} \right) \frac{dN}{d \ln k} - 3 , \\ \frac{d \ln P_h}{d \ln k} &= 2 \frac{d \ln H_*}{dN} \frac{dN}{d \ln k} - 3 .\end{aligned}\tag{2.75}$$

From the definition of the Hubble slow-roll parameters (2.10) and (2.13), we obtain

$$\frac{d \ln H_*}{dN} = -\epsilon_{H_*} , \quad \frac{d \ln \epsilon_{H_*}}{dN} = 2(\epsilon_{H_*} - \eta_{H_*}) .\tag{2.76}$$

The factor $dN/(d \ln k)$ is evaluated by recalling the horizon crossing condition $k = a_* H_*$, or

$$d \ln k = dN + d \ln H_* ,\tag{2.77}$$

hence we have

$$\frac{dN}{d \ln k} = \left[\frac{d \ln k}{dN} \right]^{-1} = \left[1 + \frac{d \ln H_*}{dN} \right]^{-1} \approx 1 + \epsilon_{H_*} .\tag{2.78}$$

As the result, to first order in the Hubble slow-roll parameter, we find the consistency relations:

$$\begin{aligned}n_s - 1 &= 2\eta_{H_*} - 4\epsilon_{H_*} \approx 2\eta_* - 6\epsilon_* , \\ n_t &= -2\epsilon_{H_*} \approx -2\epsilon_* .\end{aligned}\tag{2.79}$$

Then, from (2.70), we also find the consistency relation between r and n_t as

$$r = -8n_t .\tag{2.80}$$

In the slow-roll limit, the measurements of the scalar and tensor spectra relate directly to the shape of the potential $V(\phi)$. This means that H is a measure of the scale of the potential, ϵ of its first derivative V_ϕ , η of its second derivative $V_{\phi\phi}$, etc. Therefore, the measurements of the amplitude and the scale-dependence of the cosmological perturbations encode the information about the potential driving the inflationary expansion. This allows to reconstruct a power series expansion of the potential around ϕ_{cmb} corresponding to the time when the origins of the CMB fluctuations exited the horizon.

References

- [1] D. Baumann, *TASI Lectures on Inflation*, arXiv:0907.5424.
- [2] B. A. Bassett, S. Tsujikawa, and D. Wands, *Inflation dynamics and reheating*, *Rev.Mod.Phys.* **78** (2006) 537–589, [astro-ph/0507632].
- [3] A. D. Linde, *A New Inflationary Universe Scenario: A Possible Solution of the Horizon, Flatness, Homogeneity, Isotropy and Primordial Monopole Problems*, *Phys.Lett.* **B108** (1982) 389–393.
- [4] A. Albrecht and P. J. Steinhardt, *Cosmology for Grand Unified Theories with Radiatively Induced Symmetry Breaking*, *Phys.Rev.Lett.* **48** (1982) 1220–1223.

- [5] Q. Shafi and V. N. Senoguz, *Coleman-Weinberg potential in good agreement with wmap*, *Phys.Rev.* **D73** (2006) 127301, [[astro-ph/0603830](#)].
- [6] D. Wands, *Multiple field inflation*, *Lect.Notes Phys.* **738** (2008) 275–304, [[astro-ph/0702187](#)].
- [7] J. M. Maldacena, *Non-Gaussian features of primordial fluctuations in single field inflationary models*, *JHEP* **05** (2003) 013, [[astro-ph/0210603](#)].
- [8] **WMAP** Collaboration, E. Komatsu *et al.*, *Seven-Year Wilkinson Microwave Anisotropy Probe (WMAP) Observations: Cosmological Interpretation*, *Astrophys. J. Suppl.* **192** (2011) 18, [[arXiv:1001.4538](#)].
- [9] L. Motta and R. R. Caldwell, *Non-Gaussian features of primordial magnetic fields in power-law inflation*, *Phys.Rev.* **D85** (2012) 103532, [[arXiv:1203.1033](#)].
- [10] D. H. Lyth and A. R. Liddle, *The primordial density perturbation: cosmology, inflation and the origin of structure; rev. version*. Cambridge Univ. Press, Cambridge, 2009.
- [11] M. Giovannini and K. E. Kunze, *Generalized CMB initial conditions with pre-equality magnetic fields*, *Phys.Rev.* **D77** (2008) 123001, [[arXiv:0802.1053](#)].
- [12] J. R. Shaw and A. Lewis, *Massive Neutrinos and Magnetic Fields in the Early Universe*, *Phys. Rev.* **D81** (2010) 043517, [[arXiv:0911.2714](#)].
- [13] A. Lewis, A. Challinor, and A. Lasenby, *Efficient Computation of CMB anisotropies in closed FRW models*, *Astrophys. J.* **538** (2000) 473–476, [[astro-ph/9911177](#)].
- [14] A. Lewis, *CMB anisotropies from primordial inhomogeneous magnetic fields*, *Phys. Rev.* **D70** (2004) 043011, [[astro-ph/0406096](#)].
- [15] D. H. Lyth, *What would we learn by detecting a gravitational wave signal in the cosmic microwave background anisotropy?*, *Phys. Rev. Lett.* **78** (1997) 1861–1863, [[hep-ph/9606387](#)].

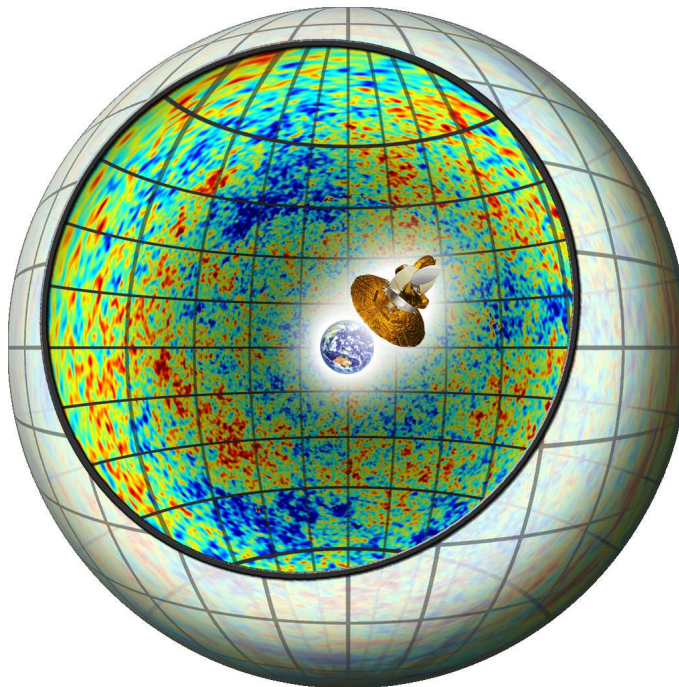


Figure 3.1: CMB anisotropy on the last scattering surface. The red (blue) parts correspond to the hot (cold) spots (Copyright 2011 by Daichi Kashino).

3 Fluctuations in cosmic microwave background radiation

Cosmic microwave background (CMB) radiation is composed of photons which have decoupled from electrons in the epoch of the hydrogen and helium recombination at $z = 1089$ and it is observed as the perfectly black body radiation whose averaged temperature is 2.725K. Historically, in 1949, Alpher and Herman predicted its existence as relics of the big bang Universe and its first detection came in 1964. More precisely, however, the CMB involves the spatial fluctuations of $\mathcal{O}(10^{-5})\text{K}$ (see Fig. 3.1). We had to wait the detection of the CMB anisotropy until the data of the COBE experiment were released in the 1990s.

Theoretically, the density contrast of the CMB is computed in the system where photons, neutrinos, baryons, dark matters and dark energy exist in the gravitational potential. Compared with the observational data, the values of several key parameters have been well-determined. The WMAP experiment established the facts that the Universe is close to spatially flat and the present structure grew from the nearly scale-invariant primordial fluctuations. These consequences are almost consistent with the prediction of the standard slow-roll inflation. Furthermore, we have a compelling evidence that the Universe is dominated by dark energy and dark matter, which implies that 96% of the total energy of the Universe remains unknown. Nowadays, some bare anomalies such as the preferred direction and the parity violation are furthermore being discussed [1], and we expect to extract more detailed information from the new precise measurements [2].

In addition to the intensity of the CMB, the polarizations also lead to better understandings. The curl-free component of the polarizations, E mode, reflects the recombination history, in particular, the reionization of the Universe. The curl component of the polarizations, B mode, is generated from the primordial vector and tensor perturbations. Hence, the detection of the B -mode polarization will provide clues as to inflation and the physics beyond the standard model of the particle physics.

In this section, we describe the original formalism of CMB fluctuations including intensity and polarization anisotropies from the scalar, vector, and tensor modes partially on the basis of our paper [3], some publications [4–7] and some academic dissertations [8–10], and summarize current outputs from the analysis of the CMB power spectra.

3.1 Einstein equations

Here, we derive the zeroth and first-order Einstein equations. Let us consider the flat ($K = 0$) FLRW metric and small perturbations in the synchronous gauge (for open and closed cases, see [11–13]):

$$ds^2 = a^2[-d\tau^2 + (\delta_{ij} + h_{ij})dx^i dx^j] . \quad (3.1)$$

We have the inverse metric to first order in perturbations as

$$g^{00} = -\frac{1}{a^2} , \quad g^{0i} = 0 , \quad g^{ij} = \frac{1}{a^2}(\delta^{ij} - h^{ij}) . \quad (3.2)$$

The Einstein equation with the cosmological constant Λ can be written as

$$G^\mu{}_\nu = R^\mu{}_\nu - \frac{1}{2}\delta^\mu{}_\nu R = 8\pi G T^\mu{}_\nu - \Lambda \delta^\mu{}_\nu , \quad (3.3)$$

where the left-hand side denotes the curvature of space-time and the right-hand one is the energy momentum tensor. The Ricci tensor $R_{\mu\nu}$ and Ricci scalar, namely a contracted form of the Ricci tensor, R , are expressed with the Christoffel symbols as

$$R_{\mu\nu} = R^\alpha{}_{\mu\alpha\nu} = \Gamma^\alpha{}_{\mu\nu,\alpha} - \Gamma^\alpha{}_{\mu\alpha,\nu} + \Gamma^\alpha{}_{\beta\alpha}\Gamma^\beta{}_{\mu\nu} - \Gamma^\alpha{}_{\beta\nu}\Gamma^\beta{}_{\mu\alpha} , \quad (3.4)$$

where $_{,\alpha} \equiv \partial_\alpha$. The Christoffel symbols in a metric space without torsion are given by

$$\Gamma^\lambda{}_{\mu\nu} = \frac{1}{2}g^{\lambda\kappa}(g_{\mu\kappa,\nu} + g_{\nu\kappa,\mu} - g_{\mu\nu,\kappa}) . \quad (3.5)$$

Up to first order, we can express as

$$\begin{aligned} \Gamma^0{}_{00} &= \mathcal{H} , \\ \Gamma^i{}_{00} &= \Gamma^0{}_{i0} = 0 , \\ \Gamma^0{}_{ij} &= \mathcal{H}(\delta_{ij} + h_{ij}) + \frac{1}{2}\dot{h}_{ij} , \\ \Gamma^i{}_{j0} &= \mathcal{H}\delta^i{}_j + \frac{1}{2}\dot{h}^i{}_j , \\ \Gamma^i{}_{jk} &= \frac{1}{2}(\partial_k h^i{}_j + \partial_j h^i{}_k - \partial^i h_{jk}) , \end{aligned} \quad (3.6)$$

therefore each component of the Ricci tensor is calculated as

$$\begin{aligned} a^2 R^0{}_0 &= 3 \left(\frac{\ddot{a}}{a} - \mathcal{H}^2 \right) + \frac{1}{2} \left(\ddot{h}^i{}_i + \mathcal{H} \dot{h}^i{}_i \right) , \\ a^2 R^i{}_0 &= -\frac{1}{2} \left(\partial^i \dot{h}^j{}_j - \partial^j \dot{h}^i{}_j \right) , \\ a^2 R^i{}_j &= \left(\frac{\ddot{a}}{a} + \mathcal{H}^2 \right) \delta^i{}_j + \frac{1}{2} \ddot{h}^i{}_j + \mathcal{H} \dot{h}^i{}_j + \frac{1}{2} \mathcal{H} \dot{h}^k{}_k \delta^i{}_j \\ &\quad - \frac{1}{2} \left(\partial^i \partial_j h^k{}_k + \nabla^2 h^i{}_j - \partial^i \partial_k h^k{}_j - \partial^k \partial_j h^i{}_k \right) . \end{aligned} \quad (3.7)$$

Here, $\mathcal{H} \equiv \dot{a}/a = aH$ is the Hubble parameter in terms of conformal time with H being the observable Hubble parameter. Then the Ricci scalar is also given by

$$R = R^\mu{}_\mu = \frac{1}{a^2} \left(6\frac{\ddot{a}}{a} + \ddot{h}^i{}_i + 3\mathcal{H}\dot{h}^i{}_i - \nabla^2 h^i{}_i + \partial_i \partial^i h^i{}_i \right) . \quad (3.8)$$

Contracting the Einstein equation (3.3) allows one to eliminate the Ricci scalar and reduce the Einstein equation to

$$R^\mu{}_\nu = 8\pi G \left(T^\mu{}_\nu - \frac{1}{2} \delta^\mu{}_\nu T^\sigma{}_\sigma \right) + \Lambda \delta^\mu{}_\nu . \quad (3.9)$$

Hence, in vacuum, we have $R^\mu{}_\nu = 0$.

3.1.1 Homogeneous contribution

At zeroth order, the 00 and ii components of Eq. (3.3) lead to the Friedmann constraint equation and the Raychaudhuri evolution equation, respectively. Substituting Eq. (3.7) into Eq. (3.9), these are obtained as

$$\begin{aligned} \mathcal{H}^2 &= -\frac{8\pi G}{3} a^2 \bar{T}^0{}_0 + \frac{a^2}{3} \Lambda , \\ 2\frac{\ddot{a}}{a} - \mathcal{H}^2 &= -\frac{8\pi G}{3} a^2 \bar{T}^i{}_i + a^2 \Lambda . \end{aligned} \quad (3.10)$$

The physical meaning of these equations can be illustrated with the perfect fluid form as follows. The energy momentum tensor of the perfect fluid is given by

$$T^\mu{}_\nu = (\rho + p)u^\mu u_\nu + p\delta^\mu{}_\nu , \quad (3.11)$$

hence the above equations change to

$$\begin{aligned} \mathcal{H}^2 &= \frac{8\pi G}{3} a^2 \left(\bar{\rho} + \frac{\Lambda}{8\pi G} \right) , \\ 2\frac{\ddot{a}}{a} - \mathcal{H}^2 &= -8\pi G a^2 \left(\bar{p} - \frac{\Lambda}{8\pi G} \right) . \end{aligned} \quad (3.12)$$

Note that we may identify the cosmological constant as a component of the perfect fluid as

$$\bar{T}^\mu{}_\nu = \frac{\Lambda}{8\pi G} \text{diag}(1, -1, -1, -1) . \quad (3.13)$$

To use a different phrase, an unperturbed perfect fluid of density and pressure are given by $\rho_\Lambda = \Lambda/(8\pi G)$, $p_\Lambda = -\rho_\Lambda$. If we use $w = p/\rho$, then $w_\Lambda = -1$.

For convenience, we change the Friedmann equation to

$$1 = \frac{8\pi G}{3\mathcal{H}^2} a^2 \bar{\rho} = \frac{8\pi G}{3H^2} \bar{\rho} = \sum_i \frac{8\pi G}{3H^2} \bar{\rho}_i , \quad (3.14)$$

where in third equality, we decompose the total energy density in the Universe into individual species $\bar{\rho}_i$. Introducing a quantity which means the ratio between the energy density of each

	w	$\rho(a)$	$a(t)$	$a(\tau)$	τ_i
rad dom	1/3	a^{-4}	$t^{1/2}$	τ	0
mat dom	0	a^{-3}	$t^{2/3}$	τ^2	0
curv dom	-	a^{-2}	t	$e^{H_0\Omega_k^{1/2}\tau}$	$-\infty$
Λ dom	-1	a^0	e^{Ht}	$-\tau^{-1}$	$-\infty$

Table 3.1: FLRW solutions dominated by radiation, matter, curvature, or a cosmological constant.

species and the critical density in the Universe at the present time, Ω_i , and which is expressed as $\Omega_i \equiv 8\pi G\bar{\rho}_{i0}/(3H_0^2)$, and using the scaling relation as $\bar{\rho}_i = \bar{\rho}_{i0}/a^{n_i}$, this equation is rewritten as

$$\sum_i \frac{\Omega_i}{a^{n_i}} = \left(\frac{H}{H_0} \right)^2. \quad (3.15)$$

For radiations, matters and cosmological constant, we have $n_i = 4, 3, 0$, respectively. In this notation, we can also include a curvature term as a component of $n_i = 2$. In Table 3.1, we summarize the solutions of Eq. (3.15) if the cosmological fluid consists of a single component.

3.1.2 Perturbed contribution

At first order, 00 and ij components of Eq. (3.9) generate the evolution equations as

$$\begin{aligned} \ddot{h}^i_i + \mathcal{H}\dot{h}^i_i &= 8\pi G a^2 (\delta T^0_0 - \delta T^i_i), \\ \ddot{h}^i_j + 2\mathcal{H}\dot{h}^i_j + \mathcal{H}\dot{h}^k_k \delta^i_j - (\partial^i \partial_j h^k_k + \nabla^2 h^i_j - \partial^k \partial_j h^i_k - \partial_k \partial^i h^k_j) \\ &= 16\pi G a^2 \left(\delta T^i_j - \frac{1}{2} \delta^i_j \delta T^\mu_\mu \right), \end{aligned} \quad (3.16)$$

and 00 and $i0$ components of Eq. (3.3) generate the constraint equations as

$$\begin{aligned} 2\mathcal{H}\dot{h}^i_i + \partial^j \partial_i h^i_j - \nabla^2 h^i_i &= -16\pi G a^2 \delta T^0_0, \\ \partial^j \dot{h}^i_j - \partial^i \dot{h}^j_j &= 16\pi G a^2 \delta T^i_0. \end{aligned} \quad (3.17)$$

From here, let us express these equations with the variables in the helicity states. To do it, we decompose all kind of vectors and tensors, such as metric, velocities and energy momentum tensors, into each helicity part in accordance with the formulae:

$$\begin{aligned} \omega_i(\mathbf{x}, \tau) &= \int \frac{d^3\mathbf{k}}{(2\pi)^3} \left(\omega^{(0)} O_i^{(0)} + \sum_{\lambda=\pm 1} \omega^{(\lambda)} O_i^{(\lambda)} \right) e^{i\mathbf{k}\cdot\mathbf{x}}, \\ \chi_{ij}(\mathbf{x}, \tau) &= \int \frac{d^3\mathbf{k}}{(2\pi)^3} \left(-\frac{1}{3} \chi_{\text{iso}} \delta_{ij} + \chi^{(0)} O_{ij}^{(0)} + \sum_{\lambda=\pm 1} \chi^{(\lambda)} O_{ij}^{(\lambda)} + \sum_{\lambda=\pm 2} \chi^{(\lambda)} O_{ij}^{(\lambda)} \right) e^{i\mathbf{k}\cdot\mathbf{x}}, \end{aligned} \quad (3.18)$$

where we define the projection vectors and tensors as

$$\begin{aligned}
O_a^{(0)}(\hat{\mathbf{k}}) &\equiv i\hat{k}_a , \\
O_a^{(\pm 1)}(\hat{\mathbf{k}}) &\equiv -i\epsilon_a^{(\pm 1)}(\hat{\mathbf{k}}) , \\
O_{ab}^{(0)}(\hat{\mathbf{k}}) &\equiv -\hat{k}_a\hat{k}_b + \frac{1}{3}\delta_{a,b} , \\
O_{ab}^{(\pm 1)}(\hat{\mathbf{k}}) &\equiv \hat{k}_a\epsilon_b^{(\pm 1)}(\hat{\mathbf{k}}) + \hat{k}_b\epsilon_a^{(\pm 1)}(\hat{\mathbf{k}}) , \\
O_{ab}^{(\pm 2)}(\hat{\mathbf{k}}) &\equiv e_{ab}^{(\pm 2)}(\hat{\mathbf{k}}) .
\end{aligned} \tag{3.19}$$

The polarization vector and tensor, $\epsilon_i^{(\pm 1)}, e_{ij}^{(\pm 2)}$, satisfy the divergenceless and transverse-traceless conditions as

$$\hat{k}_i\epsilon_i^{(\pm 1)}(\hat{\mathbf{k}}) = \hat{k}_ie_{ij}^{(\pm 2)}(\hat{\mathbf{k}}) = e_{ii}^{(\pm 2)}(\hat{\mathbf{k}}) = 0 . \tag{3.20}$$

The prescription for the scalar-vector-tensor decomposition and explicit forms of the polarization vector and tensor are presented in Appendix D. Then, from Eqs. (3.16) and (3.17), we can rewrite the evolution equations as

$$\begin{aligned}
\ddot{h}_{\text{iso}} + \mathcal{H}\dot{h}_{\text{iso}} &= -8\pi Ga^2 (\delta T_0^0 + \delta T_t^{\text{iso}}) , \\
\ddot{h}^{(0)} + 2\mathcal{H}\dot{h}^{(0)} + \frac{1}{3}k^2(h_{\text{iso}} - h^{(0)}) &= 16\pi Ga^2 \delta T_t^{(0)} , \\
\ddot{h}^{(\pm 1)} + 2\mathcal{H}\dot{h}^{(\pm 1)} &= 16\pi Ga^2 \delta T_t^{(\pm 1)} , \\
\ddot{h}^{(\pm 2)} + 2\mathcal{H}\dot{h}^{(\pm 2)} + k^2 h^{(\pm 2)} &= 16\pi Ga^2 \delta T_t^{(\pm 2)} ,
\end{aligned} \tag{3.21}$$

and the constraint equations as

$$\begin{aligned}
\mathcal{H}\dot{h}_{\text{iso}} + \frac{1}{3}k^2(h_{\text{iso}} - h^{(0)}) &= 8\pi Ga^2 \delta T_0^0 , \\
k \left(\dot{h}_{\text{iso}} - \dot{h}^{(0)} \right) &= 24\pi Ga^2 \delta T_v^{(0)} , \\
k\dot{h}^{(\pm 1)} &= -16\pi Ga^2 \delta T_v^{(\pm 1)} .
\end{aligned} \tag{3.22}$$

Here, we have obeyed the convention as

$$\begin{aligned}
\delta T_0^i(\mathbf{x}, \tau) &= \int \frac{d^3\mathbf{k}}{(2\pi)^3} \left(\delta T_v^{(0)} O_i^{(0)} + \sum_{\lambda=\pm 1} \delta T_v^{(\lambda)} O_i^{(\lambda)} \right) e^{i\mathbf{k}\cdot\mathbf{x}} , \\
\delta T_j^i(\mathbf{x}, \tau) &= \int \frac{d^3\mathbf{k}}{(2\pi)^3} \left(-\frac{1}{3}\delta T_t^{\text{iso}}\delta_{ij} + \delta T_t^{(0)} O_{ij}^{(0)} + \sum_{\lambda=\pm 1} \delta T_t^{(\lambda)} O_{ij}^{(\lambda)} + \sum_{\lambda=\pm 2} \delta T_t^{(\lambda)} O_{ij}^{(\lambda)} \right) e^{i\mathbf{k}\cdot\mathbf{x}} ,
\end{aligned} \tag{3.23}$$

Our perturbation quantities are related to the variables for the scalar mode in the synchronous gauge of Ref. [14], namely h and η , as

$$h_{\text{iso}} = -h, \quad h^{(0)} = -(h + 6\eta) . \tag{3.24}$$

Hence, we understand the correspondence to the gauge-invariant variables by Bardeen (Φ_A, Φ_H) [15] and Kodama-Sasaki (Ψ, Φ) [16]:

$$\begin{aligned}
\Phi_A = \Psi &= -\frac{1}{2k^2} \left(\ddot{h}^{(0)} + \mathcal{H}\dot{h}^{(0)} \right) , \\
\Phi_H = \Phi &= \frac{1}{6} (h^{(0)} - h_{\text{iso}}) - \frac{1}{2k^2} \mathcal{H}\dot{h}^{(0)} .
\end{aligned} \tag{3.25}$$

3.2 Boltzmann equations

The distribution function of several species evolves in accordance with the Boltzmann equation as

$$\frac{df}{d\tau} = \frac{\partial f}{\partial \tau} + \frac{\partial f}{\partial x^i} \frac{\partial x^i}{\partial \tau} + \frac{\partial f}{\partial p^\mu} \frac{\partial p^\mu}{\partial \tau} = \left(\frac{\partial f}{\partial \tau} \right)_C, \quad (3.26)$$

where τ is the conformal time, p^μ is the proper momentum of species, and a subscript C denotes the collision term. In this Boltzmann equation, there exist two contributions: the gravitational redshift and the effect of scattering, which correspond to the third term of the first equality and the term of the second equality, respectively. For convenience, we introduce the comoving momentum and energy as $q^i \equiv ap^i$, $\epsilon \equiv a\sqrt{p^2 + m^2}$. Setting a unit vector parallel to the fluid momentum as $\mathbf{q} = q\hat{\mathbf{n}}$ and expanding the distribution function up to first order:

$$f(\mathbf{x}, q, \hat{\mathbf{n}}, \tau) = f^{(0)}(q) [1 + f^{(1)}(\mathbf{x}, q, \hat{\mathbf{n}}, \tau)] , \quad (3.27)$$

the above Boltzmann equation is rewritten as

$$\begin{aligned} \frac{df}{d\tau} = & f^{(0)} \left(\frac{\partial f^{(1)}}{\partial \tau} + \frac{\partial f^{(1)}}{\partial x^i} \frac{dx^i}{d\tau} \right) \\ & + \frac{\partial f^{(0)}}{\partial q} \frac{dq}{d\tau} + f^{(0)} \frac{\partial f^{(1)}}{\partial q} \frac{dq}{d\tau} + f^{(1)} \frac{\partial f^{(0)}}{\partial q} \frac{dq}{d\tau} + f^{(0)} \frac{\partial f^{(1)}}{\partial \hat{n}^i} \frac{d\hat{n}^i}{d\tau} = \left(\frac{\partial f}{\partial \tau} \right)_C . \end{aligned} \quad (3.28)$$

To estimate $dq/d\tau$, $d\hat{n}^i/d\tau$, we consider the geodesic equation as

$$P^0 \frac{dP^\mu}{d\tau} + \Gamma^\mu_{\alpha\beta} P^\alpha P^\beta = 0 , \quad (3.29)$$

where P^μ is the canonical momentum as

$$P^\mu = \frac{1}{a^2} \left(\epsilon, q_j \left(\delta^{ij} - \frac{1}{2} h^{ij} \right) \right) , \quad P_\mu = \left(-\epsilon, q^j \left(\delta_{ij} + \frac{1}{2} h_{ij} \right) \right) . \quad (3.30)$$

The contraction is given by $P^\mu P_\mu = p^2 - (\epsilon/a)^2 = -m^2$. From $\mu = 0$ component, we obtain

$$\frac{dq}{d\tau} = -\frac{1}{2} q \hat{n}^i \hat{n}^j \frac{\partial h_{ij}}{\partial \tau} . \quad (3.31)$$

Similarly, from the spatial components, we have

$$2 \frac{d\hat{n}^i}{d\tau} = \hat{n}^i \hat{n}_m \hat{n}_n \frac{\partial h^{mn}}{\partial \tau} - \hat{n}_j \frac{\partial h^{ij}}{\partial \tau} - \frac{2q}{\epsilon} \hat{n}_m \hat{n}_n \partial^m h^{in} + \frac{q}{\epsilon} \hat{n}_m \hat{n}_n \partial^i h^{mn} \approx \mathcal{O}(h) . \quad (3.32)$$

Furthermore, since we have the zeroth order expression as $dx^i/d\tau = (q/\epsilon)\hat{n}^i$, the Boltzmann equations up to first order are expressed as

$$\frac{\partial f^{(1)}}{\partial \tau} + \frac{q}{\epsilon} \hat{n}^i \frac{\partial f^{(1)}}{\partial x^i} - \frac{1}{2} \hat{n}^i \hat{n}^j \frac{\partial h_{ij}}{\partial \tau} \frac{\partial \ln f^{(0)}}{\partial \ln q} = \frac{1}{f^{(0)}} \left(\frac{\partial f}{\partial \tau} \right)_C . \quad (3.33)$$

The general expression for the energy momentum tensor is given by

$$T^\mu{}_\nu = \int \sqrt{-g} d^3\mathbf{P} \frac{P^\mu P_\nu}{P^0} f . \quad (3.34)$$

Substituting the relations:

$$d^3\mathbf{P} = \left(1 + \frac{1}{2}h^i_i\right) q^2 dq d\Omega_n, \quad \sqrt{-g} = a^{-4} \left(1 - \frac{1}{2}h^i_i\right), \quad (3.35)$$

and noting that

$$\int \hat{n}^i \hat{n}_j d\Omega_n = \frac{4\pi}{3} \delta^i_j, \quad \int \hat{n}_i d\Omega_n = \int \hat{n}_i \hat{n}_j \hat{n}_k d\Omega_n = 0, \quad (3.36)$$

the homogeneous and linearized components of the energy momentum tensor are obtained as

$$\begin{aligned} T^0_0 &= -\rho = -\frac{1}{a^4} \int \int \epsilon f^{(0)} (1 + f^{(1)}) q^2 dq d\Omega_n \\ &= -\frac{4\pi}{a^4} \int \epsilon f^{(0)} q^2 dq - \frac{1}{a^4} \int \int \epsilon f^{(0)} f^{(1)} q^2 dq d\Omega_n \equiv \bar{T}^0_0 + \delta T^0_0, \\ T^i_0 &= -\frac{1}{a^4} \int \int q \left(\hat{n}^i - \frac{1}{2} \hat{n}_j h^{ij} \right) f^{(0)} (1 + f^{(1)}) q^2 dq d\Omega_n \\ &= -\frac{1}{a^4} \int \int q \hat{n}^i f^{(0)} f^{(1)} q^2 dq d\Omega_n \equiv \delta T^i_0, \\ T^i_j &= \frac{1}{a^4} \int \int \frac{q^2}{\epsilon} \left(\hat{n}^i - \frac{1}{2} \hat{n}_a h^{ia} \right) \left(\hat{n}_j + \frac{1}{2} \hat{n}^b h_{jb} \right) f^{(0)} (1 + f^{(1)}) q^2 dq d\Omega_n \\ &= \frac{4\pi}{3a^4} \delta^i_j \int \frac{q^2}{\epsilon} f^{(0)} q^2 dq + \frac{1}{a^4} \int \int \frac{q^2}{\epsilon} \hat{n}^i \hat{n}_j f^{(0)} f^{(1)} q^2 dq d\Omega_n \equiv \bar{T}^i_j + \delta T^i_j. \end{aligned} \quad (3.37)$$

These components correspond to the density contrast δ , velocity v^i and anisotropic stress Π^i_j of fluid as ¹

$$\bar{T}^0_0 = -\bar{\rho}, \quad \frac{\delta T^0_0}{\bar{\rho}} = -\delta, \quad \frac{\delta T^i_0}{\bar{\rho} + \bar{p}} = -\frac{\delta T^0_i}{\bar{\rho} + \bar{p}} = -v^i, \quad \bar{T}^i_j = \bar{p} \delta^i_j, \quad \frac{\delta T^i_j}{\bar{p}} = \Pi^i_j. \quad (3.38)$$

Therefore, equating the integral of Eq. (3.33) over $\mathbf{q}_1, \mathbf{q}_2, \mathbf{q}_3$ with Eqs. (3.37) and (3.38), we can see that the Boltzmann equation (3.33) becomes the differential equations with respect to δ, v^i, Π^i_j for each species. These equations correspond to the Euler and continuity equations. Generally, as the species of the cosmological fluid which mainly generate the inhomogeneity of the cosmological structure, there exist baryon, photon, neutrino and cold dark matter (CDM), hence we can trace the evolution of their fluctuations due to solving these Boltzmann equations coupled with the Einstein equations (3.21) and (3.22). Between baryons and photons, Thomson scattering is effective, so that their Boltzmann equations have the collision term. On the other hand, for neutrinos and CDMs, since there are no short-length interactions, the right-hand side of the Boltzmann equations vanishes. All these species couple with the metric via gravity. This relation is illustrated in Fig. 3.2.

3.3 Stokes parameters

Here, we introduce the Stokes parameters to characterize the polarization states of the radiation field. For simplicity, at first, we consider a plane electromagnetic wave propagating along the z axis. The Fourier decomposition of the radiation field is expressed as

$$\mathbf{E}(z, t) = \int_{-\infty}^{\infty} dk \left(\hat{\mathbf{x}} E_x e^{i\phi_x} + \hat{\mathbf{y}} E_y e^{i\phi_y} \right) e^{i(kz - \omega t)}, \quad (3.39)$$

¹The anisotropic stress of the magnetic field is often normalized by photon's energy density as Eq. (9.2).

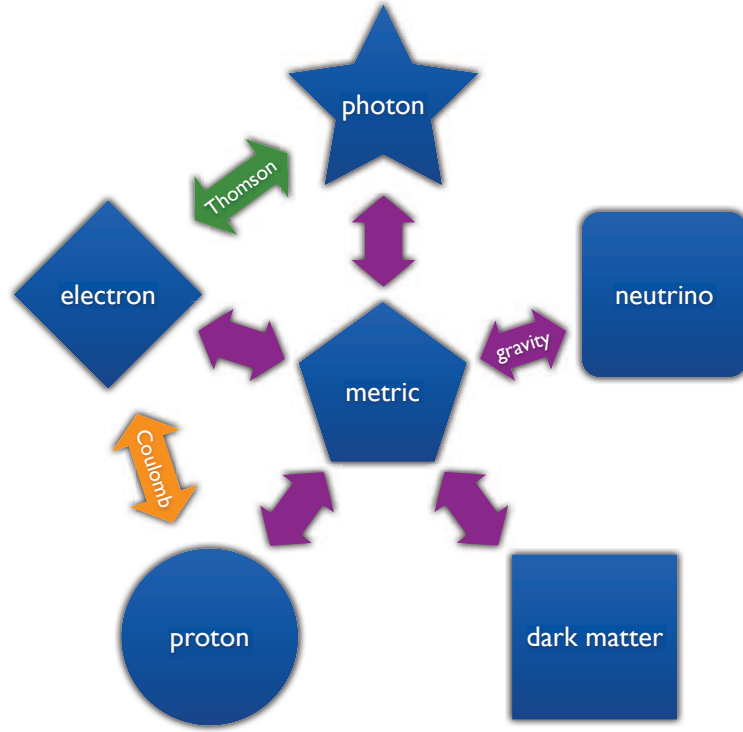


Figure 3.2: Interaction between several components in the Universe.

where E_x, E_y and ϕ_x, ϕ_y are the real quantities describing the amplitudes and phases in the $\hat{\mathbf{x}} - \hat{\mathbf{y}}$ plane, respectively, and $\omega = kc$ denotes the frequency of the wave.

The Stokes parameters are given by

$$\begin{aligned}
 I &\equiv |E_x|^2 + |E_y|^2, \\
 Q &\equiv |E_x|^2 - |E_y|^2, \\
 U &\equiv -2\text{Re}[E_x^* E_y], \\
 V &\equiv -2\text{Im}[E_x^* E_y],
 \end{aligned} \tag{3.40}$$

where these are all real quantities. For the monochromatic wave, $I^2 = Q^2 + U^2 + V^2$ is satisfied. I measures the intensity of radiation and is always positive. The other parameters represent the polarization states and can take either positive or negative values. Q and U quantify the magnitude of the linear polarization, and V parametrizes the circular polarization. While I and Q are parity-even quantities, U and V are parity-odd ones.

In order to see the transformation rule of Q and U under rotation of axes, let us introduce the new coordinate (x', y') , which is related to the original coordinate (x, y) by the rotation around the z axis as

$$\begin{pmatrix} x' \\ y' \end{pmatrix} = \begin{pmatrix} \cos \psi & \sin \psi \\ -\sin \psi & \cos \psi \end{pmatrix} \begin{pmatrix} x \\ y \end{pmatrix}. \tag{3.41}$$

Then, the radiation field is converted into

$$\begin{aligned} \mathbf{E}(z, t) &= \int_{-\infty}^{\infty} dk \left(\hat{\mathbf{x}}' E'_x e^{i\phi_x} + \hat{\mathbf{y}}' E'_y e^{i\phi_y} \right) e^{i(kz - \omega t)} , \\ (E'_x \pm iE'_y) &= e^{\pm i\psi} (E_x \pm iE_y) ; \end{aligned} \quad (3.42)$$

hence we have

$$Q' \pm iU' = e^{\mp 2i\psi} (Q \pm iU) . \quad (3.43)$$

This implies that the linear combination, $Q \pm iU$, are the spin- ± 2 quantities. Therefore, the anisotropy of the linear polarization should be expanded with the spin-2 spherical harmonics.

3.4 Boltzmann equations for photons

Here, for quantifying the CMB anisotropy, let us focus on the linearized Boltzmann equation for photons. The distribution function of photons is given by

$$f = \left[\exp \left\{ \frac{p}{T[1 + \Theta(\mathbf{x}, \hat{\mathbf{n}}, t)]} \right\} - 1 \right]^{-1} , \quad (3.44)$$

hence we have [14]

$$f^{(0)} = \frac{1}{e^{p/T} - 1} , \quad f^{(1)}(\mathbf{x}, q, \hat{\mathbf{n}}, \tau) = -\frac{q}{f^{(0)}} \frac{\partial f^{(0)}}{\partial q} \Theta = -\frac{\partial \ln f^{(0)}}{\partial \ln q} \Theta , \quad (3.45)$$

where $\Theta \equiv \Delta T/T$. Substituting Eq. (3.45) into Eq. (3.33), the Boltzmann equation in terms of Θ is expressed as

$$-q \frac{\partial f^{(0)}}{\partial q} \left(\frac{\partial \Theta}{\partial \tau} + \hat{n}^i \frac{\partial \Theta}{\partial x^i} + \frac{1}{2} \hat{n}^i \hat{n}^j \frac{\partial h_{ij}}{\partial \tau} \right) = \left(\frac{\partial f}{\partial \tau} \right)_C . \quad (3.46)$$

The first two terms in the bracket denote the free-streaming of the photon, whereas the remaining third term in the bracket account for the gravitational redshift. As for the CMB polarization, there exist no gravitational effects because Q, U and V themselves are first-order quantities and the third term in the left-hand side of Eq. (3.33) does not appear. Hence, we summarize the Boltzmann equations of Θ, Q, U and V :

$$\begin{aligned} \frac{\partial \Theta}{\partial \tau} + \hat{n}^i \frac{\partial \Theta}{\partial x^i} + \frac{1}{2} \hat{n}^i \hat{n}^j \frac{\partial h_{ij}}{\partial \tau} &= \dot{\Theta}_T , \\ \frac{\partial Q}{\partial \tau} + \hat{n}^i \frac{\partial Q}{\partial x^i} &= \dot{Q}_T , \\ \frac{\partial U}{\partial \tau} + \hat{n}^i \frac{\partial U}{\partial x^i} &= \dot{U}_T , \\ \frac{\partial V}{\partial \tau} + \hat{n}^i \frac{\partial V}{\partial x^i} &= \dot{V}_T , \end{aligned} \quad (3.47)$$

where Θ_T, Q_T, U_T and V_T denote the collision terms of Thomson scattering and $\dot{\cdot} \equiv \partial/\partial \tau$ is the derivative with respect to the conformal time. Next we consider the contribution of these terms.

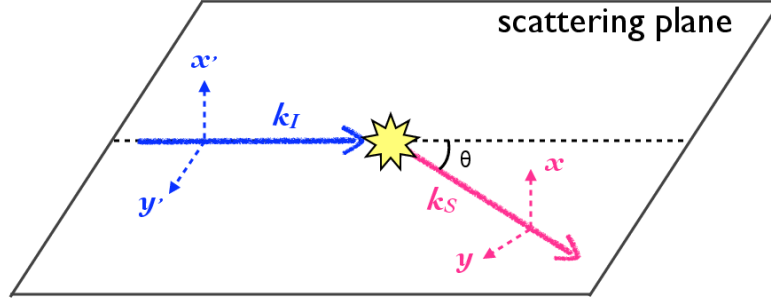


Figure 3.3: Geometry of Thomson scattering. Blue (Red) solid and two dashed arrows denote the incident (scattered) wave number vector and its orthogonal unit vectors, respectively. We set that $\hat{\mathbf{x}}' = \hat{\mathbf{x}}$

3.5 Thomson scattering

The process of scattering off a photon by a charged particle without the energy exchange of photons is called the Rayleigh scattering. In particular, when the charged particle is an electron, the process is known as Thomson scattering. During the epoch of recombination, electrons scattered off photons by Thomson scattering. Here, we consider an incoming plane wave of the radiation with a wave number vector \mathbf{k}_I parallel to the z axis and an outgoing radiation scattered off by an electron with a wave number vector \mathbf{k}_S . We take the plane spanned by \mathbf{k}_I and \mathbf{k}_S as the scattering plane as shown in Fig. 3.3.

The differential cross section of Thomson scattering is given by

$$\frac{d\sigma}{d\Omega} = \frac{3\sigma_T}{8\pi} |\hat{\mathbf{k}}_I \cdot \hat{\mathbf{k}}_S|^2, \quad (3.48)$$

where $d\Omega = d(\cos\theta)d\phi$ and σ_T is the cross section of Thomson scattering. This equation quantifies the change of the intensity by the scattering. For simplicity, we consider the case of the x' axis parallel to the x axis. Here, we suppose the incident radiation with the polarization states $I' = (I'_{y'}, I'_{x'}, U', V')$, where $I' = I'_{x'} + I'_{y'}$ and $Q' = I'_{y'} - I'_{x'}$. When there is no dependence on the azimuthal angle, namely $\phi' = 0$, from the notation of Stokes parameters (3.40) and (3.48), we obtain

$$I_y = \frac{3\sigma_T}{16\pi} \cos^2\theta I'_{y'}, \quad I_x = \frac{3\sigma_T}{16\pi} I'_{x'}, \quad U = \frac{3\sigma_T}{16\pi} \cos\theta U', \quad (3.49)$$

where we have normalized these equations so that the number of photons is conserved during a single scattering. For a general case with a non-vanishing azimuthal angle ϕ , Q' and U' are replaced

as

$$Q' \pm iU' \Rightarrow e^{\mp 2i\phi} (Q' \pm iU') . \quad (3.50)$$

Then, the changes of the Stokes parameters between the incident radiation from $\hat{\mathbf{n}}' = \hat{\mathbf{z}}$ ($\theta' = 0, \phi' = 0$), and the scattered radiation with $\hat{\mathbf{n}} = (\theta, \phi)$ are given by [17]

$$\begin{aligned} \Delta\Theta(\hat{\mathbf{n}}' = \hat{\mathbf{z}}, \hat{\mathbf{n}}) &= \frac{1}{4\pi} \left[\frac{3}{4}(1 + \cos^2 \theta)\Theta' - \sum_{s=\pm 2} \frac{3}{8} \sin^2 \theta e^{-si\phi} \left(Q' + \frac{s}{2}iU' \right) \right] , \\ \Delta(Q \pm iU)(\hat{\mathbf{n}}' = \hat{\mathbf{z}}, \hat{\mathbf{n}}) &= \frac{1}{4\pi} \left[-\frac{3}{4} \sin^2 \theta \Theta' + \sum_{s=\pm 2} \frac{3}{8} \left(1 \pm \frac{s}{2} \cos \theta \right)^2 e^{-si\phi} \left(Q' + \frac{s}{2}iU' \right) \right] , \end{aligned} \quad (3.51)$$

where we use $\Theta = \Delta I/I/4$. Using the explicit formulae of the spin-0 and spin-2 spherical harmonics described in Table A.2, we can extend this expression to the form corresponding to an arbitrary direction of $\hat{\mathbf{n}}'$:

$$\begin{aligned} \Delta\Theta(\hat{\mathbf{n}}', \hat{\mathbf{n}}) &= \sum_m \left[\left\{ \frac{1}{10} Y_{2m}(\hat{\mathbf{n}}) Y_{2m}^*(\hat{\mathbf{n}}') + Y_{0m}(\hat{\mathbf{n}}) Y_{0m}^*(\hat{\mathbf{n}}') \right\} \Theta' \right. \\ &\quad \left. - \sum_{s=\pm 2} \frac{3}{20} \sqrt{\frac{2}{3}} Y_{2m}(\hat{\mathbf{n}})_s Y_{2m}^*(\hat{\mathbf{n}}') \left(Q' + \frac{s}{2}iU' \right) \right] , \\ (\Delta Q \pm i\Delta U)(\hat{\mathbf{n}}', \hat{\mathbf{n}}) &= \sum_m \frac{3}{10} {}_{\pm 2} Y_{2m}(\hat{\mathbf{n}}) \left[-\sqrt{\frac{2}{3}} Y_{2m}^*(\hat{\mathbf{n}}') \Theta' + \sum_{s=\pm 2} {}_s Y_{2m}^*(\hat{\mathbf{n}}') \left(Q' + \frac{s}{2}iU' \right) \right] . \end{aligned} \quad (3.52)$$

We will use Eq. (3.52) in the frame satisfying $\mathbf{k} \parallel \hat{\mathbf{z}}$, where \mathbf{k} is the wave number vector. Integrating these equations over all directions $\hat{\mathbf{n}}'$, we express the scattered fields as ²

$$\begin{aligned} \dot{\Theta}_T(\hat{\mathbf{n}}) &= -\dot{\kappa} \left[\Theta(\hat{\mathbf{n}}) - \int d\Omega' \Delta\Theta(\hat{\mathbf{n}}', \hat{\mathbf{n}}) - \mathbf{v}_b \cdot \hat{\mathbf{n}} \right] , \\ \left(\dot{Q} \pm i\dot{U} \right)_T(\hat{\mathbf{n}}) &= -\dot{\kappa} \left[(Q \pm iU)(\hat{\mathbf{n}}) - \int d\Omega' (\Delta Q \pm i\Delta U)(\hat{\mathbf{n}}', \hat{\mathbf{n}}) \right] , \end{aligned} \quad (3.53)$$

where we define the differential optical depth as $\dot{\kappa} \equiv a\sigma_T n_e x_e$ with $n_e x_e$ being the density of ionized electrons, and its total value at time τ is given by

$$\kappa(\tau) \equiv \int_{\tau}^{\tau_0} \dot{\kappa}(\tau') d\tau' , \quad (3.54)$$

with τ_0 being the present conformal time.

From here, we discuss the polarization property in more detail. One of the key points in Eq. (3.52) is that the temperature anisotropy generates the polarization of the CMB photons. Then, what mode of the temperature anisotropy is related to the generation of the polarization? For simplicity, we suppose that the incident radiation field is unpolarized, $Q' = U' = V' = 0$ and consider the case for $\hat{\mathbf{n}} = \hat{\mathbf{z}}$. Integrating Eq. (3.52) over all incident radiation, we gain

$$Q \pm iU(\hat{\mathbf{z}}) = \frac{3\sigma_T}{4\pi} \sqrt{\frac{2\pi}{15}} \int d\Omega' Y_{22}(\theta', \phi') \Theta'(\theta', \phi') . \quad (3.55)$$

²The Stokes parameter, V , which means the circular polarization of photon, can be ignored because it cannot be generated through Thomson scattering if this is initially absent.

When the incident temperature (intensity) anisotropy is expanded with the spherical harmonics as $\Theta'(\theta', \phi') = \sum_{\ell m} a'_{\ell m} Y_{\ell m}(\theta', \phi')$, Eq. (3.55) is replaced with

$$Q \pm iU(\hat{\mathbf{z}}) = \frac{3\sigma_T}{4\pi} \sqrt{\frac{2\pi}{15}} a'_{22} . \quad (3.56)$$

Thus, if there exists no quadrupole moment ($\ell = 2$) in the unpolarized radiation field, the total scattered radiation along the z direction would be never polarized. Long before recombination, in the thermal equilibrium, the polarization states of photons are equally populated and the incident radiation should not have any polarization. Therefore, there are only the unpolarized radiations before recombination. Allowing the polarization at the last scatters just before the photons begin to stream freely, the polarized emission can lead to the multipole anisotropy and one has polarized quadrupole and octupole and so on. These effects are automatically involved in the Boltzmann equation.

3.6 Transfer functions

Here, we derive the CMB anisotropy sourced from scalar-, vector- and tensor-mode perturbations. We obey a Fourier transformation as

$$X(\hat{\mathbf{n}}, \tau) = \int \frac{d^3\mathbf{k}}{(2\pi)^3} \Delta_X(\tau, \mathbf{k}, \hat{\mathbf{n}}) , \quad (3.57)$$

where $X = \Theta, Q \pm iU$ and Δ_X is called the transfer function. Note that we include the factor $e^{i\mathbf{k} \cdot \hat{\mathbf{n}}}$ in Δ_X .

At first, for convenience, we derive the transfer functions of photons when $\mathbf{k} \parallel \hat{\mathbf{z}}$. For $\mathbf{k} \parallel \hat{\mathbf{z}}$, the scalar-vector-tensor decomposition of the gravitational redshift and Doppler term in the Boltzmann equation of photons (3.47) and (3.53) are given by

$$\begin{aligned} \frac{1}{2} \hat{n}^i \hat{n}^j \dot{h}_{ij}(\mathbf{k} \parallel \hat{\mathbf{z}}, \tau) &= \frac{1}{2} \left[-\frac{1}{3} \dot{h}_{\text{iso}}(\mathbf{k} \parallel \hat{\mathbf{z}}, \tau) + \dot{h}^{(0)}(\mathbf{k} \parallel \hat{\mathbf{z}}, \tau) \left(-\cos^2 \theta_{k,n} + \frac{1}{3} \right) \right] \\ &+ \sum_{\lambda=\pm 1} \frac{1}{\sqrt{2}} \sin \theta_{k,n} \cos \theta_{k,n} e^{\lambda i \phi_{k,n}} \dot{h}^{(\lambda)}(\mathbf{k} \parallel \hat{\mathbf{z}}, \tau) \\ &+ \sum_{\lambda=\pm 2} \frac{1}{2\sqrt{2}} \sin^2 \theta_{k,n} e^{\lambda i \phi_{k,n}} \dot{h}^{(\lambda)}(\mathbf{k} \parallel \hat{\mathbf{z}}, \tau) \\ &\equiv \xi^{(0)}(\mathbf{k} \parallel \hat{\mathbf{z}}) \left[\frac{1}{3} \dot{h}_{\text{iso}}^{(S)}(k, \tau) + \dot{h}^{(S)}(k, \tau) \left(\cos^2 \theta_{k,n} - \frac{1}{3} \right) \right] \\ &+ \sum_{\lambda=\pm 1} \sin \theta_{k,n} \cos \theta_{k,n} e^{\lambda i \phi_{k,n}} \xi^{(\lambda)}(\mathbf{k} \parallel \hat{\mathbf{z}}) \dot{h}^{(V)}(k, \tau) \\ &+ \sum_{\lambda=\pm 2} \sin^2 \theta_{k,n} e^{\lambda i \phi_{k,n}} \xi^{(\lambda)}(\mathbf{k} \parallel \hat{\mathbf{z}}) \dot{h}^{(T)}(k, \tau) , \\ \mathbf{v}_{\mathbf{b}}(\mathbf{k} \parallel \hat{\mathbf{z}}, \tau) \cdot \hat{\mathbf{n}} &= i \cos \theta_{k,n} v_b^{(0)}(\mathbf{k} \parallel \hat{\mathbf{z}}, \tau) + \sum_{\lambda=\pm 1} \frac{-i}{\sqrt{2}} \sin \theta_{k,n} e^{\lambda i \phi_{k,n}} v_b^{(\lambda)}(\mathbf{k} \parallel \hat{\mathbf{z}}, \tau) \\ &\equiv i \cos \theta_{k,n} \xi^{(0)}(\mathbf{k} \parallel \hat{\mathbf{z}}) v_b^{(S)}(k, \tau) \\ &+ \sum_{\lambda=\pm 1} -i \sin \theta_{k,n} e^{\lambda i \phi_{k,n}} \xi^{(\lambda)}(\mathbf{k} \parallel \hat{\mathbf{z}}) v_b^{(V)}(k, \tau) , \end{aligned} \quad (3.58)$$

where $\xi^{(0)}$, $\xi^{(\pm 1)}$ and $\xi^{(\pm 2)}$ are the initial stochastic variables of scalar, vector and tensor modes, and we use the calculation results from Appendix D as

$$\begin{aligned}\epsilon_j^{(\pm 1)}(\hat{\mathbf{z}}) &= \frac{1}{\sqrt{2}} \begin{pmatrix} 1 \\ \pm i \\ 0 \end{pmatrix}, \\ O_{ij}^{(\pm 1)}(\hat{\mathbf{z}}) &= \frac{1}{\sqrt{2}} \begin{pmatrix} 0 & 0 & 1 \\ 0 & 0 & \pm i \\ 1 & \pm i & 0 \end{pmatrix}, \\ O_{ij}^{(\pm 2)}(\hat{\mathbf{z}}) &= e_{ij}^{(\pm 2)}(\hat{\mathbf{z}}) = \frac{1}{\sqrt{2}} \begin{pmatrix} 1 & \pm i & 0 \\ \pm i & -1 & 0 \\ 0 & 0 & 0 \end{pmatrix}.\end{aligned}\tag{3.59}$$

According to Refs. [14, 18, 19], if we equate $\xi^{(0)}$ with the comoving curvature perturbation on superhorizon scales \mathcal{R} , the initial conditions of the metric perturbations and the baryon velocity are ³

$$\begin{aligned}h_{\text{iso}}^{(S)}(k, \tau_{\text{ini}}) &= -\frac{1}{4}(k\tau_{\text{ini}})^2, \\ h^{(S)}(k, \tau_{\text{ini}}) &= -3 - \frac{5}{2(15 + 4R_\nu)}(k\tau_{\text{ini}})^2, \\ v_b^{(S)}(k, \tau_{\text{ini}}) &= \frac{1}{36}(k\tau_{\text{ini}})^3.\end{aligned}\tag{3.61}$$

In the tensor mode, equating $\xi^{(\pm 2)}$ with the primordial gravitational wave on superhorizon scales $h^{(\pm 2)}$, it is satisfied that

$$h^{(T)}(k, \tau_{\text{ini}}) = \frac{1}{2\sqrt{2}} \left[1 - \frac{5}{2(15 + 4R_\nu)}(k\tau_{\text{ini}})^2 \right].\tag{3.62}$$

Note that the Doppler effect does not affect only the tensor-mode perturbation. We introduce the transfer function in the Fourier space as [4, 20]

$$\begin{aligned}\Delta_I^{(S)}(\tau, \mathbf{k} \parallel \hat{\mathbf{z}}, \hat{\mathbf{n}}) &= \xi^{(0)}(\mathbf{k} \parallel \hat{\mathbf{z}}) \tilde{\Delta}_I^{(S)}(\tau, k, \mu_{k,n}), \\ (\Delta_Q^{(S)} \pm i\Delta_U^{(S)})(\tau, \mathbf{k} \parallel \hat{\mathbf{z}}, \hat{\mathbf{n}}) &= \xi^{(0)}(\mathbf{k} \parallel \hat{\mathbf{z}}) \tilde{\Delta}_P^{(S)}(\tau, k, \mu_{k,n}), \\ \Delta_I^{(V)}(\tau, \mathbf{k} \parallel \hat{\mathbf{z}}, \hat{\mathbf{n}}) &= \sum_{\lambda=\pm 1} -i\sqrt{1 - \mu_{k,n}^2} e^{\lambda i\phi_{k,n}} \xi^{(\lambda)}(\mathbf{k} \parallel \hat{\mathbf{z}}) \tilde{\Delta}_I^{(V)}(\tau, k, \mu_{k,n}), \\ (\Delta_Q^{(V)} \pm i\Delta_U^{(V)})(\tau, \mathbf{k} \parallel \hat{\mathbf{z}}, \hat{\mathbf{n}}) &= \sum_{\lambda=\pm 1} \mp \lambda(1 \mp \lambda\mu_{k,n}) \sqrt{1 - \mu_{k,n}^2} e^{\lambda i\phi_{k,n}} \xi^{(\lambda)}(\mathbf{k} \parallel \hat{\mathbf{z}}) \tilde{\Delta}_P^{(V)}(\tau, k, \mu_{k,n}) \quad (3.63) \\ \Delta_I^{(T)}(\tau, \mathbf{k} \parallel \hat{\mathbf{z}}, \hat{\mathbf{n}}) &= (1 - \mu_{k,n}^2) \sum_{\lambda=\pm 2} e^{\lambda i\phi_{k,n}} \xi^{(\lambda)}(\mathbf{k} \parallel \hat{\mathbf{z}}) \tilde{\Delta}_I^{(T)}(\tau, k, \mu_{k,n}), \\ (\Delta_Q^{(T)} \pm i\Delta_U^{(T)})(\tau, \mathbf{k} \parallel \hat{\mathbf{z}}, \hat{\mathbf{n}}) &= \sum_{\lambda=\pm 2} \left(1 \mp \frac{\lambda}{2}\mu_{k,n} \right)^2 e^{\lambda i\phi_{k,n}} \xi^{(\lambda)}(\mathbf{k} \parallel \hat{\mathbf{z}}) \tilde{\Delta}_P^{(T)}(\tau, k, \mu_{k,n}),\end{aligned}$$

³Then, the parameters in Ref. [14] are given by

$$\begin{aligned}\eta(k, \tau_{\text{ini}}) &= -\mathcal{R} \left[1 - \frac{5 + 4R_\nu}{12(15 + 4R_\nu)}(k\tau_{\text{ini}})^2 \right], \\ h(k, \tau_{\text{ini}}) &= -\frac{1}{2}\mathcal{R}(k\tau_{\text{ini}})^2.\end{aligned}\tag{3.60}$$

where $\mu_{k,n} \equiv \hat{\mathbf{k}} \cdot \hat{\mathbf{n}}$. Then, from Eqs. (3.52) and (3.53), we can write the collision term of Thomson scattering for the scalar mode:

$$\begin{aligned}
\int d\Omega' \Delta\Theta^{(S)}(\hat{\mathbf{n}}', \hat{\mathbf{n}}) &= \int \frac{d^3\mathbf{k}}{(2\pi)^3} \int d\Omega' \sum_m \frac{1}{10} \xi^{(0)}(\mathbf{k} \parallel \hat{\mathbf{z}}) \\
&\times \left[\left\{ Y_{2m}(\hat{\mathbf{n}}) Y_{2m}^*(\hat{\mathbf{n}}') + 10 Y_{0m}(\hat{\mathbf{n}}) Y_{0m}^*(\hat{\mathbf{n}}') \right\} \tilde{\Delta}_I^{(S)}(\tau, k, \mu') \right. \\
&\quad \left. - \sqrt{\frac{3}{2}} Y_{2m}(\hat{\mathbf{n}}) \left\{ \sum_{s=\pm 2} {}_s Y_{2m}^*(\hat{\mathbf{n}}') \right\} \tilde{\Delta}_P^{(S)}(\tau, k, \mu') \right] , \\
\int d\Omega' (\Delta Q^{(S)} \pm i \Delta U^{(S)})(\hat{\mathbf{n}}', \hat{\mathbf{n}}) &= - \int \frac{d^3\mathbf{k}}{(2\pi)^3} \int d\Omega' \sum_m \frac{\sqrt{6}}{10} {}_{\pm 2} Y_{2m}(\hat{\mathbf{n}}) \xi^{(0)}(\mathbf{k} \parallel \hat{\mathbf{z}}) \\
&\times \left[Y_{2m}^*(\hat{\mathbf{n}}') \tilde{\Delta}_I^{(S)}(\tau, k, \mu') \right. \\
&\quad \left. - \sqrt{\frac{3}{2}} \left\{ \sum_{s=\pm 2} {}_s Y_{2m}^*(\hat{\mathbf{n}}') \right\} \tilde{\Delta}_P^{(S)}(\tau, k, \mu') \right] , \tag{3.64}
\end{aligned}$$

for the vector mode:

$$\begin{aligned}
\int d\Omega' \Delta\Theta^{(V)}(\hat{\mathbf{n}}', \hat{\mathbf{n}}) &= \int \frac{d^3\mathbf{k}}{(2\pi)^3} \int d\Omega' \sum_m \sum_{\lambda=\pm 1} \frac{1}{5} \sqrt{\frac{2\pi}{3}} \lambda \xi^{(\lambda)}(\mathbf{k} \parallel \hat{\mathbf{z}}) \\
&\times \left[i \left\{ Y_{2m}(\hat{\mathbf{n}}) Y_{2m}^*(\hat{\mathbf{n}}') + 10 Y_{0m}(\hat{\mathbf{n}}) Y_{0m}^*(\hat{\mathbf{n}}') \right\} \right. \\
&\quad \times Y_{1\lambda}(\hat{\mathbf{n}}') \tilde{\Delta}_I^{(V)}(\tau, k, \mu') \\
&\quad \left. - \frac{3}{\sqrt{5}} Y_{2m}(\hat{\mathbf{n}}) \left\{ \sum_{s=\pm 2} {}_s Y_{2m}^*(\hat{\mathbf{n}}') {}_s Y_{2\lambda}(\hat{\mathbf{n}}') \right\} \tilde{\Delta}_P^{(V)}(\tau, k, \mu') \right] , \tag{3.65} \\
\int d\Omega' (\Delta Q^{(V)} \pm i \Delta U^{(V)})(\hat{\mathbf{n}}', \hat{\mathbf{n}}) &= - \int \frac{d^3\mathbf{k}}{(2\pi)^3} \int d\Omega' \sum_m \frac{2\sqrt{\pi}}{5} {}_{\pm 2} Y_{2m}(\hat{\mathbf{n}}) \sum_{\lambda=\pm 1} \lambda \xi^{(\lambda)}(\mathbf{k} \parallel \hat{\mathbf{z}}) \\
&\times \left[i Y_{2m}^*(\hat{\mathbf{n}}') Y_{1\lambda}(\hat{\mathbf{n}}') \tilde{\Delta}_I^{(V)}(\tau, k, \mu') \right. \\
&\quad \left. - \frac{3}{\sqrt{5}} \left\{ \sum_{s=\pm 2} {}_s Y_{2m}^*(\hat{\mathbf{n}}') {}_s Y_{2\lambda}(\hat{\mathbf{n}}') \right\} \tilde{\Delta}_P^{(V)}(\tau, k, \mu') \right] ,
\end{aligned}$$

for the tensor mode:

$$\begin{aligned}
\int d\Omega' \Delta \Theta^{(T)}(\hat{\mathbf{n}}', \hat{\mathbf{n}}) &= \int \frac{d^3 \mathbf{k}}{(2\pi)^3} \int d\Omega' \sum_m \frac{2}{5} \sqrt{\frac{2\pi}{15}} \sum_{\lambda=\pm 2} \xi^{(\lambda)}(\mathbf{k} \parallel \hat{\mathbf{z}}) \\
&\quad \times \left[\left\{ Y_{2m}(\hat{\mathbf{n}}) Y_{2m}^*(\hat{\mathbf{n}}') + 10 Y_{0m}(\hat{\mathbf{n}}) Y_{0m}^*(\hat{\mathbf{n}}') \right\} \right. \\
&\quad \times Y_{2\lambda}(\hat{\mathbf{n}}') \tilde{\Delta}_I^{(T)}(\tau, k, \mu') \\
&\quad \left. - 3 Y_{2m}(\hat{\mathbf{n}}) \left\{ \sum_{s=\pm 2} {}_s Y_{2m}^*(\hat{\mathbf{n}}') {}_s Y_{2\lambda}(\hat{\mathbf{n}}') \right\} \tilde{\Delta}_P^{(T)}(\tau, k, \mu') \right] , \quad (3.66) \\
\int d\Omega' (\Delta Q^{(T)} \pm i \Delta U^{(T)}) (\hat{\mathbf{n}}', \hat{\mathbf{n}}) &= - \int \frac{d^3 \mathbf{k}}{(2\pi)^3} \int d\Omega' \sum_m \frac{4}{5} \sqrt{\frac{\pi}{5}} {}_{\pm 2} Y_{2m}(\hat{\mathbf{n}}) \sum_{\lambda=\pm 2} \xi^{(\lambda)}(\mathbf{k} \parallel \hat{\mathbf{z}}) \\
&\quad \times \left[Y_{2m}^*(\hat{\mathbf{n}}') Y_{2\lambda}(\hat{\mathbf{n}}') \tilde{\Delta}_I^{(T)}(\tau, k, \mu') \right. \\
&\quad \left. - 3 \left\{ \sum_{s=\pm 2} {}_s Y_{2m}^*(\hat{\mathbf{n}}') {}_s Y_{2\lambda}(\hat{\mathbf{n}}') \right\} \tilde{\Delta}_P^{(T)}(\tau, k, \mu') \right] .
\end{aligned}$$

Here, we use

$$\begin{aligned}
\sqrt{1-\mu^2} e^{\lambda i \phi} &= -\lambda \sqrt{\frac{8\pi}{3}} Y_{1\lambda} , \quad \sqrt{1-\mu^2} (1 \mp \lambda \mu) e^{\lambda i \phi} = \mp \sqrt{\frac{16\pi}{5}} {}_{\pm 2} Y_{2\lambda} \quad (\text{for } \lambda = \pm 1) , \\
(1-\mu^2) e^{\lambda i \phi} &= 4 \sqrt{\frac{2\pi}{15}} Y_{2\lambda} , \quad \left(1 \mp \frac{\lambda}{2} \mu \right)^2 e^{\lambda i \phi} = 8 \sqrt{\frac{\pi}{5}} {}_{\pm 2} Y_{2\lambda} \quad (\text{for } \lambda = \pm 2) .
\end{aligned} \quad (3.67)$$

Using the multipole expansion as

$$\tilde{\Delta}_{I/P}^{(S/V/T)}(\tau, k, \mu') = \sum_l (-i)^l \sqrt{4\pi(2l+1)} Y_{l0}(\hat{\mathbf{n}}') \tilde{\Delta}_{I/P,l}^{(S/V/T)}(\tau, k) \quad (3.68)$$

and the Ω' -integrals for $\lambda = 0$:

$$\begin{aligned}
\int d\Omega' Y_{2m}^* Y_{l0} &= \delta_{l,2} \delta_{m,0} , \\
\int d\Omega' Y_{0m}^* Y_{l0} &= \delta_{l,0} \delta_{m,0} , \\
\int d\Omega' {}_{\pm 2} Y_{2m}^* Y_{l0} &= \sqrt{\frac{5}{6}} \delta_{m,0} \left(\delta_{l,0} - \frac{1}{\sqrt{5}} \delta_{l,2} \right) ,
\end{aligned} \quad (3.69)$$

for $\lambda = \pm 1$:

$$\begin{aligned}
\int d\Omega' Y_{2m}^* Y_{1\lambda} Y_{l0} &= \sqrt{\frac{3}{20\pi}} \delta_{m,\lambda} \left(\delta_{l,1} - \sqrt{\frac{3}{7}} \delta_{l,3} \right) , \\
\int d\Omega' Y_{0m}^* Y_{2\lambda} Y_{l0} &= 0 , \\
\int d\Omega' {}_{\pm 2} Y_{2m}^* {}_{\pm 2} Y_{2\lambda} Y_{l0} &= \frac{1}{\sqrt{4\pi}} \delta_{m,\lambda} \left(\delta_{l,0} \mp \frac{\sqrt{3}}{3} \lambda \delta_{l,1} - \frac{\sqrt{5}}{7} \delta_{l,2} \pm \frac{\sqrt{7}}{7} \lambda \delta_{l,3} - \frac{2}{21} \delta_{l,4} \right) ,
\end{aligned} \quad (3.70)$$

and for $\lambda = \pm 2$:

$$\begin{aligned} \int d\Omega' Y_{2m}^* Y_{2\lambda} Y_{l0} &= \frac{1}{\sqrt{4\pi}} \delta_{m,\lambda} \left(\delta_{l,0} - \frac{2\sqrt{5}}{7} \delta_{l,2} + \frac{1}{7} \delta_{l,4} \right) , \\ \int d\Omega' Y_{0m}^* Y_{2\lambda} Y_{l0} &= 0 , \\ \int d\Omega' Y_{2m\pm 2}^* Y_{2\lambda} Y_{l0} &= \frac{1}{\sqrt{4\pi}} \delta_{m,\lambda} \left(\delta_{l,0} \mp \frac{\sqrt{3}}{3} \lambda \delta_{l,1} + \frac{2\sqrt{5}}{7} \delta_{l,2} \mp \frac{\sqrt{7}}{28} \lambda \delta_{l,3} + \frac{1}{42} \delta_{l,4} \right) , \end{aligned} \quad (3.71)$$

we can obtain the anisotropies generated via Thomson scattering for the scalar mode:

$$\begin{aligned} \int d\Omega' \Delta \Theta^{(S)}(\hat{\mathbf{n}}', \hat{\mathbf{n}}) &= \int \frac{d^3 \mathbf{k}}{(2\pi)^3} \xi^{(0)}(\mathbf{k} \parallel \hat{\mathbf{z}}) \left[\tilde{\Delta}_{I,0}^{(S)} - \sqrt{\frac{\pi}{5}} Y_{20}(\hat{\mathbf{n}}) \psi^{(S)}(k, \tau) \right] , \\ \int d\Omega' (\Delta Q^{(S)} \pm i \Delta U^{(S)})(\hat{\mathbf{n}}', \hat{\mathbf{n}}) &= \int \frac{d^3 \mathbf{k}}{(2\pi)^3} \xi^{(0)}(\mathbf{k} \parallel \hat{\mathbf{z}}) \left[\sqrt{\frac{6\pi}{5}} Y_{20}(\hat{\mathbf{n}}) \psi^{(S)}(k, \tau) \right] , \\ \psi^{(S)}(k, \tau) &\equiv \tilde{\Delta}_{I,2}^{(S)} + \tilde{\Delta}_{P,0}^{(S)} + \tilde{\Delta}_{P,2}^{(S)} , \end{aligned} \quad (3.72)$$

for the vector mode:

$$\begin{aligned} \int d\Omega' \Delta \Theta^{(V)}(\hat{\mathbf{n}}', \hat{\mathbf{n}}) &= \int \frac{d^3 \mathbf{k}}{(2\pi)^3} \left[\sum_{\lambda=\pm 1} \lambda \sqrt{\frac{8\pi}{15}} Y_{2\lambda}(\hat{\mathbf{n}}) \xi^{(\lambda)}(\mathbf{k} \parallel \hat{\mathbf{z}}) \right] \psi^{(V)}(k, \tau) , \\ \int d\Omega' (\Delta Q^{(V)} \pm i \Delta U^{(V)})(\hat{\mathbf{n}}', \hat{\mathbf{n}}) &= - \int \frac{d^3 \mathbf{k}}{(2\pi)^3} \left[\sum_{\lambda=\pm 1} \lambda \sqrt{\frac{16\pi}{5}} Y_{2\lambda}(\hat{\mathbf{n}}) \xi^{(\lambda)}(\mathbf{k} \parallel \hat{\mathbf{z}}) \right] \psi^{(V)}(k, \tau) , \\ \psi^{(V)}(k, \tau) &\equiv \frac{3}{10} \tilde{\Delta}_{I,1}^{(V)} + \frac{3}{10} \tilde{\Delta}_{I,3}^{(V)} - \frac{3}{5} \tilde{\Delta}_{P,0}^{(V)} - \frac{3}{7} \tilde{\Delta}_{P,2}^{(V)} + \frac{6}{35} \tilde{\Delta}_{P,4}^{(V)} , \end{aligned} \quad (3.73)$$

and for the tensor mode:

$$\begin{aligned} \int d\Omega' \Delta \Theta^{(T)}(\hat{\mathbf{n}}', \hat{\mathbf{n}}) &= \int \frac{d^3 \mathbf{k}}{(2\pi)^3} \left[\sum_{\lambda=\pm 2} \sqrt{\frac{32\pi}{15}} Y_{2\lambda}(\hat{\mathbf{n}}) \xi^{(\lambda)}(\mathbf{k} \parallel \hat{\mathbf{z}}) \right] \psi^{(T)}(k, \tau) , \\ \int d\Omega' (\Delta Q^{(T)} \pm i \Delta U^{(T)})(\hat{\mathbf{n}}', \hat{\mathbf{n}}) &= - \int \frac{d^3 \mathbf{k}}{(2\pi)^3} \left[\sum_{\lambda=\pm 2} \sqrt{\frac{64\pi}{5}} Y_{2\lambda}(\hat{\mathbf{n}}) \xi^{(\lambda)}(\mathbf{k} \parallel \hat{\mathbf{z}}) \right] \psi^{(T)}(k, \tau) , \\ \psi^{(T)}(k, \tau) &\equiv \frac{1}{10} \tilde{\Delta}_{I,0}^{(T)} + \frac{1}{7} \tilde{\Delta}_{I,2}^{(T)} + \frac{3}{70} \tilde{\Delta}_{I,4}^{(T)} - \frac{3}{5} \tilde{\Delta}_{P,0}^{(T)} + \frac{6}{7} \tilde{\Delta}_{P,2}^{(T)} - \frac{3}{70} \tilde{\Delta}_{P,4}^{(T)} . \end{aligned} \quad (3.74)$$

Thus, from the Boltzmann equation (3.47), the gravitational redshift and the Doppler terms (3.58), and the collision term of Thomson scattering (3.53) and (3.72) - (3.74), we derive the Boltzmann equation for the scalar mode:

$$\begin{aligned} \dot{\tilde{\Delta}}_I^{(S)} + ik \mu_{k,n} \tilde{\Delta}_I^{(S)} &= - \left[\frac{1}{3} \dot{h}_{\text{iso}}^{(S)} + \left(\mu_{k,n}^2 - \frac{1}{3} \right) \dot{h}^{(S)} \right] \\ &\quad - \dot{\kappa} \left[\tilde{\Delta}_I^{(S)} - \tilde{\Delta}_{I,0}^{(S)} + \frac{3}{4} \left(\mu_{k,n}^2 - \frac{1}{3} \right) \psi^{(S)} - i \mu_{k,n} v_b^{(S)} \right] , \\ \dot{\tilde{\Delta}}_P^{(S)} + ik \mu_{k,n} \tilde{\Delta}_P^{(S)} &= - \dot{\kappa} \left[\tilde{\Delta}_P^{(S)} - \frac{3}{4} (1 - \mu_{k,n}^2) \psi^{(S)} \right] , \end{aligned} \quad (3.75)$$

for the vector mode:

$$\begin{aligned}\dot{\tilde{\Delta}}_I^{(V)} + ik\mu_{k,n}\tilde{\Delta}_I^{(V)} &= -i\mu_{k,n}\dot{h}^{(V)} - \dot{\kappa} \left[\tilde{\Delta}_I^{(V)} + i\mu_{k,n}\psi^{(V)} - v_b^{(V)} \right] , \\ \dot{\tilde{\Delta}}_P^{(V)} + ik\mu_{k,n}\tilde{\Delta}_P^{(V)} &= -\dot{\kappa} \left[\tilde{\Delta}_P^{(V)} + \psi^{(V)} \right] ,\end{aligned}\tag{3.76}$$

and for the tensor mode:

$$\begin{aligned}\dot{\tilde{\Delta}}_I^{(T)} + ik\mu_{k,n}\tilde{\Delta}_I^{(T)} &= -\dot{h}^{(T)} - \dot{\kappa} \left[\tilde{\Delta}_I^{(T)} - \psi^{(T)} \right] , \\ \dot{\tilde{\Delta}}_P^{(T)} + ik\mu_{k,n}\tilde{\Delta}_P^{(T)} &= -\dot{\kappa} \left[\tilde{\Delta}_P^{(T)} + \psi^{(T)} \right] .\end{aligned}\tag{3.77}$$

The multipole expansion of these equations gives

$$\dot{\tilde{\Delta}}_{I/P,l}^{(S/V/T)} + \frac{k}{2l+1} \left[(l+1)\tilde{\Delta}_{I/P,l}^{(S/V/T)} - l\tilde{\Delta}_{I/P,l-1}^{(S/V/T)} \right] = V_{I/P,l}^{(S/V/T)} ,\tag{3.78}$$

where

$$\begin{aligned}V_{I,l}^{(S)} &= - \left[\frac{1}{3}\dot{h}_{\text{iso}}^{(S)}\delta_{l,0} - \frac{2}{15}\dot{h}^{(S)}\delta_{l,2} \right] - \dot{\kappa} \left[\tilde{\Delta}_{I,l}^{(S)}(1 - \delta_{l,0}) - \frac{1}{10}\psi^{(S)}\delta_{l,2} + \frac{1}{3}v_b^{(S)}\delta_{l,1} \right] , \\ V_{P,l}^{(S)} &= -\dot{\kappa} \left[\tilde{\Delta}_{P,l}^{(S)} - \frac{1}{10}\psi^{(S)}(\delta_{l,2} + 5\delta_{l,0}) \right] , \\ V_{I,l}^{(V)} &= \frac{1}{3}\dot{h}^{(V)}\delta_{l,1} - \dot{\kappa} \left[\tilde{\Delta}_{I,l}^{(V)} - \frac{1}{3}\psi^{(V)}\delta_{l,1} - v_b^{(V)}\delta_{l,0} \right] , \\ V_{P,l}^{(V)} &= -\dot{\kappa} \left[\tilde{\Delta}_{P,l}^{(V)} + \psi^{(V)}\delta_{l,0} \right] , \\ V_{I,l}^{(T)} &= -\dot{h}^{(T)}\delta_{l,0} - \dot{\kappa} \left[\tilde{\Delta}_{I,l}^{(T)} - \psi^{(T)}\delta_{l,0} \right] , \\ V_{P,l}^{(T)} &= -\dot{\kappa} \left[\tilde{\Delta}_{P,l}^{(T)} + \psi^{(T)}\delta_{l,0} \right] .\end{aligned}\tag{3.79}$$

Following the line of sight integration [21], we can give the explicit solution of this Boltzmann equation as follows. At first, let us present the derivation for tensor mode. Using $de^{-\kappa}/d\tau = \dot{\kappa}e^{-\kappa}$ and multiplying $e^{ik\mu_{k,n}\tau-\kappa}$ in both sides of Eq. (3.77), we have

$$\begin{aligned}\frac{d}{d\tau} \left(\tilde{\Delta}_I^{(T)} e^{ik\mu_{k,n}\tau-\kappa} \right) &= e^{ik\mu_{k,n}\tau-\kappa} \left[-\dot{h}^{(T)} e^{-\kappa} + g\psi^{(T)} \right] , \\ \frac{d}{d\tau} \left(\tilde{\Delta}_P^{(T)} e^{ik\mu_{k,n}\tau-\kappa} \right) &= -e^{ik\mu_{k,n}\tau-\kappa} g\psi^{(T)} .\end{aligned}\tag{3.80}$$

where $g(\tau) \equiv \dot{\kappa}e^{-\kappa}$ is the visibility function which describes the probability that a given CMB photon last scattered at a given time. Through the integral over conformal time and some treatments, we obtain each from of the transfer function at $\tau = \tau_0$ as

$$\begin{aligned}\tilde{\Delta}_I^{(T)} &= \int_0^{\tau_0} d\tau e^{-i\mu_{k,n}x} \left[-\dot{h}^{(T)} e^{-\kappa} + g\psi^{(T)} \right] , \\ \tilde{\Delta}_P^{(T)} &= - \int_0^{\tau_0} d\tau e^{-i\mu_{k,n}x} g\psi^{(T)} ,\end{aligned}\tag{3.81}$$

Here we use $\kappa(\tau_0) = 0, \kappa(\tau = 0) \rightarrow \infty$ and $x \equiv k(\tau_0 - \tau)$. In the same manner, we also obtain the scalar-mode function:

$$\begin{aligned}
\tilde{\Delta}_I^{(S)} &= \int_0^{\tau_0} d\tau e^{-i\mu_{k,n}x} \left[-\left\{ \frac{1}{3}\dot{h}_{\text{iso}}^{(S)} + \left(\mu_{k,n}^2 - \frac{1}{3} \right) \dot{h}^{(S)} \right\} e^{-\kappa} \right. \\
&\quad \left. + g \left\{ \tilde{\Delta}_{I,0}^{(S)} - \frac{3}{4} \left(\mu_{k,n}^2 - \frac{1}{3} \right) \psi^{(S)} + i\mu_{k,n} v_b^{(S)} \right\} \right] , \\
&= \int_0^{\tau_0} d\tau e^{-i\mu_{k,n}x} \left[\left(-\frac{1}{3}\dot{h}_{\text{iso}}^{(S)} + \frac{\ddot{h}^{(S)}}{k^2} + \frac{1}{3}\dot{h}^{(S)} \right) e^{-\kappa} \right. \\
&\quad + g \left(\frac{2\ddot{h}^{(S)}}{k^2} + \tilde{\Delta}_{I,0}^{(S)} + \frac{3}{4} \frac{\ddot{\psi}^{(S)}}{k^2} + \frac{1}{4} \psi^{(S)} - \frac{\dot{v}_b^{(S)}}{k} \right) \\
&\quad \left. + \dot{g} \left(\frac{\dot{h}^{(S)}}{k^2} + \frac{3}{2} \frac{\dot{\psi}^{(S)}}{k^2} - \frac{v_b^{(S)}}{k} \right) + \frac{3}{4} \frac{\ddot{g}\psi^{(S)}}{k^2} \right] , \\
\tilde{\Delta}_P^{(S)} &= \int_0^{\tau_0} d\tau e^{-i\mu_{k,n}x} (1 - \mu_{k,n}^2) \frac{3}{4} g\psi^{(S)} ,
\end{aligned} \tag{3.82}$$

and the vector-mode one:

$$\begin{aligned}
\tilde{\Delta}_I^{(V)} &= \int_0^{\tau_0} d\tau e^{-i\mu_{k,n}x} \left[-i\mu_{k,n} \left(\dot{h}^{(V)} e^{-\kappa} + g\psi^{(V)} \right) + g v_b^{(V)} \right] \\
&= \int_0^{\tau_0} d\tau e^{-i\mu_{k,n}x} \left[\frac{\ddot{h}^{(V)}}{k} e^{-\kappa} + g \left(\frac{\dot{h} + \dot{\psi}^{(V)}}{k} + v_b^{(V)} \right) + \dot{g} \frac{\psi^{(V)}}{k} \right] , \\
\tilde{\Delta}_P^{(V)} &= - \int_0^{\tau_0} d\tau e^{-i\mu_{k,n}x} g\psi^{(V)} .
\end{aligned} \tag{3.83}$$

where in the second equality of each equation, we neglect the topological terms.

Consequently, we can summarize the transfer functions when $\mathbf{k} \parallel \hat{\mathbf{z}}$ for the scalar mode:

$$\begin{aligned}
\Delta_I^{(S)}(\tau_0, \mathbf{k} \parallel \hat{\mathbf{z}}, \hat{\mathbf{n}}) &= \xi^{(0)}(\mathbf{k} \parallel \hat{\mathbf{z}}) \int_0^{\tau_0} d\tau e^{-i\mu_{k,n}x} S_I^{(S)}(k, \tau) , \\
(\Delta_Q^{(S)} \pm i\Delta_U^{(S)})(\tau_0, \mathbf{k} \parallel \hat{\mathbf{z}}, \hat{\mathbf{n}}) &= \frac{4}{3} \sqrt{\frac{6\pi}{5}} {}_{\pm 2}Y_{20}(\hat{\mathbf{n}}) \xi^{(0)}(\mathbf{k} \parallel \hat{\mathbf{z}}) \int_0^{\tau_0} d\tau e^{-i\mu_{k,n}x} S_P^{(S)}(k, \tau) , \\
S_I^{(S)}(k, \tau) &\equiv \left(-\frac{1}{3}\dot{h}_{\text{iso}}^{(S)} + \frac{\ddot{h}^{(S)}}{k^2} + \frac{1}{3}\dot{h}^{(S)} \right) e^{-\kappa} \\
&\quad + g \left(\frac{2\ddot{h}^{(S)}}{k^2} + \tilde{\Delta}_{I,0}^{(S)} + \frac{3}{4} \frac{\ddot{\psi}^{(S)}}{k^2} + \frac{1}{4} \psi^{(S)} - \frac{\dot{v}_b^{(S)}}{k} \right) \\
&\quad + \dot{g} \left(\frac{\dot{h}^{(S)}}{k^2} + \frac{3}{2} \frac{\dot{\psi}^{(S)}}{k^2} - \frac{v_b^{(S)}}{k} \right) + \frac{3}{4} \frac{\ddot{g}\psi^{(S)}}{k^2} , \\
S_P^{(S)}(k, \tau) &\equiv \frac{3}{4} g\psi^{(S)}(k, \tau) ,
\end{aligned} \tag{3.84}$$

for the vector mode:

$$\begin{aligned}
\Delta_I^{(V)}(\tau_0, \mathbf{k} \parallel \hat{\mathbf{z}}, \hat{\mathbf{n}}) &= \left[\sum_{\lambda=\pm 1} i\lambda \sqrt{\frac{8\pi}{3}} Y_{1\lambda}(\hat{\mathbf{n}}) \xi^{(\lambda)}(\mathbf{k} \parallel \hat{\mathbf{z}}) \right] \int_0^{\tau_0} d\tau e^{-i\mu_{k,n}x} S_I^{(V)}(k, \tau) , \\
(\Delta_Q^{(V)} \pm i\Delta_U^{(V)})(\tau_0, \mathbf{k} \parallel \hat{\mathbf{z}}, \hat{\mathbf{n}}) &= \left[\sum_{\lambda=\pm 1} \lambda \sqrt{\frac{16\pi}{5}} {}_{\pm 2}Y_{2\lambda}(\hat{\mathbf{n}}) \xi^{(\lambda)}(\mathbf{k} \parallel \hat{\mathbf{z}}) \right] \int_0^{\tau_0} d\tau e^{-i\mu_{k,n}x} S_P^{(V)}(k, \tau) , \quad (3.85) \\
S_I^{(V)}(k, \tau) &\equiv \frac{\ddot{h}^{(V)}}{k} e^{-\kappa} + g \left(\frac{\dot{h} + \dot{\psi}^{(V)}}{k} + v_b^{(V)} \right) + \dot{g} \frac{\psi^{(V)}}{k} , \\
S_P^{(V)}(k, \tau) &\equiv -g\psi^{(V)} ,
\end{aligned}$$

and for the tensor mode:

$$\begin{aligned}
\Delta_I^{(T)}(\tau_0, \mathbf{k} \parallel \hat{\mathbf{z}}, \hat{\mathbf{n}}) &= \left[\sum_{\lambda=\pm 2} \sqrt{\frac{32\pi}{15}} Y_{2\lambda}(\hat{\mathbf{n}}) \xi^{(\lambda)}(\mathbf{k} \parallel \hat{\mathbf{z}}) \right] \int_0^{\tau_0} d\tau e^{-i\mu_{k,n}x} S_I^{(T)}(k, \tau) , \\
(\Delta_Q^{(T)} \pm i\Delta_U^{(T)})(\tau_0, \mathbf{k} \parallel \hat{\mathbf{z}}, \hat{\mathbf{n}}) &= \left[\sum_{\lambda=\pm 2} \sqrt{\frac{64\pi}{5}} {}_{\pm 2}Y_{2\lambda}(\hat{\mathbf{n}}) \xi^{(\lambda)}(\mathbf{k} \parallel \hat{\mathbf{z}}) \right] \int_0^{\tau_0} d\tau e^{-i\mu_{k,n}x} S_P^{(T)}(k, \tau) , \quad (3.86) \\
S_I^{(T)}(k, \tau) &\equiv -\dot{h}^{(T)} e^{-\kappa} + g\psi^{(T)} , \\
S_P^{(T)}(k, \tau) &\equiv -g\psi^{(T)} .
\end{aligned}$$

Here, we have introduced the source function, $S_{I/P}^{(S/V/T)}(k, \tau)$.

3.7 All-sky formulae for the CMB scalar-, vector- and tensor-mode anisotropies

In this subsection, let us formulate the all-mode CMB coefficients $a_{\ell m}$ in the all-sky analysis on the basis of the derivation in Refs. [3, 7].

Since the CMB anisotropy is described in the spherical coordinate system, its intensity (I) and two polarization (Q and U) fields should be expanded by the spin-0 and spin-2 spherical harmonics, respectively, as

$$\begin{aligned}
\Theta^{(Z)}(\hat{\mathbf{n}}) &= \sum_{\ell, m} a_{I, \ell m}^{(Z)} Y_{\ell m}(\hat{\mathbf{n}}) , \\
(Q^{(Z)} \pm iU^{(Z)})(\hat{\mathbf{n}}) &= \sum_{\ell, m} a_{\pm 2, \ell m}^{(Z)} {}_{\pm 2}Y_{\ell m}(\hat{\mathbf{n}}) . \quad (3.87)
\end{aligned}$$

Here, the index Z denotes the mode of perturbations: $Z = S$ (scalar), $= V$ (vector) or $= T$ (tensor). The main difficulty when computing the spectrum of polarization arises from the variance under rotations in the plane perpendicular to $\hat{\mathbf{n}}$. While Q and U are easily calculated in a coordinate system where $\mathbf{k} \parallel \hat{\mathbf{z}}$, the superposition of the different modes is complicated by the behavior of Q and U under rotations. However, using the spin raising and lowering operators $\hat{\mathcal{D}}$, $\hat{\bar{\mathcal{D}}}$ defined in Appendix A, we can obtain spin-0 quantities. This leads to the rotational invariant fields like the intensity one and there are no ambiguities connected with the rotation of coordinate system arise.

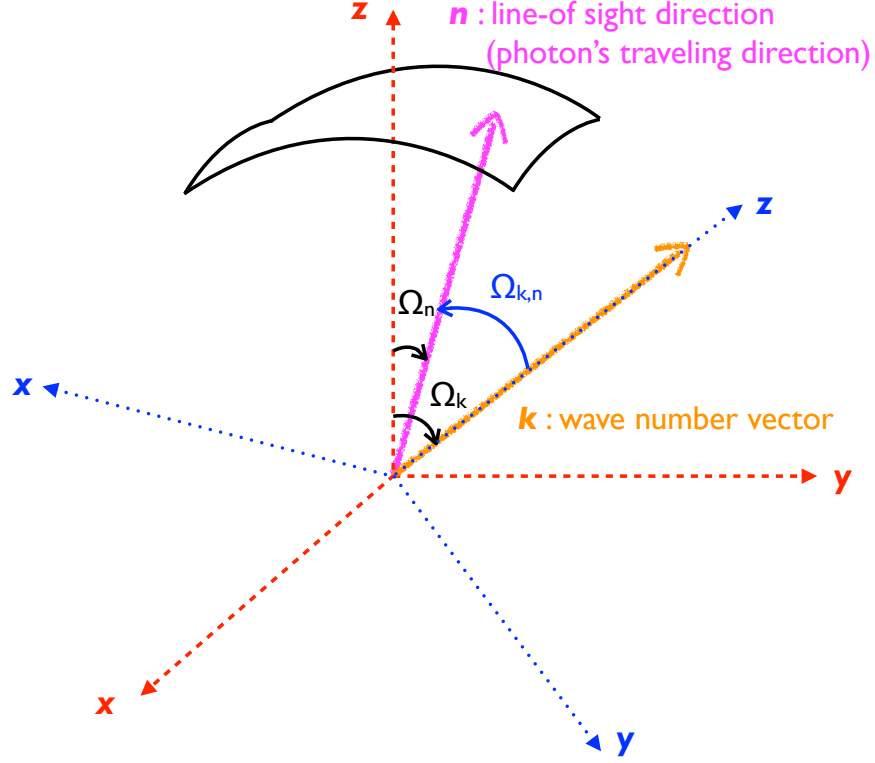


Figure 3.4: Geometry for the line-of-sight direction.

Acting these operators on $Q \pm iU$ in Eq. (3.87), we have

$$\begin{aligned} \bar{\partial}^2 (Q^{(Z)} + iU^{(Z)}) (\hat{\mathbf{n}}) &= \sum_{\ell m} \left[\frac{(\ell+2)!}{(\ell-2)!} \right]^{1/2} a_{2,\ell m}^{(Z)} Y_{\ell m}(\hat{\mathbf{n}}) , \\ \partial^2 (Q^{(Z)} - iU^{(Z)}) (\hat{\mathbf{n}}) &= \sum_{\ell m} \left[\frac{(\ell+2)!}{(\ell-2)!} \right]^{1/2} a_{-2,\ell m}^{(Z)} Y_{\ell m}(\hat{\mathbf{n}}) , \end{aligned} \quad (3.88)$$

Instead of $a_{\pm 2, \ell m}^{(Z)}$, it is convenient to introduce their linear combinations as [22]

$$\begin{aligned} a_{E, \ell m}^{(Z)} &\equiv -\frac{1}{2} \left(a_{2, \ell m}^{(Z)} + a_{-2, \ell m}^{(Z)} \right) , \\ a_{B, \ell m}^{(Z)} &\equiv \frac{i}{2} \left(a_{2, \ell m}^{(Z)} - a_{-2, \ell m}^{(Z)} \right) . \end{aligned} \quad (3.89)$$

These fields E and B have parity-even and odd properties, respectively, in analogy with the electric

and magnetic fields. Then, from Eqs. (3.88) and (3.89), we can express

$$\begin{aligned}
a_{X,\ell m}^{(Z)} &= \int d\Omega_n Y_{\ell m}^*(\Omega_n) \int \frac{d^3\mathbf{k}}{(2\pi)^3} \Delta_X^{(Z)}(\tau_0, \mathbf{k}, \hat{\mathbf{n}}) , \\
\Delta_E^{(Z)}(\tau_0, \mathbf{k}, \hat{\mathbf{n}}) &\equiv -\frac{1}{2} \left[\frac{(\ell-2)!}{(\ell+2)!} \right]^{1/2} \left[\bar{\partial}^2 (\Delta_Q^{(Z)} + i\Delta_U^{(Z)}) + \partial^2 (\Delta_Q^{(Z)} - i\Delta_U^{(Z)}) \right] (\tau_0, \mathbf{k}, \hat{\mathbf{n}}) , \\
\Delta_B^{(Z)}(\tau_0, \mathbf{k}, \hat{\mathbf{n}}) &\equiv \frac{i}{2} \left[\frac{(\ell-2)!}{(\ell+2)!} \right]^{1/2} \left[\bar{\partial}^2 (\Delta_Q^{(Z)} + i\Delta_U^{(Z)}) - \partial^2 (\Delta_Q^{(Z)} - i\Delta_U^{(Z)}) \right] (\tau_0, \mathbf{k}, \hat{\mathbf{n}}) .
\end{aligned} \tag{3.90}$$

Here, X discriminates between intensity and two polarization (electric and magnetic) modes, respectively, as $X = I, E, B$. When $\mathbf{k} \parallel \hat{\mathbf{z}}$, using Eqs. (3.84) - (3.86) and the operations derived from Eq. (A.3) as

$$\begin{aligned}
\bar{\partial}^2 [{}_2Y_{2\lambda}(\hat{\mathbf{n}})e^{-i\mu_{k,n}x}] &= \left(-\partial_{\mu_{k,n}} + \frac{\lambda}{1-\mu_{k,n}^2} \right)^2 [(1-\mu_{k,n}^2){}_2Y_{2\lambda}(\Omega_{k,n})e^{-i\mu_{k,n}x}] , \\
\partial^2 [{}_{-2}Y_{2\lambda}(\hat{\mathbf{n}})e^{-i\mu_{k,n}x}] &= \left(-\partial_{\mu_{k,n}} - \frac{\lambda}{1-\mu_{k,n}^2} \right)^2 [(1-\mu_{k,n}^2){}_{-2}Y_{2\lambda}(\Omega_{k,n})e^{-i\mu_{k,n}x}] ,
\end{aligned} \tag{3.91}$$

we obtain more explicit expressions as

$$\begin{aligned}
\Delta_E^{(S)}(\tau_0, \mathbf{k} \parallel \hat{\mathbf{z}}, \hat{\mathbf{n}}) &= \left[\frac{(\ell-2)!}{(\ell+2)!} \right]^{1/2} \xi^{(0)}(\mathbf{k} \parallel \hat{\mathbf{z}}) \int_0^{\tau_0} d\tau S_P^{(S)}(k, \tau) \hat{\mathcal{E}}^{(S)}(x) e^{-i\mu_{k,n}x} , \\
\Delta_E^{(V)}(\tau_0, \mathbf{k} \parallel \hat{\mathbf{z}}, \hat{\mathbf{n}}) &= \left[\frac{(\ell-2)!}{(\ell+2)!} \right]^{1/2} \left[\sum_{\lambda=\pm 1} -\lambda i \sqrt{\frac{8\pi}{3}} Y_{1\lambda}(\hat{\mathbf{n}}) \xi^{(\lambda)}(\mathbf{k} \parallel \hat{\mathbf{z}}) \right] \\
&\quad \times \int_0^{\tau_0} d\tau S_P^{(V)}(k, \tau) \hat{\mathcal{E}}^{(V)}(x) e^{-i\mu_{k,n}x} , \\
\Delta_B^{(V)}(\tau_0, \mathbf{k} \parallel \hat{\mathbf{z}}, \hat{\mathbf{n}}) &= \left[\frac{(\ell-2)!}{(\ell+2)!} \right]^{1/2} \left[\sum_{\lambda=\pm 1} -i \sqrt{\frac{8\pi}{3}} Y_{1\lambda}(\hat{\mathbf{n}}) \xi^{(\lambda)}(\mathbf{k} \parallel \hat{\mathbf{z}}) \right] \\
&\quad \times \int_0^{\tau_0} d\tau S_P^{(V)}(k, \tau) \hat{\mathcal{B}}^{(V)}(x) e^{-i\mu_{k,n}x} , \\
\Delta_E^{(T)}(\tau_0, \mathbf{k} \parallel \hat{\mathbf{z}}, \hat{\mathbf{n}}) &= \left[\frac{(\ell-2)!}{(\ell+2)!} \right]^{1/2} \left[\sum_{\lambda=\pm 2} \sqrt{\frac{32\pi}{15}} Y_{2\lambda}(\hat{\mathbf{n}}) \xi^{(\lambda)}(\mathbf{k} \parallel \hat{\mathbf{z}}) \right] \\
&\quad \times \int_0^{\tau_0} d\tau S_P^{(T)}(k, \tau) \hat{\mathcal{E}}^{(T)}(x) e^{-i\mu_{k,n}x} , \\
\Delta_B^{(T)}(\tau_0, \mathbf{k} \parallel \hat{\mathbf{z}}, \hat{\mathbf{n}}) &= \left[\frac{(\ell-2)!}{(\ell+2)!} \right]^{1/2} \left[\sum_{\lambda=\pm 2} -\frac{\lambda}{2} \sqrt{\frac{32\pi}{15}} Y_{2\lambda}(\hat{\mathbf{n}}) \xi^{(\lambda)}(\mathbf{k} \parallel \hat{\mathbf{z}}) \right] \\
&\quad \times \int_0^{\tau_0} d\tau S_P^{(T)}(k, \tau) \hat{\mathcal{B}}^{(T)}(x) e^{-i\mu_{k,n}x}
\end{aligned} \tag{3.92}$$

with the operators $\hat{\mathcal{E}}, \hat{\mathcal{B}}$ defined as

$$\begin{aligned}
\hat{\mathcal{E}}^{(S)}(x) &\equiv (1 + \partial_x^2)^2 x^2 , \\
\hat{\mathcal{E}}^{(V)}(x) &\equiv 4x + (12 + x^2)\partial_x + 8x\partial_x^2 + x^2\partial_x^3 , \\
\hat{\mathcal{B}}^{(V)}(x) &\equiv x^2 + 4x\partial_x + x^2\partial_x^2 , \\
\hat{\mathcal{E}}^{(T)}(x) &\equiv -12 + x^2(1 - \partial_x^2) - 8x\partial_x , \\
\hat{\mathcal{B}}^{(T)}(x) &\equiv 8x + 2x^2\partial_x .
\end{aligned} \tag{3.93}$$

From here, we want to show analytical expressions of $a_{\ell m}$'s. In the above discussion, we have analytical formulae of the transfer functions when $\mathbf{k} \parallel \hat{\mathbf{z}}$. This implies that we consider the physics in the blue basis of Fig. 3.4 and their transfer functions are completely determined by not the angle between $\hat{\mathbf{z}}$ and $\hat{\mathbf{n}}$, namely Ω_n , but the angle between \mathbf{k} and $\hat{\mathbf{n}}$, namely $\Omega_{k,n}$. However, as shown in Eq. (3.90), to obtain $a_{\ell m}$'s, we have to consider the physics in the red basis Fig. 3.4 and perform the Ω_n -integral. Here, instead of the transformation of the transfer functions, it is a better way to transform the integration variable in the $a_{\ell m}$ as $\Omega_n \rightarrow \Omega_{k,n}$. This can be done by using the Wigner D -matrix $D_{mm'}^{(\ell)}$, which is the unitary irreducible matrix of rank $2\ell + 1$ that forms a representation of the rotational group. The property of this matrix and the relation with spin-weighted spherical harmonics are explained in Appendix B. If we consider the rotational matrix

$$S(\Omega_k) \equiv \begin{pmatrix} \cos \theta_k \cos \phi_k & -\sin \phi_k & \sin \theta_k \cos \phi_k \\ \cos \theta_k \sin \phi_k & \cos \phi_k & \sin \theta_k \sin \phi_k \\ -\sin \theta_k & 0 & \cos \theta_k \end{pmatrix} \tag{3.94}$$

corresponding to the configuration $(\alpha = \phi_k, \beta = \theta_k, \gamma = 0)$ of Eq. (B.3) and satisfying

$$\Omega_n = S(\Omega_k)\Omega_{k,n} , \tag{3.95}$$

the transformation equation (B.1) can be equated with

$$Y_{\ell m}^*(\Omega_n) = \sum_{m'} D_{mm'}^{(\ell)}(S(\Omega_k)) Y_{\ell m'}^*(\Omega_{k,n}) . \tag{3.96}$$

Using this equation and the relation of the coordinate transformation as $d\Omega_n = d\Omega_{k,n}$, the $a_{\ell m}$ of arbitrary mode is written as

$$\begin{aligned}
a_{X,\ell m}^{(Z)} &= \int \frac{d^3 \mathbf{k}}{(2\pi)^3} \left[\sum_{m'} D_{mm'}^{(\ell)}(S(\Omega_k)) \int d\Omega_{k,n} Y_{\ell m'}^*(\Omega_{k,n}) \Delta_X^{(Z)}(\tau_0, \mathbf{k} \parallel \hat{\mathbf{z}}, \hat{\mathbf{n}}) \right] \\
&= \left[\frac{4\pi}{2\ell + 1} \right]^{1/2} \int \frac{d^3 \mathbf{k}}{(2\pi)^3} \left[\sum_{m'} (-1)^{m'} Y_{\ell m}^*(\Omega_k) \int d\Omega_{k,n} Y_{\ell m'}^*(\Omega_{k,n}) \Delta_X^{(Z)}(\tau_0, \mathbf{k} \parallel \hat{\mathbf{z}}, \hat{\mathbf{n}}) \right] .
\end{aligned} \tag{3.97}$$

In the second equality, we have obeyed the relation of Eq. (B.4) in this case as

$$D_{mm'}^{(\ell)}(S(\Omega_k)) = \left[\frac{4\pi}{2\ell + 1} \right]^{1/2} (-1)^{m'} Y_{\ell m}^*(\Omega_k) . \tag{3.98}$$

Using the mathematical results of the $\Omega_{k,n}$ -integrals

$$\begin{aligned}
e^{-i\mu_{k,n}x} &= \sum_L 4\pi(-i)^L j_L(x) \sqrt{\frac{2L+1}{4\pi}} Y_{L0}(\Omega_{k,n}) , \\
\int d\Omega_{k,n} Y_{\ell m'}^* e^{-i\mu_{k,n}x} &= (-i)^\ell \delta_{m',0} \sqrt{4\pi(2\ell+1)} j_\ell(x) , \\
\int d\Omega_{k,n} Y_{\ell m'}^* Y_{1\pm 1} e^{-i\mu_{k,n}x} &= (-i)^{\ell-1} \delta_{m',\pm 1} \sqrt{\frac{3}{2}(2\ell+1)} \frac{(\ell+1)!}{(\ell-1)!} \frac{j_\ell(x)}{x} , \\
\int d\Omega_{k,n} Y_{\ell m'}^* Y_{2\pm 2} e^{-i\mu_{k,n}x} &= (-i)^{\ell-2} \delta_{m',\pm 2} \sqrt{\frac{15}{8}(2\ell+1)} \frac{(\ell+2)!}{(\ell-2)!} \frac{j_\ell(x)}{x^2} ,
\end{aligned} \tag{3.99}$$

we can find the general formulae of the $a_{\ell m}$ for all-mode perturbations:

$$a_{X,\ell m}^{(Z)} = 4\pi(-i)^\ell \int \frac{d^3\mathbf{k}}{(2\pi)^3} \sum_\lambda [\text{sgn}(\lambda)]^{\lambda+x} {}_{-\lambda}Y_{\ell m}^*(\Omega_k) \xi^{(\lambda)}(\mathbf{k}) \mathcal{T}_{X,\ell}^{(Z)}(k) , \tag{3.100}$$

where the helicity of the perturbations is expressed by λ : $\lambda = 0$ for $(Z = S)$, $= \pm 1$ for $(Z = V)$ or $= \pm 2$ for $(Z = T)$, the index x discriminates between the two parity states: $x = 0$ for $X = I, E$, $x = 1$ for $X = B$, and the time-integrated transfer functions $\mathcal{T}_{X,\ell}^{(Z)}(k)$ are expressed as ⁴

$$\begin{aligned}
\mathcal{T}_{I,\ell}^{(S)}(k) &= \int_0^{\tau_0} d\tau S_I^{(S)}(k, \tau) j_\ell(x) , \\
\mathcal{T}_{E,\ell}^{(S)}(k) &= \left[\frac{(\ell-2)!}{(\ell+2)!} \right]^{1/2} \int_0^{\tau_0} d\tau S_P^{(S)}(k, \tau) \hat{\mathcal{E}}^{(S)}(x) j_\ell(x) , \\
\mathcal{T}_{I,\ell}^{(V)}(k) &= \left[\frac{(\ell+1)!}{(\ell-1)!} \right]^{1/2} \int_0^{\tau_0} d\tau S_I^{(V)}(k, \tau) \frac{j_\ell(x)}{x} , \\
\mathcal{T}_{E,\ell}^{(V)}(k) &= - \left[\frac{(\ell+1)!}{(\ell-1)!} \frac{(\ell-2)!}{(\ell+2)!} \right]^{1/2} \int_0^{\tau_0} d\tau S_P^{(V)}(k, \tau) \hat{\mathcal{E}}^{(V)}(x) \frac{j_\ell(x)}{x} , \\
\mathcal{T}_{B,\ell}^{(V)}(k) &= - \left[\frac{(\ell+1)!}{(\ell-1)!} \frac{(\ell-2)!}{(\ell+2)!} \right]^{1/2} \int_0^{\tau_0} d\tau S_P^{(V)}(k, \tau) \hat{\mathcal{B}}^{(V)}(x) \frac{j_\ell(x)}{x} , \\
\mathcal{T}_{I,\ell}^{(T)}(k) &= - \left[\frac{(\ell+2)!}{(\ell-2)!} \right]^{1/2} \int_0^{\tau_0} d\tau S_I^{(T)}(k, \tau) \frac{j_\ell(x)}{x^2} , \\
\mathcal{T}_{E,\ell}^{(T)}(k) &= - \int_0^{\tau_0} d\tau S_P^{(T)}(k, \tau) \hat{\mathcal{E}}^{(T)}(x) \frac{j_\ell(x)}{x^2} , \\
\mathcal{T}_{B,\ell}^{(T)}(k) &= \int_0^{\tau_0} d\tau S_P^{(T)}(k, \tau) \hat{\mathcal{B}}^{(T)}(x) \frac{j_\ell(x)}{x^2} .
\end{aligned} \tag{3.101}$$

Note that in the all-sky analysis, due to the dependence of transfer functions on $\phi_{k,n}$, $a_{\ell m}$'s depend on the helicity state through the spin spherical harmonics. In the above discussion, we take the synchronous gauge and derive the $a_{\ell m}$. However, in the same manner, we can obtain the identical form of Eq. (3.100) even in another gauge. In this case, the different points can be confined only

⁴In Ref. [3], there are three typos: right-hand sides of Eqs. (B21), (B22) and (B23) must be multiplied by a factor -1 , respectively.

in the transfer function (3.101). In a numerical code CAMB [13, 19], these transfer functions of polarization modes are expanded as, e.g.,

$$\begin{aligned}\mathcal{T}_{E,\ell}^{(T)}(k) &= - \int_0^{\tau_0} d\tau \left[\frac{\ddot{g}\psi^{(T)} + 2\dot{g}\dot{\psi}^{(T)} + g\ddot{\psi}^{(T)}}{k^2} + \frac{4}{k} \frac{\dot{g}\psi^{(T)} + g\dot{\psi}^{(T)}}{x} - g\psi^{(T)} \left(1 - \frac{6}{x^2} \right) \right] j_\ell(x) , \\ \mathcal{T}_{B,\ell}^{(T)}(k) &= -2 \int_0^{\tau_0} d\tau \left[g \left(\frac{2\psi^{(T)}}{x} + \frac{\dot{\psi}^{(T)}}{k} \right) + \frac{\dot{g}\psi^{(T)}}{k} \right] j_\ell(x) .\end{aligned}\tag{3.102}$$

3.8 Flat-sky formulae for the CMB scalar-, vector- and tensor-mode anisotropies

The flat-sky approximation uses the (2D) plane wave expansion of the CMB fluctuation instead of the spherical harmonics one, and it is valid if we restrict observed direction (parallel to $\hat{\mathbf{n}}$) only close to the z axis [4, 23]. As confirmed in Ref. [4], the flat-sky power spectra of E - and B -mode polarizations sourced from the primordial scalar and tensor perturbations are in good agreement with the all-sky ones for $\ell \gtrsim 40$. On the basis of these studies, we have also compared the all-sky power spectra with the flat-sky ones for the I , E , and B modes from scalar, vector, and tensor perturbations and found their consistencies at $\ell \gtrsim 40$.

As mentioned in the previous subsection, in order to estimate the $a_{\ell m}$, one must construct the transfer functions for arbitrary \mathbf{k} . In other words, we want to obtain the transfer functions expressed by arbitrary \mathbf{k} (whose direction is denoted by Ω_k) and $\hat{\mathbf{n}}$ (denoted by Ω_n) instead of $\Omega_{k,n}$ in Fig. 3.4. In the I modes, only by changing $\Omega_{k,n}$ to Ω_k and Ω_n with the relation (3.95), the transfer functions for arbitrary \mathbf{k} can be obtained. In the E and B modes, in addition to this treatment, one must consider the mixing between Δ_Q and Δ_U under the transformation $S(\Omega_k)$ as described in Ref. [4]. This effect is expressed as

$$(\Delta_Q^{(Z)'} \pm i\Delta_U^{(Z)'}) (\tau_0, \mathbf{k}, \hat{\mathbf{n}}) = e^{\mp 2i\psi} (\Delta_Q^{(Z)} \pm i\Delta_U^{(Z)}) (\tau_0, \mathbf{k} \parallel \hat{\mathbf{z}}, \hat{\mathbf{n}}) .\tag{3.103}$$

with the mixing angle ψ . The angle ψ represents the rotation angle between $\hat{\theta}_{k,n}$ and $\hat{\theta}_n$, where $\hat{\theta}_{k,n}$ and $\hat{\theta}_n$ are the unit vectors orthogonal to $\hat{\mathbf{n}}$ in a particular basis in which $\mathbf{k} \parallel \hat{\mathbf{z}}$ and a general basis, respectively (see Fig. 3.4).

In the flat-sky analysis, i.e., $\theta_n \rightarrow 0$, by using Eqs. (3.84) - (3.86) and by using the limit of ψ

as $\psi \rightarrow \phi_n - \phi_k + \pi$, the transfer functions for arbitrary \mathbf{k} are derived as

$$\begin{aligned}
\Delta_I^{(S)}(\tau_0, \mathbf{k}, \hat{\mathbf{n}}) &\rightarrow \xi(\mathbf{k}) \int_0^{\tau_0} d\tau S_I^{(S)}(k, \tau) e^{-i\mathbf{k} \cdot \hat{\mathbf{n}} D}, \\
(\Delta_Q^{(S)} \pm i\Delta_U^{(S)})(\tau_0, \mathbf{k}, \hat{\mathbf{n}}) &\rightarrow e^{\mp 2i(\phi_n - \phi_k)} \sin^2 \theta_k \xi(\mathbf{k}) \int_0^{\tau_0} d\tau S_P^{(S)}(k, \tau) e^{-i\mathbf{k} \cdot \hat{\mathbf{n}} D}, \\
\Delta_I^{(V)}(\tau_0, \mathbf{k}, \hat{\mathbf{n}}) &\rightarrow i \sin \theta_k \left(\sum_{\lambda=\pm 1} \xi^{(\lambda)}(\mathbf{k}) \right) \int_0^{\tau_0} d\tau S_I^{(V)}(k, \tau) e^{-i\mathbf{k} \cdot \hat{\mathbf{n}} D}, \\
(\Delta_Q^{(V)} \pm i\Delta_U^{(V)})(\tau_0, \mathbf{k}, \hat{\mathbf{n}}) &\rightarrow e^{\mp 2i(\phi_n - \phi_k)} \sin \theta_k \\
&\quad \times \left[-\cos \theta_k \left(\sum_{\lambda=\pm 1} \xi^{(\lambda)}(\mathbf{k}) \right) \pm \left(\sum_{\lambda=\pm 1} \lambda \xi^{(\lambda)}(\mathbf{k}) \right) \right] \\
&\quad \times \int_0^{\tau_0} d\tau S_P^{(V)}(k, \tau) e^{-i\mathbf{k} \cdot \hat{\mathbf{n}} D}, \\
\Delta_I^{(T)}(\tau_0, \mathbf{k}, \hat{\mathbf{n}}) &\rightarrow \sin^2 \theta_k \left(\sum_{\lambda=\pm 2} \xi^{(\lambda)}(\mathbf{k}) \right) \int_0^{\tau_0} d\tau S_I^{(T)}(k, \tau) e^{-i\mathbf{k} \cdot \hat{\mathbf{n}} D}, \\
(\Delta_Q^{(T)} \pm i\Delta_U^{(T)})(\tau_0, \mathbf{k}, \hat{\mathbf{n}}) &\rightarrow e^{\mp 2i(\phi_n - \phi_k)} \left[(1 + \cos^2 \theta_k) \left(\sum_{\lambda=\pm 2} \xi^{(\lambda)}(\mathbf{k}) \right) \right. \\
&\quad \left. \mp 2 \cos \theta_k \left(\sum_{\lambda=\pm 2} \frac{\lambda}{2} \xi^{(\lambda)}(\mathbf{k}) \right) \right] \int_0^{\tau_0} d\tau S_P^{(T)}(k, \tau) e^{-i\mathbf{k} \cdot \hat{\mathbf{n}} D}.
\end{aligned} \tag{3.104}$$

It is important to note that the ϕ_k dependence which are inherent in the vector and tensor perturbations vanishes in the flat-sky approximation, besides a trivial ϕ_k dependence due to a spin-2 nature of the Stokes Q and U parameters. One may explicitly see that $\phi_{k,n}$ dependence vanishes in the transfer functions when taking $\theta_n \rightarrow 0$ because the $S(\Omega_k)$ matrix rotates the basis with the new z axis always being on the $x-z$ plane in a particular basis in which $\mathbf{k} \parallel \hat{\mathbf{z}}$ (see Fig. 3.4). This approximation means that for $\theta_n \ll 1$, it is valid to calculate the CMB fluctuation on the basis of vector and tensor perturbations fixed as $\theta_n = 0$, namely, $\phi_{k,n} = \pi$.

In the flat-sky limit, $a_{\ell m}$ in the all-sky analysis described as Eq. (3.90) is modified by using the plane wave as

$$\begin{aligned}
a_{X, \ell m}^{(Z)} &\rightarrow \int d^2 \Theta e^{-i\boldsymbol{\ell} \cdot \Theta} \int \frac{d^3 \mathbf{k}}{(2\pi)^3} \Delta_X^{(Z)}(\tau_0, \mathbf{k}, \hat{\mathbf{n}}) \equiv a_X^{(Z)}(\boldsymbol{\ell}), \\
\Delta_E^{(Z)}(\tau_0, \mathbf{k}, \hat{\mathbf{n}}) &\rightarrow \frac{1}{2} \left[\sum_{s=\pm 2} \left(\Delta_Q^{(Z)} + \frac{s}{2} i \Delta_U^{(Z)} \right) (\tau_0, \mathbf{k}, \hat{\mathbf{n}}) e^{-si(\phi_\ell - \phi_n)} \right], \\
\Delta_B^{(Z)}(\tau_0, \mathbf{k}, \hat{\mathbf{n}}) &\rightarrow -\frac{i}{2} \left[\sum_{s=\pm 2} \frac{s}{2} \left(\Delta_Q^{(Z)} + \frac{s}{2} i \Delta_U^{(Z)} \right) (\tau_0, \mathbf{k}, \hat{\mathbf{n}}) e^{-si(\phi_\ell - \phi_n)} \right],
\end{aligned} \tag{3.105}$$

where Θ is the 2D vector projecting $\hat{\mathbf{n}}$ to the flat-sky plane expressed as $\Theta = (\Theta \cos \phi_n, \Theta \sin \phi_n)$ ⁵.

For example, in order to obtain $a_{I, \ell m}^{(T)}$, we substitute Eq. (3.104) into Eq. (3.105) and calculate

⁵Not confuse Θ with the CMB temperature fluctuation.

as follows:

$$\begin{aligned}
a_I^{(T)}(\ell) &= \int \frac{d^3\mathbf{k}}{(2\pi)^3} \sin^2 \theta_k \left(\sum_{\lambda=\pm 2} \xi^{(\lambda)}(\mathbf{k}) \right) \int_0^{\tau_0} d\tau \int d^2\Theta e^{-i(\mathbf{k}^\parallel D + \ell) \cdot \Theta} S_I^{(T)}(k, \tau) e^{-ik_z D} \\
&= \int \frac{d^3\mathbf{k}}{(2\pi)^3} \sin^2 \theta_k \left(\sum_{\lambda=\pm 2} \xi^{(\lambda)}(\mathbf{k}) \right) \int_0^{\tau_0} d\tau (2\pi)^2 \delta(\mathbf{k}^\parallel D + \ell) S_I^{(T)}(k, \tau) e^{-ik_z D} \\
&= \int_0^{\tau_0} d\tau \int_{-\infty}^{\infty} \frac{dk_z}{2\pi} \left(\sum_{\lambda=\pm 2} \xi^{(\lambda)}(\mathbf{k}^\parallel = -\ell/D, k_z) \right) \\
&\quad \times \frac{\ell^2}{(k_z D)^2 + \ell^2} S_I^{(T)}(k = \sqrt{k_z^2 + (\ell/D)^2}, \tau) \frac{1}{D^2} e^{-ik_z D} , \tag{3.106}
\end{aligned}$$

where $D = \tau_0 - \tau$ is the conformal distance and we have decomposed \mathbf{k} into two-dimensional vector parallel to the flat sky and that orthogonal to it, $\mathbf{k} = (\mathbf{k}^\parallel, k_z)$. In order to obtain the last equation, we use following relations which are satisfied under $\mathbf{k}^\parallel = -\ell/D$ as

$$\begin{aligned}
k &= \sqrt{k_z^2 + \left(\frac{\ell}{D} \right)^2} , \\
\sin \theta_k &= \frac{\ell}{kD} = \frac{\ell}{\sqrt{(k_z D)^2 + \ell^2}} , \\
\cos \theta_k &= \text{sgn}(k_z) \sqrt{1 - \left(\frac{\ell}{kD} \right)^2} , \\
\phi_k &= \phi_\ell + \pi .
\end{aligned} \tag{3.107}$$

The other-mode $a_{\ell m}$'s can be calculated in the same manner. Thus, we summarize the all-mode

$a(\ell)$'s:

$$\begin{aligned}
a_X^{(Z)}(\ell) &= \int_0^{\tau_0} d\tau \int_{-\infty}^{\infty} \frac{dk_z}{2\pi} \sum_{\lambda} [\text{sgn}(\lambda)]^x \xi^{(\lambda)}(\mathbf{k}_{\parallel} = -\ell/D, k_z) \frac{1}{D^2} e^{-ik_z D} \mathcal{S}_{X,\ell}^{(Z)}(k_z, \tau) \\
\mathcal{S}_{I,\ell}^{(S)}(k_z, \tau) &= S_I^{(S)}(k = \sqrt{k_z^2 + (\ell/D)^2}, \tau) , \\
\mathcal{S}_{E,\ell}^{(S)}(k_z, \tau) &= \frac{\ell^2}{(k_z D)^2 + \ell^2} S_P^{(S)}(k = \sqrt{k_z^2 + (\ell/D)^2}, \tau) , \\
\mathcal{S}_{I,\ell}^{(V)}(k_z, \tau) &= i \frac{\ell}{\sqrt{(k_z D)^2 + \ell^2}} S_I^{(V)}(k = \sqrt{k_z^2 + (\ell/D)^2}, \tau) , \\
\mathcal{S}_{E,\ell}^{(V)}(k_z, \tau) &= -\text{sgn}(k_z) \frac{\ell}{\sqrt{(k_z D)^2 + \ell^2}} \sqrt{1 - \frac{\ell^2}{(k_z D)^2 + \ell^2}} S_P^{(V)}(k = \sqrt{k_z^2 + (\ell/D)^2}, \tau) , \quad (3.108) \\
\mathcal{S}_{B,\ell}^{(V)}(k_z, \tau) &= -i \frac{\ell}{\sqrt{(k_z D)^2 + \ell^2}} S_P^{(V)}(k = \sqrt{k_z^2 + (\ell/D)^2}, \tau) , \\
\mathcal{S}_{I,\ell}^{(T)}(k_z, \tau) &= \frac{\ell^2}{(k_z D)^2 + \ell^2} S_I^{(T)}(k = \sqrt{k_z^2 + (\ell/D)^2}, \tau) , \\
\mathcal{S}_{E,\ell}^{(T)}(k_z, \tau) &= \left(2 - \frac{\ell^2}{(k_z D)^2 + \ell^2} \right) S_P^{(T)}(k = \sqrt{k_z^2 + (\ell/D)^2}, \tau) , \\
\mathcal{S}_{B,\ell}^{(T)}(k_z, \tau) &= 2i \text{sgn}(k_z) \sqrt{1 - \frac{\ell^2}{(k_z D)^2 + \ell^2}} S_P^{(T)}(k = \sqrt{k_z^2 + (\ell/D)^2}, \tau) ,
\end{aligned}$$

where we label $\mathcal{S}_{X,\ell}^{(Z)}$ as the modified source function. One can formulate the flat-sky CMB power spectrum and bispectrum by using these formulae [3, 24–26].

3.9 CMB power spectrum

To extract several information about the Universe from the observational data, the two-point correlation function of the CMB fluctuations (called CMB power spectrum) is often-used. Here, we formulate the CMB power spectrum and summarize the constraints on several model parameters from the current observational data.

If we assume the Gaussianity and the symmetry under the parity and rotational transformations in the initial stochastic variables, their power spectrum can be expressed as

$$\langle \xi^{(\lambda_1)}(\mathbf{k}_1) \xi^{(\lambda_2)*}(\mathbf{k}_2) \rangle = (2\pi)^3 P_Z(k_1) \delta(\mathbf{k}_1 - \mathbf{k}_2) \delta_{\lambda_1, \lambda_2} \times \begin{cases} 1 & (Z = S) \\ 1/2 & (Z = V, T) \end{cases} \quad (3.109)$$

This implies that the couplings between the different modes of the perturbation vanish in the power spectrum. Then, from the formula of the all-sky $a_{\ell m}$ (3.100), the CMB power spectra of all modes are derived as

$$\begin{aligned}
\left\langle \prod_{n=1}^2 a_{X_n, \ell_n m_n}^{(Z_n)} \right\rangle &\equiv C_{X_1 X_2, \ell_1}^{(Z_1)} (-1)^{m_1} \delta_{\ell_1, \ell_2} \delta_{m_1, -m_2} \delta_{Z_1, Z_2} \delta_{x_1, x_2} , \\
C_{X_1 X_2, \ell_1}^{(Z_1)} &= \frac{2}{\pi} \int k_1^2 dk_1 P_{Z_1}(k_1) \mathcal{T}_{X_1, \ell_1}^{(Z_1)}(k_1) \mathcal{T}_{X_2, \ell_1}^{(Z_1)}(k_1)
\end{aligned} \quad (3.110)$$

where we use the relation derived by the reality condition of the metric perturbation:

$$\xi^{(\lambda)}(\mathbf{k}) = (-1)^\lambda \xi^{(\lambda)*}(-\mathbf{k}) . \quad (3.111)$$

In Fig. 3.5, we plot the CMB intensity and polarization power spectra of the scalar and tensor modes. Here we think that the scalar and tensor perturbations are sourced from the primordial curvature perturbations ($\xi^{(0)} = \mathcal{R}$) and primordial gravitational waves ($\xi^{(\pm 2)} = h^{(\pm 2)}$), respectively. The ratio between these power spectra, called the tensor-to-scalar ratio r , is defined as ⁶

$$r \equiv \frac{2P_T(k)}{P_S(k)} . \quad (3.112)$$

At first, let us focus on the II spectra in the left top panel. In the scalar spectrum, the dominant signal is generated from the acoustic oscillation of the photon and baryon fluid. The first acoustic peak is located at $\ell_1 \sim 220$. This scale is corresponding to the angle of the sound horizon at the recombination epoch as $\ell_1 \sim 2\pi\tau_0/r_s(z_*)$. At small scales corresponding to $\ell \gg \ell_1$, due to the difference between the photon and baryon speeds, the coupling between photons and baryons is ineffective and the acoustic oscillation is highly damped. This effect is well-known as the Silk damping [28]. On the other hand, the gravitational blue shift due to the potential decay in the late time affects the fluctuations for $\ell \ll \ell_1$. This is called the integrate Sachs Wolfe (ISW) effect [29] and arises from the terms proportional to $e^{-\kappa}$ of the source function $S_I^{(Z)}$ in Eqs. (3.84) and (3.86). In the tensor spectrum, the ISW effect leads to the dominant signals and the scattering effect (the second term of the source function $S_I^{(T)}$ in Eq. (3.86)) is subdominant [6]. As shown in Eqs. (3.84) and (3.86), the EE and BB spectra (the bottom two panels) have no gravitational redshift term and there is no ISW effect. Instead of it, the scattering term generates the CMB fluctuation. The most interesting signature in the polarization power spectra is the enhancement at $\ell \lesssim 10$. This can be caused by Thomson scattering at reionization of hydrogen which may have occurred at $z \sim 10$ [4]. Therefore, these signals can be important to determine the optical depth of the Universe, κ . The IE spectrum described in the right top panel seems to include the features of both the II and EE spectra and has both positive and negative values. Unlike the above three cases, the BB spectrum never arises from the scalar mode because the scalar mode has only one helicity, namely $\lambda = 0$ ⁷. Hence, we believe that the BB spectrum directly tells us the amplitude of the primordial gravitational waves depending on the energy scale of inflation.

Theoretically, the CMB power spectrum depends on the parameters which determine the dynamics of the Universe as the energy density of the cosmic fluids, curvature, and the Hubble constant H_0 . Figure 3.6 shows the dependence of $C_{II,\ell}^{(S)}$ on the density parameters of cold dark matters, the cosmological constant and baryons as $\omega_c \equiv \Omega_c(H_0/100\text{sec} \cdot \text{Mpc/km})^2$, Ω_Λ and $\omega_b \equiv \Omega_b(H_0/100\text{sec} \cdot \text{Mpc/km})^2$, respectively. From this figure, one can observe that as ω_c decreases, the overall amplitude of $C_{II,\ell}^{(S)}$ enlarges. This behavior is understood as follows. If ω_c decreases, since the radiation dominated era is lengthened, the gravitational potential for smaller k enters the horizon and decays. Thus, $C_{II,\ell}^{(S)}$ at corresponding multipoles as $\ell \sim k\tau$ is boosted due to the gravitational blue shift. This is the so called early ISW effect [29]. Next, focusing on the blue dotted line, one can find that if Ω_Λ becomes large, $C_{II,\ell}^{(S)}$ is boosted for $\ell \lesssim 10$. This is due to the late ISW effect, that is, Λ dominates the Universe earlier and the potential at larger scales is

⁶This definition is consistent with Eq. (2.69), and the notation of Ref. [27] and CAMB [13]

⁷The vector mode generates the BB spectrum due to its two helicities. However, due to the decay of the vector potential via the Einstein equation, this becomes the subdominant signal. To avoid this, the sources such as cosmic strings and magnetic fields need to exist and support.

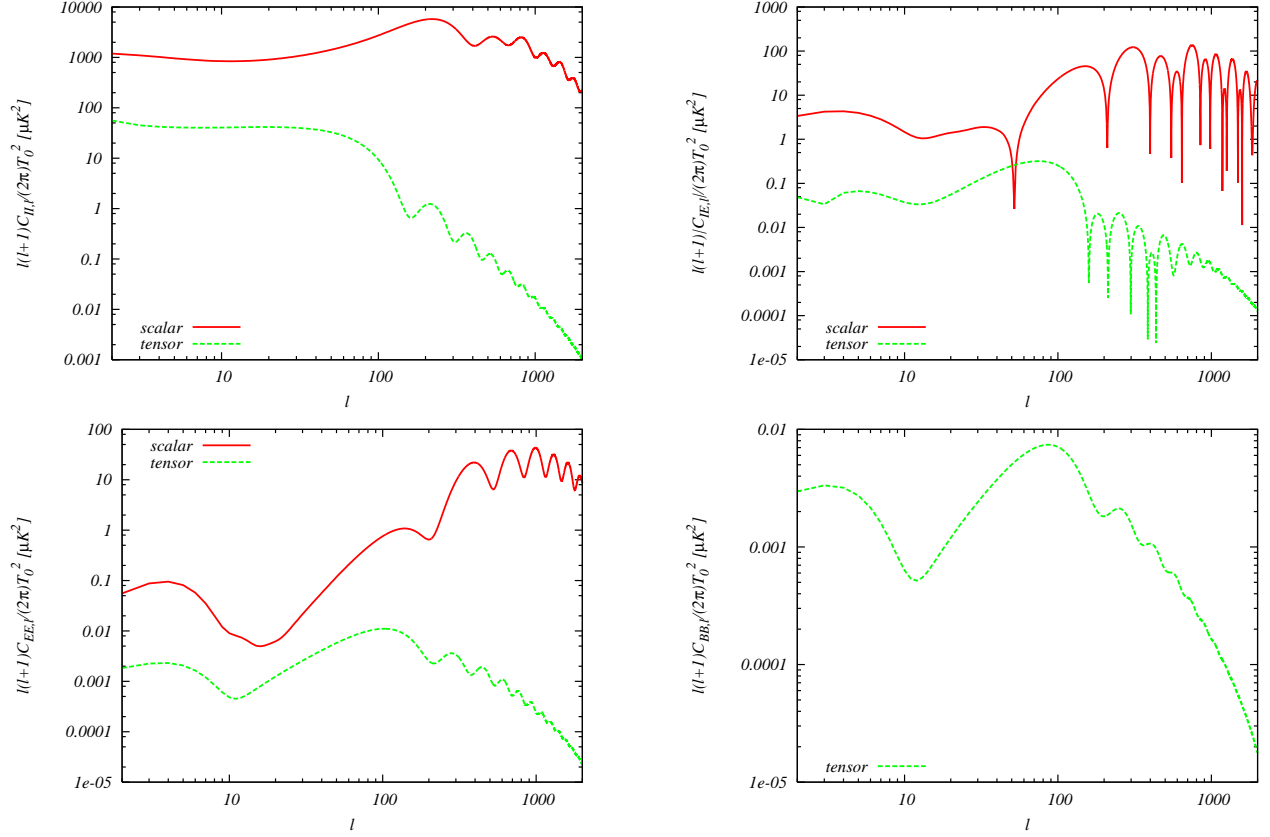


Figure 3.5: The CMB spectra of the II (left top panel), IE (right top one), EE (left bottom one) and BB (right bottom one) modes. Here we consider a power-law flat Λ CDM model and fix the tensor-to-scalar ratio as $r = 0.1$. The other cosmological parameters are fixed to the mean values reported in Ref. [27].

destroyed, hence $C_{II,\ell}^{(S)}$ at corresponding ℓ 's is amplified. We also notice that when ω_b enlarges, the ratio of the amplitude between the first and second peaks of the magenta dot-dashed line increases. Solving the coupled Boltzmann equations, the acoustic oscillation of the baryon-photon fluid in the matter dominated era is roughly given by

$$\Theta \sim \left(\frac{1}{3} + R \right) \Phi \cos(kr_s) - R\Phi, \quad (3.113)$$

where Φ is the potential of the conformal Newtonian gauge, r_s denotes the sound horizon and $R \equiv 3\rho_b/(4\rho_\gamma)$. Then if ω_b increases and R becomes large, this equation experiences increase in amplitude and suppression of the intercept. Hence, the difference of $C_{II,\ell}^{(S)} \propto \Theta^2$ between the odd and even-number peaks increases. These parameters are limited with the others from the current observational data set as Table 3.2. Other than these parameters, massive neutrinos and some relativistic components also make impacts on the CMB fluctuation (e.g. Refs. [30, 31]).

The CMB power spectrum also depends on the primordial curvature perturbations and primordial gravitational waves. Conventionally, these spectra are parametrized as

$$\frac{k^3 P_S(k)}{2\pi^2} = A_S \left(\frac{k}{0.002 \text{Mpc}^{-1}} \right)^{n_s-1}, \quad (3.114)$$

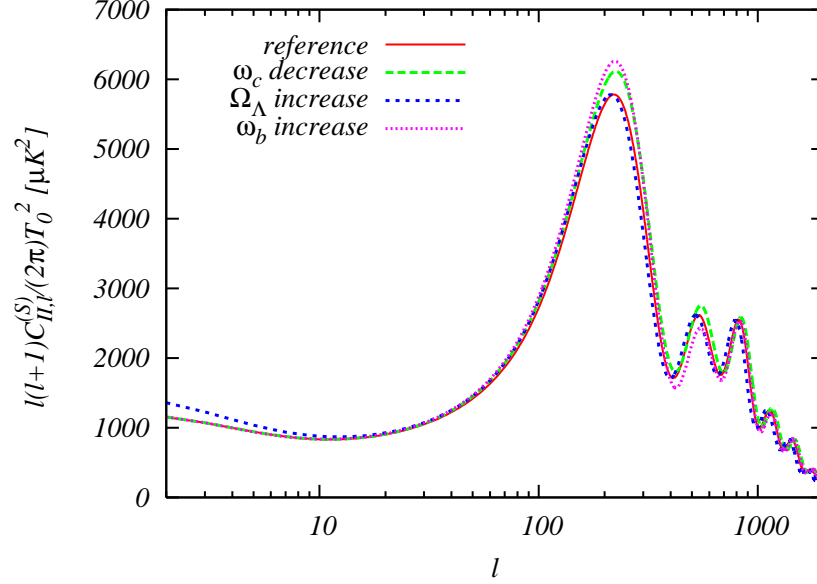


Figure 3.6: CMB II power spectra sourced from the scalar-mode perturbations in a power-law flat Λ CDM model. The red solid line is plotted with $\omega_c = 0.112$, $\Omega_\Lambda = 0.728$, $\omega_b = 0.02249$, $n_s = 0.967$, $\kappa = 0.088$ [27]. The green dashed, blue dotted and magenta dot-dashed lines are calculated if ω_c decreases to 0.1, Ω_Λ increases to 0.8, and ω_b increases to 0.028, respectively.

and Eq. (3.112). As shown in Eq. (3.100), the magnitudes of the primordial curvature perturbations A_S and gravitational waves rA_S simply determine the overall amplitude of the $C_{X_1X_2,\ell_1}^{(S)}$ and $C_{X_1X_2,\ell_1}^{(T)}$, respectively. The spectral index of the power spectrum of the curvature perturbations n_s changes in slope of $C_{X_1X_2,\ell_1}^{(Z_1)}$. From the observational data, the constraints on A_S, n_s, r are given as Table 3.2. Here, we want to note that $n_s = 1$ is excluded at about 3-sigma level. This implies the deviation from the exact de Sitter expansion in inflation. As shown in the bound on r , unlike the primordial curvature perturbation, the primordial gravitational wave has not been detected yet. However, some experimental groups aim to discover the BB spectrum through remove of some noisy foreground emission and improvement of the instruments [2, 34–36]. If these projects achieve, it will be possible to judge the existence of the primordial gravitational waves of $r < 0.01$.

So far, we discussed under the assumption that the parity and rotational invariances are kept. On the other hand, there are a lot of studies which probe the somewhat exotic scenarios where these invariances violate. As a theoretical prediction, if parity-violating action such as the Chern-Simon term exists in the early Universe, $\langle \xi^{(+2)}(\mathbf{k})\xi^{(+2)*}(\mathbf{k}') \rangle \neq \langle \xi^{(-2)}(\mathbf{k})\xi^{(-2)*}(\mathbf{k}') \rangle$ and the IB and EB spectra appear [37–40]. Using the parametrization as

$$C_{IB,\ell}^{\text{obs}} \equiv C_{IE,\ell} \sin(2\Delta\alpha) , \quad (3.115)$$

the parity violation is limited as $-5.0^\circ < \Delta\alpha < 2.8^\circ$ (95% CL) [27]. The rotational invariance is broken if the Universe has the preferred direction and this situation is realized by the anisotropic inflation [41–43]. This leads to the direction-depending power spectrum as

$$P_S(\mathbf{k}) = P_S^{\text{iso}}(k)[1 + g(\hat{\mathbf{k}} \cdot \hat{\mathbf{n}})^2] , \quad (3.116)$$

and produces the off-diagonal components in the CMB power spectrum as $\ell_1 \neq \ell_2$. From the CMB observational data, the magnitude of the statistical anisotropy has been limited as $g = 0.15 \pm 0.039$ [44]

Parameter	WMAP 7-yr	WMAP + BAO + H_0
$100\omega_b$	$2.249^{+0.056}_{-0.057}$	2.255 ± 0.054
ω_c	0.1120 ± 0.0056	0.1126 ± 0.0036
Ω_Λ	$0.727^{+0.030}_{-0.029}$	0.725 ± 0.016
n_s	0.967 ± 0.014	0.968 ± 0.012
κ	0.088 ± 0.015	0.088 ± 0.014
A_S	$(2.43 \pm 0.11) \times 10^{-9}$	$(2.430 \pm 0.091) \times 10^{-9}$
r	< 0.36	< 0.24
H_0	$70.4 \pm 2.5 \text{ km/s/Mpc}$	$70.2 \pm 1.4 \text{ km/s/Mpc}$
Ω_b	0.0455 ± 0.0028	0.0458 ± 0.0016
Ω_c	0.228 ± 0.027	0.229 ± 0.015
ω_m	$0.1345^{+0.0056}_{-0.0055}$	0.1352 ± 0.0036
z_{reion}	10.6 ± 1.2	10.6 ± 1.2
t_0	$13.77 \pm 0.13 \text{ Gyr}$	$13.76 \pm 0.11 \text{ Gyr}$

Table 3.2: Summary of the cosmological parameters of Λ CDM with finite r model from the WMAP 7-year data [27], and the data set combined with the results of the galaxy survey [32] and Hubble constant measurement [33], respectively. Here z_{reion} denotes the redshift at the reionization epoch, t_0 is the present time of the Universe, and $\omega_m \equiv \omega_b + \omega_c$.

Furthermore, owing to the progress of the observational accuracy, the deviation of the Gaussianity can be measured. Beyond the power spectrum, this is achieved by using the three-point function (bispectrum). In the next section, we discuss about how to extract the information on the early Universe from the CMB scalar, vector and tensor bispectrum.

In addition, we can add other components of fluids in the analysis of the CMB spectrum. From Sec. 9, we focus on the effect of the primordial magnetic fields on the CMB.

References

- [1] C. L. Bennett *et al.*, *Seven-Year Wilkinson Microwave Anisotropy Probe (WMAP) Observations: Are There Cosmic Microwave Background Anomalies?*, *Astrophys. J. Suppl.* **192** (2011) 17, [arXiv:1001.4758].
- [2] **PLANCK** Collaboration, *The Scientific programme of planck*, astro-ph/0604069.
- [3] M. Shiraishi, S. Yokoyama, D. Nitta, K. Ichiki, and K. Takahashi, *Analytic formulae of the CMB bispectra generated from non-Gaussianity in the tensor and vector perturbations*, *Phys. Rev.* **D82** (2010) 103505, [arXiv:1003.2096].
- [4] M. Zaldarriaga and U. Seljak, *An All-Sky Analysis of Polarization in the Microwave Background*, *Phys. Rev.* **D55** (1997) 1830–1840, [astro-ph/9609170].
- [5] M. Landriau and E. P. S. Shellard, *Fluctuations in the CMB induced by cosmic strings: Methods and formalism*, *Phys. Rev.* **D67** (2003) 103512, [astro-ph/0208540].

- [6] J. R. Pritchard and M. Kamionkowski, *Cosmic microwave background fluctuations from gravitational waves: An analytic approach*, *Annals Phys.* **318** (2005) 2–36, [astro-ph/0412581].
- [7] S. Weinberg, *Cosmology*, . Oxford, UK: Oxford Univ. Pr. (2008) 593 p.
- [8] M. Zaldarriaga, *Fluctuations in the cosmic microwave background*, astro-ph/9806122. Ph.D. Thesis.
- [9] I. A. Brown, *Primordial Magnetic Fields in Cosmology*, arXiv:0812.1781. Ph.D. Thesis.
- [10] S. Saito, *Probing circular polarization of Gravitational Wave Background with Cosmic Microwave Background anisotropy*, . Master Thesis.
- [11] M. Kamionkowski, B. Ratra, D. N. Spergel, and N. Sugiyama, *CMB anisotropy in an open inflation, CDM cosmogony*, *Astrophys.J.* **434** (1994) L1–L4, [astro-ph/9406069].
- [12] D. N. Spergel, U.-L. Pen, M. Kamionkowski, and N. Sugiyama, *Microwave background fluctuations in an open universe*, astro-ph/9402060.
- [13] A. Lewis, A. Challinor, and A. Lasenby, *Efficient Computation of CMB anisotropies in closed FRW models*, *Astrophys. J.* **538** (2000) 473–476, [astro-ph/9911177].
- [14] C.-P. Ma and E. Bertschinger, *Cosmological perturbation theory in the synchronous and conformal Newtonian gauges*, *Astrophys.J.* **455** (1995) 7–25, [astro-ph/9506072].
- [15] J. M. Bardeen, *Gauge Invariant Cosmological Perturbations*, *Phys.Rev.* **D22** (1980) 1882–1905.
- [16] H. Kodama and M. Sasaki, *Cosmological Perturbation Theory*, *Prog.Theor.Phys.Suppl.* **78** (1984) 1–166.
- [17] W. Hu and M. J. White, *CMB Anisotropies: Total Angular Momentum Method*, *Phys. Rev.* **D56** (1997) 596–615, [astro-ph/9702170].
- [18] M. Giovannini and K. E. Kunze, *Generalized CMB initial conditions with pre-equality magnetic fields*, *Phys.Rev.* **D77** (2008) 123001, [arXiv:0802.1053].
- [19] A. Lewis, *CMB anisotropies from primordial inhomogeneous magnetic fields*, *Phys. Rev.* **D70** (2004) 043011, [astro-ph/0406096].
- [20] A. Kosowsky, *Cosmic microwave background polarization*, *Annals Phys.* **246** (1996) 49–85, [astro-ph/9501045].
- [21] U. Seljak and M. Zaldarriaga, *A Line of sight integration approach to cosmic microwave background anisotropies*, *Astrophys.J.* **469** (1996) 437–444, [astro-ph/9603033].
- [22] E. T. Newman and R. Penrose, *Note on the Bondi-Metzner-Sachs group*, *J. Math. Phys.* **7** (1966) 863–870.
- [23] U. Seljak, *Measuring Polarization in the Cosmic Microwave Background*, *ApJ* **482** (June, 1997) 6, [arXiv:astro-ph/9608131].

- [24] D. Babich, P. Creminelli, and M. Zaldarriaga, *The shape of non-Gaussianities*, *JCAP* **0408** (2004) 009, [[astro-ph/0405356](#)].
- [25] C. Pitrou, J.-P. Uzan, and F. Bernardeau, *Cosmic microwave background bispectrum on small angular scales*, *Phys. Rev.* **D78** (2008) 063526, [[arXiv:0807.0341](#)].
- [26] L. Boubekur, P. Creminelli, G. D’Amico, J. Norena, and F. Vernizzi, *Sachs-Wolfe at second order: the CMB bispectrum on large angular scales*, *JCAP* **0908** (2009) 029, [[arXiv:0906.0980](#)].
- [27] **WMAP Collaboration**, E. Komatsu *et al.*, *Seven-Year Wilkinson Microwave Anisotropy Probe (WMAP) Observations: Cosmological Interpretation*, *Astrophys. J. Suppl.* **192** (2011) 18, [[arXiv:1001.4538](#)].
- [28] J. Silk, *Cosmic black body radiation and galaxy formation*, *Astrophys.J.* **151** (1968) 459–471.
- [29] W. Hu and N. Sugiyama, *The Small scale integrated Sachs-Wolfe effect*, *Phys. Rev.* **D50** (1994) 627–631, [[astro-ph/9310046](#)].
- [30] J. Lesgourgues and S. Pastor, *Massive neutrinos and cosmology*, *Phys. Rept.* **429** (2006) 307–379, [[astro-ph/0603494](#)].
- [31] M. Shiraishi, K. Ichikawa, K. Ichiki, N. Sugiyama, and M. Yamaguchi, *Constraints on neutrino masses from WMAP5 and BBN in the lepton asymmetric universe*, *JCAP* **0907** (2009) 005, [[arXiv:0904.4396](#)].
- [32] **SDSS Collaboration** Collaboration, B. A. Reid *et al.*, *Baryon Acoustic Oscillations in the Sloan Digital Sky Survey Data Release 7 Galaxy Sample*, *Mon.Not.Roy.Astron.Soc.* **401** (2010) 2148–2168, [[arXiv:0907.1660](#)].
- [33] A. G. Riess, L. Macri, S. Casertano, M. Sosey, H. Lampeitl, *et al.*, *A Redetermination of the Hubble Constant with the Hubble Space Telescope from a Differential Distance Ladder*, *Astrophys.J.* **699** (2009) 539–563, [[arXiv:0905.0695](#)].
- [34] **QUIET Collaboration** Collaboration, C. Bischoff *et al.*, *First Season QUIET Observations: Measurements of CMB Polarization Power Spectra at 43 GHz in the Multipole Range $25 \leq \ell \leq 475$* , *Astrophys.J.* **741** (2011) 111, [[arXiv:1012.3191](#)].
- [35] B. Keating, S. Moyerman, D. Boettger, J. Edwards, G. Fuller, *et al.*, *Ultra High Energy Cosmology with POLARBEAR*, [arXiv:1110.2101](#).
- [36] “LiteBIRD experiment.” <http://cmb.kek.jp/litebird/index.html>.
- [37] S. Alexander and J. Martin, *Birefringent gravitational waves and the consistency check of inflation*, *Phys. Rev.* **D71** (2005) 063526, [[hep-th/0410230](#)].
- [38] S. Saito, K. Ichiki, and A. Taruya, *Probing polarization states of primordial gravitational waves with CMB anisotropies*, *JCAP* **0709** (2007) 002, [[arXiv:0705.3701](#)].
- [39] V. Gluscevic and M. Kamionkowski, *Testing Parity-Violating Mechanisms with Cosmic Microwave Background Experiments*, *Phys. Rev.* **D81** (2010) 123529, [[arXiv:1002.1308](#)].

- [40] A. Gruppuso, P. Natoli, N. Mandolesi, A. De Rosa, F. Finelli, *et al.*, *WMAP 7 year constraints on CPT violation from large angle CMB anisotropies*, [arXiv:1107.5548](#).
- [41] S. Yokoyama and J. Soda, *Primordial statistical anisotropy generated at the end of inflation*, *JCAP* **0808** (2008) 005, [[arXiv:0805.4265](#)].
- [42] M.-a. Watanabe, S. Kanno, and J. Soda, *The Nature of Primordial Fluctuations from Anisotropic Inflation*, *Prog.Theor.Phys.* **123** (2010) 1041–1068, [[arXiv:1003.0056](#)].
- [43] M. Karciauskas, *The Primordial Curvature Perturbation from Vector Fields of General non-Abelian Groups*, *JCAP* **1201** (2012) 014, [[arXiv:1104.3629](#)].
- [44] N. E. Groeneboom and H. K. Eriksen, *Bayesian analysis of sparse anisotropic universe models and application to the 5-yr WMAP data*, *Astrophys. J.* **690** (2009) 1807–1819, [[arXiv:0807.2242](#)].

4 Primordial non-Gaussianities

The study of non-Gaussian impacts in the cosmological fluctuations provides an important information of the early Universe [1]. The primordial non-Gaussianities are measures of the interactions in inflation, hence constraining on this will lead to a great deal about the inflationary dynamics. It may also puts strong constraints on alternatives to the inflationary paradigm (e.g., Refs. [2–8]).

In the previous part, we expanded the inflationary action to second order in the comoving curvature perturbation \mathcal{R} and the gravitational waves $h^{(\pm 2)}$. These actions allowed us to compute the power spectra $P_{\mathcal{R}}(k)$ and $P_h(k)$. If the fluctuations \mathcal{R} and $h^{(\pm 2)}$ obey the exact Gaussian statistics, the power spectrum (or two-point correlation function) contains all the information¹. However, for the non-Gaussian fluctuations, higher-order correlation functions beyond the two-point function contain additional information about inflation. Estimating the leading non-Gaussian effects requires the expansion of the action to third order since we must take into account the leading non-trivial interaction terms. In this section, we review recent studies about the primordial non-Gaussianity based on e.g., Refs. [9–11].

4.1 Bispectrum of the primordial fluctuations

At first, we give the definition of the bispectrum of the initial perturbations $\xi^{(\lambda)}$ of the scalar ($\lambda = 0$), vector ($\lambda = \pm 1$), and tensor ($\lambda = \pm 2$) modes. The Fourier transformation of the two-point function is the power spectrum

$$\left\langle \prod_{n=1}^2 \xi^{(\lambda_n)}(\mathbf{k}_n) \right\rangle = (2\pi)^3 P_Z(k_1) \delta \left(\sum_{n=1}^3 \mathbf{k}_n \right) \delta_{\lambda_1, \lambda_2} (-1)^{\lambda_1} \times \begin{cases} 1 & (Z = S) \\ 1/2 & (Z = V, T) \end{cases} . \quad (4.1)$$

Similarly, the Fourier mode of the three-point function is so called the bispectrum

$$\left\langle \prod_{n=1}^3 \xi^{(\lambda_n)}(\mathbf{k}_n) \right\rangle = (2\pi)^3 F^{\lambda_1 \lambda_2 \lambda_3}(\mathbf{k}_1, \mathbf{k}_2, \mathbf{k}_3) \delta \left(\sum_{n=1}^3 \mathbf{k}_n \right) . \quad (4.2)$$

Here, the delta function enforcing the momentum conservation is a consequence of the translation invariance of the background. If the scale invariance is kept, we have

$$F^{\lambda_1 \lambda_2 \lambda_3}(b\mathbf{k}_1, b\mathbf{k}_2, b\mathbf{k}_3) = b^{-6} F^{\lambda_1 \lambda_2 \lambda_3}(\mathbf{k}_1, \mathbf{k}_2, \mathbf{k}_3) . \quad (4.3)$$

Moreover, the rotational invariance reduces the number of the independent variables to just two, namely k_2/k_1 and k_3/k_1 .

In order to compute the primordial bispectrum for a specific inflation model, we need to treat the time evolution of the vacuum in the presence of the interactions carefully. On the other hand, for the power spectrum, this is not the leading order effect. As the methodology for calculation of the cosmological correlation function, “the in-in formalism” is well-known [12–16]. In practice, computing the bispectra can be algebraically very cumbersome. In Sec. 8, using this formalism, we actually discuss the computation for the bispectrum of the gravitational waves.

¹All odd-point correlation functions vanish for the Gaussian fluctuations, while all even-point functions can be expressed in terms of the two-point function due to the Wick’s theorem. In other words, all connected higher-point functions vanish for the Gaussian fluctuations.

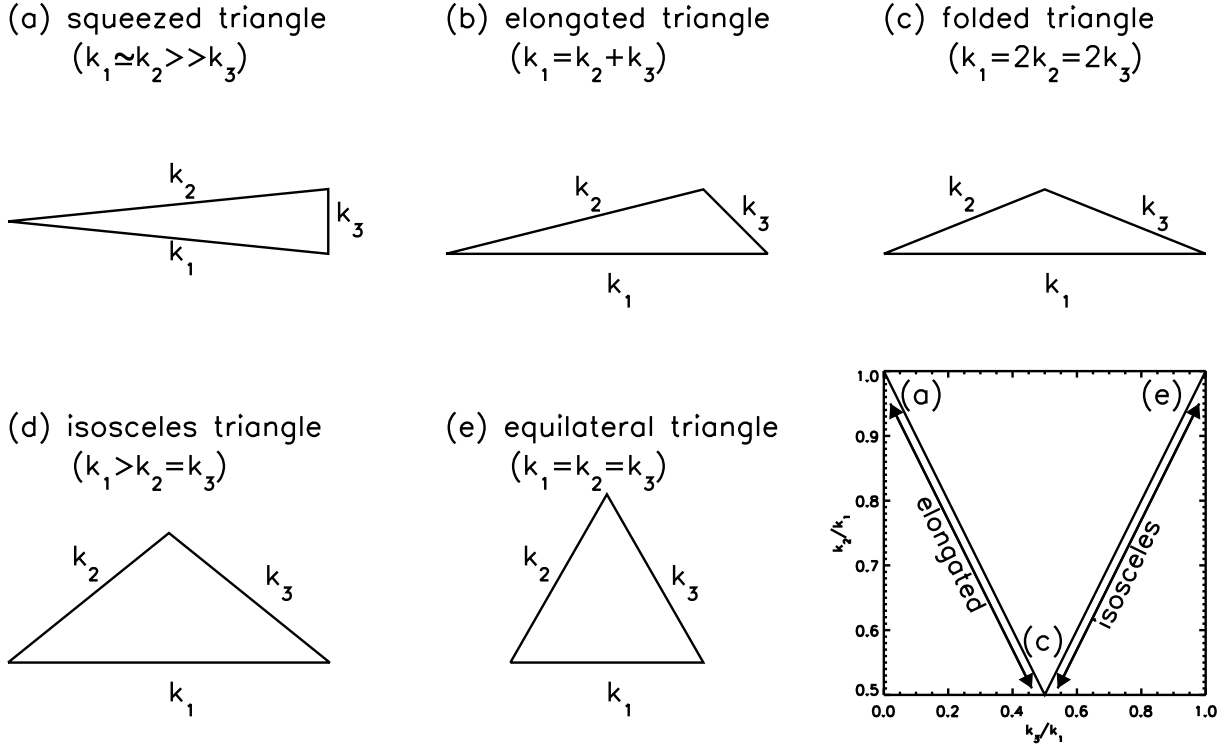


Figure 4.1: Representations of triangles forming the bispectrum, $F^{\lambda_1 \lambda_2 \lambda_3}(k_1, k_2, k_3)$, with various combinations of the wave numbers satisfying $k_3 \leq k_2 \leq k_1$. This figure is adopted from Ref. [19].

4.2 Shape of the non-Gaussianities

The delta function in Eq. (4.2) enforces that the three wave number vectors form a closed triangle. Depending on the inflation models, the maximal signals arise from the several triangle configurations. Therefore, specifying the shape of the non-Gaussianity is a powerful probe of the mechanism that laid down the primordial fluctuations [17, 18].

We have a useful way to visualize the shape dependence of the bispectrum. We study the structure of the bispectrum by plotting the magnitude of $F^{\lambda_1 \lambda_2 \lambda_3}(k_1, k_2, k_3)(k_2/k_1)^2(k_3/k_1)^2$ as a function of k_2/k_1 and k_3/k_1 for $k_3 \leq k_2 \leq k_1$. To classify various shapes of the triangles, let us utilize the following names: squeezed ($k_1 \approx k_2 \gg k_3$), elongated ($k_1 = k_2 + k_3$), folded ($k_1 = 2k_2 = 2k_3$), isosceles ($k_2 = k_3$), and equilateral ($k_1 = k_2 = k_3$). In Fig. 4.1, the visual representations of these triangles are presented.

From here, we focus on the three representative shapes of the primordial bispectrum: “local”, “equilateral”, and “orthogonal”. Then, it may be convenient to decompose the non-Gaussianity of the curvature perturbations into the magnitude-depending and shape-depending parts:

$$F^{000}(k_1, k_2, k_3) = \frac{3}{5} f_{\text{NL}} (2\pi^2 A_S)^2 S(k_1, k_2, k_3) , \quad (4.4)$$

where A_S is the magnitude of curvature perturbations defined in Eq. (3.114).

4.2.1 Local type

The simplest way to parametrize the non-Gaussianity was via a non-linear correction to a Gaussian curvature perturbation \mathcal{R}_g [20]

$$\mathcal{R}(\mathbf{x}) = \mathcal{R}_g(\mathbf{x}) + \frac{3}{5} f_{\text{NL}}^{\text{local}} [\mathcal{R}_g(\mathbf{x})^2 - \langle \mathcal{R}_g(\mathbf{x})^2 \rangle] . \quad (4.5)$$

From this equation, we can see that the non-Gaussianity is localized at a given point in the real space. Therefore, we call this the local-type non-Gaussianity, and $f_{\text{NL}}^{\text{local}}$ is called “the local-type nonlinear parameter”. Then, the bispectrum of the local-type non-Gaussianity of the curvature perturbations is derived as

$$F_{\text{local}}^{000}(k_1, k_2, k_3) = \frac{6}{5} f_{\text{NL}}^{\text{local}} [P_{\mathcal{R}}(k_1)P_{\mathcal{R}}(k_2) + 2 \text{ perms.}] , \quad (4.6)$$

where we fix the spectral index as $n_s = 1$. Hence, equating with Eq. (4.4), we can write

$$S^{\text{local}}(k_1, k_2, k_3) = 2 \left[\frac{1}{(k_1 k_2)^3} + 2 \text{ perms.} \right] . \quad (4.7)$$

Without loss of generality, we shall order the momenta such that $k_3 \leq k_2 \leq k_1$. Then, the bispectrum of the local non-Gaussianity dominates in the squeezed limit: $k_3 \ll k_1 \approx k_2$ as shown in the top-left panel of Fig. 4.2. In this limit, we obtain

$$F_{\text{local}}^{000}(k_1, k_2, k_3 \rightarrow 0) = \frac{12}{5} f_{\text{NL}}^{\text{local}} P_{\mathcal{R}}(k_1)P_{\mathcal{R}}(k_3) . \quad (4.8)$$

How large is $f_{\text{NL}}^{\text{local}}$ generated from inflation? If the single-field slow-roll inflation occurs, $f_{\text{NL}}^{\text{local}}$ would be of order the slow-roll parameter, $\epsilon \sim 10^{-2}$ [21–23]. More accurately, in Refs. [12, 24], the authors found that the coefficient of $P_{\mathcal{R}}(k_1)P_{\mathcal{R}}(k_3)$ from the simplest single-field slow-roll inflation with the canonical kinetic term in the squeezed limit is $(1 - n_s)$. Therefore, one has a consistency relation between the scalar spectral index and the local-type nonlinear parameter in the single-field slow-roll inflation:

$$f_{\text{NL}}^{\text{local}} = \frac{5}{12} (1 - n_s) , \quad (4.9)$$

which gives $f_{\text{NL}}^{\text{local}} = 0.015$ for $n_s = 0.963$. In contrast, the large local-type non-Gaussianity will be able to be realized in the models with multiple light fields during inflation [25–35], the curvaton scenario [36–38], inhomogeneous reheating [39, 40].

4.2.2 Equilateral type

The equilateral bispectrum is parametrized as [41]

$$S^{\text{equil}}(k_1, k_2, k_3) = 6 \left[\left\{ -\frac{1}{(k_1 k_2)^3} + 2 \text{ perms.} \right\} - \frac{2}{(k_1 k_2 k_3)^2} + \left\{ \frac{1}{k_1 k_2^2 k_3^3} + 5 \text{ perms.} \right\} \right] . \quad (4.10)$$

This function approximately expresses the bispectra arising from the inflation models where the scalar fields have non-canonical kinetic terms. An example is the so-called Dirac-Born-Infeld (DBI) inflation [42, 43], where $f_{\text{NL}}^{\text{equil}} \propto -1/c_s^2$ for $c_s \ll 1$ with c_s being the effective sound speed at which

the scalar field fluctuations propagate. We can also find a lot of other models that can produce large $f_{\text{NL}}^{\text{equil}}$ [44–48]. The normalized equilateral spectrum $S^{\text{equil}}(k_1, k_2, k_3)(k_2/k_1)^2(k_3/k_1)^2$, peaks at the equilateral limit, namely, $k_1 = k_2 = k_3$ as described in the bottom-left panel of Fig. 4.2. The local- and equilateral-type bispectra are nearly orthogonal to each other, which denotes that both can be measured almost independently.

In Sec. 8, we confirm that the graviton non-Gaussianity originated from the Weyl cubic action is also categorized as the equilateral type.

4.2.3 Orthogonal type

In addition to the local- and equilateral-type non-Gaussianities, we have the following parametrization:

$$S^{\text{orthog}}(k_1, k_2, k_3) = 6 \left[\left\{ -\frac{3}{(k_1 k_2)^3} + 2 \text{ perms.} \right\} - \frac{8}{(k_1 k_2 k_3)^2} + \left\{ \frac{3}{k_1 k_2^2 k_3^3} + 5 \text{ perms.} \right\} \right]. \quad (4.11)$$

This is the so called orthogonal-type non-Gaussianity and constructed such that it is nearly orthogonal to both the local-type and equilateral-type non-Gaussianities [49]. This shape approximately represents the forms appearing in a linear combination of the higher-derivative scalar-field interaction terms, each of which yields forms similar to the equilateral shape. In Ref. [49], the authors discovered that on the basis of the effective field theory of inflation approach [47], a certain linear combination of similarly equilateral shapes can lead to a distinct shape which is orthogonal to both the local and equilateral forms. The orthogonal bispectrum $S^{\text{orthog}}(k_1, k_2, k_3)(k_2/k_1)^2(k_3/k_1)^2$ has a positive peak at the equilateral configuration, and negative valley along the elongated configurations as seen in the top-right panel of Fig. 4.2.

4.3 Observational aspects

Observational limits on the primordial non-Gaussianities are beginning to reach the interesting levels. Using the optimal estimators [11, 49–52], the latest constraints on the nonlinearity parameters from the CMB data (WMAP 7-yr data) are obtained as [53]

$$-10 < f_{\text{NL}}^{\text{local}} < 74, \quad -214 < f_{\text{NL}}^{\text{equil}} < 266, \quad -410 < f_{\text{NL}}^{\text{orthog}} < 6 \quad (95\% \text{ CL}). \quad (4.12)$$

As another approach for extracting the non-Gaussianity from the CMB data, the methods with the Minkowski functionals have been developed [54–56].

The PLANCK satellite [57] and the proposed CMBPol mission [58] will give tighter bounds as $\sigma(f_{\text{NL}}^{\text{local}}) \sim 5$ and 2. At the level of $f_{\text{NL}}^{\text{local}} \sim \mathcal{O}(1)$, we expect to see a signal from the secondary effects not associated with the non-linear effects in inflation. In order not to confuse these effects with the primordial signals, some researchers have been estimating in detail how the gravitational non-linear evolution of the fluctuations can induce its own non-Gaussianity (see, e.g., [59–62]).

In addition, the primordial non-Gaussianity also leaves the signatures in the large scale structure in the Universe. In general, extracting the information of the primordial non-Gaussianity from the observational data of the large scale structure is complicated due to the fact that the gravitational nonlinear evolution of the density fluctuations produces the secondary non-Gaussianity completely dominating over the signals from the primordial origin. However, recently, the scale-dependent bias has been considered as a promising probe of the primordial non-Gaussianity [63, 64]. In these

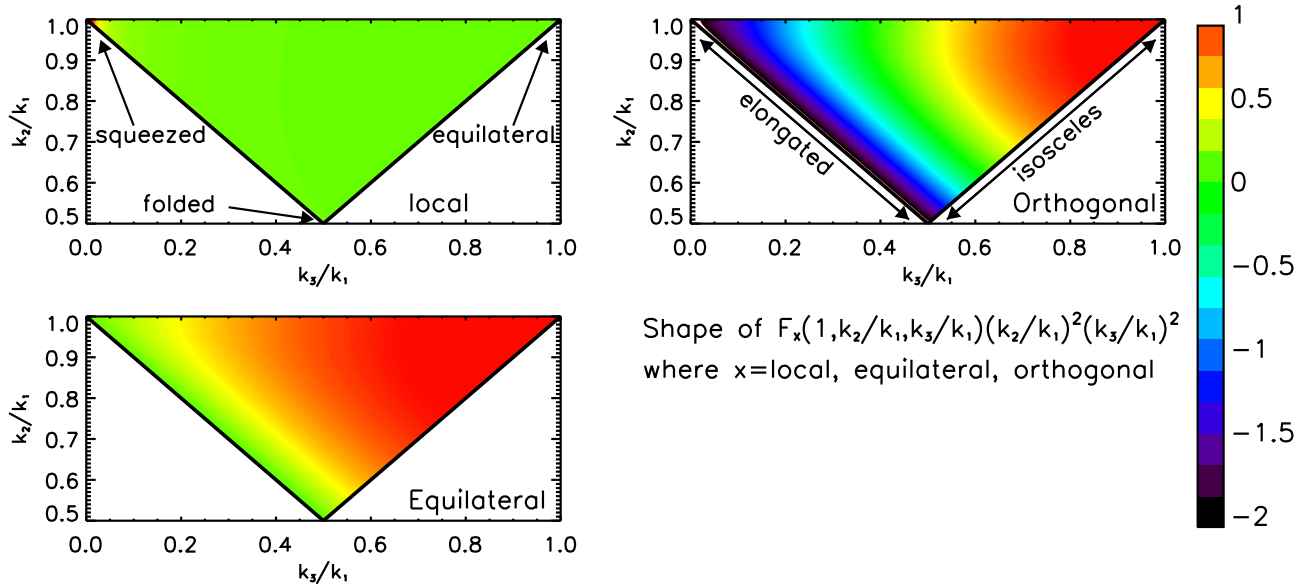


Figure 4.2: Two dimensional color contour for the shapes of the primordial bispectra. Each panel describes the normalized amplitude of $S(k_1, k_2, k_3)(k_2/k_1)^2(k_3/k_1)^2$ as a function of k_2/k_1 and k_3/k_1 for $k_3 \leq k_2 \leq k_1$. Since the primordial bispectra shown here are nearly scale invariant, the shapes may look similar regardless of the values of k_1 . The amplitude is normalized by a rule that it is unity at the point where $S(k_1, k_2, k_3)(k_2/k_1)^2(k_3/k_1)^2$ takes on the maximum value. The top-left panel is the local form given by Eq. (4.7), which peaks at the squeezed configuration. The bottom-left panel is the equilateral form given by Eq. (4.10), which peaks at the equilateral configuration. The top-right panel is the orthogonal form given by Eq. (4.11), which has a positive peak at the equilateral configuration, and a negative valley along the elongated configurations. Note that all of these shapes are almost orthogonal to each other. This is quoted in Ref. [11].

papers, it has been confirmed that for highly biased tracers of the underlying density field, the bias parameter depends on scale and f_{NL} , namely,

$$P_{\delta_{\text{gal}}}(k) = [b + \Delta b(k, f_{\text{NL}}^{\text{local}})]^2 P_{\delta}(k) . \quad (4.13)$$

Application of the method to the luminous red galaxies (LRGs) sample of SDSS leads to a bound as [64]

$$-29 < f_{\text{NL}}^{\text{local}} < 70 \quad (95\% \text{ CL}) . \quad (4.14)$$

As one see, this limit is comparable to the bounds from the CMB data. The way to extract the information on the primordial non-Gaussianity from the matter distribution has continuously been studied (see, e.g., Refs. [65–67]).

4.4 Beyond the standard scalar-mode non-Gaussianities

Historically, as described above, only the non-Gaussianity of curvature perturbations has been well-known studied. However, the non-Gaussianity of vector- or tensor-mode perturbation can be generated from the cosmological defects [68, 69], the magnetic fields [70], the nonlinear gravitational waves [12, 71–74], and so on. Furthermore, somewhat exotic non-Gaussianities including the violation of the rotational or parity invariance in the early Universe have recently been discussed

(see, e.g., Refs. [72, 75–77]). Hence, for precise comprehension of the early Universe, detailed analyses of these signals are necessary.

This is the main motivation of our studies: construction of the general formulae for the CMB bispectrum with not only scalar- but also vector- and tensor-mode contributions, and computation and analysis of the CMB bispectrum sources from these novel non-Gaussianities. In the following sections, we focus on our studies.

References

- [1] E. Komatsu, N. Afshordi, N. Bartolo, D. Baumann, J. Bond, *et al.*, *Non-Gaussianity as a Probe of the Physics of the Primordial Universe and the Astrophysics of the Low Redshift Universe*, [arXiv:0902.4759](#).
- [2] P. Creminelli and L. Senatore, *A Smooth bouncing cosmology with scale invariant spectrum*, *JCAP* **0711** (2007) 010, [[hep-th/0702165](#)].
- [3] K. Koyama, S. Mizuno, F. Vernizzi, and D. Wands, *Non-Gaussianities from ekpyrotic collapse with multiple fields*, *JCAP* **0711** (2007) 024, [[arXiv:0708.4321](#)].
- [4] E. I. Buchbinder, J. Khoury, and B. A. Ovrut, *Non-Gaussianities in New Ekpyrotic Cosmology*, *Phys. Rev. Lett.* **100** (2008) 171302, [[arXiv:0710.5172](#)].
- [5] J.-L. Lehnert and P. J. Steinhardt, *Non-Gaussian density fluctuations from entropically generated curvature perturbations in Ekpyrotic models*, *Phys.Rev.* **D77** (2008) 063533, [[arXiv:0712.3779](#)].
- [6] J.-L. Lehnert and P. J. Steinhardt, *Intuitive understanding of non-gaussianity in ekpyrotic and cyclic models*, *Phys.Rev.* **D78** (2008) 023506, [[arXiv:0804.1293](#)].
- [7] K. Koyama, S. Mizuno, and D. Wands, *Curvature perturbations from ekpyrotic collapse with multiple fields*, *Class.Quant.Grav.* **24** (2007) 3919–3932, [[arXiv:0704.1152](#)].
- [8] K. Koyama and D. Wands, *Ekpyrotic collapse with multiple fields*, *JCAP* **0704** (2007) 008, [[hep-th/0703040](#)].
- [9] D. Baumann, *TASI Lectures on Inflation*, [arXiv:0907.5424](#).
- [10] N. Bartolo, E. Komatsu, S. Matarrese, and A. Riotto, *Non-Gaussianity from inflation: Theory and observations*, *Phys. Rept.* **402** (2004) 103–266, [[astro-ph/0406398](#)].
- [11] E. Komatsu, *Hunting for Primordial Non-Gaussianity in the Cosmic Microwave Background*, *Class. Quant. Grav.* **27** (2010) 124010, [[arXiv:1003.6097](#)].
- [12] J. M. Maldacena, *Non-Gaussian features of primordial fluctuations in single field inflationary models*, *JHEP* **05** (2003) 013, [[astro-ph/0210603](#)].
- [13] J. S. Schwinger, *Brownian motion of a quantum oscillator*, *J.Math.Phys.* **2** (1961) 407–432.
- [14] E. Calzetta and B. Hu, *Closed Time Path Functional Formalism in Curved Space-Time: Application to Cosmological Back Reaction Problems*, *Phys.Rev.* **D35** (1987) 495.

- [15] R. Jordan, *Effective Field Equations for Expectation Values*, *Phys.Rev.* **D33** (1986) 444–454.
- [16] S. Weinberg, *Quantum contributions to cosmological correlations*, *Phys. Rev.* **D72** (2005) 043514, [[hep-th/0506236](#)].
- [17] D. Babich, P. Creminelli, and M. Zaldarriaga, *The shape of non-Gaussianities*, *JCAP* **0408** (2004) 009, [[astro-ph/0405356](#)].
- [18] J. Fergusson and E. Shellard, *The shape of primordial non-Gaussianity and the CMB bispectrum*, *Phys.Rev.* **D80** (2009) 043510, [[arXiv:0812.3413](#)].
- [19] D. Jeong and E. Komatsu, *Perturbation Theory Reloaded II: Non-linear Bias, Baryon Acoustic Oscillations and Millennium Simulation In Real Space*, *Astrophys.J.* **691** (2009) 569–595, [[arXiv:0805.2632](#)].
- [20] E. Komatsu and D. N. Spergel, *Acoustic signatures in the primary microwave background bispectrum*, *Phys. Rev.* **D63** (2001) 063002, [[astro-ph/0005036](#)].
- [21] D. Salopek and J. Bond, *Nonlinear evolution of long wavelength metric fluctuations in inflationary models*, *Phys.Rev.* **D42** (1990) 3936–3962.
- [22] T. Falk, R. Rangarajan, and M. Srednicki, *The Angular dependence of the three point correlation function of the cosmic microwave background radiation as predicted by inflationary cosmologies*, *Astrophys.J.* **403** (1993) L1, [[astro-ph/9208001](#)].
- [23] A. Gangui, F. Lucchin, S. Matarrese, and S. Mollerach, *The Three point correlation function of the cosmic microwave background in inflationary models*, *Astrophys.J.* **430** (1994) 447–457, [[astro-ph/9312033](#)].
- [24] V. Acquaviva, N. Bartolo, S. Matarrese, and A. Riotto, *Second order cosmological perturbations from inflation*, *Nucl.Phys.* **B667** (2003) 119–148, [[astro-ph/0209156](#)].
- [25] N. Bartolo, S. Matarrese, and A. Riotto, *Non-Gaussianity from inflation*, *Phys. Rev.* **D65** (2002) 103505, [[hep-ph/0112261](#)].
- [26] F. Bernardeau and J.-P. Uzan, *NonGaussianity in multifield inflation*, *Phys.Rev.* **D66** (2002) 103506, [[hep-ph/0207295](#)].
- [27] F. Bernardeau and J.-P. Uzan, *Inflationary models inducing non-Gaussian metric fluctuations*, *Phys.Rev.* **D67** (2003) 121301, [[astro-ph/0209330](#)].
- [28] M. Sasaki, *Multi-brid inflation and non-Gaussianity*, *Prog.Theor.Phys.* **120** (2008) 159–174, [[arXiv:0805.0974](#)].
- [29] A. Naruko and M. Sasaki, *Large non-Gaussianity from multi-brid inflation*, *Prog.Theor.Phys.* **121** (2009) 193–210, [[arXiv:0807.0180](#)].
- [30] C. T. Byrnes, K.-Y. Choi, and L. M. Hall, *Conditions for large non-Gaussianity in two-field slow-roll inflation*, *JCAP* **0810** (2008) 008, [[arXiv:0807.1101](#)].
- [31] C. T. Byrnes and D. Wands, *Curvature and isocurvature perturbations from two-field inflation in a slow-roll expansion*, *Phys.Rev.* **D74** (2006) 043529, [[astro-ph/0605679](#)].

- [32] H. Assadullahi, J. Valiviita, and D. Wands, *Primordial non-Gaussianity from two curvaton decays*, *Phys.Rev.* **D76** (2007) 103003, [arXiv:0708.0223].
- [33] J. Valiviita, M. Sasaki, and D. Wands, *Non-Gaussianity and constraints for the variance of perturbations in the curvaton model*, *astro-ph/0610001*.
- [34] F. Vernizzi and D. Wands, *Non-gaussianities in two-field inflation*, *JCAP* **0605** (2006) 019, [astro-ph/0603799].
- [35] L. E. Allen, S. Gupta, and D. Wands, *Non-gaussian perturbations from multi-field inflation*, *JCAP* **0601** (2006) 006, [astro-ph/0509719].
- [36] A. D. Linde and V. F. Mukhanov, *Nongaussian isocurvature perturbations from inflation*, *Phys.Rev.* **D56** (1997) 535–539, [astro-ph/9610219].
- [37] T. Moroi and T. Takahashi, *Effects of cosmological moduli fields on cosmic microwave background*, *Phys.Lett.* **B522** (2001) 215–221, [hep-ph/0110096].
- [38] D. H. Lyth, C. Ungarelli, and D. Wands, *The Primordial density perturbation in the curvaton scenario*, *Phys.Rev.* **D67** (2003) 023503, [astro-ph/0208055].
- [39] G. Dvali, A. Gruzinov, and M. Zaldarriaga, *A new mechanism for generating density perturbations from inflation*, *Phys.Rev.* **D69** (2004) 023505, [astro-ph/0303591].
- [40] L. Kofman, *Probing string theory with modulated cosmological fluctuations*, *astro-ph/0303614*.
- [41] P. Creminelli, A. Nicolis, L. Senatore, M. Tegmark, and M. Zaldarriaga, *Limits on non-Gaussianities from WMAP data*, *JCAP* **0605** (2006) 004, [astro-ph/0509029].
- [42] M. Alishahiha, E. Silverstein, and D. Tong, *DBI in the sky*, *Phys. Rev.* **D70** (2004) 123505, [hep-th/0404084].
- [43] E. Silverstein and D. Tong, *Scalar Speed Limits and Cosmology: Acceleration from D-celeration*, *Phys. Rev.* **D70** (2004) 103505, [hep-th/0310221].
- [44] N. Arkani-Hamed, P. Creminelli, S. Mukohyama, and M. Zaldarriaga, *Ghost Inflation*, *JCAP* **0404** (2004) 001, [hep-th/0312100].
- [45] D. Seery and J. E. Lidsey, *Primordial non-Gaussianities in single field inflation*, *JCAP* **0506** (2005) 003, [astro-ph/0503692].
- [46] X. Chen, M.-x. Huang, S. Kachru, and G. Shiu, *Observational signatures and non-Gaussianities of general single field inflation*, *JCAP* **0701** (2007) 002, [hep-th/0605045].
- [47] C. Cheung, P. Creminelli, A. L. Fitzpatrick, J. Kaplan, and L. Senatore, *The Effective Field Theory of Inflation*, *JHEP* **03** (2008) 014, [arXiv:0709.0293].
- [48] M. Li, T. Wang, and Y. Wang, *General Single Field Inflation with Large Positive Non-Gaussianity*, *JCAP* **0803** (2008) 028, [arXiv:0801.0040].

- [49] L. Senatore, K. M. Smith, and M. Zaldarriaga, *Non-Gaussianities in Single Field Inflation and their Optimal Limits from the WMAP 5-year Data*, *JCAP* **1001** (2010) 028, [[arXiv:0905.3746](#)].
- [50] A. P. Yadav, E. Komatsu, and B. D. Wandelt, *Fast Estimator of Primordial Non-Gaussianity from Temperature and Polarization Anisotropies in the Cosmic Microwave Background*, *Astrophys.J.* **664** (2007) 680–686, [[astro-ph/0701921](#)]. PhD Thesis (Advisor: Alfonso Arag on-Salamanca).
- [51] A. P. Yadav, E. Komatsu, B. D. Wandelt, M. Liguori, F. K. Hansen, *et al.*, *Fast Estimator of Primordial Non-Gaussianity from Temperature and Polarization Anisotropies in the Cosmic Microwave Background II: Partial Sky Coverage and Inhomogeneous Noise*, *Astrophys.J.* **678** (2008) 578–582, [[arXiv:0711.4933](#)].
- [52] K. M. Smith, L. Senatore, and M. Zaldarriaga, *Optimal limits on f_{NL}^{local} from WMAP 5-year data*, *JCAP* **0909** (2009) 006, [[arXiv:0901.2572](#)].
- [53] **WMAP** Collaboration, E. Komatsu *et al.*, *Seven-Year Wilkinson Microwave Anisotropy Probe (WMAP) Observations: Cosmological Interpretation*, *Astrophys. J. Suppl.* **192** (2011) 18, [[arXiv:1001.4538](#)].
- [54] H. K. Eriksen, D. Novikov, P. Lilje, A. Banday, and K. Gorski, *Testing for non-Gaussianity in the WMAP data: Minkowski functionals and the length of the skeleton*, *Astrophys.J.* **612** (2004) 64–80, [[astro-ph/0401276](#)].
- [55] C. Hikage, T. Matsubara, P. Coles, M. Liguori, F. K. Hansen, *et al.*, *Limits on Primordial Non-Gaussianity from Minkowski Functionals of the WMAP Temperature Anisotropies*, *Mon.Not.Roy.Astron.Soc.* **389** (2008) 1439–1446, [[arXiv:0802.3677](#)].
- [56] T. Matsubara, *Analytic Minkowski Functionals of the Cosmic Microwave Background: Second-order Non-Gaussianity with Bispectrum and Trispectrum*, *Phys.Rev.* **D81** (2010) 083505, [[arXiv:1001.2321](#)].
- [57] **PLANCK** Collaboration, *The Scientific programme of planck*, [astro-ph/0604069](#).
- [58] **CMBPol Study Team** Collaboration, D. Baumann *et al.*, *CMBPol Mission Concept Study: Probing Inflation with CMB Polarization*, *AIP Conf.Proc.* **1141** (2009) 10–120, [[arXiv:0811.3919](#)].
- [59] N. Bartolo and A. Riotto, *On the non-Gaussianity from Recombination*, *JCAP* **0903** (2009) 017, [[arXiv:0811.4584](#)].
- [60] C. Pitrou, *The radiative transfer at second order: a full treatment of the Boltzmann equation with polarization*, *Class. Quant. Grav.* **26** (2009) 065006, [[arXiv:0809.3036](#)].
- [61] D. Nitta, E. Komatsu, N. Bartolo, S. Matarrese, and A. Riotto, *CMB anisotropies at second order III: bispectrum from products of the first-order perturbations*, *JCAP* **0905** (2009) 014, [[arXiv:0903.0894](#)].
- [62] C. Pitrou, J.-P. Uzan, and F. Bernardeau, *The cosmic microwave background bispectrum from the non-linear evolution of the cosmological perturbations*, *JCAP* **1007** (2010) 003, [[arXiv:1003.0481](#)].

- [63] N. Dalal, O. Dore, D. Huterer, and A. Shirokov, *The imprints of primordial non-gaussianities on large-scale structure: scale dependent bias and abundance of virialized objects*, *Phys.Rev.* **D77** (2008) 123514, [[arXiv:0710.4560](#)].
- [64] A. Slosar, C. Hirata, U. Seljak, S. Ho, and N. Padmanabhan, *Constraints on local primordial non-Gaussianity from large scale structure*, *JCAP* **0808** (2008) 031, [[arXiv:0805.3580](#)].
- [65] Y. Takeuchi, K. Ichiki, and T. Matsubara, *Constraints on primordial non-Gaussianity from Galaxy-CMB lensing cross-correlation*, *Phys.Rev.* **D82** (2010) 023517, [[arXiv:1005.3492](#)].
- [66] J.-O. Gong and S. Yokoyama, *Scale-dependent bias from primordial non-Gaussianity with trispectrum*, *MNRAS* **417** (Oct., 2011) L79–L82, [[arXiv:1106.4404](#)].
- [67] S. Yokoyama, *Scale-dependent bias from the primordial non-Gaussianity with a Gaussian-squared field*, *JCAP* **1111** (2011) 001, [[arXiv:1108.5569](#)].
- [68] K. Takahashi *et al.*, *Non-Gaussianity in Cosmic Microwave Background Temperature Fluctuations from Cosmic (Super-)Strings*, *JCAP* **0910** (2009) 003, [[arXiv:0811.4698](#)].
- [69] M. Hindmarsh, C. Ringeval, and T. Suyama, *The CMB temperature bispectrum induced by cosmic strings*, *Phys. Rev.* **D80** (2009) 083501, [[arXiv:0908.0432](#)].
- [70] I. Brown and R. Crittenden, *Non-Gaussianity from Cosmic Magnetic Fields*, *Phys. Rev.* **D72** (2005) 063002, [[astro-ph/0506570](#)].
- [71] P. Adshead and E. A. Lim, *3-pt Statistics of Cosmological Stochastic Gravitational Waves*, *Phys. Rev.* **D82** (2010) 024023, [[arXiv:0912.1615](#)].
- [72] J. M. Maldacena and G. L. Pimentel, *On graviton non-Gaussianities during inflation*, *JHEP* **1109** (2011) 045, [[arXiv:1104.2846](#)].
- [73] P. McFadden and K. Skenderis, *Cosmological 3-point correlators from holography*, *JCAP* **1106** (2011) 030, [[arXiv:1104.3894](#)].
- [74] X. Gao, T. Kobayashi, M. Yamaguchi, and J. Yokoyama, *Primordial non-Gaussianities of gravitational waves in the most general single-field inflation model*, *Phys.Rev.Lett.* **107** (2011) 211301, [[arXiv:1108.3513](#)].
- [75] S. Yokoyama and J. Soda, *Primordial statistical anisotropy generated at the end of inflation*, *JCAP* **0808** (2008) 005, [[arXiv:0805.4265](#)].
- [76] K. Dimopoulos, M. Karciauskas, D. H. Lyth, and Y. Rodriguez, *Statistical anisotropy of the curvature perturbation from vector field perturbations*, *JCAP* **0905** (2009) 013, [[arXiv:0809.1055](#)].
- [77] J. Soda, H. Kodama, and M. Nozawa, *Parity Violation in Graviton Non-gaussianity*, *JHEP* **1108** (2011) 067, [[arXiv:1106.3228](#)].

5 General formalism for the CMB bispectrum from primordial scalar, vector and tensor non-Gaussianities

In this section, on the basis of the formulation of the CMB anisotropy in Sec. 3, we develop the formulae for the CMB bispectrum sourced from scalar-, vector-, and tensor-mode non-Gaussianity. These results have been published in our paper [1].

At first, we should remember an expression of CMB fluctuation discussed in Sec. 3. In the all-sky analysis, the CMB fluctuations of intensity, and E and B -mode polarizations are expanded with the spin-0 spherical harmonics, respectively. Then, the coefficients of CMB fluctuations, called $a_{\ell m}$'s, are described as

$$a_{X,\ell m}^{(Z)} = 4\pi(-i)^\ell \int \frac{d^3\mathbf{k}}{(2\pi)^3} \sum_\lambda [\text{sgn}(\lambda)]^{\lambda+x} {}_{-\lambda}Y_{\ell m}^*(\hat{\mathbf{k}}) \xi^{(\lambda)}(\mathbf{k}) \mathcal{T}_{X,\ell}^{(Z)}(k) , \quad (5.1)$$

where the index Z denotes the mode of perturbations: $Z = S$ (scalar), $= V$ (vector) or $= T$ (tensor) and its helicity is expressed by λ ; $\lambda = 0$ for $Z = S$, $= \pm 1$ for $Z = V$ or $= \pm 2$ for $Z = T$, X discriminates between intensity and two polarization (electric and magnetic) modes, respectively, as $X = I, E, B$ and x is determined by it: $x = 0$ for $X = I, E$ or $= 1$ for $X = B$, $\xi^{(\lambda)}$ is the initial perturbation decomposed on each helicity state and $\mathcal{T}_{X,\ell}^{(Z)}$ is the time-integrated transfer function in each sector given by Eq. (3.101)¹.

Next, we expand $\xi^{(\lambda)}$ with spin- $(-\lambda)$ spherical harmonics as

$$\xi^{(\lambda)}(\mathbf{k}) \equiv \sum_{\ell m} \xi_{\ell m}^{(\lambda)}(k) {}_{-\lambda}Y_{\ell m}(\hat{\mathbf{k}}) , \quad (5.2)$$

and eliminate the angular dependence in Eq. (5.1) by performing $\hat{\mathbf{k}}$ -integral:

$$a_{X,\ell m}^{(Z)} = 4\pi(-i)^\ell \int_0^\infty \frac{k^2 dk}{(2\pi)^3} \sum_\lambda [\text{sgn}(\lambda)]^{\lambda+x} \xi_{\ell m}^{(\lambda)}(k) \mathcal{T}_{X,\ell}^{(Z)}(k) . \quad (5.3)$$

Here, we use the orthogonality relation of the spin- λ spherical harmonics described in Appendix A as

$$\int d^2\hat{\mathbf{n}} {}_{\lambda}Y_{\ell' m'}^*(\hat{\mathbf{n}}) {}_{\lambda}Y_{\ell m}(\hat{\mathbf{n}}) = \delta_{\ell, \ell'} \delta_{m, m'} . \quad (5.4)$$

Then the CMB bispectrum generated from the primordial non-Gaussianity of the scalar, vector and tensor perturbations is written down as

$$\begin{aligned} \left\langle \prod_{n=1}^3 a_{X_n, \ell_n m_n}^{(Z_n)} \right\rangle &= \left[\prod_{n=1}^3 4\pi(-i)^{\ell_n} \int_0^\infty \frac{k_n^2 dk_n}{(2\pi)^3} \mathcal{T}_{X_n, \ell_n}^{(Z_n)}(k_n) \sum_{\lambda_n} [\text{sgn}(\lambda_n)]^{\lambda_n+x_n} \right] \\ &\quad \times \left\langle \prod_{n=1}^3 \xi_{\ell_n m_n}^{(\lambda_n)}(k_n) \right\rangle , \\ \left\langle \prod_{n=1}^3 \xi_{\ell_n m_n}^{(\lambda_n)}(k_n) \right\rangle &= \left[\prod_{n=1}^3 \int d^2\hat{\mathbf{k}}_n {}_{-\lambda_n}Y_{\ell_n m_n}^*(\hat{\mathbf{k}}_n) \right] \left\langle \prod_{n=1}^3 \xi^{(\lambda_n)}(\mathbf{k}_n) \right\rangle . \end{aligned} \quad (5.5)$$

¹Here, we set $0^0 = 1$.

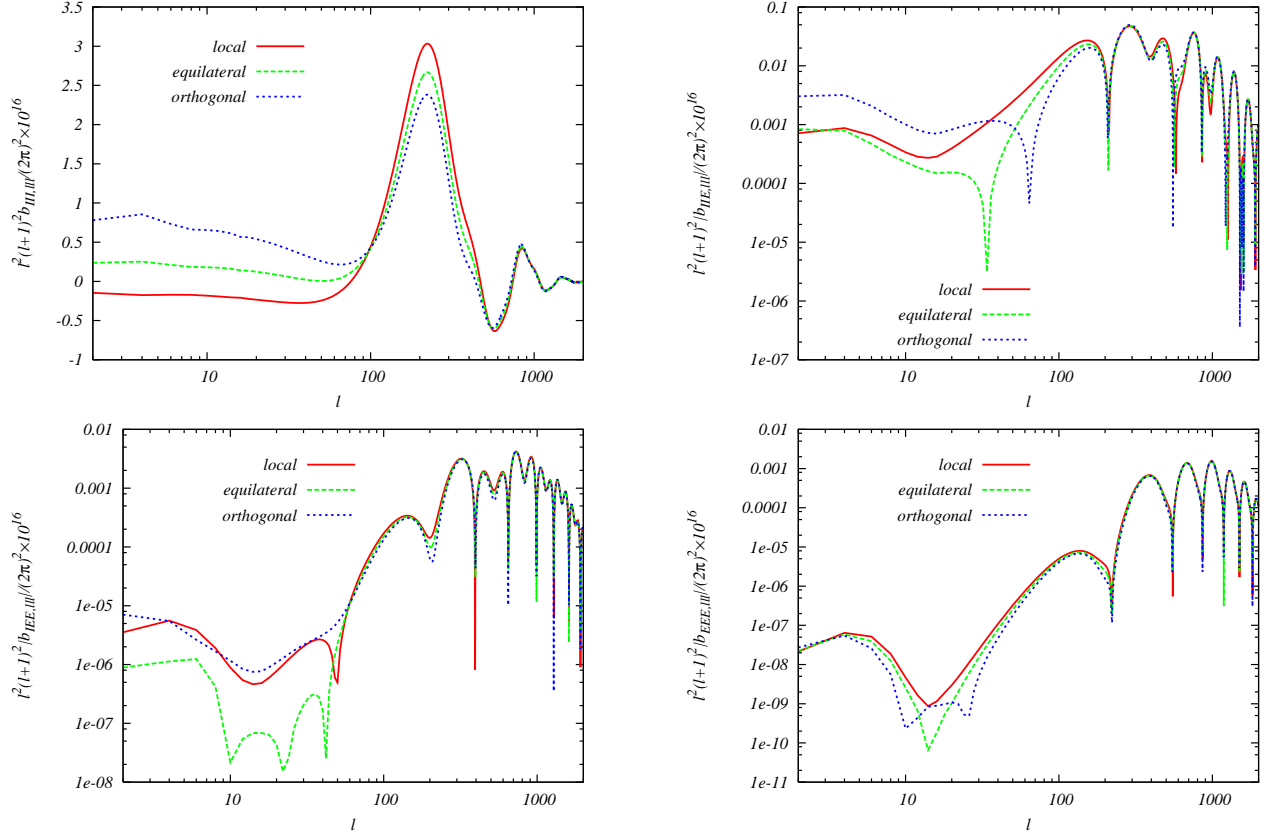


Figure 5.1: The CMB III (left top panel), IIE (right top one), IEE (left bottom one), and EEE (right bottom one) bispectra induced from the local-type (red solid line), equilateral-type (green dashed one), and orthogonal-type (blue dotted one) non-Gaussianities of curvature perturbations. The three multipoles are fixed as $\ell_1 = \ell_2 = \ell_3 \equiv \ell$. Here we consider a power-law flat Λ CDM model and fix the nonlinear parameters as $f_{\text{NL}}^{\text{local}} = f_{\text{NL}}^{\text{equil}} = f_{\text{NL}}^{\text{orthog}} = 100$. The other cosmological parameters are fixed to the mean values reported in Ref. [9].

This formalism will be applicable to diverse sources of the scalar, vector and tensor non-Gaussianities, such as, a scalar-graviton coupling [1] (Sec. 6), cosmic strings [2, 3], primordial magnetic fields [4–6] (Sec. 9), and statistically-anisotropic and parity-violating interactions [7, 8] (Secs. 7 and 8).

To compute the CMB bispectrum composed of arbitrary perturbation modes, we have to reduce the expanded primordial bispectrum, $\langle \prod_{n=1}^3 \xi_{\ell_n m_n}^{(\lambda_n)}(k_n) \rangle$, involving the contractions of the wave number vector and polarization vector and tensor, and the integrals over the angles of the wave number vectors. As shown later, this is elegantly completed by utilizing the Wigner symbols and spin-weighted spherical harmonics.

If the initial bispectrum satisfies the rotational invariance, the CMB bispectrum is divided into the Wigner- $3j$ symbol depending on the azimuthal quantum numbers and the angle-averaged function as

$$\left\langle \prod_{n=1}^3 a_{\ell_n m_n}^{(Z_n)} \right\rangle = \begin{pmatrix} \ell_1 & \ell_2 & \ell_3 \\ m_1 & m_2 & m_3 \end{pmatrix} B_{X_1 X_2 X_3, \ell_1 \ell_2 \ell_3}^{(Z_1 Z_2 Z_3)}. \quad (5.6)$$

Let us focus on the CMB bispectrum from the curvature perturbations. Then, from Eqs. (4.2), (4.4), (4.7), (4.10), (4.11), (5.5), (5.6) and the knowledge of Appendix C, we derive the reduced

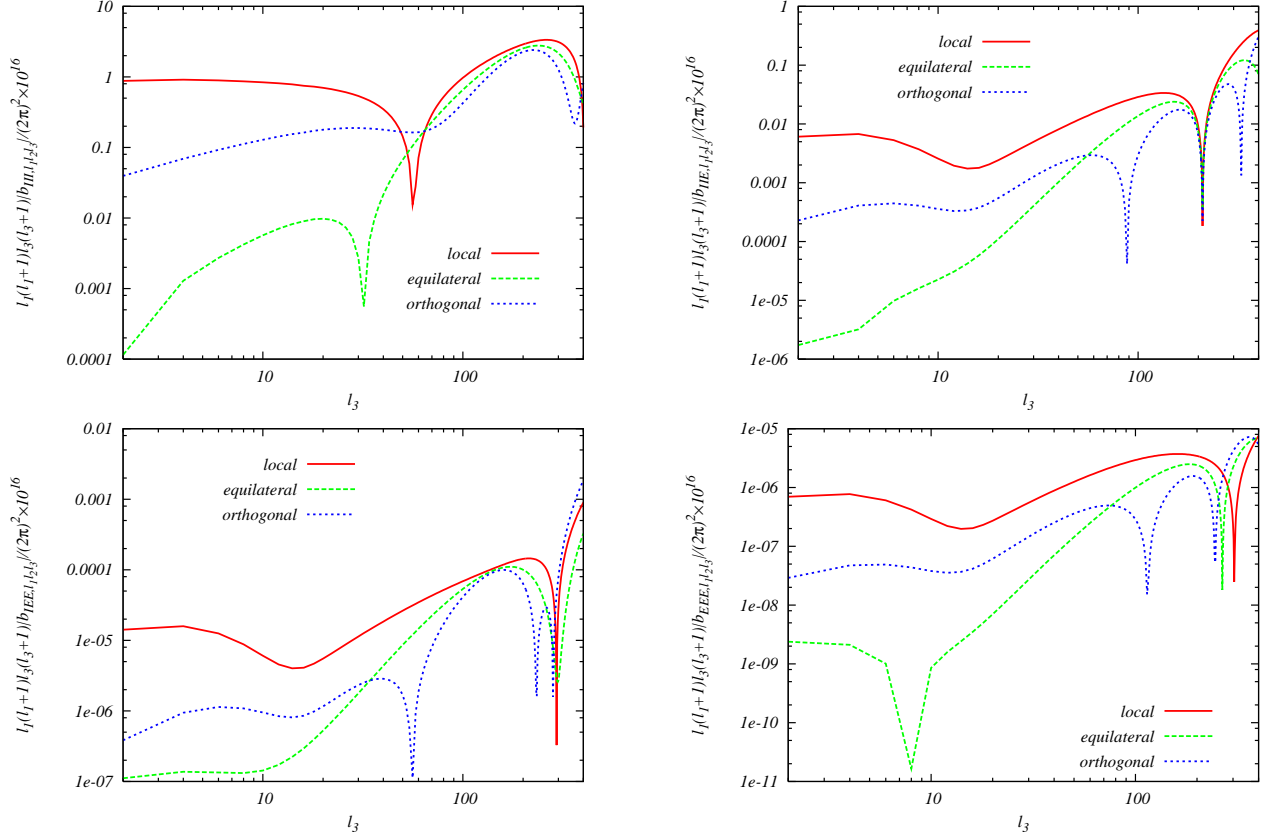


Figure 5.2: The CMB III (left top panel), IIE (right top one), IEE (left bottom one), and EEE (right bottom one) bispectra induced from the local-type (red solid line), equilateral-type (green dashed one), and orthogonal-type (blue dotted one) non-Gaussianities of curvature perturbations with $f_{\text{NL}}^{\text{local}} = f_{\text{NL}}^{\text{equil}} = f_{\text{NL}}^{\text{orthog}} = 100$. Here, we fix the two multipoles as $\ell_1 = \ell_2 = 200$, and plot each curve as the function in terms of ℓ_3 . The cosmological parameters are identical to those in Fig. 5.1.

bispectra as

$$\begin{aligned}
 b_{X_1 X_2 X_3, \ell_1 \ell_2 \ell_3}^{(SSS)} &= (I_{\ell_1 \ell_2 \ell_3}^{0 \ 0 \ 0})^{-1} B_{X_1 X_2 X_3, \ell_1 \ell_2 \ell_3}^{(SSS)} \\
 &= \int_0^\infty y^2 dy \left[\prod_{n=1}^3 \frac{2}{\pi} \int_0^\infty k_n^2 dk_n \mathcal{T}_{X_n, \ell_n}^{(S)}(k_n) j_{\ell_n}(k_n y) \right] F^{000}(k_1, k_2, k_3), \quad (5.7)
 \end{aligned}$$

where we have introduced the I symbol as

$$I_{\ell_1 \ell_2 \ell_3}^{s_1 s_2 s_3} \equiv \sqrt{\frac{(2\ell_1 + 1)(2\ell_2 + 1)(2\ell_3 + 1)}{4\pi}} \begin{pmatrix} \ell_1 & \ell_2 & \ell_3 \\ s_1 & s_2 & s_3 \end{pmatrix}. \quad (5.8)$$

In Figs. 5.1 and 5.2, we plot these CMB bispectra for each multipole configuration. From these, one can see that depending on the shape of the primordial non-Gaussianity, the overall magnitudes of the bispectra do not change, but the shapes in ℓ space change. Comparing these with the CMB data, the bounds on the nonlinearity parameters (4.12) are obtained.

In this simple CMB bispectrum, there exists no dependence of the initial bispectrum on the polarization vector and tensor, hence we can derive the above formulae easily. Considering the

vector- and tensor-mode contributions in the CMB bispectrum, however, the computation becomes so cumbersome due to the complicated angular dependence of the polarization vector and tensor. This difficulty is also true for the bispectrum where the rotational or parity invariance is broken. From the next section, we deal with these complicated bispectra depending on the several scenarios by applying the wonderful mathematical tools such as the Wigner symbols and the spin-weighted spherical harmonics.

References

- [1] M. Shiraishi, D. Nitta, S. Yokoyama, K. Ichiki, and K. Takahashi, *CMB Bispectrum from Primordial Scalar, Vector and Tensor non-Gaussianities*, *Prog. Theor. Phys.* **125** (2011) 795–813, [[arXiv:1012.1079](#)].
- [2] K. Takahashi *et al.*, *Non-Gaussianity in Cosmic Microwave Background Temperature Fluctuations from Cosmic (Super-)Strings*, *JCAP* **0910** (2009) 003, [[arXiv:0811.4698](#)].
- [3] M. Hindmarsh, C. Ringeval, and T. Suyama, *The CMB temperature bispectrum induced by cosmic strings*, *Phys. Rev.* **D80** (2009) 083501, [[arXiv:0908.0432](#)].
- [4] M. Shiraishi, D. Nitta, S. Yokoyama, K. Ichiki, and K. Takahashi, *Cosmic microwave background bispectrum of vector modes induced from primordial magnetic fields*, *Phys. Rev.* **D82** (2010) 121302, [[arXiv:1009.3632](#)].
- [5] M. Shiraishi, D. Nitta, S. Yokoyama, K. Ichiki, and K. Takahashi, *Computation approach for CMB bispectrum from primordial magnetic fields*, *Phys. Rev.* **D83** (2011) 123523, [[arXiv:1101.5287](#)].
- [6] M. Shiraishi, D. Nitta, S. Yokoyama, K. Ichiki, and K. Takahashi, *Cosmic microwave background bispectrum of tensor passive modes induced from primordial magnetic fields*, *Phys. Rev.* **D83** (2011) 123003, [[arXiv:1103.4103](#)].
- [7] M. Shiraishi and S. Yokoyama, *Violation of the Rotational Invariance in the CMB Bispectrum*, *Prog.Theor.Phys.* **126** (2011) 923–935, [[arXiv:1107.0682](#)].
- [8] M. Shiraishi, D. Nitta, and S. Yokoyama, *Parity Violation of Gravitons in the CMB Bispectrum*, *Prog.Theor.Phys.* **126** (2011) 937–959, [[arXiv:1108.0175](#)].
- [9] **WMAP** Collaboration, E. Komatsu *et al.*, *Seven-Year Wilkinson Microwave Anisotropy Probe (WMAP) Observations: Cosmological Interpretation*, *Astrophys. J. Suppl.* **192** (2011) 18, [[arXiv:1001.4538](#)].

6 CMB bispectrum induced by the two scalars and a graviton correlator

In this section, adapting Eq. (5.5) to the primordial non-Gaussianity in two scalars and a graviton correlation [1], we compute the CMB scalar-scalar-tensor bispectrum. This discussion is based on our paper [2].

6.1 Two scalars and a graviton interaction during inflation

We consider a general single-field inflation model with Einstein-Hilbert action [3] :

$$S = \int d^4x \sqrt{-g} \left[\frac{M_{\text{pl}}^2}{2} R + p(\phi, X) \right] , \quad (6.1)$$

where g is the determinant of the metric, R is the Ricci scalar, $M_{\text{pl}}^2 \equiv 1/(8\pi G)$, ϕ is a scalar field, and $X \equiv -g^{\mu\nu} \partial_\mu \phi \partial_\nu \phi / 2$. Using the background equations, the slow-roll parameter and the sound speed for perturbations are given by

$$\epsilon \equiv -\frac{\dot{H}}{H^2} = \frac{X p_{,X}}{H^2 M_{\text{pl}}^2} , \quad c_s^2 \equiv \frac{p_{,X}}{2X p_{,XX} + p_{,X}} , \quad (6.2)$$

where H is the Hubble parameter, the dot means a derivative with respect to the physical time t and $p_{,X}$ denotes partial derivative of p with respect to X . We write a metric by ADM formalism

$$ds^2 = -N^2 dt^2 + a^2 e^{\gamma_{ab}} (dx^a + N^a dt)(dx^b + N^b dt) , \quad (6.3)$$

where N and N^a are respectively the lapse function and shift vector, γ_{ab} is a transverse and traceless tensor as $\gamma_{aa} = \partial_a \gamma_{ab} = 0$, and $e^{\gamma_{ab}} \equiv \delta_{ab} + \gamma_{ab} + \gamma_{ac} \gamma_{cb} / 2 + \dots$. On the flat hypersurface, the gauge-invariant curvature perturbation ζ is related to the first-order fluctuation of the scalar field φ as $\zeta = -H\varphi/\dot{\phi}$ ¹. Following the conversion equations (D.15) and (D.22), we decompose ζ and γ_{ab} into the helicity states as

$$\xi^{(0)}(\mathbf{k}) = \zeta(\mathbf{k}) , \quad \xi^{(\pm 2)}(\mathbf{k}) = \frac{1}{2} e_{ab}^{(\mp 2)}(\hat{\mathbf{k}}) \gamma_{ab}(\mathbf{k}) . \quad (6.4)$$

Here, $e_{ab}^{(\pm 2)}$ is a transverse and traceless polarization tensor explained in Appendix D. The interaction parts of this action have been derived by Maldacena [1] up to the third-order terms. In particular, we will focus on an interaction between two scalars and a graviton. This is because the correlation between a small wave number of the tensor mode and large wave numbers of the scalar modes will remain despite the tensor mode decays after the mode reenters the cosmic horizon. We find a leading term of the two scalars and a graviton interaction in the action coming from the matter part of the Lagrangian through X as

$$X|_{\text{3rd-order}} \supset a^{-2} \frac{p_{,X}}{2} \gamma_{ab} \partial_a \varphi \partial_b \varphi , \quad (6.5)$$

therefore, the interaction part is given by

$$S_{\text{int}} \supset \int d^4x a g_{tss} \gamma_{ab} \partial_a \zeta \partial_b \zeta . \quad (6.6)$$

¹Here, ζ and γ_{ab} are equivalent to \mathcal{R} and h_{ab} in Eq. (2.40), respectively.

Here, we introduce a coupling constant g_{tss} . From the definition of ζ, γ_{ab} and the slow-roll parameter, $g_{tss} = \epsilon$. For a general consideration, let us deal with g_{tss} as a free parameter. In this sense, constraining on this parameter may offer a probe of the nature of inflation and gravity in the early Universe. The primordial bispectrum is then computed using in-in formalism in the next subsection.

6.2 Calculation of the initial bispectrum

In the same manner as discussed in Ref. [1], we calculate the primordial bispectrum generated from two scalars and a graviton in the lowest order of the slow-roll parameter:

$$\begin{aligned} \langle \xi^{(\pm 2)}(\mathbf{k}_1) \xi^{(0)}(\mathbf{k}_2) \xi^{(0)}(\mathbf{k}_3) \rangle &= (2\pi)^3 F^{\pm 200}(\mathbf{k}_1, \mathbf{k}_2, \mathbf{k}_3) \delta \left(\sum_{n=1}^3 \mathbf{k}_n \right) , \\ F^{\pm 200}(\mathbf{k}_1, \mathbf{k}_2, \mathbf{k}_3) &\equiv \frac{4g_{tss} I(k_1, k_2, k_3) k_2 k_3}{\prod_i (2k_i^3)} \frac{H_*^4}{2c_{s*}^2 \epsilon_*^2 M_{\text{pl}}^4} e_{ab}^{(\mp 2)}(\hat{\mathbf{k}}_1) \hat{k}_{2a} \hat{k}_{3b} , \\ I(k_1, k_2, k_3) &\equiv -k_t + \frac{k_1 k_2 + k_2 k_3 + k_3 k_1}{k_t} + \frac{k_1 k_2 k_3}{k_t^2} , \end{aligned} \quad (6.7)$$

where $k_t \equiv k_1 + k_2 + k_3$, and $*$ means that it is evaluated at the time of horizon crossing, i.e., $a_* H_* = k$. Here, we keep the angular and polarization dependences, $e_{ab}^{(\mp 2)}(\hat{\mathbf{k}}_1) \hat{k}_{2a} \hat{k}_{3b}$, which have sometimes been omitted in the literature for simplicity [4–6]. We show, however, that expanding this term with spin-weighted spherical harmonics enables us to formulate the rotational-invariant bispectrum in an explicit way. The statistically isotropic power spectra of $\xi^{(0)}$ and $\xi^{(\pm 2)}$ are respectively given by

$$\begin{aligned} \langle \xi^{(0)}(\mathbf{k}) \xi^{(0)*}(\mathbf{k}') \rangle &\equiv (2\pi)^3 P_S(k) \delta(\mathbf{k} - \mathbf{k}') , \\ \frac{k^3 P_S(k)}{2\pi^2} &= \frac{H_*^2}{8\pi^2 c_{s*} \epsilon_* M_{\text{pl}}^2} \equiv A_S , \\ \langle \xi^{(\lambda)}(\mathbf{k}) \xi^{(\lambda')*}(\mathbf{k}') \rangle &\equiv (2\pi)^3 \frac{P_T(k)}{2} \delta(\mathbf{k} - \mathbf{k}') \delta_{\lambda, \lambda'} \text{ (for } \lambda, \lambda' = \pm 2) , \\ \frac{k^3 P_T(k)}{2\pi^2} &= \frac{H_*^2}{\pi^2 M_{\text{pl}}^2} = 8c_{s*} \epsilon_* A_S \equiv \frac{r}{2} A_S , \end{aligned} \quad (6.8)$$

where r is the tensor-to-scalar ratio and A_S is the amplitude of primordial curvature perturbations². Note that the power spectra satisfy the scale invariance because we consider them in the lowest order of the slow-roll parameter. Using these equations, we parametrize the initial bispectrum in this case from Eq. (6.7) as

$$F^{\pm 200}(\mathbf{k}_1, \mathbf{k}_2, \mathbf{k}_3) = f^{(TSS)}(k_1, k_2, k_3) e_{ab}^{(\mp 2)}(\hat{\mathbf{k}}_1) \hat{k}_{2a} \hat{k}_{3b} , \quad (6.9)$$

$$f^{(TSS)}(k_1, k_2, k_3) \equiv \frac{16\pi^4 A_S^2 g_{tss}}{k_1^2 k_2^2 k_3^2} \frac{I(k_1, k_2, k_3)}{k_t} \frac{k_t}{k_1} . \quad (6.10)$$

Note that $f^{(TSS)}$ seems not to depend on the tensor-to-scalar ratio. In Fig. 6.1, we show the shape of I/k_1 . From this, we confirm that the initial bispectrum $f^{(TSS)}$ (6.10) dominates in the squeezed limit as $k_1 \ll k_2 \simeq k_3$ like the local-type bispectrum of scalar modes given by Eq. (4.7).

²For $c_{s*} = 1$, these results are identical to Eqs. (2.59) and (2.68).

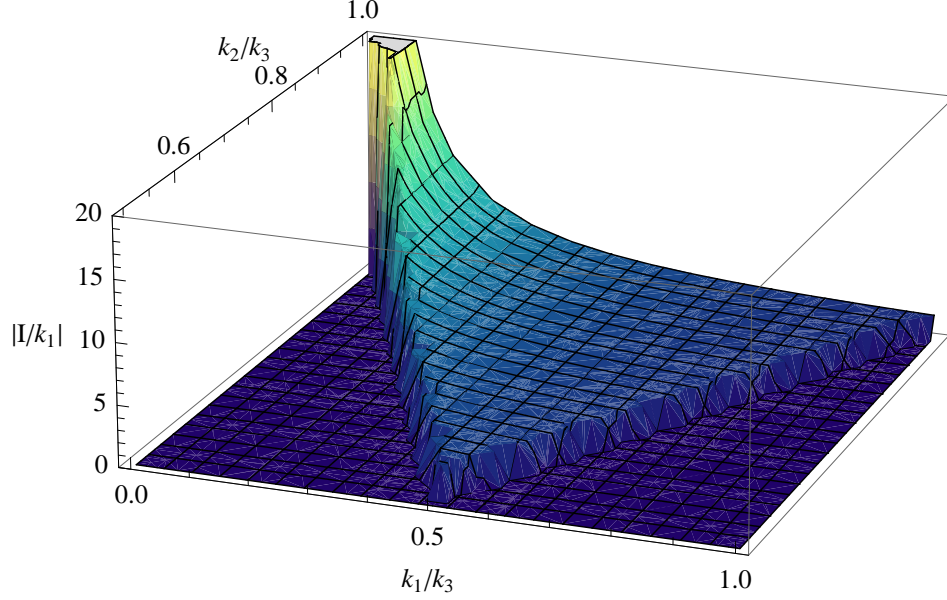


Figure 6.1: Shape of I/k_1 . For the symmetric property and the triangle condition, we limit the plot range as $k_1 \leq k_2 \leq k_3$ and $|k_1 - k_2| \leq k_3 \leq k_1 + k_2$.

In the squeezed limit, the ratio of $f^{(TSS)}$ to the scalar-scalar-scalar counterpart $f^{(SSS)} = \frac{6}{5}f_{\text{NL}}P_S(k_1)P_S(k_2)$, which has been considered frequently, reads

$$\frac{f^{(TSS)}}{f^{(SSS)}} = \frac{10g_{tss}}{3f_{\text{NL}}} \frac{I}{k_t} \frac{k_t k_2}{k_3^2} \rightarrow \frac{20g_{tss}}{3f_{\text{NL}}} \frac{I}{k_t}. \quad (6.11)$$

In the standard slow-roll inflation model, this ratio becomes $\mathcal{O}(1)$ and does not depend on the tensor-to-scalar ratio because g_{tss} and f_{NL} are proportional to the slow-roll parameter ϵ , and I/k_t has a nearly flat shape. The average of amplitude is evaluated as $I/k_t \approx -0.6537$. Therefore, it manifests the comparable importance of the higher order correlations of tensor modes to the scalar ones in the standard inflation scenario.

6.3 Formulation of the CMB bispectrum

Here, using Eqs. (5.5), (6.7) and (6.9), we explicitly calculate the CMB tensor-scalar-scalar bispectrum as

$$\begin{aligned} \left\langle a_{X_1, \ell_1 m_1}^{(T)} a_{X_2, \ell_2 m_2}^{(S)} a_{X_3, \ell_3 m_3}^{(S)} \right\rangle &= \left[\prod_{n=1}^3 4\pi (-i)^{\ell_n} \int_0^\infty \frac{k_n^2 dk_n}{(2\pi)^3} \mathcal{T}_{X_n, \ell_n}^{(Z_n)}(k_n) \right] \\ &\times \sum_{\lambda_1 = \pm 2} \left(\frac{\lambda_1}{2} \right)^{x_1} \left[\prod_{n=1}^3 \int d^2 \hat{\mathbf{k}}_n \right] {}_{-\lambda_1} Y_{\ell_1 m_1}^*(\hat{\mathbf{k}}_1) Y_{\ell_2 m_2}^*(\hat{\mathbf{k}}_2) Y_{\ell_3 m_3}^*(\hat{\mathbf{k}}_3) \\ &\times (2\pi)^3 f^{(TSS)}(k_1, k_2, k_3) e_{ab}^{(\mp 2)}(\hat{\mathbf{k}}_1) \hat{k}_{2a} \hat{k}_{3b} \delta \left(\prod_{n=1}^3 \mathbf{k}_n \right). \end{aligned} \quad (6.12)$$

At first, we express all parts containing the angular dependence with the spin spherical har-

monics³:

$$e_{ab}^{(\mp 2)}(\hat{\mathbf{k}}_1)\hat{k}_{2a}\hat{k}_{3b} = \frac{(8\pi)^{3/2}}{6} \sum_{M m_a m_b} \pm 2 Y_{2M}^*(\hat{\mathbf{k}}_1) Y_{1m_a}^*(\hat{\mathbf{k}}_2) Y_{1m_b}^*(\hat{\mathbf{k}}_3) \begin{pmatrix} 2 & 1 & 1 \\ M & m_a & m_b \end{pmatrix}, \quad (6.13)$$

$$\begin{aligned} \delta \left(\sum_{i=1}^3 \mathbf{k}_i \right) &= 8 \int_0^\infty y^2 dy \left[\prod_{i=1}^3 \sum_{L_i M_i} (-1)^{L_i/2} j_{L_i}(k_i y) Y_{L_i M_i}^*(\hat{\mathbf{k}}_i) \right] \\ &\quad \times I_{L_1 L_2 L_3}^{0 \ 0 \ 0} \begin{pmatrix} L_1 & L_2 & L_3 \\ M_1 & M_2 & M_3 \end{pmatrix}, \end{aligned} \quad (6.14)$$

where we used the relations listed in Appendices C and D and

$$I_{l_1 l_2 l_3}^{s_1 s_2 s_3} \equiv \sqrt{\frac{(2l_1+1)(2l_2+1)(2l_3+1)}{4\pi}} \begin{pmatrix} l_1 & l_2 & l_3 \\ s_1 & s_2 & s_3 \end{pmatrix}. \quad (6.15)$$

Secondly, using Eq. (C.8), we replace all the integrals of spin spherical harmonics with the Wigner symbols:

$$\begin{aligned} \int d^2 \hat{\mathbf{k}}_1 \mp 2 Y_{\ell_1 m_1}^*(\hat{\mathbf{k}}_1) Y_{L_1 M_1}^*(\hat{\mathbf{k}}_1) \pm 2 Y_{2M}^*(\hat{\mathbf{k}}_1) &= I_{\ell_1 L_1 2}^{\pm 2 0 \mp 2} \begin{pmatrix} \ell_1 & L_1 & 2 \\ m_1 & M_1 & M \end{pmatrix}, \\ \int d^2 \hat{\mathbf{k}}_2 Y_{\ell_2 m_2}^*(\hat{\mathbf{k}}_2) Y_{L_2 M_2}^*(\hat{\mathbf{k}}_2) Y_{1m_a}^*(\hat{\mathbf{k}}_2) &= I_{\ell_2 L_2 1}^{0 \ 0 \ 0} \begin{pmatrix} \ell_2 & L_2 & 1 \\ m_2 & M_2 & m_a \end{pmatrix}, \\ \int d^2 \hat{\mathbf{k}}_3 Y_{\ell_3 m_3}^*(\hat{\mathbf{k}}_3) Y_{L_3 M_3}^*(\hat{\mathbf{k}}_3) Y_{1m_b}^*(\hat{\mathbf{k}}_3) &= I_{\ell_3 L_3 1}^{0 \ 0 \ 0} \begin{pmatrix} \ell_3 & L_3 & 1 \\ m_3 & M_3 & m_b \end{pmatrix}. \end{aligned} \quad (6.16)$$

Thirdly, using the summation formula of five Wigner-3j symbols as Eq. (C.20), we sum up the Wigner-3j symbols with respect to azimuthal quantum numbers in the above equations and express with the Wigner-9j symbol as

$$\begin{aligned} \sum_{\substack{M_1 M_2 M_3 \\ M m_a m_b}} \begin{pmatrix} L_1 & L_2 & L_3 \\ M_1 & M_2 & M_3 \end{pmatrix} \begin{pmatrix} 2 & 1 & 1 \\ M & m_a & m_b \end{pmatrix} \\ \times \begin{pmatrix} \ell_1 & L_1 & 2 \\ m_1 & M_1 & M \end{pmatrix} \begin{pmatrix} \ell_2 & L_2 & 1 \\ m_2 & M_2 & m_a \end{pmatrix} \begin{pmatrix} \ell_3 & L_3 & 1 \\ m_3 & M_3 & m_b \end{pmatrix} \\ = \begin{pmatrix} \ell_1 & \ell_2 & \ell_3 \\ m_1 & m_2 & m_3 \end{pmatrix} \left\{ \begin{matrix} \ell_1 & \ell_2 & \ell_3 \\ L_1 & L_2 & L_3 \\ 2 & 1 & 1 \end{matrix} \right\}. \end{aligned} \quad (6.17)$$

After these treatments and the summation over $\lambda_1 = \pm 2$ as

$$\sum_{\lambda_1 = \pm 2} \left(\frac{\lambda_1}{2} \right)^{x_1} I_{\ell_1 L_1 2}^{\lambda_1 0 - \lambda_1} = \begin{cases} 2 I_{\ell_1 L_1 2}^{20-2} & (\text{for } x_1 + L_1 + \ell_1 = \text{even}), \\ 0 & (\text{for } x_1 + L_1 + \ell_1 = \text{odd}), \end{cases} \quad (6.18)$$

we can obtain the CMB angle-averaged bispectrum induced from the nonlinear coupling between two scalars and a graviton as

$$B_{X_1 X_2 X_3, \ell_1 \ell_2 \ell_3}^{(TSS)} = \frac{(8\pi)^{3/2}}{3} \sum_{L_1 L_2 L_3} (-1)^{\frac{L_1+L_2+L_3}{2}} I_{L_1 L_2 L_3}^{0 \ 0 \ 0} I_{\ell_1 L_1 2}^{20-2} I_{\ell_2 L_2 1}^{0 \ 0 \ 0} I_{\ell_3 L_3 1}^{0 \ 0 \ 0} \left\{ \begin{matrix} \ell_1 & \ell_2 & \ell_3 \\ L_1 & L_2 & L_3 \\ 2 & 1 & 1 \end{matrix} \right\}$$

³Equations (3.14) and (3.21) in Ref. [2] include typos.

$$\times \int_0^\infty y^2 dy \left[\prod_{n=1}^3 \frac{2}{\pi} (-i)^{\ell_n} \int_0^\infty k_n^2 dk_n \mathcal{T}_{X_n, \ell_n}^{(Z_n)} j_{L_n}(k_n y) \right] f^{(TSS)}(k_1, k_2, k_3) \quad (6.19)$$

Note that the absence of the summation over m_1, m_2 and m_3 in this equation means that the tensor-scalar-scalar bispectrum maintains the rotational invariance. As described above, this consequence is derived from the angular dependence in the polarization tensor. Also in vector modes, if their power spectra obey the statistical isotropy like Eq. (6.8), one can obtain the rotational invariant bispectrum by considering the angular dependence in the polarization vector as Eq. (D.11). Considering Eq. (6.18) and the selection rules of the Wigner symbols explained in Appendix C, we can see that the values of L_1, L_2 and L_3 are limited as

$$L_1 = \begin{cases} |\ell_1 \pm 2|, \ell_1 & (\text{for } X_1 = I, E) \\ |\ell_1 \pm 1| & (\text{for } X_1 = B) \end{cases}, \quad L_2 = |\ell_2 \pm 1|, \quad L_3 = |\ell_3 \pm 1|, \quad (6.20)$$

$$|L_1 - L_2| \leq L_3 \leq L_1 + L_2, \quad \sum_{i=1}^3 L_i = \text{even},$$

and the bispectrum (6.19) has nonzero value under the conditions:

$$|\ell_1 - \ell_2| \leq \ell_3 \leq \ell_1 + \ell_2, \quad \sum_{i=1}^3 \ell_i = \begin{cases} \text{even} & (\text{for } X_1 = I, E) \\ \text{odd} & (\text{for } X_1 = B) \end{cases}. \quad (6.21)$$

In Figs. 6.2 and 6.3, we describe the reduced CMB bispectra of intensity mode sourced from two scalars and a graviton coupling:

$$b_{III, \ell_1 \ell_2 \ell_3}^{(TSS)} + b_{III, \ell_1 \ell_2 \ell_3}^{(STS)} + b_{III, \ell_1 \ell_2 \ell_3}^{(SST)} = (I_{\ell_1 \ell_2 \ell_3}^{0 \ 0 \ 0})^{-1} \left(B_{III, \ell_1 \ell_2 \ell_3}^{(TSS)} + B_{III, \ell_1 \ell_2 \ell_3}^{(STS)} + B_{III, \ell_1 \ell_2 \ell_3}^{(SST)} \right), \quad (6.22)$$

and primordial curvature perturbations (5.7):

$$b_{III, \ell_1 \ell_2 \ell_3}^{(SSS)} = (I_{\ell_1 \ell_2 \ell_3}^{0 \ 0 \ 0})^{-1} B_{III, \ell_1 \ell_2 \ell_3}^{(SSS)}. \quad (6.23)$$

For the numerical computation, we modify the Boltzmann Code for Anisotropies in the Microwave Background (CAMB) [7, 8]⁴. In the calculation of the Wigner-3j and 9j symbols, we use the Common Mathematical Library SLATEC [9] and the summation formula of three Wigner-6j symbols (C.21). As the radiation transfer functions of scalar and tensor modes, namely, $\mathcal{T}_{X_i, \ell_i}^{(S)}$ and $\mathcal{T}_{X_i, \ell_i}^{(T)}$, we use Eq. (3.101). From the behavior of each line shown in Fig. 6.3 at small ℓ_3 that the reduced CMB bispectrum is roughly proportional to ℓ^{-2} , we can confirm that the tensor-scalar-scalar bispectrum has a nearly squeezed-type configuration corresponding to the shape of the initial bispectrum as discussed above. From Fig. 6.2, by comparing the green dashed line with the red solid line roughly estimated as

$$|b_{III, \ell \ell \ell}^{(TSS)} + b_{III, \ell \ell \ell}^{(STS)} + b_{III, \ell \ell \ell}^{(SST)}| \sim \ell^{-4} \times 8 \times 10^{-18} |g_{tss}|, \quad (6.24)$$

we find that $|g_{tss}| \sim 5$ is comparable to $f_{\text{NL}}^{\text{local}} = 5$ corresponding to the upper bound expected from the PLANCK experiment.

⁴The CMB bispectra generated from the two scalars and a graviton correlator in Figs. 6.2 and 6.3 become slightly smaller than those in Ref. [2] due to the accuracy enhancement of the numerical calculation.

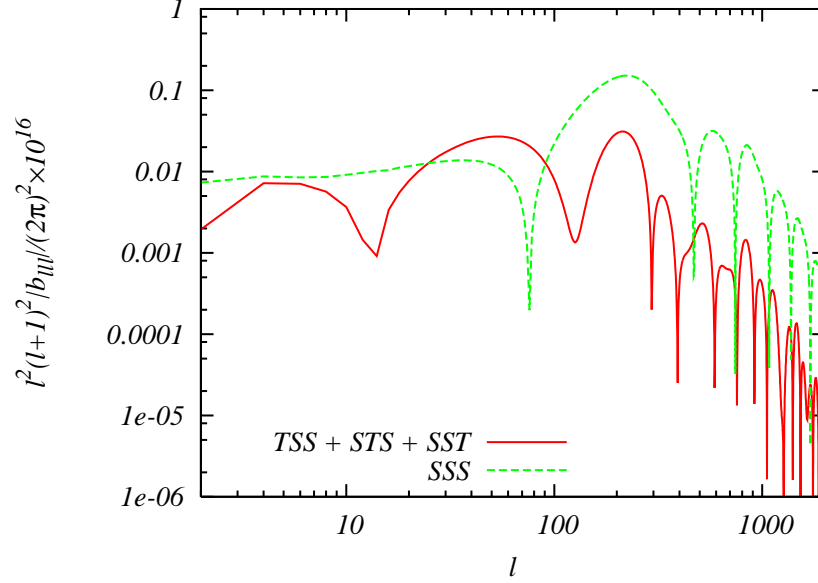


Figure 6.2: Absolute values of the CMB reduced bispectra of temperature fluctuation for $\ell_1 = \ell_2 = \ell_3 \equiv \ell$. The lines correspond to the spectra generated from tensor-scalar-scalar correlation given by Eq. (6.22) with $g_{tss} = 5$ (red solid line) and the primordial non-Gaussianity in the scalar curvature perturbations with $f_{\text{NL}}^{\text{local}} = 5$ (green dashed line). The other cosmological parameters are fixed to the mean values limited from WMAP-7yr data reported in Ref. [10].

6.4 Estimation of the signal-to-noise ratio

Here, we compute the signal-to-noise ratio by comparing the intensity bispectrum of Eq. (6.19) with the zero-noise (ideal) data and examine the bound on the absolute value of g_{tss} . The formulation of (the square of) the signal-to-noise ratio (S/N) is reported in Refs. [11] and [12]. In our case, it can be expressed as

$$\left(\frac{S}{N}\right)^2 = \sum_{2 \leq \ell_1 \leq \ell_2 \leq \ell_3 \leq \ell} \frac{\left(B_{III\ell_1\ell_2\ell_3}^{(TSS)} + B_{III\ell_1\ell_2\ell_3}^{(STS)} + B_{III\ell_1\ell_2\ell_3}^{(SST)}\right)^2}{\sigma_{\ell_1\ell_2\ell_3}^2}, \quad (6.25)$$

where $\sigma_{\ell_1\ell_2\ell_3}$ denotes the variance of the bispectrum. Assuming the weakly non-Gaussianity, the variance can be estimated as [13, 14]

$$\sigma_{\ell_1\ell_2\ell_3}^2 \approx C_{\ell_1} C_{\ell_2} C_{\ell_3} \Delta_{\ell_1\ell_2\ell_3}, \quad (6.26)$$

where $\Delta_{\ell_1\ell_2\ell_3}$ takes 1, 6 or 2 for $\ell_1 \neq \ell_2 \neq \ell_3$, $\ell_1 = \ell_2 = \ell_3$, or the case that two ℓ 's are the same, respectively. C_ℓ denotes that the CMB angular power spectrum included the noise spectrum, which is neglected in our case.

In Fig. 6.4, the numerical result of Eq. (6.25) is presented. We find that (S/N) is a monotonically increasing function roughly proportional to ℓ for $\ell < 2000$. It is compared with the order estimation of Eq. (6.25) as Ref. [12]

$$\left(\frac{S}{N}\right) \sim \sqrt{\frac{\ell^3}{24}} \times \sqrt{\frac{(2\ell)^3}{4\pi}} \left| \begin{pmatrix} \ell & \ell & \ell \\ 0 & 0 & 0 \end{pmatrix} \right| \frac{\ell^3 |b_{III\ell\ell\ell}^{(TSS)} + b_{III\ell\ell\ell}^{(STS)} + b_{III\ell\ell\ell}^{(SST)}|}{(\ell^2 C_\ell)^{3/2}}$$

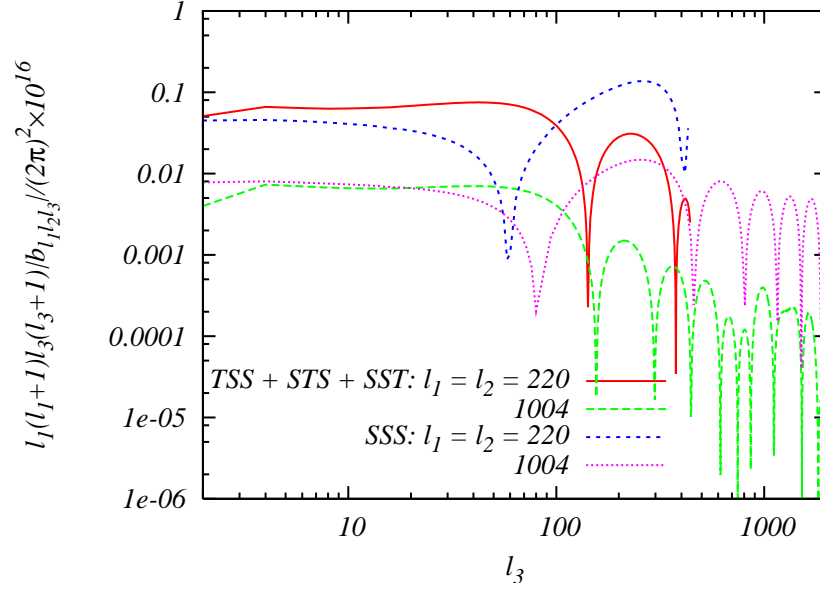


Figure 6.3: Absolute values of the CMB reduced bispectra of temperature fluctuation generated from tensor-scalar-scalar correlation given by Eq. (6.22) ($TSS + STS + SST$) and the primordial non-Gaussianity in the scalar curvature perturbations (SSS) as a function of ℓ_3 with ℓ_1 and ℓ_2 fixed to some values as indicated. The parameters are fixed to the same values defined in Fig. 6.2.

$$\sim \ell \times 5.4 \times 10^{-5} |g_{tss}|. \quad (6.27)$$

Here, we use Eq. (6.24) and the approximations as $\sum \sim \ell^3/24$, $\ell^3 \begin{pmatrix} \ell & \ell & \ell \\ 0 & 0 & 0 \end{pmatrix}^2 \sim 0.36 \times \ell$, and $\ell^2 C_\ell \sim 6 \times 10^{-10}$. We confirm that this is consistent with Fig. 6.4, which justifies our numerical calculation in some sense. This figure shows that from the WMAP and PLANCK experimental data [10, 15], which are roughly noise-free at $\ell \lesssim 500$ and 1000, respectively, expected $(S/N)/g_{tss}$ values are 0.05 and 0.11. Hence, to obtain $(S/N) > 1$, we need $|g_{tss}| > 20$ and 9. The latter value is close to a naive estimate $|g_{tss}| \lesssim 5$, which was discussed at the end of the previous subsection.

6.5 Summary and discussion

In this section, we present a full-sky formalism of the CMB bispectrum sourced from the primordial non-Gaussianity not only in the scalar but also in the vector and tensor perturbations. As an extension of the previous formalism discussed in Ref. [5], the new formalism contains the contribution of the polarization vector and tensor in the initial bispectrum. In Ref. [5], we have shown that in the all-sky analysis, the CMB bispectrum of vector or tensor mode cannot be formed as a simple angle-averaged bispectrum in the same way as that of scalar mode. This is because the angular integrals over the wave number vectors have complexities for the non-orthogonality of spin spherical harmonics whose spin values differ from each other if one neglects the angular dependence of the polarization vector or tensor. In this study, however, we find that this difficulty vanishes if we maintain the angular dependence in the initial bispectrum.

To present how to use our formalism, we compute the CMB bispectrum induced by the nonlinear mode-coupling between the two scalars and a graviton [1]. The typical value of the reduced bispectrum in temperature fluctuations is calculated as a function of the coupling constant between

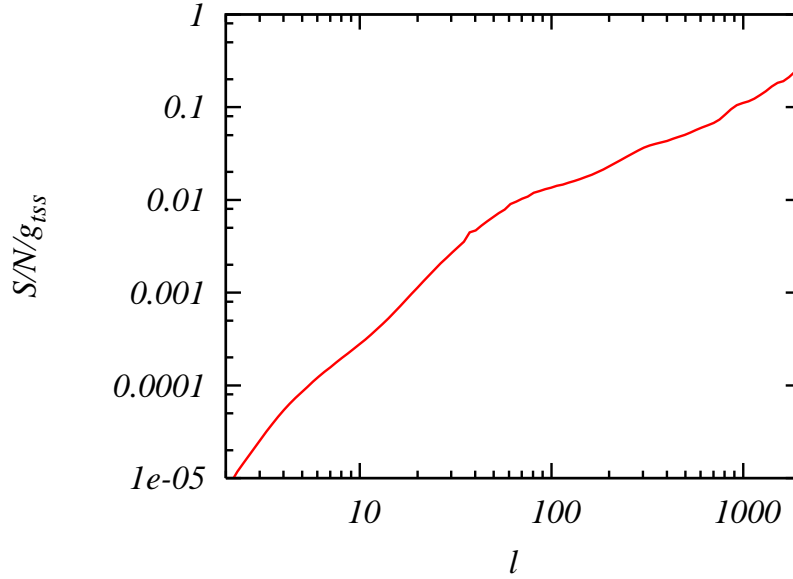


Figure 6.4: Signal-to-noise ratio normalized by g_{tss} as a function of the maximum value between ℓ_1, ℓ_2 and ℓ_3 , namely, ℓ . Each parameter is fixed to the same values defined in Fig. 6.2.

scalars and gravitons g_{tss} : $|b_{III,\ell\ell}^{(TSS)} + b_{III,\ell\ell}^{(STS)} + b_{III,\ell\ell}^{(SST)}| \sim \ell^{-4} \times 8 \times 10^{-18} |g_{tss}|$. Through the computation of the signal-to-noise ratio, we find that the two scalars and a graviton coupling can be detected by the WMAP and PLANCK experiment if $|g_{tss}| \sim \mathcal{O}(10)$. Although we do not include the effect of the polarization modes in the estimation of g_{tss} in this study, they will provide more beneficial information of the nonlinear nature of the early Universe.

References

- [1] J. M. Maldacena, *Non-Gaussian features of primordial fluctuations in single field inflationary models*, *JHEP* **05** (2003) 013, [[astro-ph/0210603](#)].
- [2] M. Shiraishi, D. Nitta, S. Yokoyama, K. Ichiki, and K. Takahashi, *CMB Bispectrum from Primordial Scalar, Vector and Tensor non-Gaussianities*, *Prog. Theor. Phys.* **125** (2011) 795–813, [[arXiv:1012.1079](#)].
- [3] J. Garriga and V. F. Mukhanov, *Perturbations in k-inflation*, *Phys. Lett.* **B458** (1999) 219–225, [[hep-th/9904176](#)].
- [4] A. Mack, T. Kahniashvili, and A. Kosowsky, *Vector and Tensor Microwave Background Signatures of a Primordial Stochastic Magnetic Field*, *Phys. Rev.* **D65** (2002) 123004, [[astro-ph/0105504](#)].
- [5] M. Shiraishi, S. Yokoyama, D. Nitta, K. Ichiki, and K. Takahashi, *Analytic formulae of the CMB bispectra generated from non-Gaussianity in the tensor and vector perturbations*, *Phys. Rev.* **D82** (2010) 103505, [[arXiv:1003.2096](#)].

- [6] C. Caprini, F. Finelli, D. Paoletti, and A. Riotto, *The cosmic microwave background temperature bispectrum from scalar perturbations induced by primordial magnetic fields*, *JCAP* **0906** (2009) 021, [[arXiv:0903.1420](#)].
- [7] A. Lewis, *CMB anisotropies from primordial inhomogeneous magnetic fields*, *Phys. Rev.* **D70** (2004) 043011, [[astro-ph/0406096](#)].
- [8] A. Lewis, A. Challinor, and A. Lasenby, *Efficient Computation of CMB anisotropies in closed FRW models*, *Astrophys. J.* **538** (2000) 473–476, [[astro-ph/9911177](#)].
- [9] “Slatec common mathematical library.” <http://www.netlib.org/slatec/>.
- [10] **WMAP** Collaboration, E. Komatsu *et al.*, *Seven-Year Wilkinson Microwave Anisotropy Probe (WMAP) Observations: Cosmological Interpretation*, *Astrophys. J. Suppl.* **192** (2011) 18, [[arXiv:1001.4538](#)].
- [11] E. Komatsu and D. N. Spergel, *Acoustic signatures in the primary microwave background bispectrum*, *Phys. Rev.* **D63** (2001) 063002, [[astro-ph/0005036](#)].
- [12] N. Bartolo, E. Komatsu, S. Matarrese, and A. Riotto, *Non-Gaussianity from inflation: Theory and observations*, *Phys. Rept.* **402** (2004) 103–266, [[astro-ph/0406398](#)].
- [13] D. N. Spergel and D. M. Goldberg, *Microwave background bispectrum. 1. Basic formalism*, *Phys. Rev.* **D59** (1999) 103001, [[astro-ph/9811252](#)].
- [14] A. Gangui and J. Martin, *Best unbiased estimators for the three point correlators of the cosmic microwave background radiation*, *Phys. Rev.* **D62** (2000) 103004, [[astro-ph/0001361](#)].
- [15] **PLANCK** Collaboration, *The Scientific programme of planck*, [astro-ph/0604069](#).

7 Violation of the rotational invariance in the CMB bispectrum

The current cosmological observations, particularly Cosmic Microwave Background (CMB), tell us that the Universe is almost isotropic, and primordial density fluctuations are almost Gaussian random fields. However, in keeping with the progress of the experiments, there have been many works that verify the possibility of the small deviation of the statistical isotropy, e.g., the so-called “Axis of Evil”. The analyses of the power spectrum by employing the current CMB data suggest that the deviation of the statistical isotropy is about 10% at most (e.g. [1–6]). Toward more precise measurements in future experiments, there are a lot of theoretical discussions about the effects of the statistical anisotropy on the CMB power spectrum, [7–11], e.g., the presence of the off-diagonal configuration of the multipoles in the CMB power spectrum, which vanishes in the isotropic spectrum.

As is well known, it might be difficult to explain such statistical anisotropy in the standard inflationary scenario. However, recently, there have been several works about the possibility of generating the statistically anisotropic primordial density fluctuations in order to introduce non-trivial dynamics of the vector field. [12–24]. In Ref. [14], the authors considered a modified hybrid inflation model where a waterfall field couples not only with an inflaton field but also with a massless vector field. They have shown that, owing to the effect of fluctuations of the vector field, the primordial density fluctuations may have a small deviation from the statistical isotropy and also the deviation from the Gaussian statistics. If the primordial density fluctuations deviate from the Gaussian statistics, they produce the non-zero higher order spectra (corresponding to higher order correlation functions), e.g., the bispectrum (3-point function), the trispectrum (4-point function) and so on. Hence, in the model presented in Ref. [14], we can expect that there are characteristic signals not only in the CMB power spectrum but also in the CMB bispectrum.

With these motivations, in this work, we calculate the CMB statistically anisotropic bispectrum sourced from the curvature perturbations generated in the modified hybrid inflation scenario proposed in Ref. [14], on the basis of the useful formula presented in Ref. [25]. Then, we find the peculiar configurations of the multipoles which never appear in the isotropic bispectrum, like off-diagonal components in the CMB power spectrum. These discussions are based on Ref. [26].

This section is organized as follows. In the next subsection, we briefly review the inflation model where the scalar waterfall field couples with the vector field and calculate the bispectrum of curvature perturbations based on Ref. [14]. In Sec. 7.2, we give an exact form of the CMB statistically anisotropic bispectrum and analyze its behavior by numerical computation. Finally, we devote the final subsection to the summary and discussion.

Throughout this section, we obey the definition of the Fourier transformation as

$$f(\mathbf{x}) \equiv \int \frac{d^3\mathbf{k}}{(2\pi)^3} \tilde{f}(\mathbf{k}) e^{i\mathbf{k}\cdot\mathbf{x}}, \quad (7.1)$$

and a normalization as $M_{\text{pl}} \equiv (8\pi G)^{-1/2} = 1$.

7.1 Statistically-anisotropic non-Gaussianity in curvature perturbations

In this subsection, we briefly review the mechanism of generating the statistically anisotropic bispectrum induced by primordial curvature perturbations proposed in Ref. [14], where the authors

set the system like the hybrid inflation wherein there are two scalar fields: inflaton ϕ and waterfall field χ , and a vector field A_μ coupled with a waterfall field. The action is given by

$$S = \int dx^4 \sqrt{-g} \left[\frac{1}{2} R - \frac{1}{2} g^{\mu\nu} (\partial_\mu \phi \partial_\nu \phi + \partial_\mu \chi \partial_\nu \chi) - V(\phi, \chi, A_\nu) - \frac{1}{4} g^{\mu\nu} g^{\rho\sigma} f^2(\phi) F_{\mu\rho} F_{\nu\sigma} \right]. \quad (7.2)$$

Here, $F_{\mu\nu} \equiv \partial_\mu A_\nu - \partial_\nu A_\mu$ is the field strength of the vector field A_μ , $V(\phi, \chi, A_\mu)$ is the potential of fields and $f(\phi)$ denotes a gauge coupling. To guarantee the isotropy of the background Universe, we need the condition that the energy density of the vector field is negligible in the total energy of the Universe and we assume a small expectation value of the vector field. Therefore, we neglect the effect of the vector field on the background dynamics and also the evolution of the fluctuations of the inflaton. In the standard hybrid inflation (only with the inflaton and the waterfall field), inflation suddenly ends owing to the tachyonic instability of the waterfall field, which is triggered when the inflaton reaches a critical value ϕ_e . In the system described using Eq. (7.2), however, ϕ_e may fluctuate owing to the fluctuation of the vector field and it generates additional curvature perturbations.

Using the δN formalism [27–32], the total curvature perturbation on the uniform-energy-density hypersurface at the end of inflation $t = t_e$ can be estimated in terms of the perturbation of the e -folding number as

$$\begin{aligned} \zeta(t_e) &= \delta N(t_e, t_*) \\ &= \frac{\partial N}{\partial \phi_*} \delta \phi_* + \frac{1}{2} \frac{\partial^2 N}{\partial \phi_*^2} \delta \phi_*^2 \\ &\quad + \frac{\partial N}{\partial \phi_e} \frac{d\phi_e(A)}{dA^\mu} \delta A_e^\mu + \frac{1}{2} \left[\frac{\partial N}{\partial \phi_e} \frac{d^2 \phi_e(A)}{dA^\mu dA^\nu} + \frac{\partial^2 N}{\partial \phi_e^2} \frac{d\phi_e(A)}{dA^\mu} \frac{d\phi_e(A)}{dA^\nu} \right] \delta A_e^\mu \delta A_e^\nu. \end{aligned} \quad (7.3)$$

Here, t_* is the time when the scale of interest crosses the horizon during the slow-roll inflation. Assuming the sudden decay of all fields into radiations just after inflation, the curvature perturbations on the uniform-energy-density hypersurface become constant after inflation ends¹. Hence, at the leading order, the power spectrum and the bispectrum of curvature perturbations are respectively derived as

$$\begin{aligned} \left\langle \prod_{n=1}^2 \zeta(\mathbf{k}_n) \right\rangle &= (2\pi)^3 N_*^2 P_\phi(k_1) \delta \left(\sum_{n=1}^2 \mathbf{k}_n \right) \\ &\quad + N_e^2 \frac{d\phi_e(A)}{dA^\mu} \frac{d\phi_e(A)}{dA^\nu} \langle \delta A_e^\mu(\mathbf{k}_1) \delta A_e^\nu(\mathbf{k}_2) \rangle, \end{aligned} \quad (7.4)$$

$$\begin{aligned} \left\langle \prod_{n=1}^3 \zeta(\mathbf{k}_n) \right\rangle &= (2\pi)^3 N_*^2 N_{**} [P_\phi(k_1) P_\phi(k_2) + 2 \text{ perms.}] \delta \left(\sum_{n=1}^3 \mathbf{k}_n \right) \\ &\quad + N_e^3 \frac{d\phi_e(A)}{dA^\mu} \frac{d\phi_e(A)}{dA^\nu} \frac{d\phi_e(A)}{dA^\rho} \langle \delta A_e^\mu(\mathbf{k}_1) \delta A_e^\nu(\mathbf{k}_2) \delta A_e^\rho(\mathbf{k}_3) \rangle \\ &\quad + N_e^4 \frac{d\phi_e(A)}{dA^\mu} \frac{d\phi_e(A)}{dA^\nu} \left(\frac{1}{N_e} \frac{d^2 \phi_e(A)}{dA^\rho dA^\sigma} + \frac{N_{ee}}{N_e^2} \frac{d\phi_e(A)}{dA^\rho} \frac{d\phi_e(A)}{dA^\sigma} \right) \\ &\quad \times [\langle \delta A_e^\mu(\mathbf{k}_1) \delta A_e^\nu(\mathbf{k}_2) (\delta A_e^\rho \star \delta A_e^\sigma)_e(\mathbf{k}_3) \rangle + 2 \text{ perms.}] , \end{aligned} \quad (7.5)$$

where $P_\phi(k) = H_*^2/(2k^3)$ is the power spectrum of the fluctuations of the inflaton, $N_* \equiv \partial N/\partial \phi_*$, $N_{**} \equiv \partial^2 N/\partial \phi_*^2$, $N_e \equiv \partial N/\partial \phi_e$, $N_{ee} \equiv \partial^2 N/\partial \phi_e^2$, and \star denotes the convolution. Here, we assume that $\delta \phi_*$ is a Gaussian random field and $\langle \delta \phi A^\mu \rangle = 0$.

¹This ζ is consistent with \mathcal{R} in Eq. (2.40).

For simplicity, we estimate the fluctuation of the vector fields in the Coulomb gauge: $\delta A_0 = 0$ and $k_i A^i = 0$. Then, the evolution equation of the fluctuations of the vector field is given by

$$\ddot{\mathcal{A}}_i - \frac{\ddot{f}}{f} \mathcal{A}_i - a^2 \partial_j \partial^j \mathcal{A}_i = 0, \quad (7.6)$$

where $\mathcal{A}_i \equiv f \delta A_i$, $\dot{}$ denotes the derivative with respect to the conformal time, and we neglect the contribution from the potential term. When $f \propto a, a^{-2}$ with appropriate quantization of the fluctuations of the vector field, we have the scale-invariant power spectrum of δA^i on superhorizon scale as [14, 18, 33]

$$\langle \delta A_e^i(\mathbf{k}_1) \delta A_e^j(\mathbf{k}_2) \rangle = (2\pi)^3 P_\phi(k) f_e^{-2} P^{ij}(\hat{\mathbf{k}}_1) \delta \left(\sum_{n=1}^2 \mathbf{k}_n \right), \quad (7.7)$$

where a is the scale factor, $P^{ij}(\hat{\mathbf{k}}) = \delta^{ij} - \hat{k}^i \hat{k}^j$, $\hat{}$ denotes the unit vector, and $f_e \equiv f(t_e)$. Therefore, substituting this expression into Eq. (7.4), we can rewrite the power spectrum of the primordial curvature perturbations, ζ , as

$$\begin{aligned} \left\langle \prod_{n=1}^2 \zeta(\mathbf{k}_n) \right\rangle &\equiv (2\pi)^3 P_\zeta(\mathbf{k}_1) \delta \left(\sum_{n=1}^2 \mathbf{k}_n \right), \\ P_\zeta(\mathbf{k}) &= P_\phi(k) \left[N_*^2 + \left(\frac{N_e}{f_e} \right)^2 q^i q^j P_{ij}(\hat{\mathbf{k}}) \right], \end{aligned} \quad (7.8)$$

where $q_i \equiv d\phi_e/dA^i$, $q_{ij} \equiv d^2\phi_e/(dA^i dA^j)$. We can divide this expression into the isotropic part and the anisotropic part as [7]

$$P_\zeta(\mathbf{k}) \equiv P_\zeta^{\text{iso}}(k) \left[1 + g_\beta (\hat{\mathbf{q}} \cdot \hat{\mathbf{k}})^2 \right], \quad (7.9)$$

with

$$P_\zeta^{\text{iso}}(k) = N_*^2 P_\phi(k) (1 + \beta), \quad g_\beta = -\frac{\beta}{1 + \beta}, \quad (7.10)$$

where $\beta = (N_e/N_*/f_e)^2 |\mathbf{q}|^2$. The bispectrum of the primordial curvature perturbation given by Eq. (7.5) can be written as

$$\left\langle \prod_{n=1}^3 \zeta(\mathbf{k}_n) \right\rangle \equiv (2\pi)^3 F_\zeta(\mathbf{k}_1, \mathbf{k}_2, \mathbf{k}_3) \delta \left(\sum_{n=1}^3 \mathbf{k}_n \right), \quad (7.11)$$

$$\begin{aligned} F_\zeta(\mathbf{k}_1, \mathbf{k}_2, \mathbf{k}_3) &= \left(\frac{g_\beta}{\beta} \right)^2 P_\zeta^{\text{iso}}(k_1) P_\zeta^{\text{iso}}(k_2) \\ &\times \left[\frac{N_{**}}{N_*^2} + \beta^2 \hat{q}^a \hat{q}^b \left(\frac{1}{N_e} \hat{q}^{cd} + \frac{N_{ee}}{N_e^2} \hat{q}^c \hat{q}^d \right) P_{ac}(\hat{\mathbf{k}}_1) P_{bd}(\hat{\mathbf{k}}_2) \right] \\ &+ 2 \text{ perms.} . \end{aligned} \quad (7.12)$$

Here $\hat{q}^{cd} \equiv q^{cd}/|\mathbf{q}|^2$ and we have assumed that the fluctuation of the vector field δA^i almost obeys Gaussian statistics; hence $\langle \delta A_e^\mu(\mathbf{k}_1) \delta A_e^\nu(\mathbf{k}_2) \delta A_e^\rho(\mathbf{k}_3) \rangle = 0$.

Hereinafter, for calculating the CMB bispectrum explicitly, we adopt a simple model whose potential looks like an Abelian Higgs model in the unitary gauge as [14]

$$V(\phi, \chi, A^i) = \frac{\lambda}{4}(\chi^2 - v^2)^2 + \frac{1}{2}g^2\phi^2\chi^2 + \frac{1}{2}m^2\phi^2 + \frac{1}{2}h^2A^\mu A_\mu\chi^2, \quad (7.13)$$

where λ, g , and h are the coupling constants, m is the inflaton mass, and v is the vacuum expectation value of χ . Since the effective mass squared of the waterfall field is given by

$$m_\chi^2 \equiv \frac{\partial^2 V}{\partial \chi^2} = -\lambda v^2 + g^2\phi_e^2 + h^2A^iA_i = 0, \quad (7.14)$$

and the critical value of the inflaton ϕ_e can be obtained as

$$g^2\phi_e^2 = \lambda v^2 - h^2A^iA_i, \quad (7.15)$$

we can express β , q^i and q^{ij} in Eq. (7.12) in terms of the model parameters as

$$\hat{q}^i = -\hat{A}^i, \quad \hat{q}^{ij} = -\frac{1}{\phi_e} \left[\left(\frac{g\phi_e}{hA} \right)^2 \delta^{ij} + \hat{A}^i \hat{A}^j \right], \quad \beta \simeq \frac{1}{f_e^2} \left(\frac{h^2A}{g^2\phi_e} \right)^2, \quad (7.16)$$

where we have used $N_* \simeq -N_e \simeq 1/\sqrt{2\epsilon}$ with $\epsilon \equiv (\partial V/\partial\phi/V)^2/2$ being a slow-roll parameter and $|\mathbf{A}| \equiv A$. Substituting these quantities into Eq. (7.12), the bispectrum of primordial curvature perturbations is obtained as

$$F_\zeta(\mathbf{k}_1, \mathbf{k}_2, \mathbf{k}_3) = CP_\zeta^{\text{iso}}(k_1)P_\zeta^{\text{iso}}(k_2)\hat{A}^a\hat{A}^b\delta^{cd}P_{ac}(\hat{\mathbf{k}}_1)P_{bd}(\hat{\mathbf{k}}_2) + 2 \text{ perms.}, \quad (7.17)$$

$$C \equiv -g_\beta^2 \frac{\phi_e}{N_e} \left(\frac{g}{hA} \right)^2.$$

Note that in the above expression, we have neglected the effect of the longitudinal polarization in the vector field for simplicity² and the terms that are suppressed by a slow-roll parameter $\eta \equiv \partial^2 V/\partial\phi^2/V$ because $-N_{**}/N_*^2 \simeq N_{ee}/N_e^2 \simeq -(N_e\phi_e)^{-1} \simeq \eta$. Since the current CMB observations suggest $g_\beta < \mathcal{O}(0.1)$ (e.g., Refs. [1, 2]) and $N_e^{-1} \simeq -\sqrt{2\epsilon}$, the overall amplitude of the bispectrum in this model, C , does not seem to be sufficiently large to be detected. However, even if $g_\beta \ll 1$ and $\epsilon \ll 1$, C can become greater than unity for $(g/hA)^2\phi_e \gg 1$. Thus, we expect meaningful signals also in the CMB bispectrum. Then, in the next subsection, we closely investigate the CMB bispectrum generated from the primordial bispectrum given by Eq. (7.17) and discuss a new characteristic feature of the CMB bispectrum induced by the statistical anisotropy of the primordial bispectrum.

7.2 CMB statistically-anisotropic bispectrum

In this subsection, we give a formula of the CMB bispectrum generated from the primordial bispectrum, which has statistical anisotropy owing to the fluctuations of the vector field, given by Eq. (7.17). We also discuss the special signals of this CMB bispectrum, which vanish in the statistically isotropic bispectrum.

²Owing to this treatment, we can use the quantities estimated in the Coulomb gauge as Eq. (7.12). In a more precise discussion, we should take into account the contribution of the longitudinal mode in the unitary gauge.

7.2.1 Formulation

The CMB fluctuation can be expanded in terms of the spherical harmonic function as

$$\frac{\Delta X(\hat{\mathbf{n}})}{X} = \sum_{\ell m} a_{X,\ell m} Y_{\ell m}(\hat{\mathbf{n}}) , \quad (7.18)$$

where $\hat{\mathbf{n}}$ is a unit vector pointing toward a line-of-sight direction, and X denotes the intensity ($\equiv I$) and polarizations ($\equiv E, B$). According to Eq. (5.3), the coefficient, $a_{\ell m}$, generated from primordial curvature perturbations, ζ , is expressed as

$$a_{X,\ell m} = 4\pi(-i)^\ell \int_0^\infty \frac{k^2 dk}{(2\pi)^3} \zeta_{\ell m}(k) \mathcal{T}_{X,\ell}(k) \quad (\text{for } X = I, E) , \quad (7.19)$$

$$\zeta_{\ell m}(k) \equiv \int d^2 \hat{\mathbf{k}} \zeta(\mathbf{k}) Y_{\ell m}^*(\hat{\mathbf{k}}) , \quad (7.20)$$

where $\mathcal{T}_{X,\ell}$ is the time-integrated transfer function of scalar modes as described in Eq. (3.101). Using these equations, the CMB bispectrum generated from the bispectrum of the primordial curvature perturbations is given by

$$\left\langle \prod_{n=1}^3 a_{X_n, \ell_n m_n} \right\rangle = \left[\prod_{n=1}^3 4\pi(-i)^{\ell_n} \int_0^\infty \frac{k_n^2 dk_n}{(2\pi)^3} \mathcal{T}_{X_n, \ell_n}(k_n) \right] \left\langle \prod_{n=1}^3 \zeta_{\ell_n m_n}(k_n) \right\rangle , \quad (7.21)$$

with

$$\left\langle \prod_{n=1}^3 \zeta_{\ell_n m_n}(k_n) \right\rangle = \left[\prod_{n=1}^3 \int d^2 \hat{\mathbf{k}}_n Y_{\ell_n m_n}^*(\hat{\mathbf{k}}_n) \right] (2\pi)^3 \delta \left(\sum_{n=1}^3 \mathbf{k}_n \right) F_\zeta(\mathbf{k}_1, \mathbf{k}_2, \mathbf{k}_3) . \quad (7.22)$$

We expand the angular dependencies which appear in the Dirac delta function, $\delta(\mathbf{k}_1 + \mathbf{k}_2 + \mathbf{k}_3)$, and the function, $F_\zeta(\mathbf{k}_1, \mathbf{k}_2, \mathbf{k}_3)$, given by Eq. (7.17) with respect to the spin spherical harmonics as

$$\delta \left(\sum_{n=1}^3 \mathbf{k}_n \right) = 8 \int_0^\infty y^2 dy \left[\prod_{n=1}^3 \sum_{L_n M_n} (-1)^{L_n/2} j_{L_n}(k_n y) Y_{L_n M_n}^*(\hat{\mathbf{k}}_n) \right] \times I_{L_1 L_2 L_3}^{0 0 0} \begin{pmatrix} L_1 & L_2 & L_3 \\ M_1 & M_2 & M_3 \end{pmatrix} , \quad (7.23)$$

$$\begin{aligned} \hat{A}^a \hat{A}^b \delta^{cd} P_{ac}(\hat{\mathbf{k}}_1) P_{bd}(\hat{\mathbf{k}}_2) &= -4 \left(\frac{4\pi}{3} \right)^3 \sum_{L, L', L_A=0,2} I_{L11}^{01-1} I_{L'11}^{01-1} I_{11L_A}^{000} \left\{ \begin{matrix} L & L' & L_A \\ 1 & 1 & 1 \end{matrix} \right\} \\ &\times \sum_{MM'M_A} Y_{LM}^*(\hat{\mathbf{k}}_1) Y_{L'M'}^*(\hat{\mathbf{k}}_2) Y_{L_A M_A}^*(\hat{\mathbf{A}}) \begin{pmatrix} L & L' & L_A \\ M & M' & M_A \end{pmatrix} \end{aligned} \quad (7.24)$$

where the 2×3 matrices of a bracket and a curly bracket denote the Wigner-3j and 6j symbols, respectively, and

$$I_{l_1 l_2 l_3}^{s_1 s_2 s_3} \equiv \sqrt{\frac{(2l_1+1)(2l_2+1)(2l_3+1)}{4\pi}} \begin{pmatrix} l_1 & l_2 & l_3 \\ s_1 & s_2 & s_3 \end{pmatrix} . \quad (7.25)$$

Here, we have used the expressions of an arbitrary unit vector and a projection tensor as Appendices C and D. Note that for $Y_{00}^*(\hat{\mathbf{A}}) = 1/\sqrt{4\pi}$, the contribution of $L_A = 0$ in Eq. (7.24) is independent of the direction of the vector field. Therefore, the statistical anisotropy is generated from the signals of $L_A = 2$. By integrating these spherical harmonics over each unit vector, the angular dependences on $\mathbf{k}_1, \mathbf{k}_2, \mathbf{k}_3$ can be reduced to the Wigner-3j symbols as

$$\begin{aligned} \int d^2\hat{\mathbf{k}}_1 Y_{\ell_1 m_1}^* Y_{L_1 M_1}^* Y_{LM}^* &= I_{\ell_1 L_1 L}^{0 0 0} \begin{pmatrix} \ell_1 & L_1 & L \\ m_1 & M_1 & M \end{pmatrix}, \\ \int d^2\hat{\mathbf{k}}_2 Y_{\ell_2 m_2}^* Y_{L_2 M_2}^* Y_{L' M'}^* &= I_{\ell_2 L_2 L'}^{0 0 0} \begin{pmatrix} \ell_2 & L_2 & L' \\ m_2 & M_2 & M' \end{pmatrix}, \\ \int d^2\hat{\mathbf{k}}_3 Y_{\ell_3 m_3}^* Y_{L_3 M_3}^* &= (-1)^{m_3} \delta_{L_3, \ell_3} \delta_{M_3, -m_3}. \end{aligned} \quad (7.26)$$

From these equations, we obtain an alternative explicit form of the bispectrum of $\zeta_{\ell m}$ as

$$\begin{aligned} \left\langle \prod_{n=1}^3 \zeta_{\ell_n m_n}(k_n) \right\rangle &= -(2\pi)^3 8 \int_0^\infty y^2 dy \sum_{L_1 L_2} (-1)^{\frac{L_1+L_2+\ell_3}{2}} I_{L_1 L_2 \ell_3}^{0 0 0} \\ &\times P_\zeta^{\text{iso}}(k_1) j_{L_1}(k_1 y) P_\zeta^{\text{iso}}(k_2) j_{L_2}(k_2 y) C j_{\ell_3}(k_3 y) \\ &\times 4 \left(\frac{4\pi}{3} \right)^3 (-1)^{m_3} \sum_{L, L', L_A=0,2} I_{L 1 1}^{0 1 -1} I_{L' 1 1}^{0 1 -1} \\ &\times I_{\ell_1 L_1 L}^{0 0 0} I_{\ell_2 L_2 L'}^{0 0 0} I_{1 1 L_A}^{0 0 0} \begin{Bmatrix} L & L' & L_A \\ 1 & 1 & 1 \end{Bmatrix} \\ &\times \sum_{M_1 M_2 M M' M_A} Y_{L_A M_A}^*(\hat{\mathbf{A}}) \begin{pmatrix} L_1 & L_2 & \ell_3 \\ M_1 & M_2 & -m_3 \end{pmatrix} \\ &\times \begin{pmatrix} \ell_1 & L_1 & L \\ m_1 & M_1 & M \end{pmatrix} \begin{pmatrix} \ell_2 & L_2 & L' \\ m_2 & M_2 & M' \end{pmatrix} \begin{pmatrix} L & L' & L_A \\ M & M' & M_A \end{pmatrix} \\ &+ 2 \text{ perms.} \end{aligned} \quad (7.27)$$

This equation implies that, owing to the vector field \mathbf{A} , the CMB bispectrum has a direction dependence, and hence, the dependence on m_1, m_2, m_3 cannot be confined only to a Wigner-3j symbol, namely,

$$\left\langle \prod_{n=1}^3 \zeta_{\ell_n m_n}(k_n) \right\rangle \neq (2\pi)^3 \mathcal{F}_{\ell_1 \ell_2 \ell_3}(k_1, k_2, k_3) \begin{pmatrix} \ell_1 & \ell_2 & \ell_3 \\ m_1 & m_2 & m_3 \end{pmatrix}. \quad (7.28)$$

This fact truly indicates the violation of the rotational invariance in the bispectrum of the primordial curvature perturbations and leads to the statistical anisotropy on the CMB bispectrum.

Let us consider the explicit form of the CMB bispectrum. Here, we set the coordinate as $\hat{\mathbf{A}} = \hat{\mathbf{z}}$. Then, by substituting Eq. (7.27) into Eq. (7.21) and using the relation $Y_{L_A M_A}^*(\hat{\mathbf{z}}) = \sqrt{(2L_A+1)/(4\pi)} \delta_{M_A, 0}$, the CMB bispectrum is expressed as

$$\begin{aligned} \left\langle \prod_{n=1}^3 a_{X_n, \ell_n m_n} \right\rangle &= - \int_0^\infty y^2 dy \left[\prod_{n=1}^3 \frac{2}{\pi} \int_0^\infty k_n^2 dk_n \mathcal{T}_{X_n, \ell_n}(k_n) \right] \\ &\times \sum_{L_1 L_2} (-1)^{\frac{\ell_1+\ell_2+L_1+L_2}{2}+\ell_3} I_{L_1 L_2 \ell_3}^{0 0 0} \end{aligned}$$

$$\begin{aligned}
& \times P_{\zeta}^{\text{iso}}(k_1) j_{L_1}(k_1 y) P_{\zeta}^{\text{iso}}(k_2) j_{L_2}(k_2 y) C j_{\ell_3}(k_3 y) \\
& \times 4 \left(\frac{4\pi}{3} \right)^3 (-1)^{m_3} \sum_{L, L', L_A=0,2} I_{L11}^{01-1} I_{L'11}^{01-1} \\
& \times I_{\ell_1 L_1 L}^{000} I_{\ell_2 L_2 L'}^{000} I_{11 L_A}^{000} \left\{ \begin{matrix} L & L' & L_A \\ 1 & 1 & 1 \end{matrix} \right\} \\
& \times \sqrt{\frac{2L_A+1}{4\pi}} \sum_{M=-2}^2 \begin{pmatrix} L_1 & L_2 & \ell_3 \\ -m_1-M & -m_2+M & -m_3 \end{pmatrix} \\
& \times \begin{pmatrix} \ell_1 & L_1 & L \\ m_1 & -m_1-M & M \end{pmatrix} \begin{pmatrix} \ell_2 & L_2 & L' \\ m_2 & -m_2+M & -M \end{pmatrix} \\
& \times \begin{pmatrix} L & L' & L_A \\ M & -M & 0 \end{pmatrix} + 2 \text{ perms.} .
\end{aligned} \tag{7.29}$$

By the selection rules of the Wigner symbols described in Appendix C, the ranges of $\ell_1, \ell_2, \ell_3, m_1, m_2$ and m_3 , and the summation ranges in terms of L_1 and L_2 are limited as

$$\begin{aligned}
& \sum_{n=1}^3 \ell_n = \text{even} , \quad \sum_{n=1}^3 m_n = 0 , \\
& L_1 = |\ell_1 - 2|, \ell_1, \ell_1 + 2 , \quad L_2 = |\ell_2 - 2|, \ell_2, \ell_2 + 2 , \\
& |L_2 - \ell_3| \leq L_1 \leq L_2 + \ell_3 .
\end{aligned} \tag{7.30}$$

7.2.2 Behavior of the CMB statistically-anisotropic bispectrum

On the basis of Eq. (7.29), we compute the CMB bispectra for the several ℓ 's and m 's. Then, we modify the Boltzmann Code for Anisotropies in the Microwave Background (CAMB) [34, 35] and use the Common Mathematical Library SLATEC [36].

In Fig. 7.1, the red solid lines are the CMB statistically anisotropic bispectra of the intensity mode given by Eq. (7.29) with $C = 1$, and the green dashed lines are the statistically isotropic one sourced from the local-type non-Gaussianity of curvature perturbations given by Eq. (4.7)

$$\begin{aligned}
\left\langle \prod_{n=1}^3 a_{X_n, \ell_n m_n} \right\rangle &= I_{\ell_1 \ell_2 \ell_3}^{000} \begin{pmatrix} \ell_1 & \ell_2 & \ell_3 \\ m_1 & m_2 & m_3 \end{pmatrix} \int_0^\infty y^2 dy \left[\prod_{n=1}^3 \frac{2}{\pi} \int_0^\infty k_n^2 dk_n \mathcal{T}_{X_n, \ell_n}(k_n) j_{\ell_n}(k_n y) \right] \\
&\times \left(P_{\zeta}^{\text{iso}}(k_1) P_{\zeta}^{\text{iso}}(k_2) \frac{6}{5} f_{\text{NL}} + 2 \text{ perms.} \right) ,
\end{aligned} \tag{7.31}$$

with $f_{\text{NL}} = 5$ for $\ell_1 = \ell_2 = \ell_3$ and two sets of m_1, m_2, m_3 . From this figure, we can see that the red solid lines are in good agreement with the green dashed line in the dependence on ℓ for both configurations of m_1, m_2, m_3 . This seems to be because the bispectrum of primordial curvature perturbations affected by the fluctuations of vector field given by Eq. (7.17) has not only the anisotropic part but also the isotropic part and both parts have the same amplitude. In this sense, it is expected that the angular dependence on the vector field $\hat{\mathbf{A}}$ does not contribute much to a change in the shape of the CMB bispectrum. We also find that the anisotropic bispectrum for $C \sim 0.3$ is comparable in magnitude to the case with $f_{\text{NL}} = 5$ for the standard local type, which corresponds to the upper bound on the local-type non-Gaussianity expected from the PLANCK experiment [37].

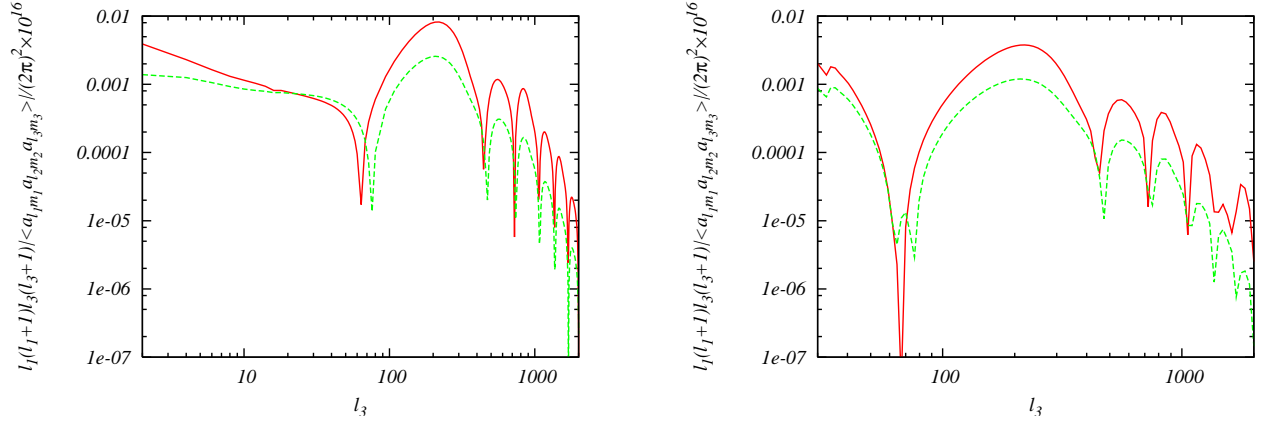


Figure 7.1: Absolute values of the CMB statistically anisotropic bispectrum of the intensity mode given by Eq. (7.29) with $C = 1$ (red solid line) and the statistically isotropic one given by Eq. (7.31) with $f_{\text{NL}} = 5$ (green dashed line) for $\ell_1 = \ell_2 = \ell_3$. The left and right figures are plotted in the configurations $(m_1, m_2, m_3) = (0, 0, 0), (10, 20, -30)$, respectively. The parameters are fixed to the mean values limited from the WMAP-7yr data as reported in Ref. [38].

In the discussion of the CMB power spectrum, if the rotational invariance is violated in the primordial power spectrum given by Eq. (7.9), the signals in the off-diagonal configurations of ℓ also have nonzero values [7, 8, 10]. Likewise, there are special configurations in the CMB bispectrum induced from the statistical anisotropy on the primordial bispectrum as Eq. (7.17). The selection rule (7.30) suggests that the statistically anisotropic bispectrum (7.29) could be nonzero in the multipole configurations given by

$$\ell_1 = |\ell_2 - \ell_3| - 4, |\ell_2 - \ell_3| - 2, \ell_2 + \ell_3 + 2, \ell_2 + \ell_3 + 4, \quad (7.32)$$

and two permutations of ℓ_1, ℓ_2, ℓ_3 . In contrast, in these configurations, the isotropic bispectrum (e.g., Eq. (7.31)) vanishes owing to the triangle condition of the Wigner-3j symbol $\begin{pmatrix} \ell_1 & \ell_2 & \ell_3 \\ m_1 & m_2 & m_3 \end{pmatrix}$ and the nonzero components arise only from

$$|\ell_2 - \ell_3| \leq \ell_1 \leq \ell_2 + \ell_3. \quad (7.33)$$

Therefore, the signals of the configurations (7.32) have the pure information of the statistical anisotropy on the CMB bispectrum.

Figure 7.2 shows the CMB anisotropic bispectra of the intensity mode given by Eq. (7.29) with $C = 1$ for the several configurations of ℓ 's and m 's as a function of ℓ_3 . The red solid line and green dashed line satisfy the special relation (7.32), namely, $\ell_1 = \ell_2 + \ell_3 + 2, |\ell_2 - \ell_3| - 2$, and the blue dotted line obeys a configuration of Eq. (7.33), namely, $\ell_1 = \ell_2 + \ell_3$. From this figure, we confirm that the signals in the special configuration (7.32) are comparable in magnitude to those for $\ell_1 = \ell_2 + \ell_3$. Therefore, if the rotational invariance is violated on the primordial bispectrum of curvature perturbations, the signals for $\ell_1 = \ell_2 + \ell_3 + 2, |\ell_2 - \ell_3| - 2$ can also become beneficial observables. Here, note that the anisotropic bispectra in the other special configurations: $\ell_1 = \ell_2 + \ell_3 + 4, |\ell_2 - \ell_3| - 4$ are zero. It is because these signals arise from only the contribution of $L = L' = L_A = 2, L_1 = \ell_1 \pm 2, L_2 = \ell_2 \pm 2$ in Eq. (7.29) owing to the selection rules of the Wigner symbols, and the summation of the four Wigner-3j symbols over M vanishes for all ℓ 's and m 's. Hence, in this anisotropic bispectrum, the additional signals arise from only two configurations $\ell_1 = \ell_2 + \ell_3 + 2, |\ell_2 - \ell_3| - 2$ and these two permutations.

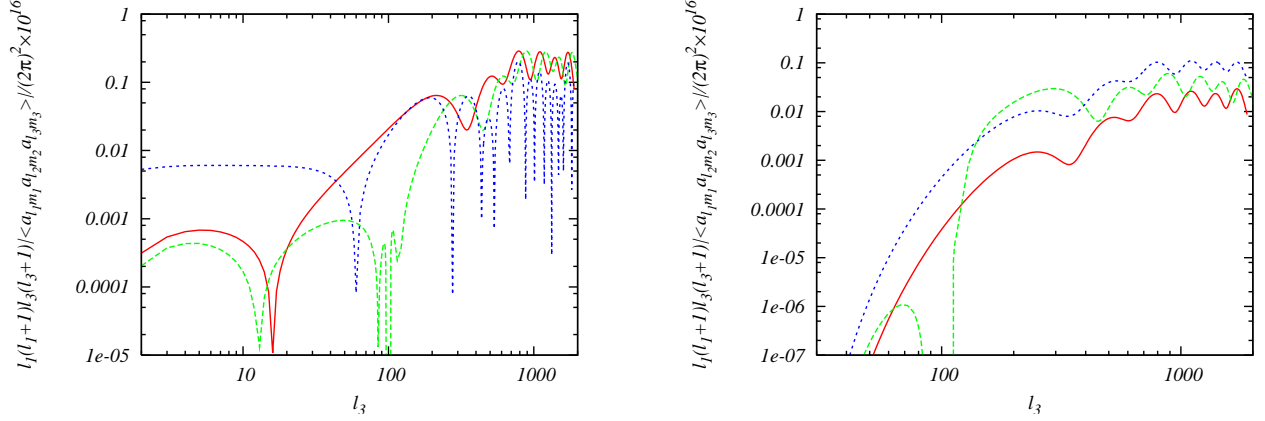


Figure 7.2: Absolute values of the CMB statistically anisotropic bispectra of the intensity mode given by Eq. (7.29) for $(m_1, m_2, m_3) = (0, 0, 0)$ (left panel) and $(10, 20, -30)$ (right one) as the function with respect to ℓ_3 . The lines correspond to the spectra for $(\ell_1, \ell_2) = (102 + \ell_3, 100)$ (red solid line), $(|100 - \ell_3| - 2, 100)$ (green dashed line) and $(100 + \ell_3, 100)$ (blue dotted line). The parameters are identical to the values defined in Fig. 7.1.

7.3 Summary and discussion

In this section, we investigated the statistical anisotropy in the CMB bispectrum by considering the modified hybrid inflation model where the waterfall field also couples with the vector field [14]. We calculated the CMB bispectrum sourced from the non-Gaussianity of curvature perturbations affected by the vector field. In this inflation model, owing to the dependence on the direction of the vector field, the correlations of the curvature perturbations violate the rotational invariance. Then, interestingly, even if the magnitude of the parameter g_β characterizing the statistical anisotropy of the CMB power spectrum is too small, the amplitude of the non-Gaussianity can become large depending on several coupling constants of the fields.

Following the procedure of Sec. 5 [25], we formulated the statistically anisotropic CMB bispectrum and confirm that three azimuthal quantum numbers m_1, m_2 and m_3 are not confined only to the Wigner symbol $\begin{pmatrix} \ell_1 & \ell_2 & \ell_3 \\ m_1 & m_2 & m_3 \end{pmatrix}$. This is evidence that the rotational invariance is violated in the CMB bispectrum and implies the existence of the signals not obeying the triangle condition of the above Wigner symbol as $|\ell_2 - \ell_3| \leq \ell_1 \leq \ell_2 + \ell_3$. We demonstrated that the signals of the CMB bispectrum for $\ell_1 = \ell_2 + \ell_3 + 2$, $|\ell_2 - \ell_3| - 2$ and these two permutations do not vanish. In fact, the statistically isotropic bispectra are exactly zero for these configurations; hence, these signals have the pure information of the statistical anisotropy. Because the amplitudes of these intensity bispectra are comparable to those for $\ell_1 = \ell_2 + \ell_3$, it might be possible to detect these contributions of the statistical anisotropy in future experiments, which would give us novel information about the physics of the early Universe. Of course, also for the E -mode polarization, we can give the same discussions and results.

Although we assume a specific potential of inflation to show the statistical anisotropy on the CMB bispectrum explicitly, the above calculation and discussion will be applicable to other inflation models where the rotational invariance violates.

References

- [1] N. E. Groeneboom and H. K. Eriksen, *Bayesian analysis of sparse anisotropic universe models and application to the 5-yr WMAP data*, *Astrophys. J.* **690** (2009) 1807–1819, [arXiv:0807.2242].
- [2] N. E. Groeneboom, L. Ackerman, I. K. Wehus, and H. K. Eriksen, *Bayesian analysis of an anisotropic universe model: systematics and polarization*, *Astrophys. J.* **722** (2010) 452–459, [arXiv:0911.0150].
- [3] M. Frommert and T. A. Enßlin, *The axis of evil - a polarization perspective*, *MNRAS* **403** (Apr., 2010) 1739–1748, [arXiv:0908.0453].
- [4] D. Hanson and A. Lewis, *Estimators for CMB Statistical Anisotropy*, *Phys. Rev.* **D80** (2009) 063004, [arXiv:0908.0963].
- [5] C. L. Bennett *et al.*, *Seven-Year Wilkinson Microwave Anisotropy Probe (WMAP) Observations: Are There Cosmic Microwave Background Anomalies?*, *Astrophys. J. Suppl.* **192** (2011) 17, [arXiv:1001.4758].
- [6] D. Hanson, A. Lewis, and A. Challinor, *Asymmetric Beams and CMB Statistical Anisotropy*, *Phys. Rev.* **D81** (2010) 103003, [arXiv:1003.0198].
- [7] L. Ackerman, S. M. Carroll, and M. B. Wise, *Imprints of a Primordial Preferred Direction on the Microwave Background*, *Phys. Rev.* **D75** (2007) 083502, [astro-ph/0701357].
- [8] C. G. Boehmer and D. F. Mota, *CMB Anisotropies and Inflation from Non-Standard Spinors*, *Phys. Lett.* **B663** (2008) 168–171, [arXiv:0710.2003].
- [9] Y. Shtanov and H. Pyatkovska, *Erratum: Statistical anisotropy in the inflationary universe*, *Phys. Rev.* **D80** (2009) 023521, [arXiv:0904.1887].
- [10] M.-a. Watanabe, S. Kanno, and J. Soda, *Imprints of Anisotropic Inflation on the Cosmic Microwave Background*, *Mon.Not.Roy.Astron.Soc.* **412** (2011) L83–L87, [arXiv:1011.3604].
- [11] A. Gumrukcuoglu, B. Himmetoglu, and M. Peloso, *Scalar-Scalar, Scalar-Tensor, and Tensor-Tensor Correlators from Anisotropic Inflation*, *Phys.Rev.* **D81** (2010) 063528, [arXiv:1001.4088].
- [12] K. Dimopoulos, *Can a vector field be responsible for the curvature perturbation in the Universe?*, *Phys.Rev.* **D74** (2006) 083502, [hep-ph/0607229].
- [13] T. Koivisto and D. F. Mota, *Vector Field Models of Inflation and Dark Energy*, *JCAP* **0808** (2008) 021, [arXiv:0805.4229].
- [14] S. Yokoyama and J. Soda, *Primordial statistical anisotropy generated at the end of inflation*, *JCAP* **0808** (2008) 005, [arXiv:0805.4265].
- [15] K. Dimopoulos, M. Karciauskas, D. H. Lyth, and Y. Rodriguez, *Statistical anisotropy of the curvature perturbation from vector field perturbations*, *JCAP* **0905** (2009) 013, [arXiv:0809.1055].

- [16] M. Karčiauskas, K. Dimopoulos, and D. H. Lyth, *Anisotropic non-Gaussianity from vector field perturbations*, *Phys.Rev.* **D80** (2009) 023509, [[arXiv:0812.0264](#)].
- [17] N. Bartolo, E. Dimastrogiovanni, S. Matarrese, and A. Riotto, *Anisotropic bispectrum of curvature perturbations from primordial non-Abelian vector fields*, *JCAP* **0910** (2009) 015, [[arXiv:0906.4944](#)].
- [18] K. Dimopoulos, M. Karčiauskas, and J. M. Wagstaff, *Vector Curvaton with varying Kinetic Function*, *Phys.Rev.* **D81** (2010) 023522, [[arXiv:0907.1838](#)].
- [19] K. Dimopoulos, M. Karčiauskas, and J. M. Wagstaff, *Vector Curvaton without Instabilities*, *Phys.Lett.* **B683** (2010) 298–301, [[arXiv:0909.0475](#)].
- [20] C. A. Valenzuela-Toledo and Y. Rodriguez, *Non-gaussianity from the trispectrum and vector field perturbations*, *Phys.Lett.* **B685** (2010) 120–127, [[arXiv:0910.4208](#)].
- [21] C. A. Valenzuela-Toledo, *Non-gaussianity and Statistical Anisotropy in Cosmological Inflationary Models*, [arXiv:1004.5363](#).
- [22] E. Dimastrogiovanni, N. Bartolo, S. Matarrese, and A. Riotto, *Non-Gaussianity and Statistical Anisotropy from Vector Field Populated Inflationary Models*, *Adv.Astron.* **2010** (2010) 752670, [[arXiv:1001.4049](#)].
- [23] K. Dimopoulos and J. M. Wagstaff, *Particle Production of Vector Fields: Scale Invariance is Attractive*, *Phys.Rev.* **D83** (2011) 023523, [[arXiv:1011.2517](#)].
- [24] M. Karčiauskas, *The Primordial Curvature Perturbation from Vector Fields of General non-Abelian Groups*, *JCAP* **1201** (2012) 014, [[arXiv:1104.3629](#)].
- [25] M. Shiraishi, D. Nitta, S. Yokoyama, K. Ichiki, and K. Takahashi, *CMB Bispectrum from Primordial Scalar, Vector and Tensor non-Gaussianities*, *Prog. Theor. Phys.* **125** (2011) 795–813, [[arXiv:1012.1079](#)].
- [26] M. Shiraishi and S. Yokoyama, *Violation of the Rotational Invariance in the CMB Bispectrum*, *Prog.Theor.Phys.* **126** (2011) 923–935, [[arXiv:1107.0682](#)].
- [27] A. A. Starobinsky, *Dynamics of Phase Transition in the New Inflationary Universe Scenario and Generation of Perturbations*, *Phys.Lett.* **B117** (1982) 175–178.
- [28] A. A. Starobinsky, *Multicomponent de Sitter (Inflationary) Stages and the Generation of Perturbations*, *JETP Lett.* **42** (1985) 152–155.
- [29] M. Sasaki and E. D. Stewart, *A General analytic formula for the spectral index of the density perturbations produced during inflation*, *Prog.Theor.Phys.* **95** (1996) 71–78, [[astro-ph/9507001](#)].
- [30] M. Sasaki and T. Tanaka, *Superhorizon scale dynamics of multiscalar inflation*, *Prog.Theor.Phys.* **99** (1998) 763–782, [[gr-qc/9801017](#)].
- [31] D. H. Lyth, K. A. Malik, and M. Sasaki, *A General proof of the conservation of the curvature perturbation*, *JCAP* **0505** (2005) 004, [[astro-ph/0411220](#)].

-
- [32] D. H. Lyth and Y. Rodriguez, *The Inflationary prediction for primordial non-Gaussianity*, *Phys.Rev.Lett.* **95** (2005) 121302, [[astro-ph/0504045](#)].
 - [33] J. Martin and J. Yokoyama, *Generation of Large-Scale Magnetic Fields in Single-Field Inflation*, *JCAP* **0801** (2008) 025, [[arXiv:0711.4307](#)].
 - [34] A. Lewis, A. Challinor, and A. Lasenby, *Efficient Computation of CMB anisotropies in closed FRW models*, *Astrophys. J.* **538** (2000) 473–476, [[astro-ph/9911177](#)].
 - [35] A. Lewis, *CMB anisotropies from primordial inhomogeneous magnetic fields*, *Phys. Rev.* **D70** (2004) 043011, [[astro-ph/0406096](#)].
 - [36] “Slatec common mathematical library.” <http://www.netlib.org/slatec/>.
 - [37] **PLANCK** Collaboration, *The Scientific programme of planck*, [astro-ph/0604069](#).
 - [38] **WMAP** Collaboration, E. Komatsu *et al.*, *Seven-Year Wilkinson Microwave Anisotropy Probe (WMAP) Observations: Cosmological Interpretation*, *Astrophys. J. Suppl.* **192** (2011) 18, [[arXiv:1001.4538](#)].

8 Parity violation of gravitons in the CMB bispectrum

Non-Gaussian features in the cosmological perturbations include detailed information on the nature of the early Universe, and there have been many works that attempt to extract them from the bispectrum (three-point function) of the cosmic microwave background (CMB) anisotropies (e.g., Refs. [1–4]). However, most of these discussions are limited in the cases that the scalar-mode contribution dominates in the non-Gaussianity and also are based on the assumption of rotational invariance and parity conservation.

In contrast, there are several studies on the non-Gaussianities of not only the scalar-mode perturbations but also the vector- and tensor-mode perturbations [5–7]. These sources produce the additional signals on the CMB bispectrum [8] and can give a dominant contribution by considering such highly non-Gaussian sources as the stochastic magnetic fields [9]. Furthermore, even in the CMB bispectrum induced from the scalar-mode non-Gaussianity, if the rotational invariance is violated in the non-Gaussianity, the characteristic signals appear [10]. Thus, it is very important to clarify these less-noted signals to understand the precise picture of the early Universe.

Recently, the parity violation in the graviton non-Gaussianities has been discussed in Refs. [11, 12]. Maldacena and Pimentel first calculated the primordial bispectrum of the gravitons sourced from parity-even (parity-conserving) and parity-odd (parity-violating) Weyl cubic terms, namely, W^3 and $\widetilde{W}W^2$, respectively, by making use of the spinor helicity formalism. [11] Soda *et al.* proved that the parity-violating non-Gaussianity of the primordial gravitational waves induced from $\widetilde{W}W^2$ emerges not in the exact de-Sitter space-time but in the quasi de-Sitter space-time, and hence, its amplitude is proportional to a slow-roll parameter. [12] In these studies, the authors assume that the coupling constant of the Weyl cubic terms is independent of time.

In this section, we estimate the primordial non-Gaussianities of gravitons generated from W^3 and $\widetilde{W}W^2$ with the time-dependent coupling parameter [13]. We consider the case where the coupling is given by a power of the conformal time. We show that in such a model, the parity violation in the non-Gaussianity of the primordial gravitational waves would not vanish even in the exact de-Sitter space-time. The effects of the parity violation on the CMB power spectrum have been well-studied, where an attractive result is that the cross-correlation between the intensity and B -mode polarization is generated [14–17]. On the other hand, in the CMB bispectrum, owing to the mathematical property of the spherical harmonic function, the parity-even and parity-odd signals should arise from just the opposite configurations of multipoles [18, 19]. Then, we formulate and numerically calculate the CMB bispectra induced by these non-Gaussianities that contain all the correlations between the intensity (I) and polarizations (E, B) and show that the signals from W^3 (parity-conserving) appear in the configuration of the multipoles where those from $\widetilde{W}W^2$ (parity-violating) vanish and vice versa. These discussions are based on Ref. [20].

This section is organized as follows. In the next subsection, we derive the primordial bispectrum of gravitons induced by W^3 and $\widetilde{W}W^2$ with the coupling constant proportional to the power of the conformal time. In Sec. 8.2, we calculate the CMB bispectra sourced from these non-Gaussianities, analyze their behavior and find some peculiar signatures of the parity violation. The final subsection is devoted to summary and discussion. In Appendices E and F, we describe the detailed calculations of the contractions of the polarization tensors and unit vectors, and of the initial bispectra by the in-in formalism.

Throughout this section, we use $M_{\text{pl}} \equiv 1/\sqrt{8\pi G}$, where G is the Newton constant and the rule that all the Greek characters and alphabets run from 0 to 3 and from 1 to 3, respectively.

8.1 Parity-even and -odd non-Gaussianity of gravitons

In this subsection, we formulate the primordial non-Gaussianity of gravitons generated from the Weyl cubic terms with the running coupling constant as a function of a conformal time, $f(\tau)$, whose action is given by

$$S = \int d\tau d^3x \frac{f(\tau)}{\Lambda^2} \left(\sqrt{-g} W^3 + \widetilde{W} W^2 \right) , \quad (8.1)$$

with

$$\begin{aligned} W^3 &\equiv W^{\alpha\beta}{}_{\gamma\delta} W^{\gamma\delta}{}_{\sigma\rho} W^{\sigma\rho}{}_{\alpha\beta} , \\ \widetilde{W} W^2 &\equiv \epsilon^{\alpha\beta\mu\nu} W_{\mu\nu\gamma\delta} W^{\gamma\delta}{}_{\sigma\rho} W^{\sigma\rho}{}_{\alpha\beta} , \end{aligned} \quad (8.2)$$

where $W^{\alpha\beta}{}_{\gamma\delta}$ denotes the Weyl tensor, $\epsilon^{\alpha\beta\mu\nu}$ is a 4D Levi-Civita tensor normalized as $\epsilon^{0123} = 1$, and Λ is a scale that sets the value of the higher derivative corrections [11]. Note that W^3 and $\widetilde{W} W^2$ have the even and odd parities, respectively. In the following discussion, we assume that the coupling constant is given by

$$f(\tau) = \left(\frac{\tau}{\tau_*} \right)^A , \quad (8.3)$$

where τ is a conformal time. Here, we have set $f(\tau_*) = 1$. Such a coupling can be readily realized by considering a dilaton-like coupling in the slow-roll inflation as discussed in Sec. 8.1.2.

8.1.1 Calculation of the primordial bispectrum

Here, let us focus on the calculation of the primordial bispectrum induced by W^3 and $\widetilde{W} W^2$ of Eq. (8.1) on the exact de-Sitter space-time in a more straightforward manner than those of Refs. [11, 12].

At first, we consider the tensor perturbations on the Friedmann-Lemaître-Robertson-Walker metric as

$$ds^2 = a^2(-d\tau^2 + e^{\gamma_{ij}} dx^i dx^j) , \quad (8.4)$$

where a denotes the scale factor and γ_{ij} obeys the transverse traceless conditions; $\gamma_{ii} = \partial\gamma_{ij}/\partial x^j = 0$ ¹. Up to the second order, even if the action includes the Weyl cubic terms given by Eq. (8.1), the gravitational wave obeys the action as [11, 12]

$$S = \frac{M_{\text{pl}}^2}{8} \int d\tau d^3x a^2 (\dot{\gamma}_{ij} \dot{\gamma}_{ij} - \gamma_{ij,k} \gamma_{ij,k}) , \quad (8.5)$$

where $\dot{\gamma} \equiv \partial/\partial\tau$ and $\gamma_{,i} \equiv \partial/\partial x^i$. We expand the gravitational wave with a transverse and traceless polarization tensor $e_{ij}^{(\lambda)}$ and the creation and annihilation operators $a^{(\lambda)\dagger}, a^{(\lambda)}$ as

$$\gamma_{ij}(\mathbf{x}, \tau) = \int \frac{d^3\mathbf{k}}{(2\pi)^3} \sum_{\lambda=\pm 2} \gamma_{dS}(k, \tau) a_{\mathbf{k}}^{(\lambda)} e_{ij}^{(\lambda)}(\hat{\mathbf{k}}) e^{i\mathbf{k}\cdot\mathbf{x}} + h.c.$$

¹ γ_{ij} is identical to h_{ij} in Sec. 2.6

$$= \int \frac{d^3\mathbf{k}}{(2\pi)^3} \sum_{\lambda=\pm 2} \gamma^{(\lambda)}(\mathbf{k}, \tau) e_{ij}^{(\lambda)}(\hat{\mathbf{k}}) e^{i\mathbf{k}\cdot\mathbf{x}} , \quad (8.6)$$

with

$$\gamma^{(\lambda)}(\mathbf{k}, \tau) \equiv \gamma_{dS}(k, \tau) a_{\mathbf{k}}^{(\lambda)} + \gamma_{dS}^*(k, \tau) a_{-\mathbf{k}}^{(\lambda)\dagger} . \quad (8.7)$$

Here, $\lambda \equiv \pm 2$ denotes the helicity of the gravitational wave and we use the polarization tensor satisfying the relations as Eq. (D.13). The creation and annihilation operators $a^{(\lambda)\dagger}, a^{(\lambda)}$ obey the relations as

$$\begin{aligned} a_{\mathbf{k}}^{(\lambda)} |0\rangle &= 0 , \\ [a_{\mathbf{k}}^{(\lambda)}, a_{\mathbf{k}'}^{(\lambda')\dagger}] &= (2\pi)^3 \delta(\mathbf{k} - \mathbf{k}') \delta_{\lambda, \lambda'} , \end{aligned} \quad (8.8)$$

where $|0\rangle$ denotes a vacuum eigenstate. Then, the mode function of gravitons on the de Sitter space-time γ_{dS} satisfies the field equation as

$$\ddot{\gamma}_{dS} - \frac{2}{\tau} \dot{\gamma}_{dS} + k^2 \gamma_{dS} = 0 , \quad (8.9)$$

and a solution is given by

$$\gamma_{dS} = i \frac{H}{M_{\text{pl}}} \frac{e^{-ik\tau}}{k^{3/2}} (1 + ik\tau) , \quad (8.10)$$

where $H = -(a\tau)^{-1}$ is the Hubble parameter and has a constant value in the exact de Sitter space-time.

On the basis of the in-in formalism (see, e.g., Refs. [5, 21]) and the above results, we calculate the tree-level bispectrum of gravitons on the late-time limit. According to this formalism, the expectation value of an operator depending on time in the interaction picture, $O(t)$, is written as

$$\langle O(t) \rangle = \left\langle 0 \left| \bar{T} e^{i \int H_{int}(t') dt'} O(t) T e^{-i \int H_{int}(t') dt'} \right| 0 \right\rangle , \quad (8.11)$$

where T and \bar{T} are respectively time-ordering and anti-time-ordering operators and $H_{int}(t)$ is the interaction Hamiltonian. Applying this equation, the primordial bispectrum of gravitons at the tree level can be expressed as

$$\left\langle \prod_{n=1}^3 \gamma^{(\lambda_n)}(\mathbf{k}_n, \tau) \right\rangle = i \int_{-\infty}^{\tau} d\tau' \left\langle 0 \left| \left[: H_{int}(\tau') : , \prod_{n=1}^3 \gamma^{(\lambda_n)}(\mathbf{k}_n, \tau) \right] \right| 0 \right\rangle , \quad (8.12)$$

where $:$ denotes normal product.

Up to the first order with respect to γ_{ij} , the nonzero components of the Weyl tensor are written as

$$\begin{aligned} W^{0i}_{0j} &= \frac{1}{4} (H\tau)^2 \gamma_{ij, \alpha\alpha} , \\ W^{ij}_{0k} &= \frac{1}{2} (H\tau)^2 (\dot{\gamma}_{ki, j} - \dot{\gamma}_{kj, i}) , \\ W^{0i}_{jk} &= \frac{1}{2} (H\tau)^2 (\dot{\gamma}_{ik, j} - \dot{\gamma}_{ij, k}) , \\ W^{ij}_{kl} &= \frac{1}{4} (H\tau)^2 (-\delta_{ik} \gamma_{jl, \alpha\alpha} + \delta_{il} \gamma_{jk, \alpha\alpha} + \delta_{jk} \gamma_{il, \alpha\alpha} - \delta_{jl} \gamma_{ik, \alpha\alpha}) , \end{aligned} \quad (8.13)$$

where $\gamma_{ij,\alpha\alpha} \equiv \ddot{\gamma}_{ij} + \nabla^2 \gamma_{ij}$. Then W^3 and $\widetilde{W}W^2$ respectively reduce to

$$\begin{aligned} W^3 &= W^{ij}_{kl} W^{kl}_{mn} W^{mn}_{ij} + 6W^{0i}_{jk} W^{jk}_{lm} W^{lm}_{0i} \\ &\quad + 12W^{0i}_{0j} W^{0j}_{kl} W^{kl}_{0i} + 8W^{0i}_{0j} W^{0j}_{0k} W^{0k}_{0i} , \\ \widetilde{W}W^2 &= 4\eta^{ijk} [W_{jkpq} (W^{pq}_{lm} W^{lm}_{0i} + 2W^{pq}_{0m} W^{0m}_{0i}) \\ &\quad + 2W_{jk0p} (W^{0p}_{lm} W^{lm}_{0i} + 2W^{0p}_{0m} W^{0m}_{0i})] , \end{aligned} \quad (8.14)$$

where $\eta^{ijk} \equiv \epsilon^{0ijk}$. Using the above expressions and $\int d\tau H_{int} = -S_{int}$, up to the third order, the interaction Hamiltonians of W^3 and $\widetilde{W}W^2$ are respectively given by

$$\begin{aligned} H_{W^3} &= - \int d^3x \Lambda^{-2} (H\tau)^2 \left(\frac{\tau}{\tau_*} \right)^A \\ &\quad \times \frac{1}{4} \gamma_{ij,\alpha\alpha} [\gamma_{jk,\beta\beta} \gamma_{ki,\sigma\sigma} + 6\dot{\gamma}_{kl,i} \dot{\gamma}_{kl,j} + 6\dot{\gamma}_{ik,l} \dot{\gamma}_{jl,k} - 12\dot{\gamma}_{ik,l} \dot{\gamma}_{kl,j}] , \\ H_{\widetilde{W}W^2} &= - \int d^3x \Lambda^{-2} (H\tau)^2 \left(\frac{\tau}{\tau_*} \right)^A \\ &\quad \times \eta^{ijk} [\gamma_{kq,\alpha\alpha} (-3\gamma_{jm,\beta\beta} \dot{\gamma}_{iq,m} + \gamma_{mi,\beta\beta} \dot{\gamma}_{mq,j}) + 4\dot{\gamma}_{pj,k} \dot{\gamma}_{pm,l} (\dot{\gamma}_{il,m} - \dot{\gamma}_{im,l})] . \end{aligned} \quad (8.15)$$

Substituting the above expressions into Eq. (8.12), using the solution given by Eq. (8.10), and considering the late-time limit as $\tau \rightarrow 0$, we can obtain an explicit form of the primordial bispectra:

$$\left\langle \prod_{n=1}^3 \gamma^{(\lambda_n)}(\mathbf{k}_n) \right\rangle_{int} = (2\pi)^3 \delta \left(\sum_{n=1}^3 \mathbf{k}_n \right) f_{int}^{(r)}(k_1, k_2, k_3) f_{int}^{(a)}(\hat{\mathbf{k}}_1, \hat{\mathbf{k}}_2, \hat{\mathbf{k}}_3) , \quad (8.16)$$

with²

$$\begin{aligned} f_{W^3}^{(r)} &= 8 \left(\frac{H}{M_{\text{pl}}} \right)^6 \left(\frac{H}{\Lambda} \right)^2 \text{Re} \left[\tau_*^{-A} \int_{-\infty}^0 d\tau' \tau'^{5+A} e^{-ik_t \tau'} \right] , \\ f_{W^3}^{(a)} &= e_{ij}^{(-\lambda_1)} \left[\frac{1}{2} e_{jk}^{(-\lambda_2)} e_{ki}^{(-\lambda_3)} + \frac{3}{4} e_{kl}^{(-\lambda_2)} e_{kl}^{(-\lambda_3)} \hat{k}_{2i} \hat{k}_{3j} \right. \\ &\quad \left. + \frac{3}{4} e_{ki}^{(-\lambda_2)} e_{jl}^{(-\lambda_3)} \hat{k}_{2l} \hat{k}_{3k} - \frac{3}{2} e_{ik}^{(-\lambda_2)} e_{kl}^{(-\lambda_3)} \hat{k}_{2l} \hat{k}_{3j} \right] + 5 \text{ perms} , \\ f_{\widetilde{W}W^2}^{(r)} &= 8 \left(\frac{H}{M_{\text{pl}}} \right)^6 \left(\frac{H}{\Lambda} \right)^2 \text{Im} \left[\tau_*^{-A} \int_{-\infty}^0 d\tau' \tau'^{5+A} e^{-ik_t \tau'} \right] , \\ f_{\widetilde{W}W^2}^{(a)} &= i\eta^{ijk} \left[e_{kq}^{(-\lambda_1)} \left\{ -3e_{jm}^{(-\lambda_2)} e_{iq}^{(-\lambda_3)} \hat{k}_{3m} + e_{mi}^{(-\lambda_2)} e_{mq}^{(-\lambda_3)} \hat{k}_{3j} \right\} \right. \\ &\quad \left. + e_{pj}^{(-\lambda_1)} e_{pm}^{(-\lambda_2)} \hat{k}_{1k} \hat{k}_{2l} \left\{ e_{il}^{(-\lambda_3)} \hat{k}_{3m} - e_{im}^{(-\lambda_3)} \hat{k}_{3l} \right\} \right] + 5 \text{ perms} . \end{aligned} \quad (8.17)$$

Here, $k_t \equiv \sum_{n=1}^3 k_n$, $int = W^3$ and $\widetilde{W}W^2$, “5 perms” denotes the five symmetric terms under the permutations of $(\hat{\mathbf{k}}_1, \lambda_1)$, $(\hat{\mathbf{k}}_2, \lambda_2)$, and $(\hat{\mathbf{k}}_3, \lambda_3)$. From the above expressions, we find that the bispectra of the primordial gravitational wave induced from W^3 and $\widetilde{W}W^2$ are proportional to the real and imaginary parts of $\tau_*^{-A} \int_{-\infty}^0 d\tau' \tau'^{5+A} e^{-ik_t \tau'}$, respectively. This difference comes from the number of $\gamma_{ij,\alpha\alpha}$ and $\dot{\gamma}_{ij,k}$. H_{W^3} consists of the products of an odd number of the former

²Here, we set that $\tau_* < 0$.

terms and an even number of the latter terms. On the other hand, in $H_{\widetilde{W}W^2}$, the situation is the opposite. Since the former and latter terms contain $\ddot{\gamma}_{dS} - k^2\gamma_{dS} = (2H\tau'/M_{\text{pl}})k^{3/2}e^{-ik\tau'}$ and $\dot{\gamma}_{dS} = i(H\tau'/M_{\text{pl}})k^{1/2}e^{-ik\tau'}$, respectively, the total numbers of i are different in each time integral. Hence, the contributions of the real and imaginary parts roll upside down in $f_{W^3}^{(r)}$ and $f_{\widetilde{W}W^2}^{(r)}$. Since the time integral in the bispectra can be analytically evaluated as

$$\tau_*^{-A} \int_{-\infty}^0 d\tau' \tau'^{5+A} e^{-ik_t\tau'} = \left[\cos\left(\frac{\pi}{2}A\right) + i \sin\left(\frac{\pi}{2}A\right) \right] \Gamma(6+A) k_t^{-6} (-k_t\tau_*)^{-A}, \quad (8.18)$$

$f_{W^3}^{(r)}$ and $f_{\widetilde{W}W^2}^{(r)}$ reduce to

$$f_{W^3}^{(r)} = 8 \left(\frac{H}{M_{\text{pl}}} \right)^6 \left(\frac{H}{\Lambda} \right)^2 \cos\left(\frac{\pi}{2}A\right) \Gamma(6+A) k_t^{-6} (-k_t\tau_*)^{-A}, \quad (8.19)$$

$$f_{\widetilde{W}W^2}^{(r)} = 8 \left(\frac{H}{M_{\text{pl}}} \right)^6 \left(\frac{H}{\Lambda} \right)^2 \sin\left(\frac{\pi}{2}A\right) \Gamma(6+A) k_t^{-6} (-k_t\tau_*)^{-A}, \quad (8.20)$$

where $\Gamma(x)$ is the Gamma function. For more detailed derivation of the graviton bispectrum, see Appendix F.

From this equation, we can see that in the case of the time-independent coupling, which corresponds to the $A = 0$ case, the bispectrum from $\widetilde{W}W^2$ vanishes. This is consistent with a claim in Ref. [12]³. On the other hand, interestingly, if A deviates from 0, it is possible to realize the nonzero bispectrum induced from $\widetilde{W}W^2$ even in the exact de Sitter limit. Thus, we expect the signals from $\widetilde{W}W^2$ without the slow-roll suppression, which can be comparable to those from W^3 and become sufficiently large to observe in the CMB.

8.1.2 Running coupling constant

Here, we discuss how to realize $f \propto \tau^A$ within the framework of the standard slow-roll inflation. During the standard slow-roll inflation, the equation of motion of the scalar field ϕ , which has a potential V , is expressed as

$$\dot{\phi} \simeq \pm \sqrt{2\epsilon_\phi} M_{\text{pl}} \tau^{-1}, \quad (8.21)$$

where $\epsilon_\phi \equiv [\partial V / \partial \phi / (3M_{\text{pl}} H^2)]^2 / 2$ is a slow-roll parameter for ϕ , $+$ and $-$ signs are taken to be for $\partial V / \partial \phi > 0$ and $\partial V / \partial \phi < 0$, respectively, and we have assumed that $aH = -1/\tau$. The solution of the above equation is given by

$$\phi = \phi_* \pm \sqrt{2\epsilon_\phi} M_{\text{pl}} \ln \left(\frac{\tau}{\tau_*} \right). \quad (8.22)$$

Hence, if we assume a dilaton-like coupling as $f \equiv e^{(\phi - \phi_*)/M}$, we have

$$f(\tau) = \left(\frac{\tau}{\tau_*} \right)^A, \quad A = \pm \sqrt{2\epsilon_\phi} \frac{M_{\text{pl}}}{M}, \quad (8.23)$$

where M is an arbitrary energy scale. Let us take τ_* to be a time when the scale of the present horizon of the Universe exits the horizon during inflation, namely, $|\tau_*| = k_*^{-1} \sim 14 \text{Gpc}$. Then, the

³ In Ref. [12], the authors have shown that for $A = 0$, the bispectrum from $\widetilde{W}W^2$ has a nonzero value upward in the first order of the slow-roll parameter.

coupling f , which determines the amplitude of the bispectrum of the primordial gravitational wave induced from the Weyl cubic terms, is on the order of unity for the current cosmological scales. From Eq. (8.23), we have $A = \pm 1/2$ with $M = \sqrt{8\epsilon_\phi} M_{\text{pl}}$. As seen in Eqs. (8.19) and (8.20), this leads to an interesting situation that the bispectra from W^3 and $\widetilde{W}W^2$ have a comparable magnitude as $f_{W^3}^{(r)} = \pm f_{\widetilde{W}W^2}^{(r)}$. Hence, we can expect that in the CMB bispectrum, the signals from these terms are almost the same.

In the next subsection, we demonstrate these through the explicit calculation of the CMB bispectra.

8.2 CMB parity-even and -odd bispectrum

In this subsection, following the calculation approach discussed in Sec. 6, we formulate the CMB bispectrum induced from the non-Gaussianities of gravitons sourced by W^3 and $\widetilde{W}W^2$ terms discussed in the previous subsection.

8.2.1 Formulation

Conventionally, the CMB fluctuation is expanded with the spherical harmonics as

$$\frac{\Delta X(\hat{\mathbf{n}})}{X} = \sum_{\ell m} a_{X,\ell m} Y_{\ell m}(\hat{\mathbf{n}}), \quad (8.24)$$

where $\hat{\mathbf{n}}$ is a unit vector pointing toward a line-of-sight direction, and X means the intensity ($\equiv I$) and the electric and magnetic polarization modes ($\equiv E, B$). By performing the line-of-sight integration, the coefficient, $a_{\ell m}$, generated from the primordial fluctuation of gravitons, $\gamma^{(\pm 2)}$, is given by [corresponding to Eq. (5.3)]

$$a_{X,\ell m} = 4\pi(-i)^\ell \int_0^\infty \frac{k^2 dk}{(2\pi)^3} \mathcal{T}_{X,\ell}(k) \sum_{\lambda=\pm 2} \left(\frac{\lambda}{2}\right)^x \gamma_{\ell m}^{(\lambda)}(k), \quad (8.25)$$

$$\gamma_{\ell m}^{(\lambda)}(k) \equiv \int d^2\hat{\mathbf{k}} \gamma^{(\lambda)}(\mathbf{k})_{-\lambda} Y_{\ell m}^*(\hat{\mathbf{k}}), \quad (8.26)$$

where x discriminates the parity of three modes: $x = 0$ for $X = I, E$ and $x = 1$ for $X = B$, and $\mathcal{T}_{X,\ell}$ is the time-integrated transfer function of tensor modes (3.101). Like Eq. (5.5), we can obtain the CMB bispectrum generated from the primordial bispectrum of gravitons as

$$\begin{aligned} \left\langle \prod_{n=1}^3 a_{X_n, \ell_n m_n} \right\rangle &= \left[\prod_{n=1}^3 4\pi(-i)^{\ell_n} \int \frac{k_n^2 dk_n}{(2\pi)^3} \mathcal{T}_{X_n, \ell_n}(k_n) \sum_{\lambda_n=\pm 2} \left(\frac{\lambda_n}{2}\right)^{x_n} \right] \\ &\times \left\langle \prod_{n=1}^3 \gamma_{\ell_n m_n}^{(\lambda_n)}(k_n) \right\rangle. \end{aligned} \quad (8.27)$$

In order to derive an explicit form of this CMB bispectrum, at first, we need to express all the functions containing the angular dependence on the wave number vectors with the spin spherical harmonics. Using the results of Appendix E, $f_{W^3}^{(a)}$ and $f_{\widetilde{W}W^2}^{(a)}$ can be calculated as

$$f_{W^3}^{(a)} = (8\pi)^{3/2} \sum_{L', L''=2,3} \sum_{M, M', M''} \begin{pmatrix} 2 & L' & L'' \\ M & M' & M'' \end{pmatrix}$$

$$\begin{aligned}
& \times_{\lambda_1} Y_{2M}^*(\hat{\mathbf{k}}_1)_{\lambda_2} Y_{L'M'}^*(\hat{\mathbf{k}}_2)_{\lambda_3} Y_{L''M''}^*(\hat{\mathbf{k}}_3) \\
& \times \left[-\frac{1}{20} \sqrt{\frac{7}{3}} \delta_{L',2} \delta_{L'',2} + (-1)^{L'} I_{L'12}^{\lambda_2 0 - \lambda_2} I_{L''12}^{\lambda_3 0 - \lambda_3} \right. \\
& \quad \times \left(-\frac{\pi}{5} \left\{ \begin{matrix} 2 & L' & L'' \\ 2 & 1 & 1 \end{matrix} \right\} - \pi \left\{ \begin{matrix} 2 & L' & L'' \\ 1 & 1 & 2 \\ 1 & 2 & 1 \end{matrix} \right\} \right. \\
& \quad \left. \left. + 2\pi \left\{ \begin{matrix} 2 & 1 & L' \\ 2 & 1 & 1 \end{matrix} \right\} \left\{ \begin{matrix} 2 & L' & L'' \\ 2 & 1 & 1 \end{matrix} \right\} \right) \right] + 5 \text{ perms} , \tag{8.28}
\end{aligned}$$

$$\begin{aligned}
f_{\widetilde{W}W^2}^{(a)} &= (8\pi)^{3/2} \sum_{L', L''=2,3} \sum_{M, M', M''} \left(\begin{matrix} 2 & L' & L'' \\ M & M' & M'' \end{matrix} \right) \\
& \times_{\lambda_1} Y_{2M}^*(\hat{\mathbf{k}}_1)_{\lambda_2} Y_{L'M'}^*(\hat{\mathbf{k}}_2)_{\lambda_3} Y_{L''M''}^*(\hat{\mathbf{k}}_3) (-1)^{L''} I_{L''12}^{\lambda_3 0 - \lambda_3} \\
& \times \left[\delta_{L',2} \left(3\sqrt{\frac{2\pi}{5}} \left\{ \begin{matrix} 2 & 2 & L'' \\ 1 & 2 & 1 \end{matrix} \right\} - 2\sqrt{2\pi} \left\{ \begin{matrix} 2 & 2 & L'' \\ 1 & 1 & 1 \\ 1 & 1 & 2 \end{matrix} \right\} \right) \right. \\
& \quad \left. + \frac{\lambda_1}{2} I_{L'12}^{\lambda_2 0 - \lambda_2} \left(-\frac{4\pi}{3} \left\{ \begin{matrix} 2 & L' & L'' \\ 1 & 2 & 1 \\ 1 & 1 & 2 \end{matrix} \right\} + \frac{2\pi}{15} \sqrt{\frac{7}{3}} \left\{ \begin{matrix} 2 & L' & L'' \\ 1 & 2 & 2 \end{matrix} \right\} \right) \right] \\
& + 5 \text{ perms} , \tag{8.29}
\end{aligned}$$

where the 2×3 matrix of a bracket, and the 2×3 and 3×3 matrices of a curly bracket denote the Wigner- $3j$, $6j$ and $9j$ symbols, respectively, and

$$I_{l_1 l_2 l_3}^{s_1 s_2 s_3} \equiv \sqrt{\frac{(2l_1+1)(2l_2+1)(2l_3+1)}{4\pi}} \begin{pmatrix} l_1 & l_2 & l_3 \\ s_1 & s_2 & s_3 \end{pmatrix} . \tag{8.30}$$

The delta function is also expanded as

$$\begin{aligned}
\delta \left(\sum_{n=1}^3 \mathbf{k}_n \right) &= 8 \int_0^\infty y^2 dy \left[\prod_{n=1}^3 \sum_{L_n M_n} (-1)^{L_n/2} j_{L_n}(k_n y) Y_{L_n M_n}^*(\hat{\mathbf{k}}_n) \right] \\
& \times I_{L_1 L_2 L_3}^{0 \ 0 \ 0} \begin{pmatrix} L_1 & L_2 & L_3 \\ M_1 & M_2 & M_3 \end{pmatrix} . \tag{8.31}
\end{aligned}$$

Next, we integrate all the spin spherical harmonics over $\hat{\mathbf{k}}_1, \hat{\mathbf{k}}_2, \hat{\mathbf{k}}_3$ as

$$\begin{aligned}
\int d^2 \hat{\mathbf{k}}_1 Y_{\ell_1 m_1}^* Y_{L_1 M_1}^* Y_{2M}^* &= I_{\ell_1 L_1 2}^{\lambda_1 0 - \lambda_1} \begin{pmatrix} \ell_1 & L_1 & 2 \\ m_1 & M_1 & M \end{pmatrix} , \\
\int d^2 \hat{\mathbf{k}}_2 Y_{\ell_2 m_2}^* Y_{L_2 M_2}^* Y_{L'M'}^* &= I_{\ell_2 L_2 L'}^{\lambda_2 0 - \lambda_2} \begin{pmatrix} \ell_2 & L_2 & L' \\ m_2 & M_2 & M' \end{pmatrix} , \\
\int d^2 \hat{\mathbf{k}}_3 Y_{\ell_3 m_3}^* Y_{L_3 M_3}^* Y_{L''M''}^* &= I_{\ell_3 L_3 L''}^{\lambda_3 0 - \lambda_3} \begin{pmatrix} \ell_3 & L_3 & L'' \\ m_3 & M_3 & M'' \end{pmatrix} . \tag{8.32}
\end{aligned}$$

Through the summation over the azimuthal quantum numbers, the product of the above five Wigner- $3j$ symbols is expressed with the Wigner- $9j$ symbols as

$$\sum_{\substack{M_1 M_2 M_3 \\ M M' M''}} \begin{pmatrix} L_1 & L_2 & L_3 \\ M_1 & M_2 & M_3 \end{pmatrix} \begin{pmatrix} 2 & L' & L'' \\ M & M' & M'' \end{pmatrix}$$

$$\begin{aligned}
& \times \begin{pmatrix} \ell_1 & L_1 & 2 \\ m_1 & M_1 & M \end{pmatrix} \begin{pmatrix} \ell_2 & L_2 & L' \\ m_2 & M_2 & M' \end{pmatrix} \begin{pmatrix} \ell_3 & L_3 & L'' \\ m_3 & M_3 & M'' \end{pmatrix} \\
& = \begin{pmatrix} \ell_1 & \ell_2 & \ell_3 \\ m_1 & m_2 & m_3 \end{pmatrix} \left\{ \begin{matrix} \ell_1 & \ell_2 & \ell_3 \\ L_1 & L_2 & L_3 \\ 2 & L' & L'' \end{matrix} \right\}.
\end{aligned} \tag{8.33}$$

Finally, performing the summation over the helicities, namely λ_1, λ_2 and λ_3 , as

$$\begin{aligned}
& \sum_{\lambda=\pm 2} \left(\frac{\lambda}{2}\right)^x I_{\ell L 2}^{\lambda 0-\lambda} = \begin{cases} 2I_{\ell L 2}^{20-2} & (\ell + L + x = \text{even}) \\ 0 & (\ell + L + x = \text{odd}) \end{cases}, \\
& \sum_{\lambda=\pm 2} \left(\frac{\lambda}{2}\right)^x I_{\ell L L'}^{\lambda 0-\lambda} I_{L' 12}^{\lambda 0-\lambda} = \begin{cases} 2I_{\ell L L'}^{20-2} I_{L' 12}^{20-2} & (\ell + L + x = \text{odd}) \\ 0 & (\ell + L + x = \text{even}) \end{cases}, \\
& \sum_{\lambda=\pm 2} \left(\frac{\lambda}{2}\right)^{x+1} I_{\ell L 2}^{\lambda 0-\lambda} = \begin{cases} 2I_{\ell L 2}^{20-2} & (\ell + L + x = \text{odd}) \\ 0 & (\ell + L + x = \text{even}) \end{cases},
\end{aligned} \tag{8.34}$$

and considering the selection rules of the Wigner symbols as described in Appendix C, we derive the CMB bispectrum generated from the non-Gaussianity of gravitons induced by W^3 as

$$\begin{aligned}
& \left\langle \prod_{n=1}^3 a_{X_n, \ell_n m_n} \right\rangle_{W^3} = \begin{pmatrix} \ell_1 & \ell_2 & \ell_3 \\ m_1 & m_2 & m_3 \end{pmatrix} \int_0^\infty y^2 dy \sum_{L_1 L_2 L_3} (-1)^{\frac{L_1+L_2+L_3}{2}} I_{L_1 L_2 L_3}^{0 \ 0 \ 0} \\
& \times \left[\prod_{n=1}^3 \frac{2}{\pi} (-i)^{\ell_n} \int k_n^2 dk_n \mathcal{T}_{X_n, \ell_n}(k_n) j_{L_n}(k_n y) \right] f_{W^3}^{(r)}(k_1, k_2, k_3) \\
& \times (8\pi)^{3/2} \sum_{L', L''=2,3} 8I_{\ell_1 L_1 2}^{20-2} I_{\ell_2 L_2 L'}^{20-2} I_{\ell_3 L_3 L''}^{20-2} \left\{ \begin{matrix} \ell_1 & \ell_2 & \ell_3 \\ L_1 & L_2 & L_3 \\ 2 & L' & L'' \end{matrix} \right\} \\
& \times \left[-\frac{1}{20} \sqrt{\frac{7}{3}} \delta_{L', 2} \delta_{L'', 2} \left(\prod_{n=1}^3 \mathcal{D}_{L_n, \ell_n, x_n}^{(e)} \right) \right. \\
& \quad \left. + (-1)^{L'} I_{L' 12}^{20-2} I_{L'' 12}^{20-2} \mathcal{D}_{L_1, \ell_1, x_1}^{(e)} \mathcal{D}_{L_2, \ell_2, x_2}^{(o)} \mathcal{D}_{L_3, \ell_3, x_3}^{(o)} \right. \\
& \quad \times \left(-\frac{\pi}{5} \left\{ \begin{matrix} 2 & L' & L'' \\ 2 & 1 & 1 \end{matrix} \right\} - \pi \left\{ \begin{matrix} 2 & L' & L'' \\ 1 & 1 & 2 \\ 1 & 2 & 1 \end{matrix} \right\} \right. \\
& \quad \left. \left. + 2\pi \left\{ \begin{matrix} 2 & 1 & L' \\ 2 & 1 & 1 \end{matrix} \right\} \left\{ \begin{matrix} 2 & L' & L'' \\ 2 & 1 & 1 \end{matrix} \right\} \right) \right] + 5 \text{ perms},
\end{aligned} \tag{8.35}$$

and $\widetilde{W}W^2$ as

$$\begin{aligned}
& \left\langle \prod_{n=1}^3 a_{X_n, \ell_n m_n} \right\rangle_{\widetilde{W}W^2} = \begin{pmatrix} \ell_1 & \ell_2 & \ell_3 \\ m_1 & m_2 & m_3 \end{pmatrix} \int_0^\infty y^2 dy \sum_{L_1 L_2 L_3} (-1)^{\frac{L_1+L_2+L_3}{2}} I_{L_1 L_2 L_3}^{0 \ 0 \ 0} \\
& \times \left[\prod_{n=1}^3 \frac{2}{\pi} (-i)^{\ell_n} \int k_n^2 dk_n \mathcal{T}_{X_n, \ell_n}(k_n) j_{L_n}(k_n y) \right] f_{\widetilde{W}W^2}^{(r)}(k_1, k_2, k_3) \\
& \times (8\pi)^{3/2} \sum_{L', L''=2,3} 8I_{\ell_1 L_1 2}^{20-2} I_{\ell_2 L_2 L'}^{20-2} I_{\ell_3 L_3 L''}^{20-2} \left\{ \begin{matrix} \ell_1 & \ell_2 & \ell_3 \\ L_1 & L_2 & L_3 \\ 2 & L' & L'' \end{matrix} \right\} (-1)^{L''} I_{L'' 12}^{20-2}
\end{aligned}$$

$$\begin{aligned}
& \times \left[\delta_{L',2} \mathcal{D}_{L_1,\ell_1,x_1}^{(e)} \mathcal{D}_{L_2,\ell_2,x_2}^{(e)} \mathcal{D}_{L_3,\ell_3,x_3}^{(o)} \right. \\
& \quad \times \left(3\sqrt{\frac{2\pi}{5}} \begin{Bmatrix} 2 & 2 & L'' \\ 1 & 2 & 1 \end{Bmatrix} - 2\sqrt{2\pi} \begin{Bmatrix} 2 & 2 & L'' \\ 1 & 1 & 1 \\ 1 & 1 & 2 \end{Bmatrix} \right) \\
& \quad + I_{L'12}^{20-2} \left(\prod_{n=1}^3 \mathcal{D}_{L_n,\ell_n,x_n}^{(o)} \right) \\
& \quad \times \left(-\frac{4\pi}{3} \begin{Bmatrix} 2 & L' & L'' \\ 1 & 2 & 1 \\ 1 & 1 & 2 \end{Bmatrix} + \frac{2\pi}{15} \sqrt{\frac{7}{3}} \begin{Bmatrix} 2 & L' & L'' \\ 1 & 2 & 2 \end{Bmatrix} \right) \Big] + 5 \text{ perms} . \quad (8.36)
\end{aligned}$$

Here, “5 perms” denotes the five symmetric terms under the permutations of (ℓ_1, m_1, x_1) , (ℓ_2, m_2, x_2) , and (ℓ_3, m_3, x_3) , and we introduce the filter functions as

$$\begin{aligned}
\mathcal{D}_{L,\ell,x}^{(e)} &\equiv (\delta_{L,\ell-2} + \delta_{L,\ell} + \delta_{L,\ell+2})\delta_{x,0} + (\delta_{L,\ell-3} + \delta_{L,\ell-1} + \delta_{L,\ell+1} + \delta_{L,\ell+3})\delta_{x,1} , \\
\mathcal{D}_{L,\ell,x}^{(o)} &\equiv (\delta_{L,\ell-2} + \delta_{L,\ell} + \delta_{L,\ell+2})\delta_{x,1} + (\delta_{L,\ell-3} + \delta_{L,\ell-1} + \delta_{L,\ell+1} + \delta_{L,\ell+3})\delta_{x,0} ,
\end{aligned} \quad (8.37)$$

where the superscripts (e) and (o) denote $L+\ell+x = \text{even}$ and $= \text{odd}$, respectively. From Eqs. (8.35) and (8.36), we can see that the azimuthal quantum numbers m_1, m_2 , and m_3 are confined only in a Wigner- $3j$ symbol as $\begin{pmatrix} \ell_1 & \ell_2 & \ell_3 \\ m_1 & m_2 & m_3 \end{pmatrix}$. This guarantees the rotational invariance of the CMB bispectrum. Therefore, this bispectrum survives if the triangle inequality is satisfied as $|\ell_1 - \ell_2| \leq \ell_3 \leq \ell_1 + \ell_2$.

Considering the products between the \mathcal{D} functions in Eq. (8.35) and the selection rules as $\sum_{n=1}^3 L_n = \text{even}$, we can notice that the CMB bispectrum from W^3 does not vanish only for

$$\sum_{n=1}^3 (\ell_n + x_n) = \text{even} . \quad (8.38)$$

Therefore, W^3 contributes the III, IIE, IEE, IBB, EEE , and EBB spectra for $\sum_{n=1}^3 \ell_n = \text{even}$ and the IIB, IEB, EEB , and BBB spectra for $\sum_{n=1}^3 \ell_n = \text{odd}$. This property can arise from any sources keeping the parity invariance such as W^3 . On the other hand, in the same manner, we understand that the CMB bispectrum from $\widetilde{W}W^2$ survives only for

$$\sum_{n=1}^3 (\ell_n + x_n) = \text{odd} . \quad (8.39)$$

By these constraints, we find that in reverse, $\widetilde{W}W^2$ generates the IIB, IEB, EEB , and BBB spectra for $\sum_{n=1}^3 \ell_n = \text{even}$ and the III, IIE, IEE, IBB, EEE , and EBB spectra for $\sum_{n=1}^3 \ell_n = \text{odd}$. This is a characteristic signature of the parity violation as mentioned in Refs. [18, 19]. Hence, if we analyze the information of the CMB bispectrum not only for $\sum_{n=1}^3 \ell_n = \text{even}$ but also for $\sum_{n=1}^3 \ell_n = \text{odd}$, it may be possible to check the parity violation at the level of the three-point correlation.

The above discussion about the multipole configurations of the CMB bispectra can be easily understood only if one consider the parity transformation of the CMB intensity and polarization

fields in the real space (8.24). The III , IIE , IEE , IBB , EEE and EBB spectra from W^3 , and the IIB , IEB , EEB , and BBB spectra from $\widetilde{W}W^2$ have even parity, namely,

$$\left\langle \prod_{i=1}^3 \frac{\Delta X_i(\hat{\mathbf{n}}_i)}{X_i} \right\rangle = \left\langle \prod_{i=1}^3 \frac{\Delta X_i(-\hat{\mathbf{n}}_i)}{X_i} \right\rangle. \quad (8.40)$$

Then, from the multipole expansion (8.24) and its parity flip version as

$$\frac{\Delta X(-\hat{\mathbf{n}})}{X} = \sum_{\ell m} a_{X,\ell m} Y_{\ell m}(-\hat{\mathbf{n}}) = \sum_{\ell m} (-1)^\ell a_{X,\ell m} Y_{\ell m}(\hat{\mathbf{n}}), \quad (8.41)$$

one can notice that $\sum_{n=1}^3 \ell_n = \text{even}$ must be satisfied. On the other hand, since the IIB , IEB , EEB , and BBB spectra from W^3 , and the III , IIE , IEE , IBB , EEE , and EBB spectra from $\widetilde{W}W^2$ have odd parity, namely,

$$\left\langle \prod_{i=1}^3 \frac{\Delta X_i(\hat{\mathbf{n}}_i)}{X_i} \right\rangle = - \left\langle \prod_{i=1}^3 \frac{\Delta X_i(-\hat{\mathbf{n}}_i)}{X_i} \right\rangle, \quad (8.42)$$

one can obtain $\sum_{n=1}^3 \ell_n = \text{odd}$.

In Sec. 8.2.3, we compute the CMB bispectra (8.35) and (8.36) when $A = \pm 1/2, 0, 1$, that is, the signals from W^3 become as large as those from $\widetilde{W}W^2$ and either signals vanish.

8.2.2 Evaluation of $f_{W^3}^{(r)}$ and $f_{\widetilde{W}W^2}^{(r)}$

Here, to compute the CMB bispectra (8.35) and (8.36) in finite time, we express the radial functions, $f_{W^3}^{(r)}$ and $f_{\widetilde{W}W^2}^{(r)}$, with some terms of the power of k_1 , k_2 , and k_3 . Let us focus on the dependence on k_1 , k_2 , and k_3 in Eqs. (8.19) and (8.20) as

$$f_{W^3}^{(r)} \propto f_{\widetilde{W}W^2}^{(r)} \propto k_t^{-6} (-k_t \tau_*)^{-A} = \frac{S_A(k_1, k_2, k_3)}{(k_1 k_2 k_3)^{A/3} (-\tau_*)^A}, \quad (8.43)$$

where we define S_A to satisfy $S_A \propto k^{-6}$ as

$$S_A(k_1, k_2, k_3) \equiv \frac{(k_1 k_2 k_3)^{A/3}}{k_t^{6+A}}. \quad (8.44)$$

In Fig. 8.1, we plot S_A for $A = -1/2, 0, 1/2$, and 1. From this, we notice that the shapes of S_A are similar to the equilateral-type configuration as Eq. (4.10)

$$S_{\text{equil}}(k_1, k_2, k_3) = 6 \left(-\frac{1}{k_1^3 k_2^3} - \frac{1}{k_2^3 k_3^3} - \frac{1}{k_3^3 k_1^3} - \frac{2}{k_1^2 k_2^2 k_3^2} \right. \\ \left. + \frac{1}{k_1 k_2^2 k_3^3} + \frac{1}{k_1 k_3^2 k_2^3} + \frac{1}{k_2 k_3^2 k_1^3} + \frac{1}{k_2 k_1^2 k_3^3} + \frac{1}{k_3 k_1^2 k_2^3} + \frac{1}{k_3 k_2^2 k_1^3} \right). \quad (8.45)$$

To evaluate how a function S is similar in shape to a function S' , we introduce a correlation function as [3, 22]

$$\cos(S \cdot S') \equiv \frac{S \cdot S'}{(S \cdot S)^{1/2} (S' \cdot S')^{1/2}}, \quad (8.46)$$

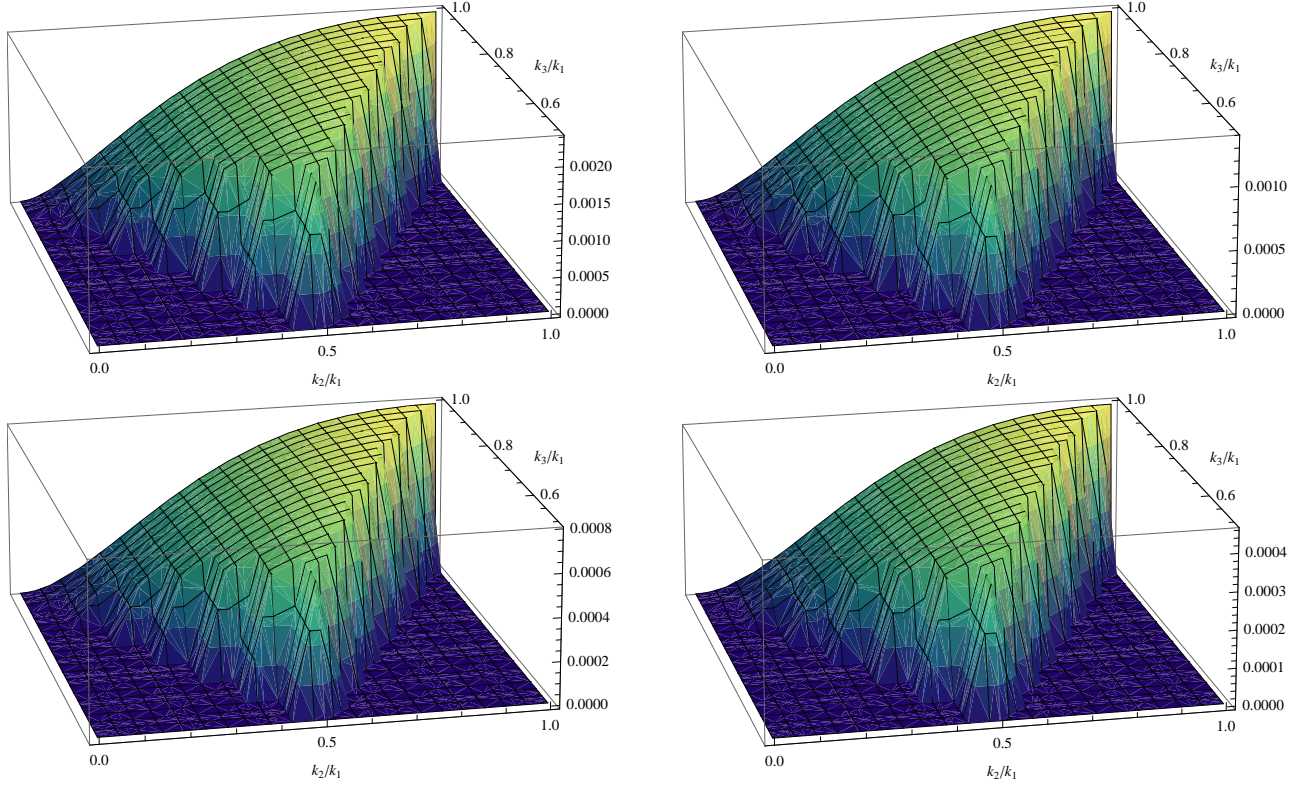


Figure 8.1: Shape of $k_1^2 k_2^2 k_3^2 S_A$ for $A = -1/2$ (top left panel), 0 (top right one), $1/2$ (bottom left one), and 1 (bottom right one) as the function of k_2/k_1 and k_3/k_1 .

with

$$\begin{aligned}
 S \cdot S' &\equiv \sum_{\mathbf{k}_i} \frac{S(k_1, k_2, k_3) S'(k_1, k_2, k_3)}{P(k_1) P(k_2) P(k_3)} \\
 &\propto \int_0^1 dx_2 \int_{1-x_2}^1 dx_3 x_2^4 x_3^4 S(1, x_2, x_3) S'(1, x_2, x_3) ,
 \end{aligned} \tag{8.47}$$

where the summation is performed over all \mathbf{k}_i , which form a triangle and $P(k) \propto k^{-3}$ denotes the power spectrum. This correlation function gets to 1 when $S = S'$. In our case, this is calculated as

$$\cos(S_A \cdot S_{\text{equil}}) \simeq \begin{cases} 0.968 , & (A = -1/2) \\ 0.970 , & (A = 0) \\ 0.971 , & (A = 1/2) \\ 0.972 , & (A = 1) \end{cases} \tag{8.48}$$

that is, an approximation that S_A is proportional to S_{equil} seems to be valid. Here, we also calculate the correlation functions with the local- and orthogonal-type non-Gaussianities [4] and conclude that these contributions are negligible. Thus, we determine the proportionality coefficient as

$$S_A \simeq \frac{S_A \cdot S_{\text{equil}}}{S_{\text{equil}} \cdot S_{\text{equil}}} S_{\text{equil}} = \begin{cases} 4.40 \times 10^{-4} S_{\text{equil}} , & (A = -1/2) \\ 2.50 \times 10^{-4} S_{\text{equil}} , & (A = 0) \\ 1.42 \times 10^{-4} S_{\text{equil}} , & (A = 1/2) \\ 8.09 \times 10^{-5} S_{\text{equil}} . & (A = 1) \end{cases} \tag{8.49}$$

Substituting this into Eqs. (8.19) and (8.20), we obtain reasonable formulae of the radial functions for $A = 1/2$ as

$$f_{W^3}^{(r)} = f_{\widetilde{W}W^2}^{(r)} \simeq \left(\frac{\pi^2}{2} r A_S\right)^4 \left(\frac{M_{\text{pl}}}{\Lambda}\right)^2 \frac{10395}{8} \sqrt{\frac{\pi}{2}} \frac{1.42 \times 10^{-4} S_{\text{equil}}}{(-\tau_*)^{1/2} (k_1 k_2 k_3)^{1/6}}, \quad (8.50)$$

and for $A = -1/2$ as

$$f_{W^3}^{(r)} = -f_{\widetilde{W}W^2}^{(r)} \simeq \left(\frac{\pi^2}{2} r A_S\right)^4 \left(\frac{M_{\text{pl}}}{\Lambda}\right)^2 \frac{945}{4} \sqrt{\frac{\pi}{2}} 4.40 \times 10^{-4} (-\tau_*)^{1/2} (k_1 k_2 k_3)^{1/6} S_{\text{equil}}. \quad (8.51)$$

Here, we also use

$$\left(\frac{H}{M_{\text{pl}}}\right)^2 = \frac{\pi^2}{2} r A_S, \quad (8.52)$$

where A_S is the amplitude of primordial curvature perturbations and r is the tensor-to-scalar ratio [4, 8]. For $A = 0$, the signals from $\widetilde{W}W^2$ disappear as $f_{\widetilde{W}W^2}^{(r)} = 0$ and the finite radial function of W^3 is given by

$$f_{W^3}^{(r)} \simeq \left(\frac{\pi^2}{2} r A_S\right)^4 \left(\frac{M_{\text{pl}}}{\Lambda}\right)^2 960 \times 2.50 \times 10^{-4} S_{\text{equil}}. \quad (8.53)$$

In contrast, for $A = 1$, since $f_{W^3}^{(r)} = 0$, we have only the parity-violating contribution from $\widetilde{W}W^2$ as

$$f_{\widetilde{W}W^2}^{(r)} \simeq \left(\frac{\pi^2}{2} r A_S\right)^4 \left(\frac{M_{\text{pl}}}{\Lambda}\right)^2 5760 \times \frac{8.09 \times 10^{-5} S_{\text{equil}}}{(-\tau_*) (k_1 k_2 k_3)^{1/3}}. \quad (8.54)$$

8.2.3 Results

On the basis of the analytical formulae (8.35), (8.36), (8.50), (8.51), (8.53) and (8.54), we compute the CMB bispectra from W^3 and $\widetilde{W}W^2$ for $A = -1/2, 0, 1/2$, and 1. Then, we modify the Boltzmann Code for Anisotropies in the Microwave Background (CAMB) [23, 24]. In calculating the Wigner symbols, we use the Common Mathematical Library SLATEC [25] and some analytic formulae described in Appendices C and D. From the dependence of the radial functions $f_{W^3}^{(r)}$ and $f_{\widetilde{W}W^2}^{(r)}$ on the wave numbers, we can see that the shapes of the CMB bispectra from W^3 and $\widetilde{W}W^2$ are similar to the equilateral-type configuration. Then, the significant signals arise from multipoles satisfying $\ell_1 \simeq \ell_2 \simeq \ell_3$. We confirm this by calculating the CMB bispectrum for several ℓ 's. Hence, in the following discussion, we give the discussion with the spectra for $\ell_1 \simeq \ell_2 \simeq \ell_3$. However, we do not focus on the spectra from $\sum_{n=1}^3 \ell_n = \text{odd}$ for $\ell_1 = \ell_2 = \ell_3$ because these vanish due to the asymmetric nature.

In Fig. 8.2, we present the reduced CMB III , IIB , IBB , and BBB spectra given by

$$b_{X_1 X_2 X_3, \ell_1 \ell_2 \ell_3} = (G_{\ell_1 \ell_2 \ell_3})^{-1} \sum_{m_1 m_2 m_3} \begin{pmatrix} \ell_1 & \ell_2 & \ell_3 \\ m_1 & m_2 & m_3 \end{pmatrix} \left\langle \prod_{n=1}^3 a_{X_n, \ell_n m_n} \right\rangle, \quad (8.55)$$

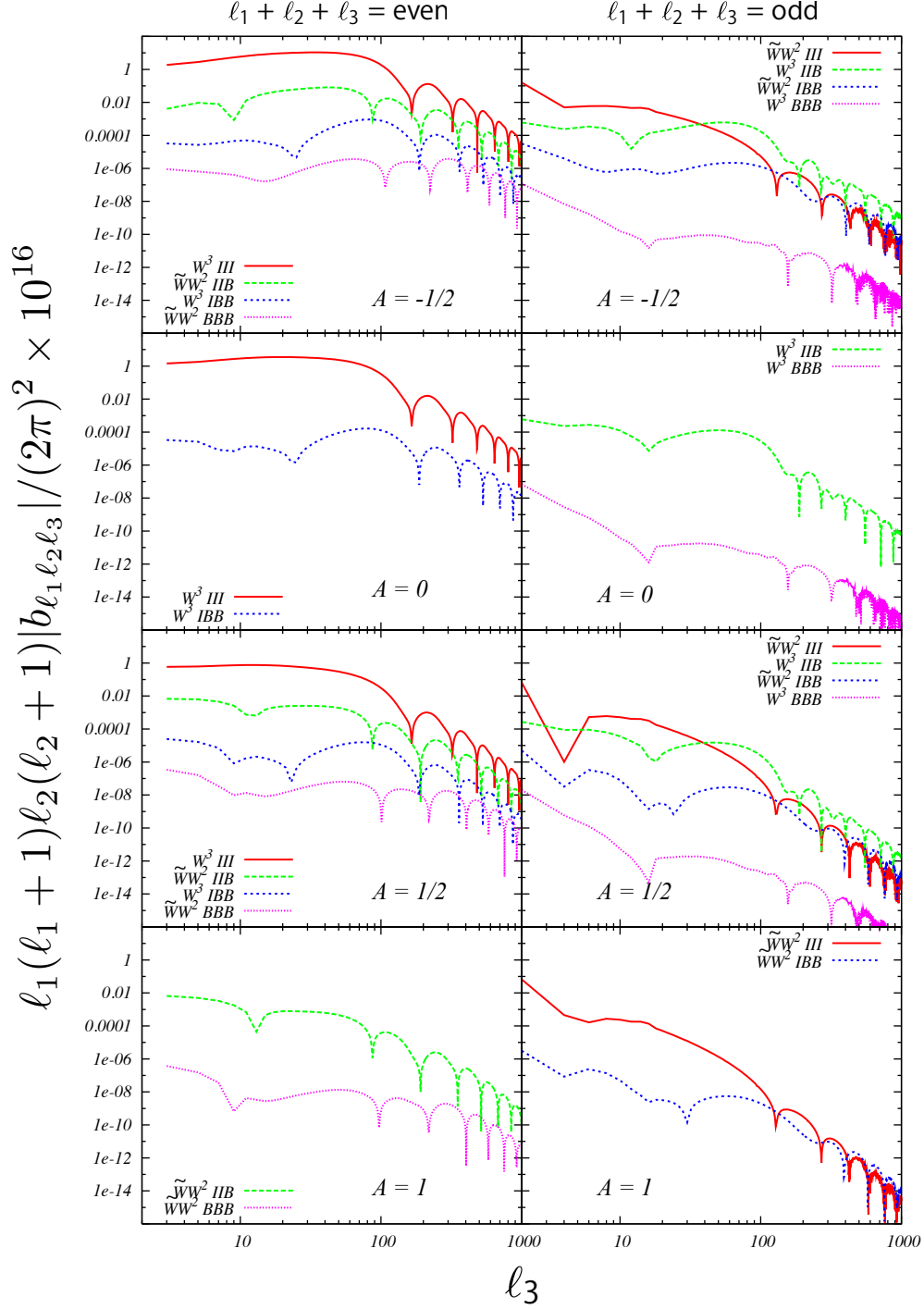


Figure 8.2: Absolute values of the CMB III, IIB, IBB , and BBB spectra induced by W^3 and $\tilde{W}W^2$ for $A = -1/2, 0, 1/2$, and 1 . We set that three multipoles have identical values as $\ell_1 - 2 = \ell_2 - 1 = \ell_3$. The left figures show the spectra not vanishing for $\sum_{n=1}^3 \ell_n = \text{even}$ (parity-even mode) and the right ones present the spectra for $\sum_{n=1}^3 \ell_n = \text{odd}$ (parity-odd mode). Here, we fix the parameters as $\Lambda = 3 \times 10^6 \text{ GeV}$, $r = 0.1$, and $\tau_* = -k_*^{-1} = -14 \text{ Gpc}$, and other cosmological parameters are fixed as the mean values limited from the WMAP 7-yr data [4].

for $\ell_1 - 2 = \ell_2 - 1 = \ell_3$. Here, the G symbol is defined by [19]⁴

$$G_{\ell_1 \ell_2 \ell_3} \equiv \frac{2\sqrt{\ell_3(\ell_3+1)\ell_2(\ell_2+1)}}{\ell_1(\ell_1+1) - \ell_2(\ell_2+1) - \ell_3(\ell_3+1)} \sqrt{\frac{\prod_{n=1}^3 (2\ell_n+1)}{4\pi}} \begin{pmatrix} \ell_1 & \ell_2 & \ell_3 \\ 0 & -1 & 1 \end{pmatrix}. \quad (8.57)$$

At first, from this figure, we can confirm that there are similar features of the CMB power spectrum of tensor modes [26, 27]. In the III spectra, the dominant signals are located in $\ell_3 < 100$ due to the enhancement of the integrated Sachs-Wolfe effect. On the other hand, since the fluctuation of polarizations is mainly produced through Thomson scattering at around the recombination and reionization epoch, the BBB spectra have two peaks for $\ell_3 < 10$ and $\ell_3 \sim 100$, respectively. The cross-correlated bispectra between I and B modes seem to contain both these effects. These features back up the consistency of our calculation.

The curves in Fig. 8.2 denote the spectra for $A = -1/2, 0, 1/2$, and 1 , respectively. We notice that the spectra for large A become red compared with those for small A . The difference in tilt of ℓ between these spectra is just one corresponding to the difference in A . The curves of the left and right figures obey $\sum_{n=1}^3 \ell_n = \text{even}$ and $= \text{odd}$, respectively. As mentioned in Sec. 8.2.1, we stress again that in the ℓ configuration where the bispectrum from W^3 vanishes, the bispectrum from $\widetilde{W}W^2$ survives, and vice versa for each correlation. This is because the parities of these terms are opposite each other. For example, this predicts a nonzero III spectrum not only for $\sum_{n=1}^3 \ell_n = \text{even}$ due to W^3 but also for $\sum_{n=1}^3 \ell_n = \text{odd}$ due to $\widetilde{W}W^2$.

We can also see that each bispectrum induced by W^3 has a different shape from that induced by $\widetilde{W}W^2$ corresponding to the difference in the primordial bispectra. Regardless of this, the overall amplitudes of the spectra for $A = \pm 1/2$ are almost identical. However, if we consider A deviating from these values, the balance between the contributions of W^3 and $\widetilde{W}W^2$ breaks. For example, if $-1/2 < A < 1/2$, the contribution of W^3 dominates. Assuming the time-independent coupling, namely, $A = 0$, since $f_{\widetilde{W}W^2}^{(r)} = 0$, the CMB bispectra are generated only from W^3 . Thus, we will never observe the parity violation of gravitons in the CMB bispectrum. On the other hand, when $-3/2 < A < -1/2$ or $1/2 < A < 3/2$, the contribution of $\widetilde{W}W^2$ dominates. In an extreme case, if $A = \text{odd}$, since $f_{W^3}^{(r)} = 0$, the CMB bispectra arise only from $\widetilde{W}W^2$ and violate the parity invariance. Then, the information of the signals under $\sum_{n=1}^3 \ell_n = \text{odd}$ will become more important in the analysis of the III spectrum.

In Fig. 8.3, we focus on the III spectra from W^3 for $\ell_1 = \ell_2 = \ell_3 \equiv \ell$ to compare these with the III spectrum generated from the equilateral-type non-Gaussianity of curvature perturbations given by

$$b_{III, \ell_1 \ell_2 \ell_3}^{(SSS)} = \int_0^\infty y^2 dy \left[\prod_{n=1}^3 \frac{2}{\pi} \int_0^\infty k_n^2 dk_n \mathcal{T}_{I, \ell_n}^{(S)}(k_n) j_{\ell_n}(k_n y) \right] \times \frac{3}{5} f_{\text{NL}}^{\text{equil}} (2\pi^2 A_S)^2 S_{\text{equil}}(k_1, k_2, k_3), \quad (8.58)$$

⁴The conventional expression of the CMB-reduced bispectrum as

$$b_{X_1 X_2 X_3, \ell_1 \ell_2 \ell_3} \equiv (I_{\ell_1 \ell_2 \ell_3}^{0 \ 0 \ 0})^{-1} \sum_{m_1 m_2 m_3} \begin{pmatrix} \ell_1 & \ell_2 & \ell_3 \\ m_1 & m_2 & m_3 \end{pmatrix} \left\langle \prod_{n=1}^3 a_{X_n, \ell_n m_n} \right\rangle \quad (8.56)$$

breaks down for $\sum_{n=1}^3 \ell_n = \text{odd}$ due to the divergence behavior of $(I_{\ell_1 \ell_2 \ell_3}^{0 \ 0 \ 0})^{-1}$. Here, replacing the I symbol with the G symbol, this problem is avoided. Of course, for $\sum_{n=1}^3 \ell_n = \text{even}$, $G_{\ell_1 \ell_2 \ell_3}$ is identical to $I_{\ell_1 \ell_2 \ell_3}^{0 \ 0 \ 0}$.

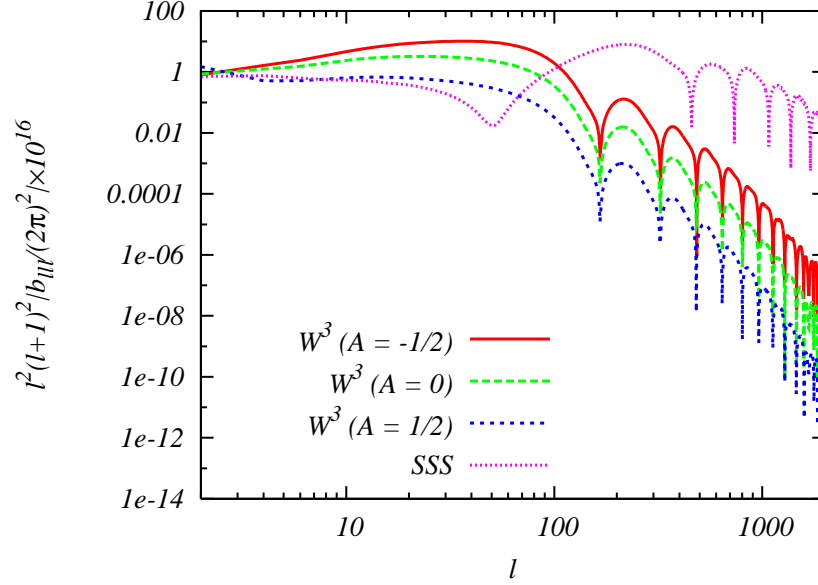


Figure 8.3: Absolute value of the CMB *III* spectra generated from W^3 for $A = -1/2$ (red solid line), 0 (green dashed one) and $1/2$ (blue dotted one), and generated from the equilateral-type non-Gaussianity given by Eq. (8.58) with $f_{\text{NL}}^{\text{equil}} = 300$ (magenta dot-dashed one). We set that three multipoles have identical values as $\ell_1 = \ell_2 = \ell_3 \equiv \ell$. Here, we fix the parameters as the same values mentioned in Fig. 8.2.

where $f_{\text{NL}}^{\text{equil}}$ is the nonlinearity parameter of the equilateral non-Gaussianity and $\mathcal{T}_{I,\ell}^{(S)}$ is the transfer function of scalar mode described in Eq. (3.101). Note that these three spectra vanish for $\sum_{n=1}^3 \ell_n = \text{odd}$. From this figure, we can estimate the typical amplitude of the *III* spectra from W^3 at large scale as

$$|b_{\ell\ell\ell}| \sim \ell^{-4} \times 3.2 \times 10^{-2} \left(\frac{\text{GeV}}{\Lambda} \right)^2 \left(\frac{r}{0.1} \right)^4. \quad (8.59)$$

This equation also seems to be applicable to the *III* spectra from $\widetilde{W}W^2$. On the other hand, the CMB bispectrum generated from the equilateral-type non-Gaussianity on a large scale is evaluated with $f_{\text{NL}}^{\text{equil}}$ as

$$|b_{\ell\ell\ell}| \sim \ell^{-4} \times 4 \times 10^{-15} \left| \frac{f_{\text{NL}}^{\text{equil}}}{300} \right|. \quad (8.60)$$

From these estimations and ideal upper bounds on $f_{\text{NL}}^{\text{equil}}$ estimated only from the cosmic variance for $\ell < 100$ [28–30], namely $f_{\text{NL}}^{\text{equil}} \lesssim 300$ and $r \sim 0.1$, we find a rough limit: $\Lambda \gtrsim 3 \times 10^6 \text{GeV}$. Here, we use only the signals for $\sum_{n=1}^3 \ell_n = \text{even}$ due to the comparison with the parity-conserving bispectrum from scalar-mode non-Gaussianity. Of course, to estimate more precisely, we will have to calculate the signal-to-noise ratio with the information of $\sum_{n=1}^3 \ell_n = \text{odd}$ [19].

8.3 Summary and discussion

In this section, we have studied the CMB bispectrum generated from the graviton non-Gaussianity induced by the parity-even and parity-odd Weyl cubic terms, namely, W^3 and $\widetilde{W}W^2$, which have a

dilaton-like coupling depending on the conformal time as $f \propto \tau^A$. Through the calculation based on the in-in formalism, we have found that the primordial non-Gaussianities from $\widetilde{W}W^2$ can have a magnitude comparable to that from W^3 even in the exact de Sitter space-time.

Using the explicit formulae of the primordial bispectrum, we have derived the CMB bispectra of the intensity (I) and polarization (E, B) modes. Then, we have confirmed that, owing to the difference in the transformation under parity, the spectra from W^3 vanish in the ℓ space where those from $\widetilde{W}W^2$ survive and vice versa. For example, owing to the parity-violating $\widetilde{W}W^2$ term, the III spectrum can be produced not only for $\sum_{n=1}^3 \ell_n = \text{even}$ but also for $\sum_{n=1}^3 \ell_n = \text{odd}$, and the IIB spectrum can also be produced for $\sum_{n=1}^3 \ell_n = \text{even}$. These signals are powerful lines of evidence the parity violation in the non-Gaussian level; hence, to reanalyze the observational data for $\sum_{n=1}^3 \ell_n = \text{odd}$ is meaningful work.

When $A = -1/2, 0, 1/2$, and 1, we have obtained reasonable numerical results of the CMB bispectra from the parity-conserving W^3 and the parity-violating $\widetilde{W}W^2$. For $A = \pm 1/2$, we have found that the spectra from W^3 and $\widetilde{W}W^2$ have almost the same magnitudes even though these have a small difference in the shapes. In contrast, if $A = 0$ and 1, we have confirmed that the signals from $\widetilde{W}W^2$ and W^3 vanish, respectively. In the latter case, we will observe only the parity-violating signals in the CMB bispectra generated from the Weyl cubic terms. We have also found that the shape of the non-Gaussianity from such Weyl cubic terms is quite similar to the equilateral-type non-Gaussianity of curvature perturbations. In comparison with the III spectrum generated from the equilateral-type non-Gaussianity, we have found that if $r = 0.1$, $\Lambda \gtrsim 3 \times 10^6 \text{ GeV}$ corresponds approximately to $f_{\text{NL}}^{\text{equil}} \lesssim 300$.

Strictly speaking, to obtain the bound on the scale Λ , we need to calculate the signal-to-noise ratio with the information of not only $\sum_{n=1}^3 \ell_n = \text{even}$ but also $\sum_{n=1}^3 \ell_n = \text{odd}$ for each A by the application of Ref. [19]. This will be discussed in the future.

References

- [1] E. Komatsu and D. N. Spergel, *Acoustic signatures in the primary microwave background bispectrum*, *Phys. Rev.* **D63** (2001) 063002, [[astro-ph/0005036](#)].
- [2] N. Bartolo, E. Komatsu, S. Matarrese, and A. Riotto, *Non-Gaussianity from inflation: Theory and observations*, *Phys. Rept.* **402** (2004) 103–266, [[astro-ph/0406398](#)].
- [3] D. Babich, P. Creminelli, and M. Zaldarriaga, *The shape of non-Gaussianities*, *JCAP* **0408** (2004) 009, [[astro-ph/0405356](#)].
- [4] **WMAP** Collaboration, E. Komatsu *et al.*, *Seven-Year Wilkinson Microwave Anisotropy Probe (WMAP) Observations: Cosmological Interpretation*, *Astrophys. J. Suppl.* **192** (2011) 18, [[arXiv:1001.4538](#)].
- [5] J. M. Maldacena, *Non-Gaussian features of primordial fluctuations in single field inflationary models*, *JHEP* **05** (2003) 013, [[astro-ph/0210603](#)].
- [6] I. Brown and R. Crittenden, *Non-Gaussianity from Cosmic Magnetic Fields*, *Phys. Rev.* **D72** (2005) 063002, [[astro-ph/0506570](#)].
- [7] P. Adshead and E. A. Lim, *3-pt Statistics of Cosmological Stochastic Gravitational Waves*, *Phys. Rev.* **D82** (2010) 024023, [[arXiv:0912.1615](#)].

- [8] M. Shiraishi, D. Nitta, S. Yokoyama, K. Ichiki, and K. Takahashi, *CMB Bispectrum from Primordial Scalar, Vector and Tensor non-Gaussianities*, *Prog. Theor. Phys.* **125** (2011) 795–813, [[arXiv:1012.1079](#)].
- [9] M. Shiraishi, D. Nitta, S. Yokoyama, K. Ichiki, and K. Takahashi, *Cosmic microwave background bispectrum of tensor passive modes induced from primordial magnetic fields*, *Phys. Rev.* **D83** (2011) 123003, [[arXiv:1103.4103](#)].
- [10] M. Shiraishi and S. Yokoyama, *Violation of the Rotational Invariance in the CMB Bispectrum*, *Prog.Theor.Phys.* **126** (2011) 923–935, [[arXiv:1107.0682](#)].
- [11] J. M. Maldacena and G. L. Pimentel, *On graviton non-Gaussianities during inflation*, *JHEP* **1109** (2011) 045, [[arXiv:1104.2846](#)].
- [12] J. Soda, H. Kodama, and M. Nozawa, *Parity Violation in Graviton Non-gaussianity*, *JHEP* **1108** (2011) 067, [[arXiv:1106.3228](#)].
- [13] S. Weinberg, *Effective Field Theory for Inflation*, *Phys. Rev.* **D77** (2008) 123541, [[arXiv:0804.4291](#)].
- [14] S. Alexander and J. Martin, *Birefringent gravitational waves and the consistency check of inflation*, *Phys. Rev.* **D71** (2005) 063526, [[hep-th/0410230](#)].
- [15] S. Saito, K. Ichiki, and A. Taruya, *Probing polarization states of primordial gravitational waves with CMB anisotropies*, *JCAP* **0709** (2007) 002, [[arXiv:0705.3701](#)].
- [16] V. Gluscevic and M. Kamionkowski, *Testing Parity-Violating Mechanisms with Cosmic Microwave Background Experiments*, *Phys. Rev.* **D81** (2010) 123529, [[arXiv:1002.1308](#)].
- [17] L. Sorbo, *Parity violation in the Cosmic Microwave Background from a pseudoscalar inflaton*, *JCAP* **1106** (2011) 003, [[arXiv:1101.1525](#)].
- [18] T. Okamoto and W. Hu, *The Angular Trispectra of CMB Temperature and Polarization*, *Phys. Rev.* **D66** (2002) 063008, [[astro-ph/0206155](#)].
- [19] M. Kamionkowski and T. Souradeep, *The Odd-Parity CMB Bispectrum*, *Phys. Rev.* **D83** (2011) 027301, [[arXiv:1010.4304](#)].
- [20] M. Shiraishi, D. Nitta, and S. Yokoyama, *Parity Violation of Gravitons in the CMB Bispectrum*, *Prog.Theor.Phys.* **126** (2011) 937–959, [[arXiv:1108.0175](#)].
- [21] S. Weinberg, *Quantum contributions to cosmological correlations*, *Phys. Rev.* **D72** (2005) 043514, [[hep-th/0506236](#)].
- [22] L. Senatore, K. M. Smith, and M. Zaldarriaga, *Non-Gaussianities in Single Field Inflation and their Optimal Limits from the WMAP 5-year Data*, *JCAP* **1001** (2010) 028, [[arXiv:0905.3746](#)].
- [23] A. Lewis, A. Challinor, and A. Lasenby, *Efficient Computation of CMB anisotropies in closed FRW models*, *Astrophys. J.* **538** (2000) 473–476, [[astro-ph/9911177](#)].

- [24] A. Lewis, *CMB anisotropies from primordial inhomogeneous magnetic fields*, *Phys. Rev.* **D70** (2004) 043011, [astro-ph/0406096].
- [25] “Slatec common mathematical library.” <http://www.netlib.org/slatec/>.
- [26] J. R. Pritchard and M. Kamionkowski, *Cosmic microwave background fluctuations from gravitational waves: An analytic approach*, *Annals Phys.* **318** (2005) 2–36, [astro-ph/0412581].
- [27] D. Baskaran, L. P. Grishchuk, and A. G. Polnarev, *Imprints of relic gravitational waves in cosmic microwave background radiation*, *Phys. Rev.* **D74** (2006) 083008, [gr-qc/0605100].
- [28] P. Creminelli, A. Nicolis, L. Senatore, M. Tegmark, and M. Zaldarriaga, *Limits on non-Gaussianities from WMAP data*, *JCAP* **0605** (2006) 004, [astro-ph/0509029].
- [29] P. Creminelli, L. Senatore, M. Zaldarriaga, and M. Tegmark, *Limits on f_{NL} parameters from WMAP 3yr data*, *JCAP* **0703** (2007) 005, [astro-ph/0610600].
- [30] K. M. Smith and M. Zaldarriaga, *Algorithms for bispectra: Forecasting, optimal analysis, and simulation*, *Mon.Not.Roy.Astron.Soc.* **417** (2011) 2–19, [astro-ph/0612571].

9 CMB bispectrum generated from primordial magnetic fields

Recent observational consequences have shown the existence of $\mathcal{O}(10^{-6})\text{G}$ magnetic fields in galaxies and clusters of galaxies at redshift $z \sim 0.7 - 2.0$ [1–3]. One of the scenarios to realize this is an amplification of the magnetic fields by the galactic dynamo mechanism (e.g. [4]), which requires $\mathcal{O}(10^{-20})\text{G}$ seed fields prior to the galaxy formation. A variety of studies have suggested the possibility of generating the seed fields at the inflationary epoch [5, 6], the cosmic phase transitions [7, 8], and cosmological recombination [9–11] and also there have been many studies about constraints on the strength of primordial magnetic fields (PMFs) through the impact on the cosmic microwave background (CMB) anisotropies, in particular, the CMB power spectrum sourced from the PMFs [12–17]. The PMFs excite not only the scalar fluctuation but also the vector and tensor fluctuations in the CMB fields. For example, the gravitational waves and curvature perturbations, which come from the tensor and scalar components of the PMF anisotropic stresses, produce additional CMB fluctuations at large and intermediate scales [15, 17]. In addition, it has been known that the magnetic vector mode may dominate the CMB small-scale fluctuations by the Doppler effect (e.g. [14, 15]).

The PMF anisotropic stresses depend quadratically on the magnetic seed fields. Thus, assuming the gaussianity of the PMF, the anisotropic stress and CMB fluctuation obey the highly non-Gaussian statistics [18, 19]. Owing to the Wick’s theorem, the CMB bispectrum contains the pure non-Gaussian information. Hence, to extract the information of the PMF from the CMB fields, the analysis of the CMB bispectrum is of great utility. Recently, in Refs. [20–23], the authors investigated the contribution of the scalar-mode anisotropic stresses of PMFs to the bispectrum of the CMB temperature fluctuations. From current CMB experimental data, some authors obtained rough limits on the PMF strength smoothed on 1Mpc scale as $B_{1\text{Mpc}} < \mathcal{O}(1)\text{nG}$. However, since in all these studies, the complicated angular dependence on the wave number vectors are neglected, there may exist any uncertainties. In addition, the authors have never considered the dependence on the vector- and tensor-mode contributions and hence more precise discussion including these concerns should be realized.

With these motivations, we have studied the CMB scalar, vector and tensor bispectra induced from PMFs and firstly succeeded in the exact computation of them with the full-angular dependence [24–26] by applying the all-sky formulae for the CMB bispectrum [27]¹. In our studies, we also updated constraints on the PMF strength.

In this section, after reviewing the impact of PMFs on the CMB anisotropies, we present the derivation of the CMB bispectra induced from PMFs and discuss their behaviors. In addition, we put limits on the PMFs by considering the WMAP data and the expected PLANCK data [29, 30]. Finally, we mention our future works. These discussions are based on our studies [24–26],

9.1 CMB fluctuation induced from PMFs

The PMFs drive the Lorentz force and the anisotropic stress, and change the motion of baryons (protons and electrons) and the growth of the gravitational potential via the Euler and Einstein equations. Consequently, the photon’s anisotropy is also affected. We illustrate this in Fig. 9.1. In the following discussion, we summarize the impacts of PMFs on the CMB fluctuations in detail

¹In Ref. [28], after us, the authors presented an analytic formula for the CMB temperature bispectrum generated from vector anisotropic stresses of the PMF.

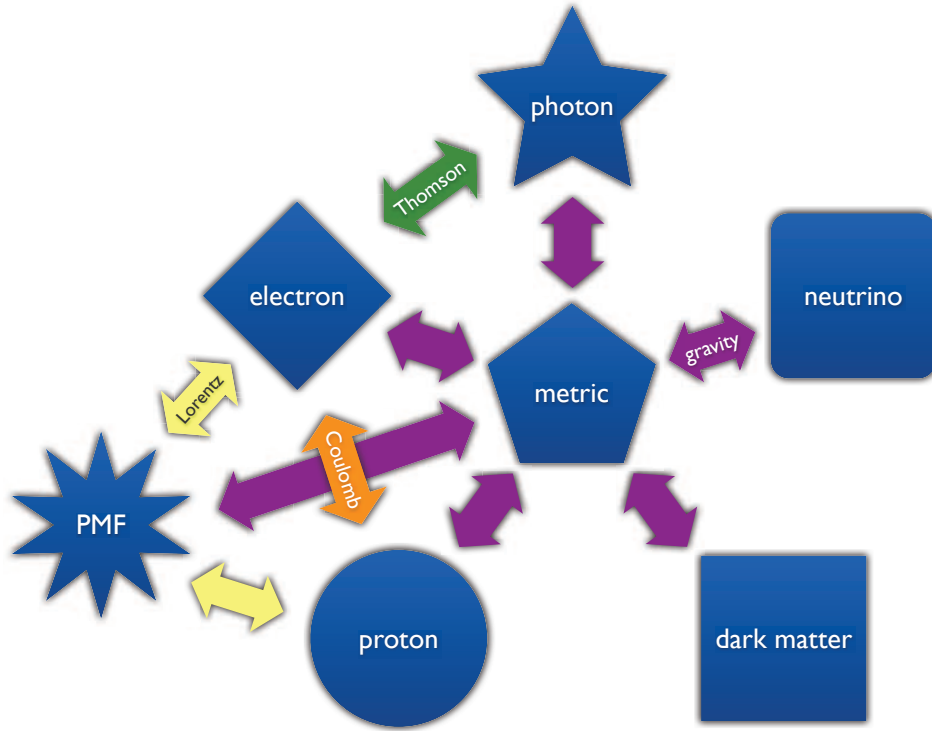


Figure 9.1: Interaction between several components in the Universe if the PMF exists.

and current constraints on the PMFs obtained from the CMB power spectrum.

9.1.1 Setting for the PMFs

Let us consider the stochastic PMFs $B^b(\mathbf{x}, \tau)$ on the homogeneous background Universe which is characterized by the Friedmann-Robertson-Walker metric,

$$ds^2 = a(\tau)^2 [-d\tau^2 + \delta_{bc} dx^b dx^c] , \quad (9.1)$$

where τ is a conformal time and $a(\tau)$ is a scale factor. The expansion of the Universe makes the amplitude of the magnetic fields decay as $1/a^2$ and hence we can draw off the time dependence as $B^b(\mathbf{x}, \tau) = B^b(\mathbf{x})/a^2$. Each component of the energy momentum tensor (EMT) of PMFs is given by

$$\begin{aligned} T^0_0(x^\mu) &= -\rho_B = -\frac{1}{8\pi a^4} B^2(\mathbf{x}) \equiv -\rho_\gamma(\tau) \Delta_B(x^\mu) , \\ T^0_c(x^\mu) &= T^b_0(x^\mu) = 0 , \\ T^b_c(x^\mu) &= \frac{1}{4\pi a^4} \left[\frac{B^2(\mathbf{x})}{2} \delta^b_c - B^b(\mathbf{x}) B_c(\mathbf{x}) \right] \equiv \rho_\gamma(\tau) [\Delta_B(x^\mu) \delta^b_c + \Pi^b_{Bc}(x^\mu)] . \end{aligned} \quad (9.2)$$

The Fourier components of the spatial parts are described as

$$\begin{aligned} T_c^b(\mathbf{k}, \tau) &\equiv \rho_\gamma(\tau) [\delta_c^b \Delta_B(\mathbf{k}) + \Pi_{Bc}^b(\mathbf{k})] , \\ \Delta_B(\mathbf{k}) &= \frac{1}{8\pi\rho_{\gamma,0}} \int \frac{d^3\mathbf{k}'}{(2\pi)^3} B^b(\mathbf{k}') B_b(\mathbf{k} - \mathbf{k}') , \\ \Pi_{Bc}^b(\mathbf{k}) &= -\frac{1}{4\pi\rho_{\gamma,0}} \int \frac{d^3\mathbf{k}'}{(2\pi)^3} B^b(\mathbf{k}') B_c(\mathbf{k} - \mathbf{k}') , \end{aligned} \quad (9.3)$$

where we have introduced the photon energy density ρ_γ in order to include the time dependence of a^{-4} and $\rho_{\gamma,0}$ denotes the present energy density of photons. In the following discussion, for simplicity of calculation, we ignore the trivial time-dependence. Hence, the index is lowered by δ_{bc} and the summation is implied for repeated indices.

Assuming that $B^a(\mathbf{x})$ is a Gaussian field, the statistically isotropic power spectrum of PMFs $P_B(k)$ is defined by ²

$$\langle B_a(\mathbf{k}) B_b(\mathbf{p}) \rangle = (2\pi)^3 \frac{P_B(k)}{2} P_{ab}(\hat{\mathbf{k}}) \delta(\mathbf{k} + \mathbf{p}) , \quad (9.4)$$

with a projection tensor

$$P_{ab}(\hat{\mathbf{k}}) \equiv \sum_{\sigma=\pm 1} \epsilon_a^{(\sigma)}(\hat{\mathbf{k}}) \epsilon_b^{(-\sigma)}(\hat{\mathbf{k}}) = \delta_{ab} - \hat{k}_a \hat{k}_b , \quad (9.5)$$

which comes from the divergence free nature of PMFs. Here $\hat{\mathbf{k}}$ denotes a unit vector and $\epsilon_a^{(\pm 1)}$ is a normalized divergenceless polarization vector which satisfies the orthogonal condition; $\hat{k}^a \epsilon_a^{(\pm 1)} = 0$. The details of the relations and conventions of the polarization vector are described in Appendix D. Although the form of the power spectrum $P_B(k)$ is strongly dependent on the production mechanism, we assume a simple power law shape given by

$$P_B(k) = A_B k^{n_B} , \quad (9.6)$$

where A_B and n_B denote the amplitude and the spectral index of the power spectrum of magnetic fields, respectively. In order to parametrize the strength of PMFs, we smooth the magnetic fields with a conventional Gaussian filter on a comoving scale r :

$$B_r^2 \equiv \int_0^\infty \frac{k^2 dk}{2\pi^2} e^{-k^2 r^2} P_B(k) , \quad (9.7)$$

then, A_B is calculated as

$$A_B = \frac{(2\pi)^{n_B+5} B_r^2}{\Gamma(\frac{n_B+3}{2}) k_r^{n_B+3}} , \quad (9.8)$$

where $\Gamma(x)$ is the Gamma function and $k_r \equiv 2\pi/r$.

We focus on the scalar, vector and tensor contributions induced from the PMFs, which come from the anisotropic stress of the EMT, i.e., Π_{Bab} . Following the definition of the projection

²Here we neglect the helical component. This effect will be considered in Ref. [31].

operators in Appendix D, the PMF anisotropic stress fluctuation is decomposed into

$$\begin{aligned}\Pi_{Bs}^{(0)}(\mathbf{k}) &= \frac{3}{2}O_{ij}^{(0)}(\hat{\mathbf{k}})\Pi_{Bij}(\mathbf{k}) , \\ \Pi_{Bv}^{(\pm 1)}(\mathbf{k}) &= \frac{1}{2}O_{ij}^{(\mp 1)}(\hat{\mathbf{k}})\Pi_{Bij}(\mathbf{k}) , \\ \Pi_{Bt}^{(\pm 2)}(\mathbf{k}) &= \frac{1}{2}O_{ij}^{(\mp 2)}(\hat{\mathbf{k}})\Pi_{Bij}(\mathbf{k}) .\end{aligned}\tag{9.9}$$

These act as sources of the CMB scalar-, vector- and tensor-mode fluctuations as follow.

9.1.2 Scalar and tensor modes

If the seed magnetic fields exist in the early Universe, the scalar and tensor components of the PMF anisotropic stress are not compensated prior to neutrino decoupling [15, 17], and the scalar and tensor metric perturbations generated from them survive passively. These residual metric perturbations generate the CMB anisotropies of the scalar and tensor modes. These kind of CMB anisotropies are so called “the passive mode” and may dominate at intermediate and large scales depending on the PMF strength [17].

To estimate the curvature perturbations generated from PMFs, let us consider the metric perturbation

$$ds^2 = a^2[-(1 + 2A)d\tau^2 - 2C_i d\tau dx^i + (\delta_{ij} + 2H_{ij})dx^i dx^j] .\tag{9.10}$$

Then, the Gauge-invariant Bardeen potentials [32] are

$$\begin{aligned}\Psi &= A + \frac{i}{k} \left(\dot{C}^{(0)} + \mathcal{H}C^{(0)} \right) - \frac{1}{k^2} \left(\ddot{H}^{(0)} + \mathcal{H}\dot{H}^{(0)} \right) , \\ \Phi &= \frac{1}{3} \left(H^{\text{iso}} - H^{(0)} \right) - \frac{i\mathcal{H}}{k} C^{(0)} + \frac{\mathcal{H}}{k^2} \dot{H}^{(0)} ,\end{aligned}\tag{9.11}$$

where we obey the vector and tensor decomposition of Appendix D as

$$\begin{aligned}C_a(\mathbf{k}) &= C^{(0)}(\mathbf{k})O_a^{(0)} + \sum_{\lambda=\pm 1} C^{(\lambda)}(\mathbf{k})O_a^{(\lambda)} , \\ H_{ab}(\mathbf{k}) &= -\frac{1}{3}H^{\text{iso}}(\mathbf{k})\delta_{ab} + H^{(0)}(\mathbf{k})O_{ab}^{(0)} + \sum_{\lambda=\pm 1} H^{(\lambda)}(\mathbf{k})O_{ab}^{(\lambda)} + \sum_{\lambda=\pm 2} H^{(\lambda)}(\mathbf{k})O_{ab}^{(\lambda)} .\end{aligned}\tag{9.12}$$

The energy momentum tensor is given by

$$\begin{aligned}T^0_0 &= -\rho(1 + \Delta) , \\ T^i_j &= \rho \left[\frac{p}{\rho} \left(1 + \Gamma + \frac{c_s^2}{w} \Delta \right) \delta^i_j + \Pi^i_j \right] ,\end{aligned}\tag{9.13}$$

where $w = p/\rho$ is the coefficient of the equation of state and $c_s^2 = \dot{p}/\dot{\rho}$ is the sound speed. The anisotropic stress is also decomposed into

$$\Pi_{ab}(\mathbf{k}) = \Pi_s^{(0)}(\mathbf{k})O_{ab}^{(0)} + \sum_{\lambda=\pm 1} \Pi_v^{(\lambda)}(\mathbf{k})O_{ab}^{(\lambda)} + \sum_{\lambda=\pm 2} \Pi_t^{(\lambda)}(\mathbf{k})O_{ab}^{(\lambda)} .\tag{9.14}$$

Before neutrino decoupling, the Universe is dominated by the radiative fluid with $c_s^2 = w = 1/3$. The fluid is tightly coupled to the trace amount of baryons and can not create any anisotropic

stress. Hence, in this period, the total anisotropic stress comes from only PMFs, namely, the constant $\Pi_{Bs}^{(0)}$. Until neutrino decoupling, there is no mechanism to compensate $\Pi_{Bs}^{(0)}$, and it will be a source of the gravitational potential via the Einstein equation. Using $\mathcal{H} = \tau^{-1}$ and taking into account the radiation-dominated limit, the Einstein equation is written as

$$3(k\tau)^2 \left[\tau^2 \ddot{\Phi} + 4\tau \dot{\Phi} \right] + (k\tau)^4 \Phi = -3R_\gamma \Pi_{Bs}^{(0)} [6 + (k\tau)^2] , \quad (9.15)$$

where $R_\gamma \sim 0.6$ is the ratio by the energy density of photons to all relativistic particles and we assume $\Gamma = 0$. This can be solved exactly and the superhorizon limit, when $k\tau \ll 1$, is

$$\Phi \approx \frac{3R_\gamma \Pi_{Bs}^{(0)}}{(k\tau)^2} - \frac{c_1}{(k\tau)^3} - \frac{c_1}{6k\tau} + c_2 - \frac{2}{3}R_\gamma \Pi_{Bs}^{(0)} \ln \tau . \quad (9.16)$$

We have the interest in the contribution on the comoving curvature perturbation

$$\zeta = \Phi + \frac{2}{3(1+w)} \left(\Psi + \frac{\dot{\Phi}}{\mathcal{H}} \right) . \quad (9.17)$$

From the above estimation, this superhorizon limit becomes

$$\zeta(\tau) = \zeta(\tau_B) - R_\gamma \Pi_{Bs}^{(0)} \left[\ln \left(\frac{\tau}{\tau_B} \right) + \frac{\tau_B}{2\tau} - \frac{1}{2} \right] , \quad (9.18)$$

where τ_B is the conformal times at the generation of the PMF. At $\tau_\nu = 1\text{MeV}^{-1}$, neutrinos decouple from the radiative fluid. By considering the Boltzmann equations of neutrinos, we find the solution for $\tau \gg \tau_\nu$ as $\Pi_\nu^{(0)} = -(R_\gamma/R_\nu)\Pi_{Bs}^{(0)}$ with $R_\nu \sim 0.4$ being the ratio by the energy density of neutrinos to all relativistic particles. This implies that the neutrino anisotropic stress compensates the magnetic anisotropic stress. Hence, when this compensation is effective, the source term of the Einstein equation become zero and the gravitational potentials stop growing. Including the further bare growth, the total curvature perturbation in the superhorizon limit for $\tau \gg \tau_\nu$ is evaluated as ³

$$\zeta(\mathbf{k}) \approx \zeta(\mathbf{k}, \tau_B) - R_\gamma \Pi_{Bs}^{(0)}(\mathbf{k}) \ln \left(\frac{\tau_\nu}{\tau_B} \right) . \quad (9.19)$$

Note that this logarithmic growth and saturation of the curvature perturbation even on superhorizon scales is caused by only the property of the sources as $\rho \propto a^{-4}$, hence the above discussion is valid for the general radiation fluid other than PMFs [33]. This curvature perturbation acts as a source of the CMB fluctuation of the scalar mode.

Similar discussion can be given in the tensor perturbation. Here, we shall consider the spatial metric and decomposition into the helicity states as ⁴

$$g_{ij} = a^2 e^{h_{ij}} , \quad h^{(\pm 2)}(\mathbf{k}, \tau) = \frac{1}{2} e_{ab}^{(\mp 2)}(\hat{\mathbf{k}}) h_{ab}(\mathbf{k}, \tau) . \quad (9.20)$$

As is well known, the gravitational potential of tensor modes can be generated from anisotropic stresses via the Einstein equation. Like the scalar case, after neutrino decoupling, the anisotropic

³On superhorizon scales, this ζ is equal to $-\mathcal{R}$ in Eq. (2.40).

⁴ $h^{(\pm 2)}$ is equal to $-\sqrt{3}H_T$ of Refs. [15, 17].

stresses of PMFs vanish via the compensation of those of neutrinos. However, prior to this epoch, there is no compensation process due to the absence of the neutrino anisotropic stresses. Hence, from the Einstein equation, we find the evolution equation of the tensor-mode metric perturbations as

$$\ddot{h}^{(\pm 2)} + 2\mathcal{H}\dot{h}^{(\pm 2)} + k^2 h^{(\pm 2)} \approx \begin{cases} 16\pi G a^2 \rho_\gamma \Pi_{Bt}^{(\pm 2)} & (\tau_B \lesssim \tau \lesssim \tau_\nu) \\ 0 & (\tau \gtrsim \tau_\nu) \end{cases}, \quad (9.21)$$

From this equation, we can find a superhorizon solution of the tensor metric perturbation for $\tau \gg \tau_\nu$ as

$$h^{(\pm 2)}(\mathbf{k}) \approx h^{(\pm 2)}(\mathbf{k}, \tau_B) + 6R_\gamma \Pi_{Bt}^{(\pm 2)}(\mathbf{k}) \ln \left(\frac{\tau_\nu}{\tau_B} \right). \quad (9.22)$$

This gravitational wave also generates additional CMB fluctuation.

Note that the effects of PMFs on the transfer functions $\mathcal{T}_{X,\ell}^{(S)}$ and $\mathcal{T}_{X,\ell}^{(T)}$ are inconsiderable at larger scales [17], hence it is safe to use the non-magnetic transfer functions (3.101) in the computation of the CMB spectra induced from scalar and tensor modes of the PMF anisotropic stress.

9.1.3 Vector mode

The vector mode has no equivalent passive mode as the gravitational potential of the vector mode decays away via the Einstein equation posterior to neutrino decoupling. Thus, in the vector mode, we need to consider the impact of the PMF on the transfer function. In Refs. [13, 14, 25, 28], it is discussed that the temperature fluctuations are generated via Doppler and integrated Sachs-Wolfe effects on the CMB vector modes. On the basis of them, we derive the transfer function of the vector magnetic mode as follows.

When we decompose the metric perturbations into vector components as

$$\begin{aligned} \delta g_{0c} &= \delta g_{c0} = a^2 A_c, \\ \delta g_{cd} &= a^2 \left(\partial_c h_d^{(V)} + \partial_d h_c^{(V)} \right), \end{aligned} \quad (9.23)$$

we can construct two gauge-invariant variables, namely a vector perturbation of the extrinsic curvature and a vorticity, as

$$\begin{aligned} \mathbf{V} &\equiv \mathbf{A} - \dot{\mathbf{h}}, \\ \mathbf{\Omega} &\equiv \mathbf{v} - \mathbf{A}, \end{aligned} \quad (9.24)$$

where \mathbf{v} is the spatial part of the four-velocity perturbation of a stationary fluid element and a dash denotes a partial derivative of the conformal time τ . Here, choosing a gauge as $\dot{\mathbf{h}} = 0$, we can express the Einstein equation

$$\dot{\mathbf{V}} + 2\mathcal{H}\mathbf{V} = -\frac{16\pi G \rho_{\gamma,0} (\Pi_\gamma^{(\mathbf{V})} + \Pi_\nu^{(\mathbf{V})} + \Pi_{\mathbf{B}}^{(\mathbf{V})})}{a^2 k}, \quad (9.25)$$

and the Euler equations for photons and baryons

$$\dot{\mathbf{\Omega}}_\gamma + \kappa(\mathbf{v}_\gamma - \mathbf{v}_b) = 0, \quad (9.26)$$

$$\dot{\Omega}_{\mathbf{b}} + \mathcal{H}\Omega_{\mathbf{b}} - \frac{\dot{\kappa}}{R}(\mathbf{v}_{\gamma} - \mathbf{v}_{\mathbf{b}}) = \frac{\mathbf{L}^{(\mathbf{V})}}{a^4(\rho_b + p_b)}. \quad (9.27)$$

Here $\mathbf{L}^{(\mathbf{V})} \equiv k\rho_{\gamma,0}\mathbf{\Pi}_{\mathbf{B}}^{(\mathbf{V})}$ is the Lorentz force of vector mode and $\Pi_a^{(V)} = -i\hat{k}_b P_{ac}\Pi_{bc}$, p is the isotropic pressure, the indices γ, ν and b denote the photon, neutrino and baryon, κ is the optical depth, and $R \equiv (\rho_b + p_b)/(\rho_{\gamma} + p_{\gamma}) \simeq 3\rho_b/(4\rho_{\gamma})$. In the tight-coupling limit as $\mathbf{v}_{\gamma} \simeq \mathbf{v}_{\mathbf{b}}$, the photon vorticity is comparable to the baryon one: $\Omega_{\gamma} \simeq \Omega_{\mathbf{b}} \equiv \Omega$. Then, the Euler equations (9.26) and (9.27) are combined into

$$(1 + R)\dot{\Omega} + R\mathcal{H}\Omega = \frac{\mathbf{L}^{(\mathbf{V})}}{a^4(\rho_{\gamma} + p_{\gamma})}, \quad (9.28)$$

and this solution is given by

$$\Omega(\mathbf{k}, \tau) \simeq \frac{\tau \mathbf{L}^{(\mathbf{V})}(\mathbf{k})}{(1 + R)(\rho_{\gamma,0} + p_{\gamma,0})}, \quad (9.29)$$

Note that Eq. (9.28) and the above solution are valid for perturbation wavelengths larger than the comoving Silk damping scale $L_S \equiv 2\pi/k_S$, namely, $k < k_S$, where photon viscosity can be neglected compared to the Lorentz force. For $k > k_S$, due to the effect of the photon vorticity, the Euler equation (9.28) is changed as [12]

$$(1 + R)\dot{\Omega} + R\left(\mathcal{H} + \frac{k^2\chi}{a\rho_b}\right)\Omega = \frac{\mathbf{L}^{(\mathbf{V})}}{a^4(\rho_{\gamma} + p_{\gamma})}, \quad (9.30)$$

where $\chi = (4/15)\rho_{\gamma}L_{\gamma}a$ is the photon shear viscosity coefficient and $L_{\gamma} = \dot{\kappa}^{-1}$ is the photon comoving mean-free path. We can obtain this analytical solution:

$$\Omega(\mathbf{k}, \tau) \simeq \frac{\mathbf{L}^{(\mathbf{V})}(\mathbf{k})}{(k^2 L_{\gamma}/5)(\rho_{\gamma,0} + p_{\gamma,0})}. \quad (9.31)$$

Hence, we can summarize the vorticity of the baryon and photon fluids as

$$\begin{aligned} \Omega(\mathbf{k}, \tau) &\simeq \beta(k, \tau)\mathbf{\Pi}_{\mathbf{B}}^{(\mathbf{V})}(\mathbf{k}), \\ \beta(k, \tau) &= \frac{\rho_{\gamma,0}}{\rho_{\gamma,0} + p_{\gamma,0}} \times \begin{cases} k\tau/(1 + R) & \text{for } k < k_S \\ 5\dot{\kappa}/k & \text{for } k > k_S \end{cases}. \end{aligned} \quad (9.32)$$

As mentioned above, the CMB temperature anisotropies of vector modes are produced through the Doppler and integrated Sachs-Wolfe effects as

$$\frac{\Delta I(\hat{\mathbf{n}})}{I} = -\mathbf{v}_{\gamma} \cdot \hat{\mathbf{n}}|_{\tau_*}^{\tau_0} + \int_{\tau_*}^{\tau_0} d\tau \dot{\mathbf{V}} \cdot \hat{\mathbf{n}}, \quad (9.33)$$

where τ_0 is today and τ_* is the recombination epoch in conformal time, $\mu_{k,n} \equiv \hat{\mathbf{k}} \cdot \hat{\mathbf{n}}$, $x \equiv k(\tau_0 - \tau)$, and $\hat{\mathbf{n}}$ is a unit vector along the line-of-sight direction. Because of compensation of the anisotropic stresses, a solution of the Einstein equation (9.25) expresses the decaying signature as $\mathbf{V} \propto a^{-2}$ after neutrino decoupling. Therefore, in an integrated Sachs-Wolfe effect term, the contribution around the recombination epoch is dominant. Furthermore, neglecting dipole contribution due to \mathbf{v} today, we can form the coefficient of anisotropies as

$$a_{I,\ell m}^{(V)} \equiv \int d^2\hat{\mathbf{n}} \frac{\Delta I(\hat{\mathbf{n}})}{I} Y_{\ell m}^*(\hat{\mathbf{n}})$$

$$\simeq \int \frac{d^3\mathbf{k}}{(2\pi)^3} \int d^2\hat{\mathbf{n}} [\Pi_{\mathbf{B}}^{(V)}(\mathbf{k}) \cdot \hat{\mathbf{n}}] Y_{\ell m}^*(\hat{\mathbf{n}}) \beta(k, \tau_*) e^{-i\mu_{k,n}x_*} . \quad (9.34)$$

In the transformation $\hat{\mathbf{n}} \rightarrow (\mu_{k,n}, \phi_{k,n})$, the functions are rewritten as

$$\begin{aligned} \Pi_{\mathbf{B}}^{(V)}(\mathbf{k}) \cdot \hat{\mathbf{n}} &\rightarrow -i \sqrt{\frac{1 - \mu_{k,n}^2}{2}} \sum_{\lambda=\pm 1} \Pi_{Bv}^{(\lambda)}(\mathbf{k}) e^{i\lambda\phi_{k,n}} , \\ Y_{\ell m}^*(\hat{\mathbf{n}}) &\rightarrow \sum_{m'} D_{mm'}^{(\ell)} \left(S(\hat{\mathbf{k}}) \right) Y_{\ell m'}^*(\Omega_{k,n}) , \\ d^2\hat{\mathbf{n}} &\rightarrow d\Omega_{k,n} , \end{aligned} \quad (9.35)$$

where we use the relation: $\Pi_a^{(V)} = \sum_{\lambda=\pm 1} -i \Pi_{Bv}^{(\lambda)} \epsilon_a^{(\lambda)}$ and the Wigner D matrix under the rotational transformation of a unit vector parallel to z axis into $\hat{\mathbf{k}}$ corresponding to Eq. (3.96). Therefore, performing the integration over $\Omega_{k,n}$ in the same manner as Sec. 3, we can obtain the explicit form of $a_{I,\ell m}^{(V)}$ and express the radiation transfer function introduced in Eq. (3.100) as

$$\begin{aligned} a_{I,\ell m}^{(V)} &= 4\pi(-i)^\ell \int \frac{d^3\mathbf{k}}{(2\pi)^3} \sum_{\lambda=\pm 1} \lambda_{-\lambda} Y_{\ell m}^*(\hat{\mathbf{k}}) \Pi_{Bv}^{(\lambda)}(\mathbf{k}) \mathcal{T}_{I,\ell}^{(V)}(k) , \\ \mathcal{T}_{I,\ell}^{(V)}(k) &\simeq \left[\frac{(\ell+1)!}{(\ell-1)!} \right]^{1/2} \frac{\beta(k, \tau_*)}{\sqrt{2}} \frac{j_\ell(x_*)}{x_*} . \end{aligned} \quad (9.36)$$

This is consistent with the results presented in Refs. [15, 34]. In the same manner, the vector-mode transfer functions of polarizations are derived [14, 19]. Then, we can also express as

$$a_{X,\ell m}^{(V)} = 4\pi(-i)^\ell \int \frac{d^3\mathbf{k}}{(2\pi)^3} \sum_{\lambda=\pm 1} \lambda^{x+1} {}_{-\lambda}Y_{\ell m}^*(\hat{\mathbf{k}}) \Pi_{Bv}^{(\lambda)}(\mathbf{k}) \mathcal{T}_{X,\ell}^{(V)}(k) . \quad (9.37)$$

9.1.4 Expression of $a_{\ell m}$'s

As the above results and Eq. (5.3), the CMB intensity and polarization fluctuations induced from PMFs are expressed as

$$\begin{aligned} a_{X,\ell m}^{(Z)} &= 4\pi(-i)^\ell \int \frac{k^2 dk}{(2\pi)^3} \sum_{\lambda} [\text{sgn}(\lambda)]^{\lambda+x} \xi_{\ell m}^{(\lambda)}(k) \mathcal{T}_{X,\ell}^{(Z)}(k) , \\ \xi_{\ell m}^{(0)}(k) &\approx \int d^2\hat{\mathbf{k}} Y_{\ell m}^*(\hat{\mathbf{k}}) \left[R_\gamma \ln \left(\frac{\tau_\nu}{\tau_B} \right) \right] \Pi_{Bs}^{(0)}(\mathbf{k}) , \\ \xi_{\ell m}^{(\pm 1)}(k) &\approx \int d^2\hat{\mathbf{k}} {}_{\mp 1}Y_{\ell m}^*(\hat{\mathbf{k}}) \Pi_{Bv}^{(\pm 1)}(\mathbf{k}) , \\ \xi_{\ell m}^{(\pm 2)}(k) &\approx \int d^2\hat{\mathbf{k}} {}_{\mp 2}Y_{\ell m}^*(\hat{\mathbf{k}}) \left[6R_\gamma \ln \left(\frac{\tau_\nu}{\tau_B} \right) \right] \Pi_{Bt}^{(\pm 2)}(\mathbf{k}) , \end{aligned} \quad (9.38)$$

where we take $\zeta(\mathbf{k}, \tau_B) = h^{(\pm 2)}(\mathbf{k}, \tau_B) = 0$, and regard $\xi^{(0)}$ and $\xi^{(\pm 2)}$ as $-\zeta(= \mathcal{R})$ and $h^{(\pm 2)}$, respectively ⁵.

⁵In Refs. [31, 35], we equate $\xi^{(0)}$ to ζ .

9.1.5 CMB power spectrum from PMFs

From the formulae (9.38), the CMB power spectra from PMFs are written as

$$\left\langle \prod_{n=1}^2 a_{X_n, \ell_n m_n}^{(Z_n)} \right\rangle = \left[\prod_{n=1}^2 4\pi(-i)^{\ell_n} \int \frac{k_n^2 dk_n}{(2\pi)^3} \mathcal{T}_{X_n, \ell_n}^{(Z_n)}(k_n) \sum_{\lambda_n} [\text{sgn}(\lambda_n)]^{\lambda_n + x_n} \right] \left\langle \prod_{n=1}^2 \xi_{\ell_n m_n}^{(\lambda_n)}(k_n) \right\rangle. \quad (9.39)$$

To compute the initial power spectrum $\langle \prod_{n=1}^2 \xi_{\ell_n m_n}^{(\lambda_n)}(k_n) \rangle$, we need to deal with the power spectrum of the anisotropic stresses as

$$\begin{aligned} \langle \Pi_{Bab}(\mathbf{k}_1) \Pi_{Bcd}(\mathbf{k}_2) \rangle &= (-4\pi\rho_{\gamma,0})^{-2} \left[\prod_{n=1}^2 \int \frac{d^3 \mathbf{k}'_n}{(2\pi)^3} \right] \\ &\quad \times \langle B_a(\mathbf{k}'_1) B_b(\mathbf{k}_1 - \mathbf{k}'_1) B_c(\mathbf{k}'_2) B_d(\mathbf{k}_2 - \mathbf{k}'_2) \rangle \\ &= \delta \left(\prod_{n=1}^2 \mathbf{k}_n \right) (-4\pi\rho_{\gamma,0})^{-2} \int d^3 \mathbf{k}'_1 P_B(k'_1) P_B(|\mathbf{k}_1 - \mathbf{k}'_1|) \\ &\quad \times \frac{1}{4} [P_{ad}(\hat{\mathbf{k}}'_1) P_{bc}(\widehat{\mathbf{k}_1 - \mathbf{k}'_1}) + P_{ac}(\hat{\mathbf{k}}'_1) P_{bd}(\widehat{\mathbf{k}_1 - \mathbf{k}'_1})]. \end{aligned} \quad (9.40)$$

Note that this equation includes the convolution integral and the complicated angular dependence. In Refs. [16, 36–38], the authors performed the numerical and analytical computation of this convolution integral over \mathbf{k}'_1 and provided the fitting formulae with respect to the magnitude of the wave numbers k_1 for each value of the magnetic spectral index n_B .

In Fig. 9.2, we plot the power spectra of the intensity anisotropies (9.39) for the scalar, vector and tensor modes when magnetic spectrum is nearly scale invariant as $n_B = -2.9$. Here, we assume that the PMFs generate from the epoch of the grand unification $\tau_B^{-1} = 10^{14} \text{GeV}$ to that of the electroweak phase transition $\tau_B^{-1} = 10^3 \text{GeV}$. Firstly, we will see that the shapes of the tensor and scalar power spectra are similar to those of the non-magnetic case coming from the scale-invariant primordial spectra shown in Fig. 3.5. This is because PMFs impact on only the primordial gravitational waves and primordial curvature perturbations, and do not change the transfer functions of the tensor and scalar modes. For $\ell \lesssim 100$, the tensor mode dominates over the intensity signal. The scalar mode seems to dominate in the intermediate scale as $100 \lesssim \ell \lesssim 2000$. The vector-mode spectrum monotonically increases for larger than Silk damping scale, namely, $\ell \lesssim k_S \tau_0 \sim 2000$, and decreases for $\ell \gtrsim 2000$. These features seem to trace the scaling relation of the transfer function in terms of the wave number (9.32). Hence, we can understand that the latter damping effect arises from the viscosity of photons. The vector mode seems to show up for very small scale, namely, $\ell \gtrsim 2000$.

In this figure, for comparison, we also plot the CMB intensity power spectrum from the primordial curvature perturbations not depending on the PMF. In principle, comparing this spectrum with that sourced from PMFs leads to bounds on the PMF parameters. Actually, the researchers perform the parameter estimation by the Malkov Chain Monte Carlo approach [36, 37, 39–43]. So far, the most stringent limit on the PMF strength from the CMB two-point function data of the intensity and polarizations are $B_{1\text{Mpc}} < 5\text{nG}$ and $n_B < -0.12$ [41]. In Refs. [36, 43], combining the CMB data with the information of the matter power spectrum, tighter bounds are gained.

As discussed above, conventionally, the CMB power spectra from PMFs are computed by using the fitting formulae for the power spectra of the magnetic anisotropic stresses. However, without these formulae, we can obtain the CMB power spectra by applying the mathematical tools such

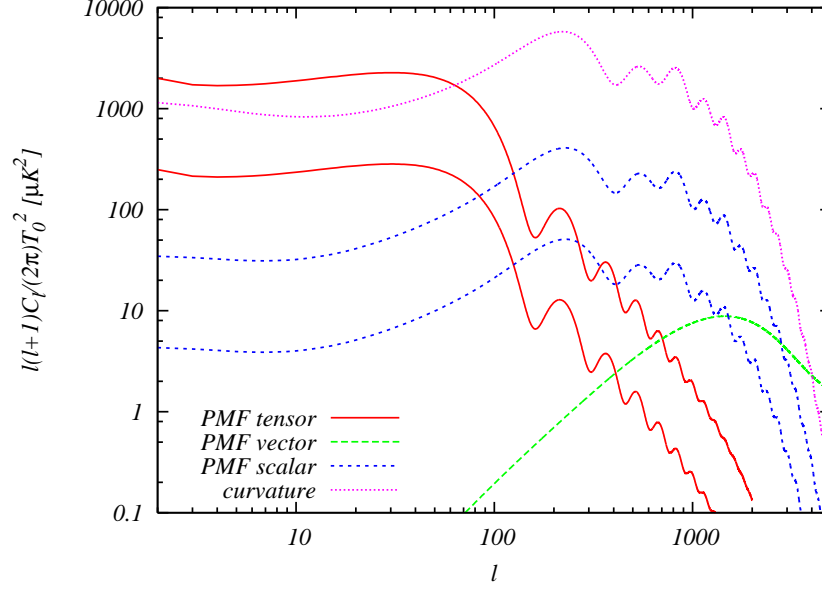


Figure 9.2: Power spectra of the CMB intensity fluctuations. The red solid, green dashed and blue dotted lines correspond to the spectra generated from the tensor, vector and scalar components of the PMF anisotropic stress for $n_B = -2.9$, respectively. The upper (lower) line of the red solid and blue dotted ones are calculated when $\tau_\nu/\tau_B = 10^{17}(10^6)$. The magenta dot-dashed line expresses the spectrum sourced from the primordial curvature perturbations. The strength of PMFs is fixed to $B_{1\text{Mpc}} = 4.7\text{nG}$ and the other cosmological parameters are fixed to the mean values limited from WMAP-7yr data reported in Ref. [29].

as the Wigner symbols [25]. In the remaining part, focusing on the vector mode, we present this new approach and show the consistency with the conventional result. Then, we use some colors in the equations for readers to follow the complex equations more easily.

From Eq. (9.39), the CMB power spectrum of the intensity mode induced from the magnetic-vector-mode anisotropic stress is formulated as

$$\begin{aligned}
 \left\langle a_{I,\ell_1 m_1}^{(V)} a_{I,\ell_2 m_2}^{(V)*} \right\rangle &= \left[\prod_{n=1}^2 4\pi \int_0^\infty \frac{k_n^2 dk_n}{(2\pi)^3} \mathcal{T}_{I,\ell_n}^{(V)}(k_n) \right] (-i)^{\ell_1} i^{\ell_2} \\
 &\times \sum_{\lambda_1, \lambda_2 = \pm 1} \lambda_1 \lambda_2 \left\langle \Pi_{Bv,\ell_1 m_1}^{(\lambda_1)}(k_1) \Pi_{Bv,\ell_2 m_2}^{(\lambda_2)*}(k_2) \right\rangle \\
 &\equiv C_{II,\ell_1}^{(V)} \delta_{\ell_1, \ell_2} \delta_{m_1, m_2} ,
 \end{aligned} \tag{9.41}$$

where the initial power spectrum, which is expanded by the spin spherical harmonics, is

$$\begin{aligned}
 \left\langle \Pi_{Bv,\ell_1 m_1}^{(\lambda_1)}(k_1) \Pi_{Bv,\ell_2 m_2}^{(\lambda_2)*}(k_2) \right\rangle &= (-4\pi \rho_{\gamma,0})^{-2} \int d^2 \hat{\mathbf{k}}_1 \int d^2 \hat{\mathbf{k}}_2 {}_{-\lambda_1} Y_{\ell_1 m_1}^*(\hat{\mathbf{k}}_1) {}_{-\lambda_2} Y_{\ell_2 m_2}(\hat{\mathbf{k}}_2) \\
 &\times \int_0^{k_D} k_1'^2 dk_1' P_B(k_1') \int_0^{k_D} k_2'^2 dk_2' P_B(k_2') \\
 &\times \int d^2 \hat{\mathbf{k}}_1' \int d^2 \hat{\mathbf{k}}_2' \delta(\mathbf{k}_1 - \mathbf{k}_1' - \mathbf{k}_2') \delta(\mathbf{k}_2 - \mathbf{k}_2' - \mathbf{k}_1')
 \end{aligned}$$

$$\times \frac{1}{4} \hat{k}_{1a} \epsilon_b^{(-\lambda_1)}(\hat{\mathbf{k}}_1) \hat{k}_{2c} \epsilon_d^{(\lambda_2)}(\hat{\mathbf{k}}_2) \left[P_{ad}(\hat{\mathbf{k}}_1) P_{bc}(\hat{\mathbf{k}}_2) + P_{ac}(\hat{\mathbf{k}}_1) P_{bd}(\hat{\mathbf{k}}_2) \right] , \quad (9.42)$$

where we use Eq. (9.9) and the definition of the vector projection operator, $O_{ab}^{(\pm 1)}(\hat{\mathbf{k}})$, in Appendix D. Note that we rewrote the power spectrum (9.40) as more symmetric form in terms of $\mathbf{k}_1, \mathbf{k}_2$ and \mathbf{k}_3 . Then, we should simplify this initial power spectrum.

For the first part in two permutations, we calculate δ -functions and the summations with respect to a, b, c and d :

$$\begin{aligned} \delta(\mathbf{k}_1 - \mathbf{k}'_1 - \mathbf{k}'_2) &= 8 \int_0^\infty A^2 dA \sum_{\substack{L_1 L_2 L_3 \\ M_1 M_2 M_3}} (-1)^{\frac{L_1+3L_2+3L_3}{2}} I_{L_1 L_2 L_3}^{0 \ 0 \ 0} j_{L_1}(k_1 A) j_{L_2}(k'_1 A) j_{L_3}(k'_2 A) \\ &\quad \times Y_{L_1 M_1}^*(\hat{\mathbf{k}}_1) Y_{L_2 M_2}(\hat{\mathbf{k}}'_1) Y_{L_3 - M_3}^*(\hat{\mathbf{k}}'_2) (-1)^{M_2} \begin{pmatrix} L_1 & L_2 & L_3 \\ M_1 & -M_2 & -M_3 \end{pmatrix} , \\ \delta(\mathbf{k}_2 - \mathbf{k}'_2 - \mathbf{k}'_1) &= 8 \int_0^\infty B^2 dB \sum_{\substack{L'_1 L'_2 L'_3 \\ M'_1 M'_2 M'_3}} (-1)^{\frac{L'_1+3L'_2+3L'_3}{2}} I_{L'_1 L'_2 L'_3}^{0 \ 0 \ 0} j_{L'_1}(k_2 B) j_{L'_2}(k'_2 B) j_{L'_3}(k'_1 B) \\ &\quad \times Y_{L'_1 M'_1}^*(\hat{\mathbf{k}}_2) Y_{L'_2 M'_2}(\hat{\mathbf{k}}'_2) Y_{L'_3 - M'_3}^*(\hat{\mathbf{k}}'_1) (-1)^{M'_2} \begin{pmatrix} L'_1 & L'_2 & L'_3 \\ M'_1 & -M'_2 & -M'_3 \end{pmatrix} , \quad (9.43) \\ \hat{k}_{1a} \epsilon_d^{(\lambda_2)}(\hat{\mathbf{k}}_2) P_{ad}(\hat{\mathbf{k}}'_1) &= \sum_{\sigma=\pm 1} \sum_{m_a, m_d=\pm 1, 0} \left(\frac{4\pi}{3} \right)^2 \lambda_2 \\ &\quad \times Y_{1m_a}(\hat{\mathbf{k}}_1)_{\lambda_2} Y_{1m_d}(\hat{\mathbf{k}}_2)_{-\sigma} Y_{1m_a}^*(\hat{\mathbf{k}}'_1)_{\sigma} Y_{1m_d}^*(\hat{\mathbf{k}}'_1) , \\ \hat{k}_{2c} \epsilon_b^{(-\lambda_1)}(\hat{\mathbf{k}}_1) P_{bc}(\hat{\mathbf{k}}'_2) &= \sum_{\sigma'=\pm 1} \sum_{m_c, m_b=\pm 1, 0} \left(\frac{4\pi}{3} \right)^2 (-\lambda_1) \\ &\quad \times Y_{1m_c}(\hat{\mathbf{k}}_2)_{-\lambda_1} Y_{1m_b}(\hat{\mathbf{k}}_1)_{-\sigma'} Y_{1m_c}^*(\hat{\mathbf{k}}'_2)_{\sigma'} Y_{1m_b}^*(\hat{\mathbf{k}}'_2) , \end{aligned}$$

perform the angular integrals of the spin spherical harmonics:

$$\begin{aligned}
& \int d^2\mathbf{k}'_{\mathbf{1}-\sigma} Y_{1m_a}^* Y_{L_2 M_2 \sigma} Y_{1m_d}^* Y_{L'_3 - M'_3}^* \\
&= \sum_{LMS} (-1)^{\sigma+m_a} I_{L'_3 1 L}^{0-\sigma-S} I_{L_2 1 L}^{0-\sigma-S} \begin{pmatrix} L'_3 & 1 & L \\ -M'_3 & m_d & M \end{pmatrix} \begin{pmatrix} L_2 & 1 & L \\ M_2 & -m_a & M \end{pmatrix}, \\
& \int d^2\mathbf{k}'_{\mathbf{2}-\sigma'} Y_{1m_c}^* Y_{L'_2 M'_2 \sigma'} Y_{1m_b}^* Y_{L_3 - M_3}^* \\
&= \sum_{L'M'S'} (-1)^{\sigma'+m_c} I_{L_3 1 L'}^{0-\sigma'-S'} I_{L'_2 1 L'}^{0-\sigma'-S'} \begin{pmatrix} L_3 & 1 & L' \\ -M_3 & m_b & M' \end{pmatrix} \begin{pmatrix} L'_2 & 1 & L' \\ M'_2 & -m_c & M' \end{pmatrix}, \\
& \int d^2\mathbf{k}_{\mathbf{1}-\lambda_1} Y_{1m_b} Y_{1m_a - \lambda_1} Y_{\ell_1 m_1}^* Y_{L_1 M_1}^* \\
&= \sum_{L_k M_k S_k} I_{L_1 \ell_1 L_k}^{0\lambda_1 - S_k} I_{11 L_k}^{0\lambda_1 - S_k} \begin{pmatrix} L_1 & \ell_1 & L_k \\ M_1 & m_1 & M_k \end{pmatrix} \begin{pmatrix} 1 & 1 & L_k \\ m_a & m_b & M_k \end{pmatrix}, \\
& \int d^2\mathbf{k}_{\mathbf{2}\lambda_2} Y_{1m_d} Y_{1m_c - \lambda_2} Y_{\ell_2 m_2} Y_{L'_1 M'_1}^* \\
&= \sum_{L_p M_p S_p} (-1)^{m_2 + \lambda_2} I_{L'_1 \ell_2 L_p}^{0\lambda_2 - S_p} I_{11 L_p}^{0\lambda_2 - S_p} \begin{pmatrix} L'_1 & \ell_2 & L_p \\ -M'_1 & m_2 & M_p \end{pmatrix} \begin{pmatrix} 1 & 1 & L_p \\ -m_c & -m_d & M_p \end{pmatrix},
\end{aligned} \tag{9.44}$$

sum up the Wigner-3j symbols over the azimuthal quantum numbers:

$$\begin{aligned}
& \sum_{\substack{M_1 M_2 M_3 \\ M_k m_a m_b}} (-1)^{M_2 + m_a} \begin{pmatrix} 1 & 1 & L_k \\ m_a & m_b & M_k \end{pmatrix} \begin{pmatrix} L_1 & L_2 & L_3 \\ M_1 & -M_2 & -M_3 \end{pmatrix} \\
& \times \begin{pmatrix} L_3 & 1 & L' \\ -M_3 & m_b & M' \end{pmatrix} \begin{pmatrix} L_2 & 1 & L \\ M_2 & -m_a & M \end{pmatrix} \begin{pmatrix} L_1 & \ell_1 & L_k \\ M_1 & m_1 & M_k \end{pmatrix} \\
&= (-1)^{M + \ell_1 + L_3 + L + 1} \begin{pmatrix} L' & L & \ell_1 \\ M' & -M & m_1 \end{pmatrix} \left\{ \begin{matrix} L' & L & \ell_1 \\ L_3 & L_2 & L_1 \\ 1 & 1 & L_k \end{matrix} \right\}, \\
& \sum_{\substack{M'_1 M'_2 M'_3 \\ M_p m_c m_d}} (-1)^{M'_2 + m_c} \begin{pmatrix} 1 & 1 & L_p \\ -m_c & -m_d & M_p \end{pmatrix} \begin{pmatrix} L'_1 & L'_2 & L'_3 \\ M'_1 & -M'_2 & -M'_3 \end{pmatrix} \\
& \begin{pmatrix} L'_2 & 1 & L' \\ M'_2 & -m_c & M' \end{pmatrix} \begin{pmatrix} L'_3 & 1 & L \\ -M'_3 & m_d & M \end{pmatrix} \begin{pmatrix} L'_1 & \ell_2 & L_p \\ -M'_1 & m_2 & M_p \end{pmatrix} \\
&= (-1)^{M' + \ell_2 + L'_2 + L + 1 + L_p} \begin{pmatrix} L' & L & \ell_2 \\ M' & -M & m_2 \end{pmatrix} \left\{ \begin{matrix} L' & L & \ell_2 \\ L'_2 & L'_3 & L'_1 \\ 1 & 1 & L_p \end{matrix} \right\},
\end{aligned} \tag{9.45}$$

and sum up the Wigner-3j symbols over M and M' :

$$\sum_{MM'} (-1)^{M+M'} \begin{pmatrix} L' & L & \ell_1 \\ M' & -M & m_1 \end{pmatrix} \begin{pmatrix} L' & L & \ell_2 \\ M' & -M & m_2 \end{pmatrix} = \frac{(-1)^{m_2}}{2\ell_1 + 1} \delta_{\ell_1, \ell_2} \delta_{m_1, m_2}. \tag{9.46}$$

Following the same procedures in the other permutation and calculating the summation over L_p

as

$$\sum_{L_p} I_{L'_1 \ell_2 L_p}^{0\lambda_2-\lambda_2} I_{11 L_p}^{0\lambda_2-\lambda_2} \frac{1+(-1)^{L_p}}{2} \begin{Bmatrix} L' & L & \ell_2 \\ L'_2 & L'_3 & L'_1 \\ 1 & 1 & L_p \end{Bmatrix} = -\frac{3}{2\sqrt{2\pi}} I_{L'_1 \ell_2 2}^{0\lambda_2-\lambda_2} \begin{Bmatrix} L' & L & \ell_2 \\ L'_3 & L'_2 & L'_1 \\ 1 & 1 & 2 \end{Bmatrix}, \quad (9.47)$$

we can obtain the exact solution of Eq. (9.42) as

$$\begin{aligned} \left\langle \Pi_{Bv, \ell_1 m_1}^{(\lambda_1)}(k_1) \Pi_{Bv, \ell_2 m_2}^{(\lambda_2)*}(k_2) \right\rangle &= -\frac{\sqrt{2\pi}}{3} \left(\frac{8(2\pi)^{1/2}}{3\rho_{\gamma,0}} \right)^2 / (2\ell_1 + 1) \delta_{\ell_1, \ell_2} \delta_{m_1, m_2} \\ &\times \sum_{LL'} \sum_{\substack{L_1 L_2 L_3 \\ L'_1 L'_2 L'_3}} (-1)^{\sum_{i=1}^3 \frac{L_i + L'_i}{2}} I_{L_1 L_2 L_3}^{0 \ 0 \ 0} I_{L'_1 L'_2 L'_3}^{0 \ 0 \ 0} \\ &\times \sum_{L_k} (-1)^{L'_2 + L_3} \begin{Bmatrix} L' & L & \ell_1 \\ L_3 & L_2 & L_1 \\ 1 & 1 & L_k \end{Bmatrix} \begin{Bmatrix} L' & L & \ell_2 \\ L'_2 & L'_3 & L'_1 \\ 1 & 1 & 2 \end{Bmatrix} \\ &\times \int_0^\infty A^2 dA j_{L_1}(k_1 A) \int_0^\infty B^2 dB j_{L'_1}(k_2 B) \\ &\times \int_0^{k_D} k_1'^2 dk_1' P_B(k_1') j_{L_2}(k_1' A) j_{L'_3}(k_1' B) \\ &\times \int_0^{k_D} k_2'^2 dk_2' P_B(k_2') j_{L'_2}(k_2' B) j_{L_3}(k_2' A) \\ &\times \sum_{S, S'=\pm 1} (-1)^{L_2 + L'_2 + L_3 + L'_3} I_{L'_3 1 L}^{0S-S} I_{L_2 1 L}^{0S-S} I_{L_3 1 L'}^{0S'-S'} I_{L'_2 1 L'}^{0S'-S'} \\ &\times \lambda_1 \lambda_2 I_{L_1 \ell_1 L_k}^{0\lambda_1-\lambda_1} I_{11 L_k}^{0\lambda_1-\lambda_1} I_{L'_1 \ell_2 2}^{0\lambda_2-\lambda_2}. \end{aligned} \quad (9.48)$$

Note that in this equation, the dependence on the azimuthal quantum number is included only in δ_{m_1, m_2} . In the similar discussion of the CMB bispectrum, this implies that the CMB vector-mode power spectrum generated from the magnetized anisotropic stresses is rotationally-invariant if the PMFs satisfy the statistical isotropy as Eq. (9.4).

Furthermore, using such evaluations as

$$\begin{aligned} \sum_{S, S'=\pm 1} (-1)^{L_2 + L'_2 + L_3 + L'_3} I_{L'_3 1 L}^{0S-S} I_{L_2 1 L}^{0S-S} I_{L_3 1 L'}^{0S'-S'} I_{L'_2 1 L'}^{0S'-S'} \\ = \begin{cases} 4 I_{L'_3 1 L}^{01-1} I_{L_2 1 L}^{01-1} I_{L_3 1 L'}^{01-1} I_{L'_2 1 L'}^{01-1} & (L'_3 + L_2, L_3 + L'_2 = \text{even}) \\ 0 & (\text{otherwise}) \end{cases}, \end{aligned} \quad (9.49)$$

$$\sum_{\lambda_1, \lambda_2=\pm 1} I_{L_1 \ell_1 L_k}^{0\lambda_1-\lambda_1} I_{11 L_k}^{0\lambda_1-\lambda_1} I_{L'_1 \ell_2 2}^{0\lambda_2-\lambda_2} = \begin{cases} 4 I_{L_1 \ell_1 L_k}^{01-1} I_{11 L_k}^{01-1} I_{L'_1 \ell_2 2}^{01-1} & (L_1 + \ell_1, L'_1 + \ell_2 = \text{even}) \\ 0 & (\text{otherwise}) \end{cases}, \quad (9.50)$$

$$\begin{aligned} &\left[\prod_{n=1}^2 4\pi \int_0^\infty \frac{k_n^2 dk_n}{(2\pi)^3} \mathcal{T}_{I, \ell_n}^{(V)}(k_n) \right] \int_0^\infty A^2 dA j_{L_1}(k_1 A) \int_0^\infty B^2 dB j_{L'_1}(k_2 B) \\ &\quad \times \int_0^{k_D} k_1'^2 dk_1' P_B(k_1') j_{L_2}(k_1' A) j_{L'_3}(k_1' B) \int_0^{k_D} k_2'^2 dk_2' P_B(k_2') j_{L'_2}(k_2' B) j_{L_3}(k_2' A) \\ &\simeq \left[\prod_{n=1}^2 4\pi \int_0^\infty \frac{k_n^2 dk_n}{(2\pi)^3} \mathcal{T}_{I, \ell_n}^{(V)}(k_n) j_{\ell_n}(k_n(\tau_0 - \tau_*)) \right] \end{aligned}$$

$$\times A_B^2(\tau_0 - \tau_*)^4 \left(\frac{\tau_*}{5}\right)^2 \mathcal{K}_{L_2 L'_3}^{-(n_B+1)}(\tau_0 - \tau_*) \mathcal{K}_{L'_2 L_3}^{-(n_B+1)}(\tau_0 - \tau_*) , \quad (9.51)$$

the CMB angle-averaged power spectrum is formulated as

$$\begin{aligned} C_{II,\ell}^{(V)} &\simeq -\frac{\sqrt{2\pi}}{3} \left(\frac{32(2\pi)^{1/2}}{3\rho_{\gamma,0}}\right)^2 / (2\ell + 1) \left[4\pi \int_0^\infty \frac{k^2 dk}{(2\pi)^3} \mathcal{T}_{I,\ell}^{(V)}(k) j_\ell(k(\tau_0 - \tau_*)) \right]^2 \\ &\times \sum_{L_1 L'_1} \sum_{L_k} I_{L_1 \ell L_k}^{01-1} I_{11 L_k}^{01-1} I_{L'_1 \ell 2}^{01-1} \sum_{LL'} \sum_{\substack{L_2 L'_2 \\ L'_3 L_3}} A_B^2(\tau_0 - \tau_*)^4 \left(\frac{\tau_*}{5}\right)^2 \\ &\times \mathcal{K}_{L_2 L'_3}^{-(n_B+1)}(\tau_0 - \tau_*) \mathcal{K}_{L'_2 L_3}^{-(n_B+1)}(\tau_0 - \tau_*) \\ &\times (-1)^{\sum_{i=1}^3 \frac{L_i + L'_i}{2} + L'_2 + L_3} I_{L_1 L_2 L_3}^{0 \ 0 \ 0} I_{L'_1 L'_2 L'_3}^{0 \ 0 \ 0} I_{L'_3 1 L}^{01-1} I_{L_2 1 L}^{01-1} I_{L_3 1 L'}^{01-1} I_{L'_2 1 L'}^{01-1} \\ &\times \left\{ \begin{matrix} L' & L & \ell \\ L_3 & L_2 & L_1 \\ 1 & 1 & L_k \end{matrix} \right\} \left\{ \begin{matrix} L' & L & \ell \\ L'_2 & L'_3 & L'_1 \\ 1 & 1 & 2 \end{matrix} \right\} . \end{aligned} \quad (9.52)$$

Here, we use the thin LSS approximation described in Sec. 9.3.1. This has nonzero value in the configurations:

$$\begin{aligned} (L_k, L_1) &= (2, |\ell \pm 2|), (2, \ell), (1, \ell) , \quad L'_1 = |\ell \pm 2|, \ell , \\ |\ell - L| &\leq L' \leq \ell + L , \\ (L_2, L'_3) &= (|L - 1|, |L \pm 1|), (L, L), (L + 1, |L \pm 1|) , \\ (L'_2, L_3) &= (|L' - 1|, |L' \pm 1|), (L', L'), (L' + 1, |L' \pm 1|) , \\ L_1 + L_2 + L_3 &= \text{even} , \quad L'_1 + L'_2 + L'_3 = \text{even} , \\ |L_1 - L_2| &\leq L_3 \leq L_1 + L_2 , \quad |L'_1 - L'_2| \leq L'_3 \leq L'_1 + L'_2 . \end{aligned} \quad (9.53)$$

This shape is described in Fig. 9.3. From this figure, we confirm that the amplitude and the overall behavior of the red solid line are in broad agreement with the green dashed line of Fig. 9.2 and the previous studies (e.g. [15–17, 44]). For $\ell \lesssim 2000$, using the scaling relations of the Wigner symbols at the dominant configuration $L \sim \ell, L' \sim 1$ as discussed in Sec. 9.5, we analytically find that $C_{I,\ell}^{(V)} \propto \ell^{n_B+3}$. This traces our numerical results as shown by the green dashed line.

This computation approach is of great utility in the higher-order correlations. In the next subsection, in accordance with this approach, we compute the CMB bispectra sourced from PMFs.

9.2 Formulation for the CMB bispectrum induced from PMFs

In this subsection, we derive the explicit form of the CMB bispectra induced from PMFs by calculating the full-angular dependence which has never been considered in the previous studies [20–23, 28]. The following procedures are based on the calculation rules discussed in Ref. [25]. Note that we use some colors in the following equations for readers to follow the complex equations more easily.

9.2.1 Bispectrum of the anisotropic stress fluctuations

According to Eq. (9.2), EMT of PMF at an arbitrary point, $T^\mu{}_\nu(\mathbf{x})$, depends quadratically on the Gaussian magnetic fields at that point. This non-Gaussian structure is identical to the local-type

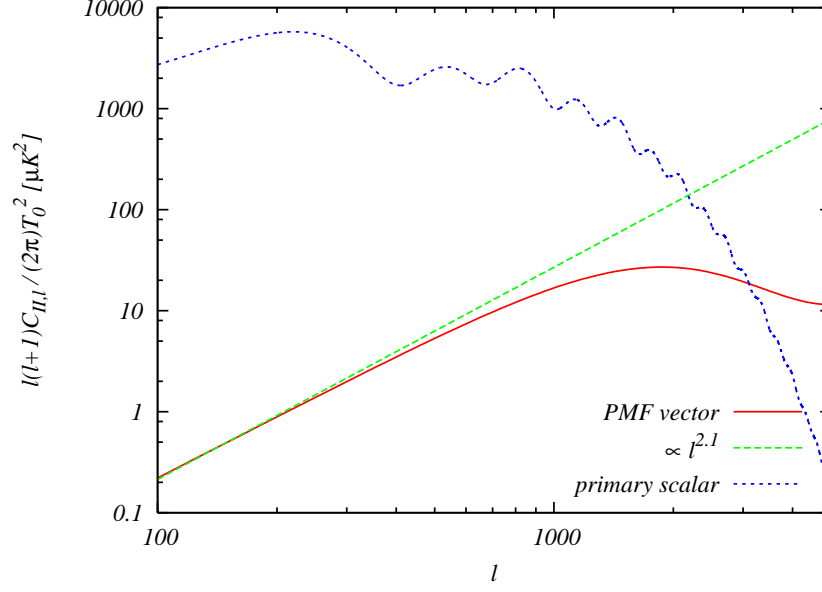


Figure 9.3: CMB power spectra of the temperature fluctuations. The lines correspond to the spectra generated from vector anisotropic stress of PMFs as Eq. (9.52) (red solid line) and primordial curvature perturbations (blue dotted line). The green dashed line expresses the asymptotic power of the red solid one. The PMF parameters are fixed to $n_B = -2.9$ and $B_{1\text{Mpc}} = 4.7\text{nG}$, and the other cosmological parameters are fixed to the mean values limited from WMAP-7yr data reported in Ref. [29].

non-Gaussianity of the curvature perturbations as mentioned in Sec 4.2, hence it is expected that the statistical properties of the magnetic fields obey those of the local-type non-Gaussianity. This will be automatically shown in Sec. 9.4.

Using Eq. (9.4) and the Wick's theorem, the bispectrum of the anisotropic stresses is calculated as

$$\begin{aligned}
 \langle \Pi_{Bab}(\mathbf{k}_1) \Pi_{Bcd}(\mathbf{k}_2) \Pi_{Bef}(\mathbf{k}_3) \rangle &= (-4\pi\rho_{\gamma,0})^{-3} \left[\prod_{n=1}^3 \int \frac{d^3\mathbf{k}'_n}{(2\pi)^3} \right] \\
 &\quad \times \langle B_a(\mathbf{k}'_1) B_b(\mathbf{k}_1 - \mathbf{k}'_1) B_c(\mathbf{k}'_2) B_d(\mathbf{k}_2 - \mathbf{k}'_2) B_e(\mathbf{k}'_3) B_f(\mathbf{k}_3 - \mathbf{k}'_3) \rangle \\
 &= (-4\pi\rho_{\gamma,0})^{-3} \left[\prod_{n=1}^3 \int_0^{k_D} k_n'^2 dk_n' P_B(k_n') \int d^2\hat{\mathbf{k}}'_n \right] \\
 &\quad \times \delta(\mathbf{k}_1 - \mathbf{k}'_1 + \mathbf{k}'_3) \delta(\mathbf{k}_2 - \mathbf{k}'_2 + \mathbf{k}'_1) \delta(\mathbf{k}_3 - \mathbf{k}'_3 + \mathbf{k}'_2) \\
 &\quad \times \frac{1}{8} [P_{ad}(\hat{\mathbf{k}}'_1) P_{be}(\hat{\mathbf{k}}'_3) P_{cf}(\hat{\mathbf{k}}'_2) + \{a \leftrightarrow b \text{ or } c \leftrightarrow d \text{ or } e \leftrightarrow f\}] ,
 \end{aligned} \tag{9.54}$$

where k_D is the Alfvén-wave damping length scale [45, 46] as $k_D^{-1} \sim \mathcal{O}(0.1)\text{Mpc}$ and the curly bracket denotes the symmetric 7 terms under the permutations of indices: $a \leftrightarrow b$, $c \leftrightarrow d$, or $e \leftrightarrow f$. Note that we express in a more symmetric form than that of Ref. [18] to perform the angular integrals which is described in Sec. 9.2. To avoid the divergence of $\langle \Pi_{Bab}(\mathbf{k}_1) \Pi_{Bcd}(\mathbf{k}_2) \Pi_{Bef}(\mathbf{k}_3) \rangle$ in the IR limit, the value range of the spectral index is limited as $n_B > -3$. We note that this

bispectrum depends on the Gaussian PMFs to six, hence this is highly non-Gaussian compared with the bispectrum of primordial curvature perturbations proportional to the Gaussian variable to four as shown in Sec. 4.2.

9.2.2 CMB all-mode bispectrum

Following the general formula (5.5) and using Eq. (9.38), the CMB bispectra induced from PMF are written as

$$\left\langle \prod_{n=1}^3 a_{X_n, \ell_n m_n}^{(Z_n)} \right\rangle = \left[\prod_{n=1}^3 4\pi(-i)^{\ell_n} \int_0^\infty \frac{k_n^2 dk_n}{(2\pi)^3} \mathcal{T}_{X_n, \ell_n}^{(Z_n)}(k_n) \sum_{\lambda_n} [\text{sgn}(\lambda_n)]^{\lambda_n + x_n} \right] \left\langle \prod_{n=1}^3 \xi_{\ell_n m_n}^{(\lambda_n)}(k_n) \right\rangle. \quad (9.55)$$

Remember that the index Z denotes the mode of perturbations: $Z = S$ (scalar), $= V$ (vector) or $= T$ (tensor) and its helicity is expressed by λ ; $\lambda = 0$ for ($Z = S$), $= \pm 1$ for ($Z = V$) or $= \pm 2$ for ($Z = T$), X discriminates between intensity and two polarization (electric and magnetic) modes, respectively, as $X = I, E, B$ and x is determined by it: $x = 0$ for $X = I, E$ or $= 1$ for $X = B$. In the following discussion, we calculate $\left\langle \prod_{n=1}^3 \xi_{\ell_n m_n}^{(\lambda_n)}(k_n) \right\rangle$ and find an explicit formulae of the CMB bispectra corresponding to an arbitrary Z .

Using Eqs. (9.38) and (9.54), we can write

$$\begin{aligned} \left\langle \prod_{n=1}^3 \xi_{\ell_n m_n}^{(\lambda_n)}(k_n) \right\rangle &= (-4\pi\rho_{\gamma,0})^{-3} \left[\prod_{n=1}^3 \int d^2\hat{\mathbf{k}}_{\mathbf{n}-\lambda_n} Y_{\ell_n m_n}^*(\hat{\mathbf{k}}_{\mathbf{n}}) \int_0^{k_D} k_n'^2 dk_n' P_B(k_n') \int d^2\hat{\mathbf{k}}_{\mathbf{n}} \right] \\ &\quad \times \delta(\mathbf{k}_1 - \mathbf{k}'_1 + \mathbf{k}'_3) \delta(\mathbf{k}_2 - \mathbf{k}'_2 + \mathbf{k}'_1) \delta(\mathbf{k}_3 - \mathbf{k}'_3 + \mathbf{k}'_2) \\ &\quad \times C'_{-\lambda_1} O_{ab}^{(-\lambda_1)}(\hat{\mathbf{k}}_1) C'_{-\lambda_2} O_{cd}^{(-\lambda_2)}(\hat{\mathbf{k}}_2) C'_{-\lambda_3} O_{ef}^{(-\lambda_3)}(\hat{\mathbf{k}}_3) \\ &\quad \times P_{ad}(\hat{\mathbf{k}}_1) P_{be}(\hat{\mathbf{k}}_3) P_{cf}(\hat{\mathbf{k}}_2), \end{aligned} \quad (9.56)$$

with

$$C'_\lambda \equiv \begin{cases} \frac{3}{2} R_\gamma \ln\left(\frac{\tau_\nu}{\tau_B}\right) & (\lambda = 0) \\ \frac{1}{2} & (\lambda = \pm 1) \\ 3R_\gamma \ln\left(\frac{\tau_\nu}{\tau_B}\right) & (\lambda = \pm 2) \end{cases}. \quad (9.57)$$

Let us consider this exact expression by expanding all the angular dependencies with the spin-weighted spherical harmonics and rewriting the angular integrals with the summations in terms of the multipoles and azimuthal quantum numbers.

In the first step, in order to perform all angular integrals, we expand each function of the wave number vectors with the spin-weighted spherical harmonics. By this concept, three delta functions

are rewritten as

$$\begin{aligned}
\delta(\mathbf{k}_1 - \mathbf{k}'_1 + \mathbf{k}'_3) &= 8 \int_0^\infty A^2 dA \sum_{\substack{L_1 L_2 L_3 \\ M_1 M_2 M_3}} (-1)^{\frac{L_1+3L_2+L_3}{2}} I_{L_1 L_2 L_3}^0 \begin{matrix} 0 & 0 & 0 \end{matrix} j_{L_1}(k_1 A) j_{L_2}(k'_1 A) j_{L_3}(k'_3 A) \\
&\quad \times Y_{L_1 M_1}^*(\hat{\mathbf{k}}_1) Y_{L_2 M_2}(\hat{\mathbf{k}}'_1) Y_{L_3 M_3}^*(\hat{\mathbf{k}}'_3) (-1)^{M_2} \begin{pmatrix} L_1 & L_2 & L_3 \\ M_1 & -M_2 & M_3 \end{pmatrix}, \\
\delta(\mathbf{k}_2 - \mathbf{k}'_2 + \mathbf{k}'_1) &= 8 \int_0^\infty B^2 dB \sum_{\substack{L'_1 L'_2 L'_3 \\ M'_1 M'_2 M'_3}} (-1)^{\frac{L'_1+3L'_2+L'_3}{2}} I_{L'_1 L'_2 L'_3}^0 \begin{matrix} 0 & 0 & 0 \end{matrix} j_{L'_1}(k_2 B) j_{L'_2}(k'_2 B) j_{L'_3}(k'_1 B) \\
&\quad \times Y_{L'_1 M'_1}^*(\hat{\mathbf{k}}_2) Y_{L'_2 M'_2}(\hat{\mathbf{k}}'_2) Y_{L'_3 M'_3}^*(\hat{\mathbf{k}}'_1) (-1)^{M'_2} \begin{pmatrix} L'_1 & L'_2 & L'_3 \\ M'_1 & -M'_2 & M'_3 \end{pmatrix}, \\
\delta(\mathbf{k}_3 - \mathbf{k}'_3 + \mathbf{k}'_2) &= 8 \int_0^\infty C^2 dC \sum_{\substack{L''_1 L''_2 L''_3 \\ M''_1 M''_2 M''_3}} (-1)^{\frac{L''_1+3L''_2+L''_3}{2}} I_{L''_1 L''_2 L''_3}^0 \begin{matrix} 0 & 0 & 0 \end{matrix} j_{L''_1}(k_3 C) j_{L''_2}(k'_3 C) j_{L''_3}(k'_2 C) \\
&\quad \times Y_{L''_1 M''_1}^*(\hat{\mathbf{k}}_3) Y_{L''_2 M''_2}(\hat{\mathbf{k}}'_3) Y_{L''_3 M''_3}^*(\hat{\mathbf{k}}'_2) (-1)^{M''_2} \begin{pmatrix} L''_1 & L''_2 & L''_3 \\ M''_1 & -M''_2 & M''_3 \end{pmatrix},
\end{aligned} \tag{9.58}$$

where

$$I_{\ell_1 \ell_2 \ell_3}^{s_1 s_2 s_3} \equiv \sqrt{\frac{(2\ell_1+1)(2\ell_2+1)(2\ell_3+1)}{4\pi}} \begin{pmatrix} \ell_1 & \ell_2 & \ell_3 \\ s_1 & s_2 & s_3 \end{pmatrix}. \tag{9.59}$$

The other functions in Eq. (9.56), which depend on the angles of the wave number vectors, can be also expanded in terms of the spin-weighted spherical harmonics as

$$\begin{aligned}
&O_{ab}^{(-\lambda_1)}(\hat{\mathbf{k}}_1) O_{cd}^{(-\lambda_2)}(\hat{\mathbf{k}}_2) O_{ef}^{(-\lambda_3)}(\hat{\mathbf{k}}_3) P_{ad}(\hat{\mathbf{k}}'_1) P_{be}(\hat{\mathbf{k}}'_3) P_{cf}(\hat{\mathbf{k}}'_2) \\
&= \sum_{\sigma_1, \sigma_2, \sigma_3 = \pm 1} -C_{-\lambda_1} \sqrt{\frac{3}{8\pi}} \sum_{\mu_1 m_a m_b} \left(\frac{4\pi}{3}\right)^2 \\
&\quad \times {}_{\lambda_1} Y_{2\mu_1}^*(\hat{\mathbf{k}}_1) \begin{pmatrix} 2 & 1 & 1 \\ \mu_1 & m_a & m_b \end{pmatrix} {}_{-\sigma_1} Y_{1m_a}^*(\hat{\mathbf{k}}'_1) {}_{\sigma_3} Y_{1m_b}^*(\hat{\mathbf{k}}'_3) \\
&\quad \times C_{-\lambda_2} \sqrt{\frac{3}{8\pi}} \sum_{\mu_2 m_c m_d} \left(\frac{4\pi}{3}\right)^2 {}_{\lambda_2} Y_{2\mu_2}^*(\hat{\mathbf{k}}_2) \begin{pmatrix} 2 & 1 & 1 \\ \mu_2 & m_c & m_d \end{pmatrix} {}_{-\sigma_2} Y_{1m_c}^*(\hat{\mathbf{k}}'_2) {}_{\sigma_1} Y_{1m_d}^*(\hat{\mathbf{k}}'_1) \\
&\quad \times C_{-\lambda_3} \sqrt{\frac{3}{8\pi}} \sum_{\mu_3 m_e m_f} \left(\frac{4\pi}{3}\right)^2 {}_{\lambda_3} Y_{2\mu_3}^*(\hat{\mathbf{k}}_3) \begin{pmatrix} 2 & 1 & 1 \\ \mu_3 & m_e & m_f \end{pmatrix} {}_{-\sigma_3} Y_{1m_e}^*(\hat{\mathbf{k}}'_3) {}_{\sigma_2} Y_{1m_f}^*(\hat{\mathbf{k}}'_2),
\end{aligned} \tag{9.60}$$

where we have used Eqs. (9.5), some relations in Appendices C and D, and the definition (D.23) as

$$\begin{aligned}
O_{ab}^{(\lambda)}(\hat{\mathbf{k}}) &= C_\lambda \sqrt{\frac{3}{8\pi}} \sum_{M m_a m_b} -{}_\lambda Y_{2M}^*(\hat{\mathbf{k}}) \alpha_a^{m_a} \alpha_b^{m_b} \begin{pmatrix} 2 & 1 & 1 \\ M & m_a & m_b \end{pmatrix}, \\
C_\lambda &= \begin{cases} -2 & (\lambda = 0) \\ 2\sqrt{3}\lambda & (\lambda = \pm 1) \\ 2\sqrt{3} & (\lambda = \pm 2) \end{cases}.
\end{aligned} \tag{9.61}$$

In the second step, let us consider performing all angular integrals and replacing them with the Wigner-3j symbols. Three angular integrals with respect to $\hat{\mathbf{k}}'_1$, $\hat{\mathbf{k}}'_2$ and $\hat{\mathbf{k}}'_3$ are given as

$$\begin{aligned}
& \int d^2 \hat{\mathbf{k}}'_1 Y_{1m_a}^* Y_{L_2 M_2 \sigma_1} Y_{1m_d}^* Y_{L'_3 M'_3}^* \\
&= - \sum_{LM} \sum_{S=\pm 1} (-1)^{m_a} I_{L'_3 1 L}^{0-\sigma_1-S} I_{L_2 1 L}^{0-\sigma_1-S} \begin{pmatrix} L'_3 & 1 & L \\ M'_3 & m_d & M \end{pmatrix} \begin{pmatrix} L_2 & 1 & L \\ M_2 & -m_a & M \end{pmatrix}, \\
& \int d^2 \hat{\mathbf{k}}'_2 Y_{1m_c}^* Y_{L'_2 M'_2 \sigma_2} Y_{1m_f}^* Y_{L''_3 M''_3}^* \\
&= - \sum_{L'M'} \sum_{S'=\pm 1} (-1)^{m_c} I_{L''_3 1 L'}^{0-\sigma_2-S'} I_{L'_2 1 L'}^{0-\sigma_2-S'} \begin{pmatrix} L''_3 & 1 & L' \\ M''_3 & m_f & M' \end{pmatrix} \begin{pmatrix} L'_2 & 1 & L' \\ M'_2 & -m_c & M' \end{pmatrix}, \\
& \int d^2 \hat{\mathbf{k}}'_3 Y_{1m_e}^* Y_{L''_2 M''_2 \sigma_3} Y_{1m_b}^* Y_{L_3 M_3}^* \\
&= - \sum_{L''M''} \sum_{S''=\pm 1} (-1)^{m_e} I_{L_3 1 L''}^{0-\sigma_3-S''} I_{L''_2 1 L''}^{0-\sigma_3-S''} \begin{pmatrix} L_3 & 1 & L'' \\ M_3 & m_b & M'' \end{pmatrix} \begin{pmatrix} L''_2 & 1 & L'' \\ M''_2 & -m_e & M'' \end{pmatrix},
\end{aligned} \tag{9.62}$$

where we have used a property of spin-weighted spherical harmonics given by Eq. (C.7). We can also perform the angular integrals with respect to $\hat{\mathbf{k}}_1$, $\hat{\mathbf{k}}_2$ and $\hat{\mathbf{k}}_3$ as

$$\begin{aligned}
& \int d^2 \hat{\mathbf{k}}_1 Y_{L_1 M_1 - \lambda_1}^* Y_{\ell_1 m_1 \lambda_1}^* Y_{2\mu_1}^* = I_{L_1 \ell_1 2}^{0\lambda_1 - \lambda_1} \begin{pmatrix} L_1 & \ell_1 & 2 \\ M_1 & m_1 & \mu_1 \end{pmatrix}, \\
& \int d^2 \hat{\mathbf{k}}_2 Y_{L'_1 M'_1 - \lambda_2}^* Y_{\ell_2 m_2 \lambda_2}^* Y_{2\mu_2}^* = I_{L'_1 \ell_2 2}^{0\lambda_2 - \lambda_2} \begin{pmatrix} L'_1 & \ell_2 & 2 \\ M'_1 & m_2 & \mu_2 \end{pmatrix}, \\
& \int d^2 \hat{\mathbf{k}}_3 Y_{L''_1 M''_1 - \lambda_3}^* Y_{\ell_3 m_3 \lambda_3}^* Y_{2\mu_3}^* = I_{L''_1 \ell_3 2}^{0\lambda_3 - \lambda_3} \begin{pmatrix} L''_1 & \ell_3 & 2 \\ M''_1 & m_3 & \mu_3 \end{pmatrix}.
\end{aligned} \tag{9.63}$$

At this point, all the angular integrals in Eq. (9.56) have been reduced into the Wigner-3j symbols.

As the third step, we consider summing up the Wigner-3j symbols in terms of the azimuthal quantum numbers and replacing them with the Wigner-6j and 9j symbols, which denote Clebsch-Gordan coefficients between two other eigenstates coupled to three and four individual momenta [27, 47–49]. Using these properties, we can express the summation of five Wigner-3j symbols with

a Wigner-9j symbol:

$$\begin{aligned}
& \sum_{\substack{M_1 M_2 M_3 \\ \mu_1 m_a m_b}} (-1)^{M_2+m_a} \begin{pmatrix} L_1 & L_2 & L_3 \\ M_1 & -M_2 & M_3 \end{pmatrix} \begin{pmatrix} 2 & 1 & 1 \\ \mu_1 & m_a & m_b \end{pmatrix} \\
& \quad \times \begin{pmatrix} L_3 & 1 & L'' \\ M_3 & m_b & M'' \end{pmatrix} \begin{pmatrix} L_2 & 1 & L \\ M_2 & -m_a & M \end{pmatrix} \begin{pmatrix} L_1 & \ell_1 & 2 \\ M_1 & m_1 & \mu_1 \end{pmatrix} \\
& = -(-1)^{M+\ell_1+L_3+L} \begin{pmatrix} L'' & L & \ell_1 \\ M'' & -M & m_1 \end{pmatrix} \left\{ \begin{matrix} L'' & L & \ell_1 \\ L_3 & L_2 & L_1 \\ 1 & 1 & 2 \end{matrix} \right\}, \\
& \sum_{\substack{M'_1 M'_2 M'_3 \\ \mu_2 m_c m_d}} (-1)^{M'_2+m_c} \begin{pmatrix} L'_1 & L'_2 & L'_3 \\ M'_1 & -M'_2 & M'_3 \end{pmatrix} \begin{pmatrix} 2 & 1 & 1 \\ \mu_2 & m_c & m_d \end{pmatrix} \\
& \quad \times \begin{pmatrix} L'_3 & 1 & L \\ M'_3 & m_d & M \end{pmatrix} \begin{pmatrix} L'_2 & 1 & L' \\ M'_2 & -m_c & M' \end{pmatrix} \begin{pmatrix} L'_1 & \ell_2 & 2 \\ M'_1 & m_2 & \mu_2 \end{pmatrix} \\
& = -(-1)^{M'+\ell_2+L'_3+L'} \begin{pmatrix} L & L' & \ell_2 \\ M & -M' & m_2 \end{pmatrix} \left\{ \begin{matrix} L & L' & \ell_2 \\ L'_3 & L'_2 & L'_1 \\ 1 & 1 & 2 \end{matrix} \right\}, \\
& \sum_{\substack{M''_1 M''_2 M''_3 \\ \mu_3 m_e m_f}} (-1)^{M''_2+m_e} \begin{pmatrix} L''_1 & L''_2 & L''_3 \\ M''_1 & -M''_2 & M''_3 \end{pmatrix} \begin{pmatrix} 2 & 1 & 1 \\ \mu_3 & m_e & m_f \end{pmatrix} \\
& \quad \times \begin{pmatrix} L''_3 & 1 & L' \\ M''_3 & m_f & M' \end{pmatrix} \begin{pmatrix} L''_2 & 1 & L'' \\ M''_2 & -m_e & M'' \end{pmatrix} \begin{pmatrix} L''_1 & \ell_3 & 2 \\ M''_1 & m_3 & \mu_3 \end{pmatrix} \\
& = -(-1)^{M''+\ell_3+L''_3+L''} \begin{pmatrix} L' & L'' & \ell_3 \\ M' & -M'' & m_3 \end{pmatrix} \left\{ \begin{matrix} L' & L'' & \ell_3 \\ L''_3 & L''_2 & L''_1 \\ 1 & 1 & 2 \end{matrix} \right\}.
\end{aligned} \tag{9.64}$$

Furthermore, we can also sum up the renewed Wigner-3j symbols arising in the above equations over M, M' and M'' with the Wigner-6j symbol as [50]

$$\begin{aligned}
& \sum_{MM'M''} (-1)^{M+M'+M''} \begin{pmatrix} L'' & L & \ell_1 \\ M'' & -M & m_1 \end{pmatrix} \begin{pmatrix} L & L' & \ell_2 \\ M & -M' & m_2 \end{pmatrix} \begin{pmatrix} L' & L'' & \ell_3 \\ M' & -M'' & m_3 \end{pmatrix} \\
& = (-1)^{L+L'+L''} \begin{pmatrix} \ell_1 & \ell_2 & \ell_3 \\ m_1 & m_2 & m_3 \end{pmatrix} \left\{ \begin{matrix} \ell_1 & \ell_2 & \ell_3 \\ L' & L'' & L \end{matrix} \right\}.
\end{aligned} \tag{9.65}$$

With this prescription, one can find that the three azimuthal numbers are confined only in the Wigner-3j symbol as $\begin{pmatrix} \ell_1 & \ell_2 & \ell_3 \\ m_1 & m_2 & m_3 \end{pmatrix}$. This 3j symbol arises from $\langle \prod_{n=1}^3 \xi_{\ell_n m_n}^{(\lambda_n)}(k_n) \rangle$ and exactly ensures the rotational invariance of the CMB bispectrum as pointed out above.

Consequently, we can obtain an exact form of the primordial angular bispectrum given by

$$\begin{aligned}
\left\langle \prod_{n=1}^3 \xi_{\ell_n m_n}^{(\lambda_n)}(k_n) \right\rangle & = \begin{pmatrix} \ell_1 & \ell_2 & \ell_3 \\ m_1 & m_2 & m_3 \end{pmatrix} (-4\pi\rho_{\gamma,0})^{-3} \left[\prod_{n=1}^3 \int_0^{k_D} k_n'^2 dk_n' P_B(k_n') \right] \\
& \quad \times \sum_{LL'L''} \sum_{S,S',S''=\pm 1} \left\{ \begin{matrix} \ell_1 & \ell_2 & \ell_3 \\ L' & L'' & L \end{matrix} \right\}
\end{aligned}$$

$$\times f_{L''L\ell_1}^{S''S\lambda_1}(k'_3, k'_1, k_1) f_{LL'\ell_2}^{SS'\lambda_2}(k'_1, k'_2, k_2) f_{L'L''\ell_3}^{S'S''\lambda_3}(k'_2, k'_3, k_3), \quad (9.66)$$

where

$$\begin{aligned} f_{L''L\ell}^{S''S\lambda}(r_3, r_2, r_1) &= \sum_{L_1 L_2 L_3} \int_0^\infty y^2 dy j_{L_3}(r_3 y) j_{L_2}(r_2 y) j_{L_1}(r_1 y) \\ &\times (-1)^{\ell+L_2+L_3} (-1)^{\frac{L_1+L_2+L_3}{2}} I_{L_1 L_2 L_3}^{000} I_{L_3 1 L''}^{0S''-S''} I_{L_2 1 L}^{0S-S} I_{L_1 \ell_2}^{0\lambda-\lambda} \begin{Bmatrix} L'' & L & \ell \\ L_3 & L_2 & L_1 \\ 1 & 1 & 2 \end{Bmatrix} \\ &\times \begin{cases} \frac{2}{\sqrt{3}}(8\pi)^{3/2} R_\gamma \ln(\tau_\nu/\tau_B) & (\lambda = 0) \\ \frac{2}{3}(8\pi)^{3/2} \lambda & (\lambda = \pm 1) \\ -4(8\pi)^{3/2} R_\gamma \ln(\tau_\nu/\tau_B) & (\lambda = \pm 2) \end{cases}. \end{aligned} \quad (9.67)$$

Here, the coefficients have been calculated as

$$C_{-\lambda} C'_{-\lambda} \sqrt{\frac{3}{8\pi}} \left(\frac{4\pi}{3}\right)^2 8 = \begin{cases} -\frac{2}{\sqrt{3}}(8\pi)^{3/2} R_\gamma \ln(\tau_\nu/\tau_B) & (\lambda = 0) \\ -\frac{2}{3}(8\pi)^{3/2} \lambda & (\lambda = \pm 1) \\ 4(8\pi)^{3/2} R_\gamma \ln(\tau_\nu/\tau_B) & (\lambda = \pm 2) \end{cases}. \quad (9.68)$$

Substituting Eq. (9.66) into Eq. (9.55), we can formulate the CMB bispectra generated from arbitrary three modes such as the scalar-scalar-vector and tensor-tensor-tensor correlations with the f function as

$$\begin{aligned} \left\langle \prod_{n=1}^3 a_{X_n, \ell_n m_n}^{(Z_n)} \right\rangle &= \begin{pmatrix} \ell_1 & \ell_2 & \ell_3 \\ m_1 & m_2 & m_3 \end{pmatrix} (-4\pi\rho_{\gamma,0})^{-3} \\ &\times \left[\prod_{n=1}^3 (-i)^{\ell_n} \int \frac{k_n^2 dk_n}{2\pi^2} \mathcal{T}_{X_n, \ell_n}^{(Z_n)}(k_n) \sum_{\lambda_n} [\text{sgn}(\lambda_n)]^{\lambda_n+x_n} \int_0^{k_D} k_n'^2 dk_n' P_B(k_n') \right] \\ &\times \sum_{LL'L''} \sum_{S,S',S''=\pm 1} \begin{Bmatrix} \ell_1 & \ell_2 & \ell_3 \\ L' & L'' & L \end{Bmatrix} \\ &\times f_{L''L\ell_1}^{S''S\lambda_1}(k'_3, k'_1, k_1) f_{LL'\ell_2}^{SS'\lambda_2}(k'_1, k'_2, k_2) f_{L'L''\ell_3}^{S'S''\lambda_3}(k'_2, k'_3, k_3). \end{aligned} \quad (9.69)$$

From this form, it can be easily seen that due to the sextuplicate dependence on the Gaussian PMFs, the Wigner-6j symbol connects the true multipoles (ℓ_1, ℓ_2 and ℓ_3) and the dummy ones (L, L' and L''), and the 1-loop calculation with respect to these multipoles is realized as illustrated in the left panel of Fig. 9.4. Due to the extra summations over L, L' and L'' , it takes a lot of time to compute this compared with the tree-level calculation presented in the previous sections.

9.3 Treatment for numerical computation

In order to perform the numerical computation of the CMB bispectra, we give the explicit angle-averaged form of Eq. (9.69) as

$$B_{X_1 X_2 X_3, \ell_1 \ell_2 \ell_3}^{(Z_1 Z_2 Z_3)} = C_{Z_1} C_{Z_2} C_{Z_3} (-4\pi\rho_{\gamma,0})^{-3} \sum_{LL'L''} \begin{Bmatrix} \ell_1 & \ell_2 & \ell_3 \\ L' & L'' & L \end{Bmatrix}$$

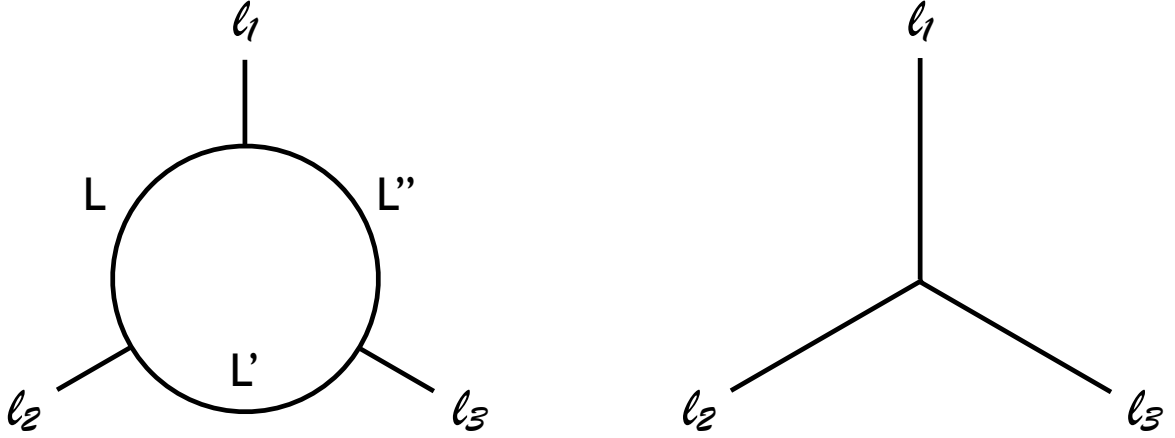


Figure 9.4: Diagrams with respect to multipoles [35]. The left panel corresponds to Eq. (9.69). Due to the Wigner-6j symbol originated with the sextuplicate dependence on the Gaussian PMFs, the true multipoles ℓ_1, ℓ_2 and ℓ_3 are linked with the dummy ones L, L' , and L'' and the 1-loop structure is realized. The right panel represents the tree-structure diagram, which arises from the CMB bispectrum induced by the four-point function of the Gaussian fields as mentioned in the previous sections.

$$\begin{aligned}
& \times \sum_{\substack{L_1 L_2 L_3 \\ L'_1 L'_2 L'_3 \\ L''_1 L''_2 L''_3}} (-1)^{\sum_{n=1}^3 \frac{L_n + L'_n + L''_n + 2\ell_n}{2}} I_{L_1 L_2 L_3}^{0 \ 0 \ 0} I_{L'_1 L'_2 L'_3}^{0 \ 0 \ 0} I_{L''_1 L''_2 L''_3}^{0 \ 0 \ 0} \\
& \times \left\{ \begin{matrix} L'' & L & \ell_1 \\ L_3 & L_2 & L_1 \\ 1 & 1 & 2 \end{matrix} \right\} \left\{ \begin{matrix} L & L' & \ell_2 \\ L'_3 & L'_2 & L'_1 \\ 1 & 1 & 2 \end{matrix} \right\} \left\{ \begin{matrix} L' & L'' & \ell_3 \\ L''_3 & L''_2 & L''_1 \\ 1 & 1 & 2 \end{matrix} \right\} \\
& \times \left[\prod_{n=1}^3 (-i)^{\ell_n} \int_0^\infty \frac{k_n^2 dk_n}{2\pi^2} \mathcal{T}_{X_n, \ell_n}^{(Z_n)}(k_n) \right] \\
& \times \int_0^\infty A^2 dA j_{L_1}(k_1 A) \int_0^\infty B^2 dB j_{L'_1}(k_2 B) \int_0^\infty C^2 dC j_{L''_1}(k_3 C) \\
& \times \int_0^{k_D} k_1'^2 dk_1' P_B(k_1') j_{L_2}(k_1' A) j_{L'_3}(k_1' B) \int_0^{k_D} k_2'^2 dk_2' P_B(k_2') j_{L'_2}(k_2' B) j_{L''_3}(k_2' C) \\
& \times \int_0^{k_D} k_3'^2 dk_3' P_B(k_3') j_{L''_2}(k_3' C) j_{L_3}(k_3' A) \\
& \times \sum_{S, S', S'' = \pm 1} (-1)^{L_2 + L'_2 + L''_2 + L_3 + L'_3 + L''_3} I_{L'_3 1 L}^{0S-S} I_{L_2 1 L}^{0S-S} I_{L''_3 1 L'}^{0S'-S'} I_{L'_2 1 L'}^{0S'-S'} I_{L_3 1 L''}^{0S''-S''} I_{L''_2 1 L''}^{0S''-S''} \\
& \times \sum_{\lambda_1 \lambda_2 \lambda_3} [\text{sgn}(\lambda_1)]^{x_1} I_{L_1 \ell_1 2}^{0\lambda_1 - \lambda_1} [\text{sgn}(\lambda_2)]^{x_2} I_{L'_1 \ell_2 2}^{0\lambda_2 - \lambda_2} [\text{sgn}(\lambda_3)]^{x_3} I_{L''_1 \ell_3 2}^{0\lambda_3 - \lambda_3}, \quad (9.70)
\end{aligned}$$

with

$$C_Z \equiv \begin{cases} \frac{2}{\sqrt{3}}(8\pi)^{3/2} R_\gamma \ln(\tau_\nu/\tau_B) & (Z = S) \\ \frac{2}{3}(8\pi)^{3/2} & (Z = V) \\ -4(8\pi)^{3/2} R_\gamma \ln(\tau_\nu/\tau_B) & (Z = T) \end{cases}. \quad (9.71)$$

We consider performing the summations with respect to the helicities. By considering the selection rules of the Wigner-3j symbol, the summations over S, S' and S'' are performed as

$$\begin{aligned} \sum_{S, S', S''=\pm 1} (-1)^{L_2+L'_2+L''_2+L_3+L'_3+L''_3} I_{L'_3 1 L}^{0S-S} I_{L_2 1 L}^{0S-S} I_{L''_3 1 L'}^{0S'-S'} I_{L'_2 1 L'}^{0S'-S'} I_{L_3 1 L''}^{0S''-S''} I_{L'_2 1 L''}^{0S''-S''} \\ = I_{L'_3 1 L}^{01-1} I_{L_2 1 L}^{01-1} I_{L''_3 1 L'}^{01-1} I_{L'_2 1 L'}^{01-1} I_{L_3 1 L''}^{01-1} I_{L'_2 1 L''}^{01-1} \\ \times \begin{cases} 8 & (L'_3 + L_2, L'_3 + L'_2, L_3 + L'_2 = \text{even}) \\ 0 & (\text{otherwise}) \end{cases} . \end{aligned} \quad (9.72)$$

By the same token, the summations over λ_1, λ_2 and λ_3 are given by

$$\begin{aligned} \sum_{\lambda_1 \lambda_2 \lambda_3} [\text{sgn}(\lambda_1)]^{x_1} I_{L_1 \ell_1 2}^{0\lambda_1-\lambda_1} [\text{sgn}(\lambda_2)]^{x_2} I_{L'_1 \ell'_2 2}^{0\lambda_2-\lambda_2} [\text{sgn}(\lambda_3)]^{x_3} I_{L''_1 \ell''_3 2}^{0\lambda_3-\lambda_3} \\ = I_{L_1 \ell_1 2}^{0|\lambda_1|-\lambda_1} I_{L'_1 \ell'_2 2}^{0|\lambda_2|-\lambda_2} I_{L''_1 \ell''_3 2}^{0|\lambda_3|-\lambda_3} \\ \times \begin{cases} 2^{3-N_S} & (L_1 + \ell_1 + x_1, L'_1 + \ell'_2 + x_2, L''_1 + \ell''_3 + x_3 = \text{even}) \\ 0 & (\text{otherwise}) \end{cases} , \end{aligned} \quad (9.73)$$

where N_S is the number of the scalar modes constituting the CMB bispectrum⁶. Thus, we rewrite the bispectrum as

$$\begin{aligned} B_{X_1 X_2 X_3, \ell_1 \ell_2 \ell_3}^{(Z_1 Z_2 Z_3)} &= C_{Z_1} C_{Z_2} C_{Z_3} (-4\pi \rho_{\gamma,0})^{-3} \sum_{LL'L''} \left\{ \begin{matrix} \ell_1 & \ell_2 & \ell_3 \\ L' & L'' & L \end{matrix} \right\} \\ &\times \sum_{\substack{L_1 L_2 L_3 \\ L'_1 L'_2 L'_3 \\ L''_1 L''_2 L''_3}} (-1)^{\sum_{n=1}^3 \frac{L_n + L'_n + L''_n + 2\ell_n}{2}} I_{L_1 L_2 L_3}^{000} I_{L'_1 L'_2 L'_3}^{000} I_{L''_1 L''_2 L''_3}^{000} \\ &\times \begin{Bmatrix} L'' & L & \ell_1 \\ L_3 & L_2 & L_1 \\ 1 & 1 & 2 \end{Bmatrix} \begin{Bmatrix} L & L' & \ell_2 \\ L'_3 & L'_2 & L'_1 \\ 1 & 1 & 2 \end{Bmatrix} \begin{Bmatrix} L' & L'' & \ell_3 \\ L''_3 & L''_2 & L''_1 \\ 1 & 1 & 2 \end{Bmatrix} \\ &\times \left[\prod_{n=1}^3 (-i)^{\ell_n} \int_0^\infty \frac{k_n^2 dk_n}{2\pi^2} \mathcal{T}_{X_n, \ell_n}^{(Z_n)}(k_n) \right] \\ &\times \int_0^\infty A^2 dA j_{L_1}(k_1 A) \int_0^\infty B^2 dB j_{L'_1}(k_2 B) \int_0^\infty C^2 dC j_{L''_1}(k_3 C) \\ &\times \int_0^{k_D} k_1'^2 dk_1' P_B(k_1') j_{L_2}(k_1' A) j_{L'_3}(k_1' B) \int_0^{k_D} k_2'^2 dk_2' P_B(k_2') j_{L'_2}(k_2' B) j_{L''_3}(k_2' C) \\ &\times \int_0^{k_D} k_3'^2 dk_3' P_B(k_3') j_{L''_2}(k_3' C) j_{L_3}(k_3' A) \\ &\times 8 I_{L'_3 1 L}^{01-1} I_{L_2 1 L}^{01-1} I_{L''_3 1 L'}^{01-1} I_{L'_2 1 L'}^{01-1} I_{L_3 1 L''}^{01-1} I_{L'_2 1 L''}^{01-1} \mathcal{Q}_{L'_3, L_2, L} \mathcal{Q}_{L'_3, L'_2, L'} \mathcal{Q}_{L_3, L'_2, L''} \\ &\times 2^{3-N_S} I_{L_1 \ell_1 2}^{0|\lambda_1|-\lambda_1} I_{L'_1 \ell'_2 2}^{0|\lambda_2|-\lambda_2} I_{L''_1 \ell''_3 2}^{0|\lambda_3|-\lambda_3} \mathcal{U}_{L_1, \ell_1, x_1} \mathcal{U}_{L'_1, \ell'_2, x_2} \mathcal{U}_{L''_1, \ell''_3, x_3} , \end{aligned} \quad (9.74)$$

where we introduce the filter functions as

$$\begin{aligned} \mathcal{Q}_{L'_3, L_2, L} &\equiv (\delta_{L'_3, L+1} + \delta_{L'_3, |L-1|})(\delta_{L_2, L+1} + \delta_{L_2, |L-1|}) + \delta_{L'_3, L} \delta_{L_2, L} \\ \mathcal{U}_{L_1, \ell_1, x_1} &\equiv (\delta_{L_1, \ell_1-2} + \delta_{L_1, \ell_1} + \delta_{L_1, \ell_1+2})\delta_{x_1, 0} + (\delta_{L_1, \ell_1-1} + \delta_{L_1, \ell_1+1})\delta_{x_1, 1} . \end{aligned} \quad (9.75)$$

⁶Caution about a fact that $|\lambda|$ is determined by Z , namely, $|\lambda| = 0, 1, 2$ for $Z = S, V, T$, respectively.

The above analytic expression seems to be quite useful to calculate the CMB bispectrum induced from PMFs with the full-angular dependence. However, it is still too hard to calculate numerically, because the full expression of the bispectrum has six integrals. In addition, when we calculate the spectra for large ℓ 's, this situation becomes worse since we spend a lot of time calculating the Wigner symbols for large ℓ 's. The CMB signals of the vector mode appear at $\ell > 2000$, hence we need the reasonable approximation in calculation of the CMB bispectra composed of the vector modes. In what follows, we introduce an approximation, the so-called thin last scattering surface (LSS) approximation to reduce the integrals.

9.3.1 Thin LSS approximation

Let us consider the parts of the integrals with respect to A, B, C, k', p' and q' in the full expression of the bispectrum (9.74) of $B_{III, \ell_1 \ell_2 \ell_3}^{(VVV)}$. In the computation of the CMB bispectrum, the integral in terms of k , (p and q) appears in the form as $\int k^2 dk \mathcal{T}_{I, \ell_1}^{(V)}(k) j_{L_1}(kA)$. We find that this integral is sharply-peaked at $A \simeq \tau_0 - \tau_*$, where τ_0 is the present conformal time and τ_* is the conformal time of the recombination epoch. According to Sec. 9.1.3, the vorticity of subhorizon scale sourced by magnetic fields around the recombination epoch mostly contributes to generate the CMB vector perturbation. On the other hand, since the vector mode in the metric decays after neutrino decoupling, the integrated Sachs-Wolfe effect after recombination is not observable. Such a behavior of the transfer function would be understood on the basis of the calculation in Sec. 9.1 and we expect $\mathcal{T}_{I, \ell_1}^{(V)}(k) \propto j_{\ell_1}(k(\tau_0 - \tau_*))$, and the k -integral behaves like $\delta(A - (\tau_0 - \tau_*))$. By the numerical computation, we found that

$$\int_0^\infty A^2 dA \int_0^\infty k_1^2 dk_1 \mathcal{T}_{I, \ell_1}^{(V)}(k_1) j_{L_1}(k_1 A) \simeq (\tau_0 - \tau_*)^2 \left(\frac{\tau_*}{5}\right) \int k_1^2 dk_1 \mathcal{T}_{I, \ell_1}^{(V)}(k_1) j_{\ell_1}(k_1(\tau_0 - \tau_*)), \quad (9.76)$$

is a good approximation for $L_1 = \ell_1 \pm 2, \ell_1$ as described in Fig. 9.5. Note that only the cases $L_1 = \ell_1 \pm 2, \ell_1$ should be considered due to the selection rules for Wigner-3j symbols as we shall see later. From this figure, we can find that the approximation (the right-handed term of Eq. (9.76)) has less than 20% uncertainty for $\ell_1 \simeq L_1 \gtrsim 100$, and therefore this approximation leads to only less than 10% uncertainty in the bound on the strength of PMFs if we place the constraint from the bispectrum data at $\ell_1, \ell_2, \ell_3 \gtrsim 100$ ⁷. Using this approximation, namely $A = B = C \rightarrow \tau_0 - \tau_*$ and $\int dA = \int dB = \int dC \rightarrow \tau_*/5$, the integrals with respect to A, B, C, k', p' and q' are estimated as

$$\begin{aligned} & \left[\prod_{n=1}^3 4\pi(-i)^{\ell_n} \int_0^\infty \frac{k_n^2 dk_n}{(2\pi)^3} \mathcal{T}_{I, \ell_n}^{(V)}(k_n) \right] \int_0^\infty A^2 dA j_{L_1}(k_1 A) \int_0^\infty B^2 dB j_{L'_1}(k_2 B) \int_0^\infty C^2 dC j_{L''_1}(k_3 C) \\ & \quad \times \int_0^{k_D} k_1'^2 dk_1' P_B(k_1') j_{L_2}(k_1' A) j_{L'_3}(k_1' B) \int_0^{k_D} k_2'^2 dk_2' P_B(k_2') j_{L'_2}(k_2' B) j_{L'_3}(k_2' C) \\ & \quad \times \int_0^{k_D} k_3'^2 dk_3' P_B(k_3') j_{L'_2}(k_3' C) j_{L'_3}(k_3' A) \\ & \simeq \left[\prod_{n=1}^3 4\pi(-i)^{\ell_n} \int_0^\infty \frac{k_n^2 dk_n}{(2\pi)^3} \mathcal{T}_{I, \ell_n}^{(V)}(k_n) j_{\ell_n}(k_n(\tau_0 - \tau_*)) \right] A_B^3(\tau_0 - \tau_*)^6 \left(\frac{\tau_*}{5}\right)^3 \\ & \quad \times \mathcal{K}_{L_2 L'_3}^{-(n_B+1)}(\tau_0 - \tau_*) \mathcal{K}_{L'_2 L''_3}^{-(n_B+1)}(\tau_0 - \tau_*) \mathcal{K}_{L'_2 L'_3}^{-(n_B+1)}(\tau_0 - \tau_*) . \end{aligned} \quad (9.77)$$

⁷Of course, if we calculate the bispectrum at smaller multipoles and the CMB bispectra are produced by other modes than the vector one, we may perform the full integration without this approximation.

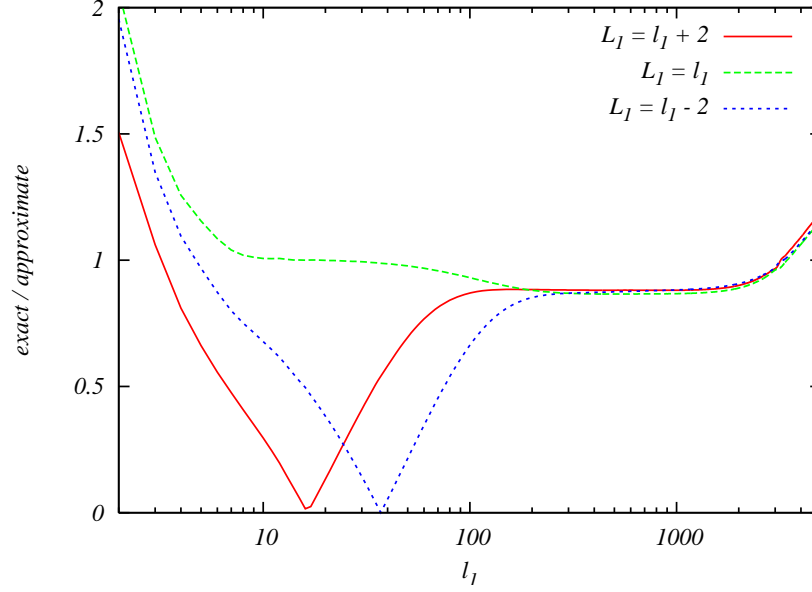


Figure 9.5: The ratio of the left-hand side (exact solution) to the right-hand side (approximate solution) in Eq. (9.76). The lines correspond to the case for $L_1 = \ell_1 + 2$ (red solid line), for $L_1 = \ell_1$ (green dashed one), and for $L_1 = \ell_1 - 2$ (blue dotted one).

Here the function $\mathcal{K}_{ll'}^N$ is defined as

$$\begin{aligned} \mathcal{K}_{ll'}^N(y) &\equiv \int_0^\infty dk k^{1-N} j_l(ky) j_{l'}(ky) \\ &= \frac{\pi}{2y} \frac{y^{N-1}}{2^N} \frac{\Gamma(N) \Gamma(\frac{l+l'+2-N}{2})}{\Gamma(\frac{l-l'+1+N}{2}) \Gamma(\frac{-l+l'+1+N}{2}) \Gamma(\frac{l+l'+2+N}{2})} \quad (\text{for } y, N, l+l'+2-N > 0), \end{aligned} \quad (9.78)$$

which behaves asymptotically as $\mathcal{K}_{ll'}^N(y) \propto l^{-N}$ for $l \sim l' \gg 1$. Here we have evaluated the k' integrals by setting $k_D \rightarrow \infty$. This is also a good approximation because the integrands are suppressed enough for $k', p', q' < k_D \sim \mathcal{O}(10) \text{Mpc}^{-1}$.

9.3.2 Selection rules of the Wigner-3j symbol

From the selection rules of the Wigner symbols as described in Appendix C, we can further limit the summation range of the multipoles as

$$\begin{aligned} |L - \ell_2| \leq L' \leq L + \ell_2, \quad \text{Max}[|L - \ell_1|, |L' - \ell_3|] \leq L'' \leq \text{Min}[L + \ell_1, L' + \ell_3], \\ L_1 + L_2 + L_3 = \text{even}, \quad L'_1 + L'_2 + L'_3 = \text{even}, \quad L''_1 + L''_2 + L''_3 = \text{even}, \\ |L_1 - L_2| \leq L_3 \leq L_1 + L_2, \quad |L'_1 - L'_2| \leq L'_3 \leq L'_1 + L'_2, \quad |L''_1 - L''_2| \leq L''_3 \leq L''_1 + L''_2, \end{aligned} \quad (9.79)$$

and from the above restrictions the multipoles in the bispectrum, ℓ_1, ℓ_2 and ℓ_3 , are also limited as

$$|\ell_1 - \ell_2| \leq \ell_3 \leq \ell_1 + \ell_2. \quad (9.80)$$

Therefore, these selection rules significantly reduce the number of calculation. In these ranges, while L' and L'' are limited by L , only L has no upper bound. However, we can show that the

summation of L is suppressed at $\ell_1 \sim \ell_2 \sim \ell_3 \ll L$ as follows. When the summations with respect to L, L' and L'' are evaluated at large L, L' and L'' , namely $\ell_1, \ell_2, \ell_3 \ll L \sim L' \sim L'', L_2 \sim L'_3 \sim L, L'_2 \sim L''_3 \sim L'$ and $L''_2 \sim L_3 \sim L''$, we get

$$\begin{aligned}
& \sum_{LL'L''} \left\{ \begin{matrix} \ell_1 & \ell_2 & \ell_3 \\ L' & L'' & L \end{matrix} \right\} \sum_{\substack{L_2 L'_2 L''_2 \\ L'_3 L''_3 L_3}} \int_0^{k_D} k_1'^2 dk_1' P_B(k_1') j_{L_2}(k_1' A) j_{L'_3}(k_1' B) \\
& \times \int_0^{k_D} k_2'^2 dk_2' P_B(k_2') j_{L'_2}(k_2' B) j_{L''_3}(k_2' C) \int_0^{k_D} k_3'^2 dk_3' P_B(k_3') j_{L''_2}(k_3' C) j_{L_3}(k_3' A) \\
& \times (-1)^{\sum_{i=1}^3 \frac{L_i + L'_i + L''_i}{2}} I_{L_1 L_2 L_3}^{0 \ 0 \ 0} I_{L'_1 L'_2 L'_3}^{0 \ 0 \ 0} I_{L''_1 L''_2 L''_3}^{0 \ 0 \ 0} I_{L'_3 1 L}^{01-1} I_{L_2 1 L}^{01-1} I_{L''_3 1 L'}^{01-1} I_{L'_2 1 L'}^{01-1} I_{L_3 1 L''}^{01-1} I_{L''_2 1 L''}^{01-1} \\
& \times \left\{ \begin{matrix} L'' & L & \ell_1 \\ L_3 & L_2 & L_1 \\ 1 & 1 & 2 \end{matrix} \right\} \left\{ \begin{matrix} L & L' & \ell_2 \\ L'_3 & L'_2 & L'_1 \\ 1 & 1 & 2 \end{matrix} \right\} \left\{ \begin{matrix} L' & L'' & \ell_3 \\ L''_3 & L''_2 & L''_1 \\ 1 & 1 & 2 \end{matrix} \right\} \\
& \propto \sum_{LL'L''} (LL'L'')^{n_B+4/3} . \tag{9.81}
\end{aligned}$$

Therefore, we may obtain a stable result with the summations over a limited number of L when we consider the magnetic power spectrum is as red as $n_B \sim -2.9$, because the summations of L' and L'' are limited by L . Here, we use the analytic formulas of the I symbols which are given by

$$\left\{ \begin{matrix} \ell_1 & \ell_2 & \ell_3 \\ L' & L'' & L \end{matrix} \right\} \propto (LL'L'')^{-1/6} , \quad \mathcal{K}_{L_2 L'_3}^{-(n_B+1)} \propto L^{n_B+1} , \quad \left\{ \begin{matrix} L'' & L & \ell_1 \\ L_3 & L_2 & L_1 \\ 1 & 1 & 2 \end{matrix} \right\} \propto (L''L)^{-1/2} , \tag{9.82}$$

as described in detail in Appendix C.

Using the thin LSS approximation and the summation rules described above, we can perform the computation of the CMB bispectrum containing full-angular dependence in a reasonable time.

9.4 Shape of the non-Gaussianity

In this subsection, in order to understand the shape of the non-Gaussianities arising from PMFs, we reduce the bispectra of the PMF anisotropic stress by the pole approximation [35].

Let us focus on the structure of the bispectrum of the PMF anisotropic stresses (9.54). If the magnetic spectrum is enough red as $n_B \sim -3$, the integral over the wave number vectors is almost determined by the behavior of the integrand around at three poles as $k'_1, k'_2, k'_3 \sim 0$. Considering the effects around at these poles, we can express the bispectrum of the PMF anisotropic stresses approximately as

$$\begin{aligned}
& \langle \Pi_{Bab}(\mathbf{k}_1) \Pi_{Bcd}(\mathbf{k}_2) \Pi_{Bef}(\mathbf{k}_3) \rangle \sim (-4\pi\rho_{\gamma,0})^{-3} \frac{\alpha A_B}{n_B+3} k_*^{n_B+3} \frac{8\pi}{3} \delta \left(\sum_{n=1}^3 \mathbf{k}_n \right) \\
& \times \frac{1}{8} \left[P_B(k_1) P_B(k_2) \delta_{ad} P_{be}(\hat{\mathbf{k}}_1) P_{cf}(\hat{\mathbf{k}}_2) + P_B(k_2) P_B(k_3) P_{ad}(\hat{\mathbf{k}}_2) P_{be}(\hat{\mathbf{k}}_3) \delta_{cf} \right. \\
& \left. + P_B(k_1) P_B(k_3) P_{ad}(\hat{\mathbf{k}}_1) \delta_{be} P_{cf}(\hat{\mathbf{k}}_3) + \{a \leftrightarrow b \text{ or } c \leftrightarrow d \text{ or } e \leftrightarrow f\} \right] , \tag{9.83}
\end{aligned}$$

where we evaluate as

$$\int d^3 \mathbf{k}' P_B(k') P_{ab}(\hat{\mathbf{k}}') \sim \alpha \int_0^{k_*} k'^2 dk' P_B(k') \int d^2 \hat{\mathbf{k}}' P_{ab}(\hat{\mathbf{k}}') = \frac{\alpha A_B}{n_B+3} k_*^{n_B+3} \frac{8\pi}{3} \delta_{ab} . \tag{9.84}$$

Note that α is an unknown parameter and should be determined by the comparison with the exact bispectra [(9.69) or (9.74)], and we take $k_* = 10\text{Mpc}^{-1}$.

Under this approximation, the angular bispectrum of the primordial tensor perturbations ($\lambda_1, \lambda_2, \lambda_3 = \pm 2$) is given by

$$\begin{aligned} \left\langle \prod_{n=1}^3 \xi_{\ell_n m_n}^{(\lambda_n)}(k_n) \right\rangle &\sim \left[\prod_{n=1}^3 \int d^2 \hat{\mathbf{k}}_{\mathbf{n}-\lambda_n} Y_{\ell_n m_n}^*(\hat{\mathbf{k}}_{\mathbf{n}}) \right] \left[\frac{R_\gamma \ln(\tau_\nu/\tau_B)}{4\pi\rho_{\gamma,0}} \right]^3 \frac{\alpha A_B}{n_B + 3} k_*^{n_B+3} \frac{8\pi}{3} \delta \left(\sum_{n=1}^3 \mathbf{k}_n \right) \\ &\times \left[P_B(k_1)P_B(k_2)\delta_{ad}P_{be}(\hat{\mathbf{k}}_1)P_{cf}(\hat{\mathbf{k}}_2) + P_B(k_2)P_B(k_3)P_{ad}(\hat{\mathbf{k}}_2)P_{be}(\hat{\mathbf{k}}_3)\delta_{cf} \right. \\ &\quad \left. + P_B(k_1)P_B(k_3)P_{ad}(\hat{\mathbf{k}}_1)\delta_{be}P_{cf}(\hat{\mathbf{k}}_3) \right] \\ &\times (-27)e_{ab}^{(-\lambda_1)}(\hat{\mathbf{k}}_1)e_{cd}^{(-\lambda_2)}(\hat{\mathbf{k}}_2)e_{ef}^{(-\lambda_3)}(\hat{\mathbf{k}}_3). \end{aligned} \quad (9.85)$$

Using Eq. (D.23), we reduce the contraction of the subscripts in the TTT spectrum to

$$\begin{aligned} &O_{ab}^{(-\lambda_1)}(\hat{\mathbf{k}}_1)O_{cd}^{(-\lambda_2)}(\hat{\mathbf{k}}_2)O_{ef}^{(-\lambda_3)}(\hat{\mathbf{k}}_3) \left[P_B(k_1)P_B(k_2)\delta_{ad}P_{be}(\hat{\mathbf{k}}_1)P_{cf}(\hat{\mathbf{k}}_2) \right. \\ &\quad \left. + P_B(k_2)P_B(k_3)P_{ad}(\hat{\mathbf{k}}_2)P_{be}(\hat{\mathbf{k}}_3)\delta_{cf} + P_B(k_1)P_B(k_3)P_{ad}(\hat{\mathbf{k}}_1)\delta_{be}P_{cf}(\hat{\mathbf{k}}_3) \right] \\ &= e_{ae}^{(-\lambda_1)}(\hat{\mathbf{k}}_1)e_{ef}^{(-\lambda_3)}(\hat{\mathbf{k}}_3)e_{fa}^{(-\lambda_2)}(\hat{\mathbf{k}}_2)[P_B(k_1)P_B(k_2) + 2 \text{ perms.}] \\ &= -\frac{(8\pi)^{5/2}}{3} I_{211}^{01-1} I_{211}^{01-1} \left\{ \begin{matrix} 2 & 2 & 2 \\ 1 & 1 & 1 \end{matrix} \right\} [P_B(k_1)P_B(k_2) + 2 \text{ perms.}] \\ &\times \sum_{M, M', M''} \lambda_1 Y_{2M}^*(\hat{\mathbf{k}}_1) \lambda_2 Y_{2M'}^*(\hat{\mathbf{k}}_2) \lambda_3 Y_{2M''}^*(\hat{\mathbf{k}}_3) \left(\begin{matrix} 2 & 2 & 2 \\ M & M' & M'' \end{matrix} \right). \end{aligned} \quad (9.86)$$

The delta function is also expanded with the spin spherical harmonics as Eq. (6.14)

$$\begin{aligned} \delta \left(\sum_{i=1}^3 \mathbf{k}_i \right) &= 8 \int_0^\infty y^2 dy \left[\prod_{i=1}^3 \sum_{L_i M_i} (-1)^{L_i/2} j_{L_i}(k_i y) Y_{L_i M_i}^*(\hat{\mathbf{k}}_i) \right] \\ &\times I_{L_1 L_2 L_3}^0 \left(\begin{matrix} L_1 & L_2 & L_3 \\ M_1 & M_2 & M_3 \end{matrix} \right). \end{aligned} \quad (9.87)$$

Then, the angular integrals are performed as

$$\begin{aligned} \int d^2 \hat{\mathbf{k}}_{1-\lambda_1} Y_{\ell_1 m_1}^* Y_{L_1 M_1 \lambda_1}^* Y_{2M}^* &= I_{\ell_1 L_1 2}^{\lambda_1 0 - \lambda_1} \left(\begin{matrix} \ell_1 & L_1 & 2 \\ m_1 & M_1 & M \end{matrix} \right), \\ \int d^2 \hat{\mathbf{k}}_{2-\lambda_2} Y_{\ell_2 m_2}^* Y_{L_2 M_2 \lambda_2}^* Y_{2M'}^* &= I_{\ell_2 L_2 2}^{\lambda_2 0 - \lambda_2} \left(\begin{matrix} \ell_2 & L_2 & 2 \\ m_2 & M_2 & M' \end{matrix} \right), \\ \int d^2 \hat{\mathbf{k}}_{3-\lambda_3} Y_{\ell_3 m_3}^* Y_{L_3 M_3 \lambda_3}^* Y_{2M''}^* &= I_{\ell_3 L_3 2}^{\lambda_3 0 - \lambda_3} \left(\begin{matrix} \ell_3 & L_3 & 2 \\ m_3 & M_3 & M'' \end{matrix} \right), \end{aligned} \quad (9.88)$$

and all the Wigner-3j symbols are summed up as

$$\begin{aligned} &\sum_{\substack{M_1 M_2 M_3 \\ M M' M''}} \left(\begin{matrix} L_1 & L_2 & L_3 \\ M_1 & M_2 & M_3 \end{matrix} \right) \left(\begin{matrix} 2 & 2 & 2 \\ M & M' & M'' \end{matrix} \right) \\ &\times \left(\begin{matrix} \ell_1 & L_1 & 2 \\ m_1 & M_1 & M \end{matrix} \right) \left(\begin{matrix} \ell_2 & L_2 & 2 \\ m_2 & M_2 & M' \end{matrix} \right) \left(\begin{matrix} \ell_3 & L_3 & 2 \\ m_3 & M_3 & M'' \end{matrix} \right) \end{aligned}$$

$$= \begin{pmatrix} \ell_1 & \ell_2 & \ell_3 \\ m_1 & m_2 & m_3 \end{pmatrix} \begin{Bmatrix} \ell_1 & \ell_2 & \ell_3 \\ L_1 & L_2 & L_3 \\ 2 & 2 & 2 \end{Bmatrix}. \quad (9.89)$$

Thus the initial bispectrum (9.85) is rewritten as

$$\begin{aligned} \left\langle \prod_{n=1}^3 \xi_{\ell_n m_n}^{(\lambda_n)}(k_n) \right\rangle &\sim \begin{pmatrix} \ell_1 & \ell_2 & \ell_3 \\ m_1 & m_2 & m_3 \end{pmatrix} \left[\frac{R_\gamma \ln(\tau_\nu/\tau_B)}{4\pi\rho_{\gamma,0}} \right]^3 \frac{\alpha A_B}{n_B + 3} k_*^{n_B+3} \frac{8\pi}{3} \\ &\times 8 \int_0^\infty y^2 dy \left[\prod_{n=1}^3 \sum_{L_n} (-1)^{L_n/2} j_{L_n}(k_n y) \right] I_{L_1 L_2 L_3}^{0 \ 0 \ 0} \\ &\times \begin{Bmatrix} 2 & 2 & 2 \\ 1 & 1 & 1 \end{Bmatrix} I_{211}^{01-1} I_{211}^{01-1} I_{\ell_1 L_1 2}^{\lambda_1 0 - \lambda_1} I_{\ell_2 L_2 2}^{\lambda_2 0 - \lambda_2} I_{\ell_3 L_3 2}^{\lambda_3 0 - \lambda_3} \begin{Bmatrix} \ell_1 & \ell_2 & \ell_3 \\ L_1 & L_2 & L_3 \\ 2 & 2 & 2 \end{Bmatrix} \\ &\times 9(8\pi)^{5/2} [P_B(k_1)P_B(k_2) + 2\text{perms.}] . \end{aligned} \quad (9.90)$$

Comparing the exact initial bispectrum of the tensor modes (9.66) with this equation, we can see that the number of the time-integrals and summations in terms of the multipoles decreases. This means that corresponding to the pole approximation, the 1-loop calculation (the left panel of Fig. 9.4) reaches the tree-level one (the right one of that figure). This approximation seems to be applicable to the non-Gaussianity generated from the chi-squared fields without the complicated angular dependence [51]. Note that the scaling behaviors of these initial bispectra with respect to k_1, k_2 and k_3 are in agreement with that of the local-type non-Gaussianity (4.7). Thus, if the pole approximation is valid, we can expect that the PMFs generate the CMB bispectra coming from the local-type non-Gaussianity. Via the summation over λ_1, λ_2 and λ_3 as Eq. (9.73), the approximate CMB bispectra of the tensor modes are quickly formulated:

$$\begin{aligned} B_{X_1 X_2 X_3, \ell_1 \ell_2 \ell_3}^{\text{app}(TTT)}(\alpha) &= \left[\frac{R_\gamma \ln(\tau_\nu/\tau_B)}{4\pi\rho_{\gamma,0}} \right]^3 \frac{\alpha A_B}{n_B + 3} k_*^{n_B+3} \frac{8\pi}{3} \sum_{L_1 L_2 L_3} (-1)^{\frac{L_1+L_2+L_3}{2}} I_{L_1 L_2 L_3}^{0 \ 0 \ 0} \\ &\times \begin{Bmatrix} 2 & 2 & 2 \\ 1 & 1 & 1 \end{Bmatrix} I_{211}^{01-1} I_{211}^{01-1} \begin{Bmatrix} \ell_1 & \ell_2 & \ell_3 \\ L_1 & L_2 & L_3 \\ 2 & 2 & 2 \end{Bmatrix} \\ &\times 8 I_{\ell_1 L_1 2}^{20-2} I_{\ell_2 L_2 2}^{20-2} I_{\ell_3 L_3 2}^{20-2} \mathcal{U}_{L_1, \ell_1, x_1} \mathcal{U}_{L_2, \ell_2, x_2} \mathcal{U}_{L_3, \ell_3, x_3} \\ &\times 8 \int_0^\infty y^2 dy \left[\prod_{n=1}^3 (-i)^{\ell_n} \int_0^\infty \frac{k_n^2 dk_n}{2\pi^2} \mathcal{T}_{X_n, \ell_n}^{(T)}(k_n) j_{L_n}(k_n y) \right] \\ &\times 9(8\pi)^{5/2} [P_B(k_1)P_B(k_2) + 2\text{perms.}] , \end{aligned} \quad (9.91)$$

where the multipoles are limited as

$$\sum_{n=1}^3 L_n = \text{even} , \quad |L_1 - L_2| \leq L_3 \leq L_1 + L_2 , \quad (9.92)$$

and the triangle inequality imposes

$$|\ell_1 - \ell_2| \leq \ell_3 \leq \ell_1 + \ell_2 . \quad (9.93)$$

In the next subsection, we compare these approximate spectra with the exact spectra given by Eq. (9.74) and evaluate the validity of the pole approximation.

9.5 Analysis

In this subsection, we show the result of the CMB intensity-intensity-intensity spectra induced from the auto-correlations of the each-mode anisotropic stress. In order to compute numerically, we insert Eq. (9.74) into the Boltzmann code for anisotropies in the microwave background (CAMB) [15, 52]. We use the transfer functions shown in Sec. 9.1. In the calculation of the Wigner- $3j$, $6j$ and $9j$ symbols, we use a common mathematical library called SLATEC [53] and analytical expressions in Appendix C.

In Fig. 9.6, we plot the CMB reduced bispectra of these modes defined as [54]

$$b_{III,\ell_1\ell_2\ell_3}^{(Z_1Z_2Z_3)} \equiv (I_{\ell_1\ell_2\ell_3}^0)^{-1} B_{III,\ell_1\ell_2\ell_3}^{(Z_1Z_2Z_3)}, \quad (9.94)$$

for $\ell_1 = \ell_2 = \ell_3$. Here, for comparison, we also write the bispectrum generated from the local-type primordial non-Gaussianities of curvature perturbations given by Eq. (4.7).

From the red solid lines, we can find the enhancement at $\ell \lesssim 100$ in tensor-tensor-tensor bispectra. It is because the ISW effect gives the dominant signal like in the CMB anisotropies of tensor modes [17, 55]. From the green dashed line, one can see that the peak of the vector-vector-vector bispectrum is located at $\ell \sim 2000$ and the position is similar to that of the angular power spectrum $C_{I,\ell}^{(V)}$ induced from the vector mode as calculated in Sec. 9.1. At small scales, the vector mode contributes to the CMB power spectrum through the Doppler effect. Thus, we can easily find that the Doppler effect can also enhance the CMB bispectrum on small scale. From the blue dotted lines, we can see that the scalar-scalar-scalar bispectra are boosted around at $\ell \sim 200$ due to the acoustic oscillation of the fluid of photons and baryons. On the other hand, as ℓ enlarges, the spectra are suppressed by the Silk damping effect. These features are also observed in the non-magnetic case (the magenta dot-dashed line), however, owing to the difference of the angular dependence on the wave number vectors in the source bispectra, the location of the nodes slightly differs. Comparing the behaviors between the three spectra arising from PMFs, we confirm that the tensor, scalar and vector modes become effective for $\ell \lesssim 100$, $100 \lesssim \ell \lesssim 2000$ and $\ell \gtrsim 2000$, respectively, like the behaviors seen in the power spectra. Thus, for $\ell < 1000$, namely the current instrumental limit of the angular resolution such as the PLANK experiment [30], we expect that the auto- and cross-correlations between the scalar and tensor modes will be primary signals of PMFs in the CMB bispectrum.

The overall amplitudes of $b_{III,\ell\ell\ell}^{(SSS)}$ and $b_{III,\ell\ell\ell}^{(TTT)}$ seem to be comparable to $[C_{II,\ell}^{(S)}]^{3/2}$ and $[C_{II,\ell}^{(T)}]^{3/2}$. However, we find that the amplitude of $b_{III,\ell\ell\ell}^{(VVV)}$ is smaller than the above expectation. This is because the configuration of multipoles, corresponding to the angles of wave number vectors, is limited to the conditions placed by the Wigner symbols. We can understand this by considering the scaling relation with respect to ℓ at high ℓ . If the magnetic power spectrum given by Eq. (9.4) is close to the scale-invariant shape, the configuration that satisfies $L \sim L'' \sim \ell$ and $L' \sim 1$ contributes dominantly in the summations. Furthermore, the other multipoles are evaluated as

$$L_1 \sim L'_1 \sim L''_1 \sim \ell, \quad L_2 \sim L''_2 \sim L_3 \sim L'_3 \sim \ell, \quad L'_2 \sim L''_3 \sim 1, \quad (9.95)$$

from the triangle conditions described in Appendix C. Then we can find $b_{III,\ell\ell\ell}^{(VVV)} \propto \ell^{2n_B+4}$ for

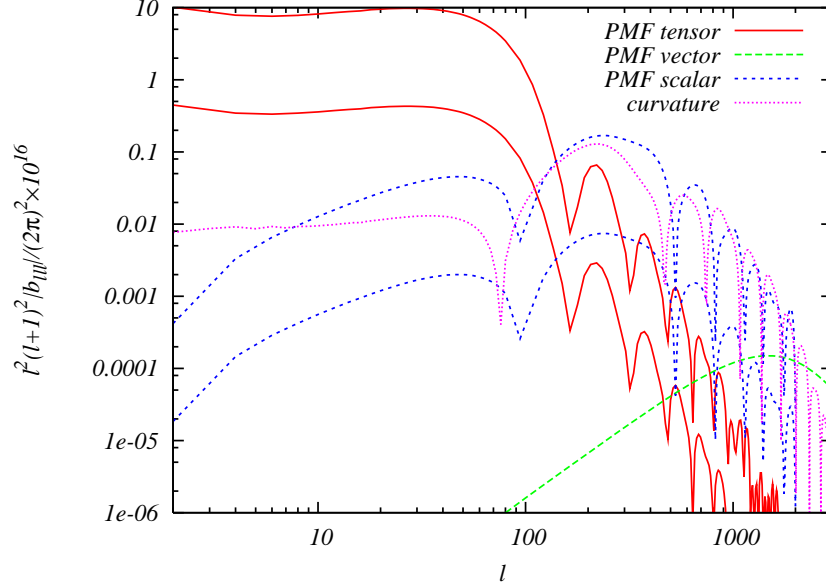


Figure 9.6: Absolute values of the normalized reduced bispectra of temperature fluctuations for a configuration $\ell_1 = \ell_2 = \ell_3 \equiv \ell$. The red solid, green dashed, and blue dotted lines correspond to the spectra generated from the auto-correlations of the PMF tensor, vector, and scalar anisotropic stresses for $n_B = -2.9$, respectively. The upper (lower) lines of the red solid and blue dotted lines are calculated when $\tau_\nu/\tau_B = 10^{17}(10^6)$. The magenta dot-dashed line expresses the spectrum sourced from the primordial non-Gaussianity with $f_{\text{NL}}^{\text{local}} = 5$. The strength of PMFs is fixed to $B_{1\text{Mpc}} = 4.7\text{nG}$ and the other cosmological parameters are fixed to the mean values limited from WMAP-7yr data reported in Ref. [29].

$\ell \lesssim 1000$, where we have also used the following relations

$$\begin{aligned} \int k^2 dk \mathcal{T}_{I,\ell_i}^{(V)}(k) j_{\ell_i}(k(\tau_0 - \tau_*)) &\propto \ell, \quad \left\{ \begin{matrix} \ell_1 & \ell_2 & \ell_3 \\ L' & L'' & L \end{matrix} \right\} \propto \ell^{-1}, \quad \mathcal{K}_{L_2 L'_3}^{-(n_B+1)} \sim \mathcal{K}_{L'_2 L_3}^{-(n_B+1)} \propto \ell^{n_B+1}, \\ \left\{ \begin{matrix} L'' & L & \ell_1 \\ L_3 & L_2 & L_1 \\ 1 & 1 & 2 \end{matrix} \right\} &\propto \ell^{-3/2}, \quad \left\{ \begin{matrix} L & L' & \ell_1 \\ L'_3 & L'_2 & L'_1 \\ 1 & 1 & 2 \end{matrix} \right\} \sim \left\{ \begin{matrix} L' & L'' & \ell_1 \\ L''_3 & L''_2 & L''_1 \\ 1 & 1 & 2 \end{matrix} \right\} \propto \ell^{-1}, \end{aligned} \quad (9.96)$$

which, except for the first relation, are also coming from the triangle conditions of the Wigner 3-j symbols. Therefore, combining with the scaling relation of the CMB power spectrum mentioned in Sec. 9.1, we find that $b_{III,\ell\ell\ell}^{(VVV)}$ is suppressed by a factor $\ell^{(n_B-1)/2}$ from $C_{II,\ell}^{(V)3/2}$.

In Fig. 9.7, we show $b_{III,\ell\ell\ell}^{(VVV)}$ for $\ell_1 = \ell_2 = \ell_3$ for the different spectral index n_B . Red solid and green dashed lines correspond to the bispectrum with the spectral index of the power spectrum of PMFs fixed as $n_B = -2.9$ and -2.8 , respectively. From this figure, we find that the CMB bispectrum becomes steeper if n_B becomes larger, which is similar to the case of the power spectrum. These spectra trace the scaling relation in the above discussion. These will lead to another constraint on the strength of PMFs.

In Figs. 9.8 and 9.9, we show the reduced bispectrum $b_{III,\ell_1\ell_2\ell_3}^{(VVV)}$ and $b_{III,\ell_1\ell_2\ell_3}^{(TTT)}$ with respect to ℓ_3 with setting $\ell_1 = \ell_2$, respectively. From Fig. 9.8, we can see that $b_{III,\ell_1\ell_2\ell_3}^{(VVV)}$ for $\ell_1, \ell_2, \ell_3 \gtrsim 100$ is

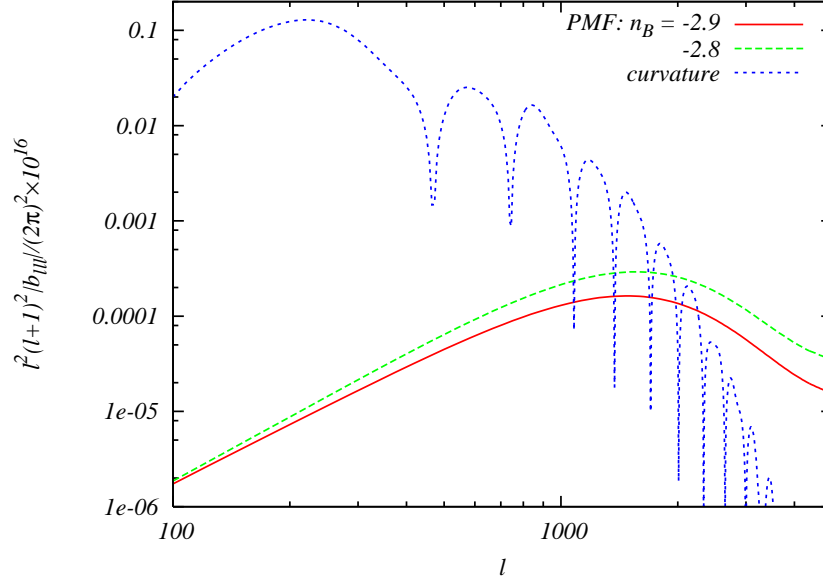


Figure 9.7: Absolute values of the normalized reduced temperature-temperature-temperature spectra arising from the auto-correlation between the PMF vector anisotropic stresses for a configuration $\ell_1 = \ell_2 = \ell_3 \equiv \ell$. The lines correspond to the spectra generated from vector anisotropic stress for $n_B = -2.9$ (red solid line) and -2.8 (green dashed line), and primordial non-Gaussianity with $f_{\text{NL}}^{\text{local}} = 5$ (blue dotted line). The strength of PMFs is fixed to $B_{1\text{Mpc}} = 4.7\text{nG}$ and the other cosmological parameters are identical to the values used in Fig. 9.6.

nearly flat and given as

$$\ell_1(\ell_1 + 1)\ell_3(\ell_3 + 1)|b_{III,\ell_1\ell_2\ell_3}^{(VVV)}| \sim 2 \times 10^{-19} \left(\frac{B_{1\text{Mpc}}}{4.7\text{nG}} \right)^6. \quad (9.97)$$

We can understand this by the analytical evaluation as follows. As mentioned above, in the summations of Eq. (9.74), the configuration that $L \sim \ell_1, L' \sim 1$ and $L'' \sim \ell_3$ contributes dominantly. By using this and the approximations that

$$L_1 \sim \ell_1, \quad L'_1 \sim \ell_2, \quad L''_1 \sim \ell_3, \quad L_2 \sim L'_3 \sim L, \quad L'_2 \sim L''_3 \sim L', \quad L''_2 \sim L_3 \sim L'', \quad (9.98)$$

which again come from the triangle conditions from the Wigner symbols, the scaling relation of ℓ_3 at large scale is evaluated as $b_{III,\ell_1\ell_2\ell_3}^{(VVV)} \propto \ell_3^{n_B+1}$. From this estimation we can find that $\ell_1(\ell_1 + 1)\ell_3(\ell_3 + 1)b_{III,\ell_1\ell_2\ell_3}^{(VVV)} \propto \ell_3^{0.1}$, for $n_B = -2.9$, and $\ell_3^{0.2}$ for $n_B = -2.8$, respectively, which match the behaviors of the bispectra in Fig. 9.8.

From Fig. 9.9, we can also see that if the PMF spectrum obeys the nearly scale-invariant shape, $b_{III,\ell_1\ell_2\ell_3}^{(TTT)}$ for $\ell_1, \ell_2, \ell_3 \lesssim 100$ is given by

$$\ell_1(\ell_1 + 1)\ell_3(\ell_3 + 1)|b_{III,\ell_1\ell_2\ell_3}^{(TTT)}| \sim (130 - 6) \times 10^{-16} \left(\frac{B_{1\text{Mpc}}}{4.7\text{nG}} \right)^6, \quad (9.99)$$

where the factor 130 corresponds to the $\tau_\nu/\tau_B = 10^{17}$ case and 6 corresponds to 10^6 . In order to obtain a rough constraint on the magnitude of the PMF, we compare the bispectrum induced from

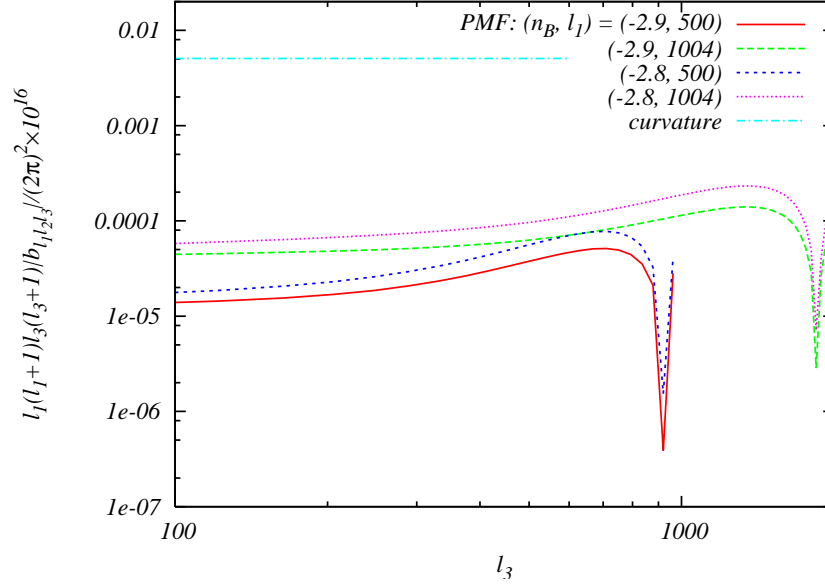


Figure 9.8: Absolute values of the normalized reduced temperature-temperature-temperature bispectra induced by the auto-correlation between the PMF vector anisotropic stresses and generated by primordial non-Gaussianity given by Eq. (9.100) as a function of ℓ_3 with ℓ_1 and ℓ_2 fixed to some value as indicated. Each parameter is fixed to the same value defined in Fig. 9.6.

the PMF with that from the local-type primordial non-Gaussianity in the curvature perturbations, which is typically estimated as [56]

$$\ell_1(\ell_1 + 1)\ell_3(\ell_3 + 1)b_{\ell_1 \ell_2 \ell_3} \sim 4 \times 10^{-18} f_{\text{NL}}^{\text{local}}. \quad (9.100)$$

By comparing this with Eq. (9.99), the relation between the magnitudes of the PMF with the nearly scale-invariant power spectrum and $f_{\text{NL}}^{\text{local}}$ is derived as

$$\left(\frac{B_{\text{1Mpc}}}{\text{1nG}} \right) \sim (1.22 - 2.04) |f_{\text{NL}}^{\text{local}}|^{1/6}. \quad (9.101)$$

Using the above equation, we can obtain the rough bound on the PMF strength. As shown in Fig. 9.6, because the tensor bispectrum is highly damped for $\ell \gtrsim 100$, we should use an upper bound on $f_{\text{NL}}^{\text{local}}$ obtained by the current observational data for $\ell < 100$, namely $f_{\text{NL}}^{\text{local}} < 100$ [57]. This value is consistent with a simple prediction from the cosmic variance [54]. From this value, we derive $B_{\text{1Mpc}} < 2.6 - 4.4 \text{nG}$.

From here, let us discuss the validity and possibility of the CMB bispectra under the pole approximation (9.91). Figure 9.10 shows the shapes of the CMB tensor-tensor-tensor spectra based on the exact form (9.74) and approximate one (9.91). Both spectra seem to have a good agreement in the shape of the ℓ space. To discuss more precisely, using the correlation

$$b \cdot b' \propto \sum_{\ell} b_{\ell\ell\ell} b'_{\ell\ell\ell}, \quad (9.102)$$

we calculate a correlation coefficient as

$$\frac{b^{\text{ex}} \cdot b^{\text{app}}}{\sqrt{(b^{\text{ex}} \cdot b^{\text{ex}})(b^{\text{app}} \cdot b^{\text{app}})}} = 0.99373, \quad (9.103)$$

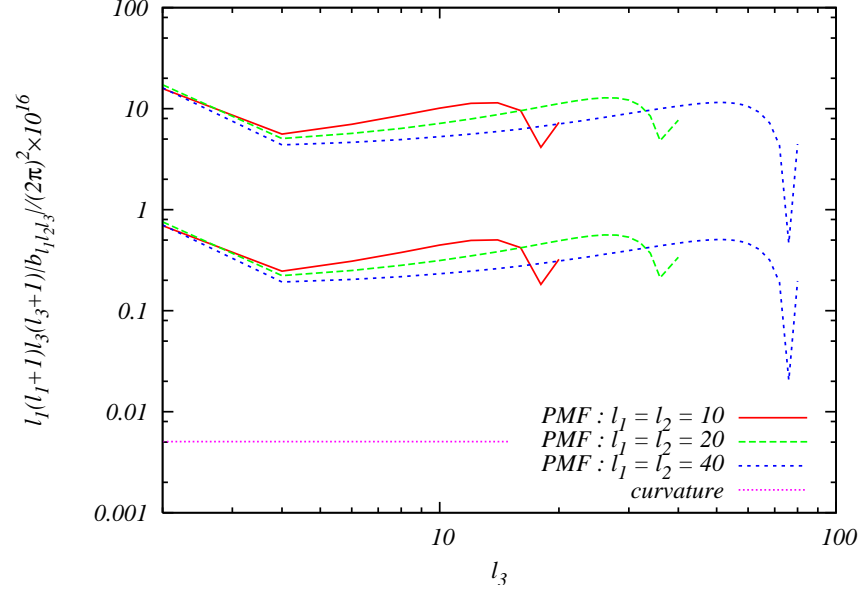


Figure 9.9: Absolute values of the normalized reduced temperature-temperature-temperature bispectra induced by the auto-correlation between the PMF tensor anisotropic stresses and generated from primordial non-Gaussianity in curvature perturbations given by Eq. (9.100) as a function of ℓ_3 with $\ell_1 = \ell_2$. Each parameter is identical to the values defined in Fig. 9.6.

where b^{ex} and b^{app} are the exact and approximate reduced bispectra, respectively. This fact, which this quantity approaches unity, implies that the pole approximation can produce an almost exact copy. An unknown parameter, α , is derived from the relation as

$$\alpha = \frac{b_{\ell\ell\ell}^{\text{ex}}}{b_{\ell\ell\ell}^{\text{app}}(\alpha = 1)} \approx \frac{b^{\text{ex}} \cdot b^{\text{app}}(\alpha = 1)}{b^{\text{app}}(\alpha = 1) \cdot b^{\text{app}}(\alpha = 1)} = 0.2991. \quad (9.104)$$

The cases other than the tensor-tensor-tensor spectrum will be presented in Ref. [35].

As shown in the previous subsections, the CMB bispectra from PMFs arise from the six-point correlation of the Gaussian magnetic fields and have one-loop structure due to the summation over the additional multipoles. Hence, it takes so long hours to estimate all ℓ 's contribution and it is actually impossible to compute the signal-to-noise ratio. However, using the pole approximation, since the summation reaches the tree-level calculation, we will obtain more precise bound through the estimation of the signal-to-noise ratio including the contribution of the cross-correlations between scalar and tensor modes [35].

9.6 Summary and discussion

In this section, on the basis of our recent works [24–26], we presented the all-sky formulae for the CMB bispectra induced by the scalar, vector, and tensor non-Gaussianities coming from the PMFs by dealing with the full-angular dependence of the bispectrum of the PMF anisotropic stresses. Then, expressing the angular dependence with the spin-weighted spherical harmonics and converting the angular integrals into the Wigner symbols were key points of the formulation. From the practical calculation, it is found that the CMB bispectra from the magnetic tensor, scalar, and vector modes dominate at large ($\ell \lesssim 100$), intermediate ($100 \lesssim \ell \lesssim 2000$), and small ($\ell \gtrsim 2000$)

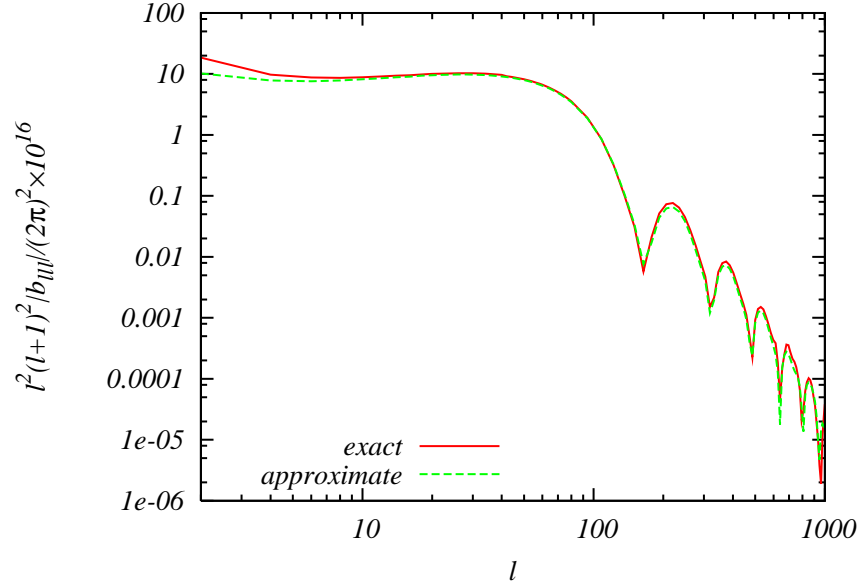


Figure 9.10: Absolute values of the normalized reduced bispectra of temperature fluctuation for a configuration $\ell_1 = \ell_2 = \ell_3 \equiv \ell$. The red solid and green dashed lines represent the exact and approximate spectra arising from the tensor-tensor-tensor correlation of the PMF anisotropic stresses for $B_{1\text{Mpc}} = 4.7\text{nG}$, $n_B = -2.9$ and $\tau_\nu/\tau_B = 10^{17}$, respectively. The cosmological parameters are identical to the values defined in Fig. 9.6.

scales. For the discussion about the shape of the non-Gaussianity in the PMF anisotropic stresses, we performed the pole approximation, which is the evaluation of the convolutions at around the divergence points of the integrands, and found that the bispectra of the PMF anisotropic stresses are classified as the local-type configuration. Owing to this, we had some significant signals of the CMB bispectra on the squeezed limit also in the multipole space. Compared with the exact formula, the approximate one reduces the computing time, hence we expect the use for the calculation of the signal-to-noise ratio [35]. We also investigated the dependence of the CMB bispectrum on the spectral index of the PMF power spectrum and confirmed that the CMB bispectrum induced from the PMFs is sensitive to it. Since the characteristic scale varies with the value of the spectral index, it is important to consider not only the contribution from the scalar mode, but also those from the vector and tensor modes.

By translating the current bound on the local-type non-Gaussianity from the CMB bispectrum into the bound on the amplitude of the magnetic fields, we obtain a new limit: $B_{1\text{Mpc}} < 2.6 - 4.4\text{nG}$. This is a rough estimate coming from the large scale information of the tensor mode and a precise constraint is expected if one considers the full ℓ contribution by using an appropriate estimator of the CMB bispectrum induced from the primordial magnetic fields.

Because of the complicated discussions and mathematical manipulations, here we restrict our numerical results to the intensity bispectra of auto-correlations between scalar, vector and tensor modes despite the fact that our formula for the CMB bispectra (9.69) contains the polarizations and the cross-correlations between scalar, vector and tensor modes. However, like the non-magnetic case [58], the modes other than our numerical results, such as $B_{IEB, \ell_1 \ell_2 \ell_3}^{(SVT)}$, will bring in more reasonable bounds on the PMFs [35]. Furthermore, the effect on the CMB four-point correlation (trispectrum) is just beginning to be roughly discussed [59]. Applying our studies, this should be

taken into account more precisely.

References

- [1] M. L. Bernet, F. Miniati, S. J. Lilly, P. P. Kronberg, and M. Dessauges-Zavadsky, *Strong magnetic fields in normal galaxies at high redshifts*, *Nature* **454** (2008) 302–304, [[arXiv:0807.3347](#)].
- [2] A. M. Wolfe, R. A. Jorgenson, T. Robishaw, C. Heiles, and J. X. Prochaska, *An 84 microGauss Magnetic Field in a Galaxy at Redshift $z=0.692$* , *Nature* **455** (2008) 638, [[arXiv:0811.2408](#)].
- [3] P. P. Kronberg *et al.*, *A Global Probe of Cosmic Magnetic Fields to High Redshifts*, *Astrophys. J.* **676** (2008) 70–79, [[arXiv:0712.0435](#)].
- [4] L. M. Widrow, *Origin of Galactic and Extragalactic Magnetic Fields*, *Rev. Mod. Phys.* **74** (2002) 775–823, [[astro-ph/0207240](#)].
- [5] J. Martin and J. Yokoyama, *Generation of Large-Scale Magnetic Fields in Single-Field Inflation*, *JCAP* **0801** (2008) 025, [[arXiv:0711.4307](#)].
- [6] K. Bamba and M. Sasaki, *Large-scale magnetic fields in the inflationary universe*, *JCAP* **0702** (2007) 030, [[astro-ph/0611701](#)].
- [7] T. Stevens and M. B. Johnson, *Theory of Magnetic Seed-Field Theory of Magnetic Seed-Field Generation during the Cosmological First-Order Electroweak Phase Transition*, [arXiv:1001.3694](#).
- [8] T. Kahniashvili, A. G. Tevzadze, and B. Ratra, *Phase Transition Generated Cosmological Magnetic Field at Large Scales*, *Astrophys.J.* **726** (2011) 78, [[arXiv:0907.0197](#)].
- [9] K. Ichiki, K. Takahashi, H. Ohno, H. Hanayama, and N. Sugiyama, *Cosmological Magnetic Field: a fossil of density perturbations in the early universe*, *Science*. **311** (2006) 827–829, [[astro-ph/0603631](#)].
- [10] S. Maeda, S. Kitagawa, T. Kobayashi, and T. Shiromizu, *Primordial magnetic fields from second-order cosmological perturbations: Tight coupling approximation*, *Class. Quant. Grav.* **26** (2009) 135014, [[arXiv:0805.0169](#)].
- [11] E. Fenu, C. Pitrou, and R. Maartens, *The seed magnetic field generated during recombination*, *Mon.Not.Roy.Astron.Soc.* **414** (2011) 2354–2366, [[arXiv:1012.2958](#)].
- [12] K. Subramanian and J. D. Barrow, *Microwave Background Signals from Tangled Magnetic Fields*, *Phys. Rev. Lett.* **81** (1998) 3575–3578, [[astro-ph/9803261](#)].
- [13] R. Durrer, T. Kahniashvili, and A. Yates, *Microwave Background Anisotropies from Alfvén waves*, *Phys. Rev.* **D58** (1998) 123004, [[astro-ph/9807089](#)].
- [14] A. Mack, T. Kahniashvili, and A. Kosowsky, *Vector and Tensor Microwave Background Signatures of a Primordial Stochastic Magnetic Field*, *Phys. Rev.* **D65** (2002) 123004, [[astro-ph/0105504](#)].

- [15] A. Lewis, *CMB anisotropies from primordial inhomogeneous magnetic fields*, *Phys. Rev.* **D70** (2004) 043011, [[astro-ph/0406096](#)].
- [16] D. Paoletti, F. Finelli, and F. Paci, *The full contribution of a stochastic background of magnetic fields to CMB anisotropies*, *Mon. Not. Roy. Astron. Soc.* **396** (2009) 523–534, [[arXiv:0811.0230](#)].
- [17] J. R. Shaw and A. Lewis, *Massive Neutrinos and Magnetic Fields in the Early Universe*, *Phys. Rev.* **D81** (2010) 043517, [[arXiv:0911.2714](#)].
- [18] I. Brown and R. Crittenden, *Non-Gaussianity from Cosmic Magnetic Fields*, *Phys. Rev.* **D72** (2005) 063002, [[astro-ph/0506570](#)].
- [19] I. A. Brown, *Primordial Magnetic Fields in Cosmology*, [arXiv:0812.1781](#). Ph.D.Thesis.
- [20] T. R. Seshadri and K. Subramanian, *CMB bispectrum from primordial magnetic fields on large angular scales*, *Phys. Rev. Lett.* **103** (2009) 081303, [[arXiv:0902.4066](#)].
- [21] C. Caprini, F. Finelli, D. Paoletti, and A. Riotto, *The cosmic microwave background temperature bispectrum from scalar perturbations induced by primordial magnetic fields*, *JCAP* **0906** (2009) 021, [[arXiv:0903.1420](#)].
- [22] R.-G. Cai, B. Hu, and H.-B. Zhang, *Acoustic signatures in the Cosmic Microwave Background bispectrum from primordial magnetic fields*, *JCAP* **1008** (2010) 025, [[arXiv:1006.2985](#)].
- [23] P. Trivedi, K. Subramanian, and T. R. Seshadri, *Primordial Magnetic Field Limits from Cosmic Microwave Background Bispectrum of Magnetic Passive Scalar Modes*, *Phys. Rev.* **D82** (2010) 123006, [[arXiv:1009.2724](#)].
- [24] M. Shiraishi, D. Nitta, S. Yokoyama, K. Ichiki, and K. Takahashi, *Cosmic microwave background bispectrum of vector modes induced from primordial magnetic fields*, *Phys. Rev.* **D82** (2010) 121302, [[arXiv:1009.3632](#)].
- [25] M. Shiraishi, D. Nitta, S. Yokoyama, K. Ichiki, and K. Takahashi, *Computation approach for CMB bispectrum from primordial magnetic fields*, *Phys. Rev.* **D83** (2011) 123523, [[arXiv:1101.5287](#)].
- [26] M. Shiraishi, D. Nitta, S. Yokoyama, K. Ichiki, and K. Takahashi, *Cosmic microwave background bispectrum of tensor passive modes induced from primordial magnetic fields*, *Phys. Rev.* **D83** (2011) 123003, [[arXiv:1103.4103](#)].
- [27] M. Shiraishi, D. Nitta, S. Yokoyama, K. Ichiki, and K. Takahashi, *CMB Bispectrum from Primordial Scalar, Vector and Tensor non-Gaussianities*, *Prog. Theor. Phys.* **125** (2011) 795–813, [[arXiv:1012.1079](#)].
- [28] T. Kahnishvili and G. Lavrelashvili, *CMB two- and three-point correlation functions from Alfvén waves*, [arXiv:1010.4543](#).
- [29] **WMAP** Collaboration, E. Komatsu *et al.*, *Seven-Year Wilkinson Microwave Anisotropy Probe (WMAP) Observations: Cosmological Interpretation*, *Astrophys. J. Suppl.* **192** (2011) 18, [[arXiv:1001.4538](#)].

- [30] **PLANCK** Collaboration, *The Scientific programme of planck*, [astro-ph/0604069](#).
- [31] M. Shiraishi, *Parity violation of primordial magnetic fields in the CMB bispectrum*, *JCAP* **1206** (2012) 015, [[arXiv:1202.2847](#)].
- [32] J. M. Bardeen, *Gauge Invariant Cosmological Perturbations*, *Phys.Rev.* **D22** (1980) 1882–1905.
- [33] K. Kojima, T. Kajino, and G. J. Mathews, *Generation of Curvature Perturbations with Extra Anisotropic Stress*, *JCAP* **1002** (2010) 018, [[arXiv:0910.1976](#)].
- [34] A. Lewis, *Observable primordial vector modes*, *Phys. Rev. D* **70** (Aug, 2004) 043518.
- [35] M. Shiraishi, D. Nitta, S. Yokoyama, and K. Ichiki, *Optimal limits on primordial magnetic fields from CMB temperature bispectrum of passive modes*, *JCAP* **1203** (2012) 041, [[arXiv:1201.0376](#)].
- [36] D. G. Yamazaki, K. Ichiki, T. Kajino, and G. J. Mathews, *Effects of a Primordial Magnetic Field on Low and High Multipoles of the CMB*, *Phys.Rev.* **D77** (2008) 043005, [[arXiv:0801.2572](#)].
- [37] F. Finelli, F. Paci, and D. Paoletti, *The Impact of Stochastic Primordial Magnetic Fields on the Scalar Contribution to Cosmic Microwave Background Anisotropies*, *Phys.Rev.* **D78** (2008) 023510, [[arXiv:0803.1246](#)].
- [38] I. A. Brown, *Concerning the statistics of cosmic magnetism*, [arXiv:1005.2982](#).
- [39] M. Giovannini and K. E. Kunze, *Generalized CMB initial conditions with pre-equality magnetic fields*, *Phys.Rev.* **D77** (2008) 123001, [[arXiv:0802.1053](#)].
- [40] K. E. Kunze, *CMB anisotropies in the presence of a stochastic magnetic field*, *Phys.Rev.* **D83** (2011) 023006, [[arXiv:1007.3163](#)].
- [41] D. Paoletti and F. Finelli, *CMB Constraints on a Stochastic Background of Primordial Magnetic Fields*, *Phys.Rev.* **D83** (2011) 123533, [[arXiv:1005.0148](#)].
- [42] D. G. Yamazaki, K. Ichiki, T. Kajino, and G. J. Mathews, *New Constraints on the Primordial Magnetic Field*, *Phys. Rev.* **D81** (2010) 023008, [[arXiv:1001.2012](#)].
- [43] J. R. Shaw and A. Lewis, *Constraining Primordial Magnetism*, [arXiv:1006.4242](#).
- [44] D. Yamazaki, K. Ichiki, T. Kajino, and G. J. Mathews, *Constraints on the Evolution of the Primordial Magnetic Field from the Small-Scale Cosmic Microwave Background Angular Anisotropy*, *Astrophys. J.* **646** (2006) 719–729, [[astro-ph/0602224](#)].
- [45] K. Jedamzik, V. Katalinic, and A. V. Olinto, *Damping of Cosmic Magnetic Fields*, *Phys. Rev.* **D57** (1998) 3264–3284, [[astro-ph/9606080](#)].
- [46] K. Subramanian and J. D. Barrow, *Magnetohydrodynamics in the early universe and the damping of nonlinear Alfvén waves*, *Phys. Rev.* **D58** (1998) 083502, [[astro-ph/9712083](#)].
- [47] W. Hu, *Angular trispectrum of the cosmic microwave background*, *Phys. Rev.* **D64** (2001) 083005, [[astro-ph/0105117](#)].

- [48] R. Gurau, *The Ponzano-Regge asymptotic of the 6j symbol: an elementary proof*, *Annales Henri Poincare* **9** (2008) 1413–1424, [arXiv:0808.3533].
- [49] H. A. Jahn and J. Hope, *Symmetry properties of the wigner 9j symbol*, *Phys. Rev.* **93** (Jan, 1954) 318–321.
- [50] “The wolfram function site.” <http://functions.wolfram.com/>.
- [51] D. H. Lyth, *Non-gaussianity and cosmic uncertainty in curvaton-type models*, *JCAP* **0606** (2006) 015, [astro-ph/0602285].
- [52] A. Lewis, A. Challinor, and A. Lasenby, *Efficient Computation of CMB anisotropies in closed FRW models*, *Astrophys. J.* **538** (2000) 473–476, [astro-ph/9911177].
- [53] “Slatec common mathematical library.” <http://www.netlib.org/slatec/>.
- [54] E. Komatsu and D. N. Spergel, *Acoustic signatures in the primary microwave background bispectrum*, *Phys. Rev.* **D63** (2001) 063002, [astro-ph/0005036].
- [55] J. R. Pritchard and M. Kamionkowski, *Cosmic microwave background fluctuations from gravitational waves: An analytic approach*, *Annals Phys.* **318** (2005) 2–36, [astro-ph/0412581].
- [56] A. Riotto, *The Quest for Non-gaussianity*, in *Inflationary Cosmology* (M. Lemoine, J. Martin, & P. Peter, ed.), vol. 738 of *Lecture Notes in Physics*, Berlin Springer Verlag, pp. 305–+, 2008.
- [57] K. M. Smith, L. Senatore, and M. Zaldarriaga, *Optimal limits on f_{NL}^{local} from WMAP 5-year data*, *JCAP* **0909** (2009) 006, [arXiv:0901.2572].
- [58] D. Babich and M. Zaldarriaga, *Primordial bispectrum information from CMB polarization*, *Phys.Rev.* **D70** (2004) 083005, [astro-ph/0408455].
- [59] P. Trivedi, T. Seshadri, and K. Subramanian, *Cosmic Microwave Background Trispectrum and Primordial Magnetic Field Limits*, *Phys.Rev.Lett.* **108** (2012) 231301, [arXiv:1111.0744].

10 Conclusion

The main purpose of this thesis was to present the formalism for the CMB bispectrum induced by the non-Gaussianities not only in the standard scalar-mode perturbations but also in the vector- and tensor-mode ones where the violation of the rotational or parity invariance is also involved, and some attempts to prove the nature of the early Universe by applying our formalism. To do this, we have discussed the following things.

In Sec. 1, we gave the introduction of this thesis. Then, we quickly summarized the history of the Universe, the paradigm in the early Universe, and the concept of this thesis. In Sec. 2, we summarized how to generate the curvature perturbations and gravitational waves and the consistency relations in the slow-roll inflation. In Sec. 3, we showed how to construct the $a_{\ell m}$'s generated from the primordial scalar, vector and tensor sources in order to formulate the CMB bispectrum easily. We also summarized the constraints on several key parameters, which characterize the nature of inflation and the dynamics of the Universe, obtained from the current CMB data. In Sec. 4, we focused on the topic of the primordial non-Gaussianities. In Sec. 5, we gave the general formulae for the CMB bispectrum coming from not only scalar-mode but also vector- and tensor-mode perturbations, which includes both the auto- and cross-correlations between the intensity and polarizations. Next, applying this formalism, we computed the CMB bispectra from several kinds of the non-Gaussianities. In Sec. 6, we treated the two scalars and a graviton correlator and obtained the CMB bispectrum including the tensor-mode perturbation. Here, we had a bound on the nonlinear scalar-scalar-tensor coupling by the computation of the signal-to-noise ratio. In Sec. 7, we considered the non-Gaussianity which has the preferred direction. Through the analysis, we found that the finite signals arise from the multipoles except for the triangle inequality. We furthermore confirmed that these special signals are comparable in magnitude with the signals keeping the triangle inequality. In Sec. 8, we dealt with the graviton non-Gaussianity arising from the parity-conserving and parity-violating Weyl cubic terms. Calculating the CMB intensity and polarization bispectra, we clarified that the intensity-intensity-intensity spectrum from the parity-violating non-Gaussianity obeys the condition as $\sum_{n=1}^3 \ell_n = \text{odd}$. These configurations will be very beneficial to check the parity violation of the Universe in the non-Gaussian level observationally. In Sec. 9, we took into account the effect of the non-Gaussianities due to the primordial magnetic fields. Depending quadratically on the magnetic fields, the magnetic anisotropic stresses obey the chi-square distributions. Since these non-Gaussian anisotropic stresses become the sources of the CMB fluctuations, their bispectra have the finite values. Computing the CMB intensity-intensity-intensity spectra, we clarified that the tensor (vector) mode dominates at large (small) scales and the scalar mode shows up at intermediate scales. By the pole approximation, we also found that the bispectrum of the magnetic anisotropic stresses is similar to the local-type bispectrum. Comparing the theoretical results with the observational limit on the local-type non-Gaussianity, we obtained a bound on the strength of the magnetic fields, $B_{1\text{Mpc}} < 2.6 - 4.4\text{nG}$. We expect that this bound will be updated by considering the impacts of the cross-correlations between scalar, vector and tensor modes, and the additional information from polarizations.

Our formalism for the CMB bispectrum is general enough to be applicable to the non-Gaussian sources other than the above ones. Moreover, this will be easily extended to the higher-order correlations. Therefore, the studies in this thesis will be very beneficial to quest for the true picture of the origin of the Universe.

A Spin-weighted spherical harmonic function

Here, we review the theory of spin-weighted functions and their expansion in spin- s spherical harmonics. In the past, these functions were mainly applied to the analysis of the gravitational wave (see e.g. Ref. [1]). This discussion is based on Refs. [2–4].

For any given direction on the sphere specified by the angles (θ, ϕ) , one can define three orthogonal vectors, one radial and two tangential to the sphere. Let us denote the radial direction vector with \mathbf{n} and the tangential with $\hat{\mathbf{e}}_1, \hat{\mathbf{e}}_2$. The latter two are only defined up to a rotation around \mathbf{n} .

A function ${}_sf(\theta, \phi)$ defined on the sphere is said to have spin- s if under a right-handed rotation of $(\hat{\mathbf{e}}_1, \hat{\mathbf{e}}_2)$ by an angle ψ it transforms as ${}_sf'(\theta, \phi) = e^{-is\psi} {}_sf(\theta, \phi)$. For example, given an arbitrary vector \mathbf{a} on the sphere the quantities, $\mathbf{a} \cdot \hat{\mathbf{e}}_1 + i\mathbf{a} \cdot \hat{\mathbf{e}}_2$, $\mathbf{n} \cdot \mathbf{a}$ and $\mathbf{a} \cdot \hat{\mathbf{e}}_1 - i\mathbf{a} \cdot \hat{\mathbf{e}}_2$ have spin 1, 0 and -1, respectively.

A scalar field on the sphere can be expanded in spherical harmonics, $Y_{lm}(\theta, \phi)$, which form a complete and orthonormal basis. These functions are not appropriate to expand spin weighted functions with $s \neq 0$. There exist analog sets of functions that can be used to expand spin- s functions, the so called spin- s spherical harmonics ${}_sY_{lm}(\theta, \phi)$. These sets of functions (one set for each particular spin) satisfy the same completeness and orthogonality relations,

$$\begin{aligned} \int_0^{2\pi} d\phi \int_{-1}^1 d\cos\theta {}_sY_{l'm'}^*(\theta, \phi) {}_sY_{lm}(\theta, \phi) &= \delta_{l',l} \delta_{m',m} , \\ \sum_{lm} {}_sY_{lm}^*(\theta, \phi) {}_sY_{lm}(\theta', \phi') &= \delta(\phi - \phi') \delta(\cos\theta - \cos\theta'). \end{aligned} \quad (\text{A.1})$$

An important property of spin- s functions is that there exists a spin raising (lowering) operator ∂ ($\bar{\partial}$) with the property of raising (lowering) the spin-weight of a function, $(\partial {}_sf)' = e^{-i(s+1)\psi} \partial {}_sf$, $(\bar{\partial} {}_sf)' = e^{-i(s-1)\psi} \bar{\partial} {}_sf$. Their explicit expression is given by

$$\begin{aligned} \partial {}_sf(\theta, \phi) &= -\sin^s\theta [\partial_\theta + i \csc\theta \partial_\phi] \sin^{-s}\theta {}_sf(\theta, \phi) , \\ \bar{\partial} {}_sf(\theta, \phi) &= -\sin^{-s}\theta [\partial_\theta - i \csc\theta \partial_\phi] \sin^s\theta {}_sf(\theta, \phi) , \end{aligned} \quad (\text{A.2})$$

Specifically, the $\bar{\partial}$ and ∂ operators acting twice on the spin- ± 2 function ${}_{\pm 2}f(\mu, \phi)$ such as the CMB polarization fields can be expressed as

$$\begin{aligned} \bar{\partial}^2 {}_2f(\mu, \phi) &= \left(-\partial_\mu + \frac{m}{1-\mu^2} \right)^2 [(1-\mu^2)_2 f(\mu, \phi)] , \\ \partial^2 {}_{-2}f(\mu, \phi) &= \left(-\partial_\mu - \frac{m}{1-\mu^2} \right)^2 [(1-\mu^2)_{-2} f(\mu, \phi)] , \end{aligned} \quad (\text{A.3})$$

where $\mu \equiv \cos\theta$ and ${}_{\pm 2}f(\mu, \phi) = {}_{\pm 2}\tilde{f}(\mu) e^{im\phi}$. With the aid of these operators, we can express ${}_sY_{lm}$ in terms of the spin-0 spherical harmonics Y_{lm} , which are the usual spherical harmonics,

$$\begin{aligned} {}_sY_{lm} &= \left[\frac{(l-s)!}{(l+s)!} \right]^{\frac{1}{2}} \partial^s Y_{lm} \quad (0 \leq s \leq l) , \\ {}_sY_{lm} &= \left[\frac{(l+s)!}{(l-s)!} \right]^{\frac{1}{2}} (-1)^s \bar{\partial}^{-s} Y_{lm} \quad (-l \leq s \leq 0) , \end{aligned} \quad (\text{A.4})$$

m	Y_{1m}	${}_1Y_{1m}$
± 1	$-m\sqrt{\frac{3}{8\pi}}\sin\theta e^{mi\phi}$	$-\frac{1}{2}\sqrt{\frac{3}{4\pi}}(1-m\cos\theta)e^{mi\phi}$
0	$\frac{1}{2}\sqrt{\frac{3}{\pi}}\cos\theta$	$\sqrt{\frac{3}{8\pi}}\sin\theta$

Table A.1: Dipole ($l = 1$) harmonics for spin-0 and 1.

m	Y_{2m}	${}_2Y_{2m}$
± 2	$\frac{1}{4}\sqrt{\frac{15}{2\pi}}\sin^2\theta e^{mi\phi}$	$\frac{1}{8}\sqrt{\frac{5}{\pi}}\left(1-\frac{m}{2}\cos\theta\right)^2 e^{mi\phi}$
± 1	$-m\sqrt{\frac{15}{8\pi}}\sin\theta\cos\theta e^{mi\phi}$	$-\frac{1}{4}\sqrt{\frac{5}{\pi}}\sin\theta(1-m\cos\theta)e^{mi\phi}$
0	$\frac{1}{2}\sqrt{\frac{5}{4\pi}}(3\cos^2\theta-1)$	$\frac{3}{4}\sqrt{\frac{5}{6\pi}}\sin^2\theta$

Table A.2: Quadrupole ($l = 2$) harmonics for spin-0 and 2.

where these equations contain

$$\begin{aligned}
\partial_s Y_{lm} &= [(l-s)(l+s+1)]^{\frac{1}{2}} {}_{s+1}Y_{lm} , \\
\bar{\partial}_s Y_{lm} &= -[(l+s)(l-s+1)]^{\frac{1}{2}} {}_{s-1}Y_{lm} , \\
\bar{\partial}\partial_s Y_{lm} &= -(l-s)(l+s+1) {}_sY_{lm} .
\end{aligned} \tag{A.5}$$

The above relations lead to an explicit expression for the spin weighted spherical harmonic function:

$$\begin{aligned}
{}_sY_{lm}(\theta, \phi) &= e^{im\phi} \left[\frac{(l+m)!(l-m)!}{(l+s)!(l-s)!} \frac{2l+1}{4\pi} \right]^{1/2} \sin^{2l}(\theta/2) \\
&\times \sum_r \binom{l-s}{r} \binom{l+s}{r+s-m} (-1)^{l-r-s+m} \cot^{2r+s-m}(\theta/2) .
\end{aligned} \tag{A.6}$$

The following properties of spin-weighted harmonics are also useful

$$\begin{aligned}
{}_sY_{lm}^*(\theta, \phi) &= (-1)^{s+m} {}_{-s}Y_{l-m}(\theta, \phi) , \\
{}_sY_{lm}(\pi - \theta, \phi + \pi) &= (-1)^l {}_{-s}Y_{lm}(\theta, \phi) .
\end{aligned} \tag{A.7}$$

Finally, we give the specific expressions for some simple cases in Tables A.1 and A.2.

B Wigner D -matrix

Here, on the basis of Refs. [3, 5, 6], we introduce the properties of the Wigner D -matrix $D_{mm'}^{(l)}$, which is the unitary irreducible matrix of rank $2l + 1$ that forms a representation of the rotational group as $SU(2)$ and $SO(3)$. With this matrix, the change of the spin wighted spherical harmonic function under the rotational transformation as $\hat{\mathbf{n}} \rightarrow R\hat{\mathbf{n}}$ is expressed as

$${}_s Y_{lm}^*(R\hat{\mathbf{n}}) = \sum_{m'} D_{mm'}^{(l)}(R) {}_s Y_{lm'}^*(\hat{\mathbf{n}}) . \quad (\text{B.1})$$

This satisfies the relation as

$$D_{mm'}^{(l)*}(R) = (-1)^{m-m'} D_{-m, m'}^{(l)}(R) = D_{m' m}^{(l)}(R^{-1}) . \quad (\text{B.2})$$

When we express the rotational matrix with three Euler angles (α, β, γ) under the $z - y - z$ convention as

$$R = \begin{pmatrix} \cos \alpha \cos \beta \cos \gamma - \sin \alpha \sin \gamma & -\cos \beta \sin \gamma \cos \alpha - \cos \gamma \sin \alpha & \cos \alpha \sin \beta \\ \cos \alpha \sin \gamma + \cos \gamma \cos \beta \sin \alpha & \cos \alpha \cos \gamma - \cos \beta \sin \alpha \sin \gamma & \sin \beta \sin \alpha \\ -\cos \gamma \sin \beta & \sin \gamma \sin \beta & \cos \beta \end{pmatrix} , \quad (\text{B.3})$$

we can write a general relationship between the Wigner D -matrix and the spin weighted spherical harmonics as

$$D_{ms}^{(l)}(\alpha, \beta, \gamma) = (-1)^s \sqrt{\frac{4\pi}{2l+1}} {}_{-s} Y_{lm}^*(\beta, \alpha) e^{-is\gamma} . \quad (\text{B.4})$$

Like the spin weighted spherical harmonics, there also exists the orthogonality of the Wigner D -matrix as

$$\int_0^{2\pi} d\alpha \int_{-1}^1 d \cos \beta \int_0^{2\pi} d\gamma D_{m's'}^{(l')*}(\alpha, \beta, \gamma) D_{ms}^{(l)}(\alpha, \beta, \gamma) = \frac{8\pi^2}{2l+1} \delta_{l', l} \delta_{m', m} \delta_{s', s} . \quad (\text{B.5})$$

C Wigner symbols

Here, we briefly review the useful properties of the Wigner- $3j$, $6j$ and $9j$ symbols. The following discussions are based on Refs. [5, 7–12].

C.1 Wigner- $3j$ symbol

In quantum mechanics, considering the coupling of two angular momenta as

$$\mathbf{l}_3 = \mathbf{l}_1 + \mathbf{l}_2 , \quad (\text{C.1})$$

the scalar product of eigenstates between the right-handed term and the left-handed one, namely, a Clebsch-Gordan coefficient, is related to the Wigner- $3j$ symbol:

$$\begin{pmatrix} l_1 & l_2 & l_3 \\ m_1 & m_2 & -m_3 \end{pmatrix} \equiv \frac{(-1)^{l_1-l_2+m_3} \langle l_1 m_1 l_2 m_2 | (l_1 l_2) l_3 m_3 \rangle}{\sqrt{2l_3+1}} . \quad (\text{C.2})$$

This symbol vanishes unless the selection rules are satisfied as follows:

$$\begin{aligned} |m_1| \leq l_1 , \quad |m_2| \leq l_2 , \quad |m_3| \leq l_3 , \quad m_1 + m_2 = m_3 , \\ |l_1 - l_2| \leq l_3 \leq l_1 + l_2 \text{ (the triangle condition) } , \quad l_1 + l_2 + l_3 \in \mathbb{Z} . \end{aligned} \quad (\text{C.3})$$

Symmetries of the Wigner- $3j$ symbol are given by

$$\begin{aligned} \begin{pmatrix} l_1 & l_2 & l_3 \\ m_1 & m_2 & m_3 \end{pmatrix} &= (-1)^{\sum_{i=1}^3 l_i} \begin{pmatrix} l_2 & l_1 & l_3 \\ m_2 & m_1 & m_3 \end{pmatrix} = (-1)^{\sum_{i=1}^3 l_i} \begin{pmatrix} l_1 & l_3 & l_2 \\ m_1 & m_3 & m_2 \end{pmatrix} \\ &\quad \text{(odd permutation of columns)} \\ &= \begin{pmatrix} l_2 & l_3 & l_1 \\ m_2 & m_3 & m_1 \end{pmatrix} = \begin{pmatrix} l_3 & l_1 & l_2 \\ m_3 & m_1 & m_2 \end{pmatrix} \\ &\quad \text{(even permutation of columns)} \\ &= (-1)^{\sum_{i=1}^3 l_i} \begin{pmatrix} l_1 & l_2 & l_3 \\ -m_1 & -m_2 & -m_3 \end{pmatrix} \\ &\quad \text{(sign inversion of } m_1, m_2, m_3 \text{)} . \end{aligned} \quad (\text{C.4})$$

The Wigner- $3j$ symbols satisfy the orthogonality as

$$\begin{aligned} \sum_{l_3 m_3} (2l_3+1) \begin{pmatrix} l_1 & l_2 & l_3 \\ m_1 & m_2 & m_3 \end{pmatrix} \begin{pmatrix} l_1 & l_2 & l_3 \\ m'_1 & m'_2 & m_3 \end{pmatrix} &= \delta_{m_1, m'_1} \delta_{m_2, m'_2} , \\ (2l_3+1) \sum_{m_1 m_2} \begin{pmatrix} l_1 & l_2 & l_3 \\ m_1 & m_2 & m_3 \end{pmatrix} \begin{pmatrix} l_1 & l_2 & l'_3 \\ m_1 & m_2 & m'_3 \end{pmatrix} &= \delta_{l_3, l'_3} \delta_{m_3, m'_3} . \end{aligned} \quad (\text{C.5})$$

For a special case that $\sum_{i=1}^3 l_i = \text{even}$ and $m_1 = m_2 = m_3 = 0$, there is an analytical expression as

$$\begin{pmatrix} l_1 & l_2 & l_3 \\ 0 & 0 & 0 \end{pmatrix} = (-1)^{\sum_{i=1}^3 \frac{-l_i}{2}} \frac{(\sum_{i=1}^3 \frac{l_i}{2})! \sqrt{(-l_1+l_2+l_3)!} \sqrt{(l_1-l_2+l_3)!} \sqrt{(l_1+l_2-l_3)!}}{(\frac{-l_1+l_2+l_3}{2})! (\frac{l_1-l_2+l_3}{2})! (\frac{l_1+l_2-l_3}{2})! \sqrt{(\sum_{i=1}^3 l_i + 1)!}} . \quad (\text{C.6})$$

This vanishes for $\sum_{i=1}^3 l_i = \text{odd}$. The Wigner-3j symbol is related to the spin-weighted spherical harmonics as

$$\prod_{i=1}^2 {}_{s_i} Y_{l_i m_i}(\hat{\mathbf{n}}) = \sum_{l_3 m_3 s_3} {}_{s_3} Y_{l_3 m_3}^*(\hat{\mathbf{n}}) I_{l_1 l_2 l_3}^{-s_1 - s_2 - s_3} \begin{pmatrix} l_1 & l_2 & l_3 \\ m_1 & m_2 & m_3 \end{pmatrix}, \quad (\text{C.7})$$

which leads to the “extended” Gaunt integral including spin dependence:

$$\int d^2 \hat{\mathbf{n}} {}_{s_1} Y_{l_1 m_1}(\hat{\mathbf{n}}) {}_{s_2} Y_{l_2 m_2}(\hat{\mathbf{n}}) {}_{s_3} Y_{l_3 m_3}(\hat{\mathbf{n}}) = I_{l_1 l_2 l_3}^{-s_1 - s_2 - s_3} \begin{pmatrix} l_1 & l_2 & l_3 \\ m_1 & m_2 & m_3 \end{pmatrix}. \quad (\text{C.8})$$

Here $I_{l_1 l_2 l_3}^{s_1 s_2 s_3} \equiv \sqrt{\frac{(2l_1+1)(2l_2+1)(2l_3+1)}{4\pi}} \begin{pmatrix} l_1 & l_2 & l_3 \\ s_1 & s_2 & s_3 \end{pmatrix}.$

C.2 Wigner-6j symbol

Considering two other ways in the coupling of three angular momenta as

$$\mathbf{l}_5 = \mathbf{l}_1 + \mathbf{l}_2 + \mathbf{l}_4 \quad (\text{C.9})$$

$$= \mathbf{l}_3 + \mathbf{l}_4 \quad (\text{C.10})$$

$$= \mathbf{l}_1 + \mathbf{l}_6, \quad (\text{C.11})$$

the Wigner-6j symbol is defined using a Clebsch-Gordan coefficient between each eigenstate of \mathbf{l}_5 corresponding to Eqs. (C.10) and (C.11) as

$$\left\{ \begin{matrix} l_1 & l_2 & l_3 \\ l_4 & l_5 & l_6 \end{matrix} \right\} \equiv \frac{(-1)^{l_1+l_2+l_4+l_5} \langle (l_1 l_2) l_3; l_4; l_5 m_5 | l_1; (l_2 l_4) l_6; l_5 m_5 \rangle}{\sqrt{(2l_3+1)(2l_6+1)}}. \quad (\text{C.12})$$

This is expressed with the summation of three Wigner-3j symbols:

$$\begin{aligned} \sum_{m_4 m_5 m_6} (-1)^{\sum_{i=4}^6 l_i - m_i} \begin{pmatrix} l_5 & l_1 & l_6 \\ m_5 & -m_1 & -m_6 \end{pmatrix} \begin{pmatrix} l_6 & l_2 & l_4 \\ m_6 & -m_2 & -m_4 \end{pmatrix} \begin{pmatrix} l_4 & l_3 & l_5 \\ m_4 & -m_3 & -m_5 \end{pmatrix} \\ = \begin{pmatrix} l_1 & l_2 & l_3 \\ m_1 & m_2 & m_3 \end{pmatrix} \left\{ \begin{matrix} l_1 & l_2 & l_3 \\ l_4 & l_5 & l_6 \end{matrix} \right\}; \end{aligned} \quad (\text{C.13})$$

hence, the triangle conditions are given by

$$\begin{aligned} |l_1 - l_2| \leq l_3 \leq l_1 + l_2, \quad |l_4 - l_5| \leq l_3 \leq l_4 + l_5, \\ |l_1 - l_5| \leq l_6 \leq l_1 + l_5, \quad |l_4 - l_2| \leq l_6 \leq l_4 + l_2. \end{aligned} \quad (\text{C.14})$$

The Wigner-6j symbol obeys 24 symmetries such as

$$\begin{aligned} \left\{ \begin{matrix} l_1 & l_2 & l_3 \\ l_4 & l_5 & l_6 \end{matrix} \right\} &= \left\{ \begin{matrix} l_2 & l_1 & l_3 \\ l_5 & l_4 & l_6 \end{matrix} \right\} = \left\{ \begin{matrix} l_2 & l_3 & l_1 \\ l_5 & l_6 & l_4 \end{matrix} \right\} \text{ (permutation of columns)} \\ &= \left\{ \begin{matrix} l_4 & l_5 & l_3 \\ l_1 & l_2 & l_6 \end{matrix} \right\} = \left\{ \begin{matrix} l_1 & l_5 & l_6 \\ l_4 & l_2 & l_3 \end{matrix} \right\} \\ &\text{(exchange of two corresponding elements between rows)}. \end{aligned} \quad (\text{C.15})$$

Geometrically, the Wigner-6j symbol is expressed using the tetrahedron composed of four triangles obeying Eq. (C.14). It is known that the Wigner-6j symbol is suppressed by the square root of the volume of the tetrahedron at high multipoles.

C.3 Wigner-9j symbol

Considering two other ways in the coupling of four angular momenta as

$$\mathbf{l}_9 = \mathbf{l}_1 + \mathbf{l}_2 + \mathbf{l}_4 + \mathbf{l}_5 \quad (\text{C.16})$$

$$= \mathbf{l}_3 + \mathbf{l}_6 \quad (\text{C.17})$$

$$= \mathbf{l}_7 + \mathbf{l}_8 , \quad (\text{C.18})$$

where $\mathbf{l}_3 \equiv \mathbf{l}_1 + \mathbf{l}_2$, $\mathbf{l}_6 \equiv \mathbf{l}_4 + \mathbf{l}_5$, $\mathbf{l}_7 \equiv \mathbf{l}_1 + \mathbf{l}_4$, $\mathbf{l}_8 \equiv \mathbf{l}_2 + \mathbf{l}_5$, the Wigner 9j symbol expresses a Clebsch-Gordan coefficient between each eigenstate of \mathbf{l}_9 corresponding to Eqs. (C.17) and (C.18) as

$$\left\{ \begin{matrix} l_1 & l_2 & l_3 \\ l_4 & l_5 & l_6 \\ l_7 & l_8 & l_9 \end{matrix} \right\} \equiv \frac{\langle (l_1 l_2) l_3; (l_4 l_5) l_6; l_9 m_9 | (l_1 l_4) l_7; (l_2 l_5) l_8; l_9 m_9 \rangle}{\sqrt{(2l_3 + 1)(2l_6 + 1)(2l_7 + 1)(2l_8 + 1)}} . \quad (\text{C.19})$$

This is expressed with the summation of five Wigner-3j symbols:

$$\begin{aligned} & \sum_{\substack{m_4 m_5 m_6 \\ m_7 m_8 m_9}} \begin{pmatrix} l_4 & l_5 & l_6 \\ m_4 & m_5 & m_6 \end{pmatrix} \begin{pmatrix} l_7 & l_8 & l_9 \\ m_7 & m_8 & m_9 \end{pmatrix} \\ & \times \begin{pmatrix} l_4 & l_7 & l_1 \\ m_4 & m_7 & m_1 \end{pmatrix} \begin{pmatrix} l_5 & l_8 & l_2 \\ m_5 & m_8 & m_2 \end{pmatrix} \begin{pmatrix} l_6 & l_9 & l_3 \\ m_6 & m_9 & m_3 \end{pmatrix} \\ & = \begin{pmatrix} l_1 & l_2 & l_3 \\ m_1 & m_2 & m_3 \end{pmatrix} \left\{ \begin{matrix} l_1 & l_2 & l_3 \\ l_4 & l_5 & l_6 \\ l_7 & l_8 & l_9 \end{matrix} \right\} , \end{aligned} \quad (\text{C.20})$$

and that of three Wigner-6j symbols:

$$\left\{ \begin{matrix} l_1 & l_2 & l_3 \\ l_4 & l_5 & l_6 \\ l_7 & l_8 & l_9 \end{matrix} \right\} = \sum_x (-1)^{2x} (2x + 1) \left\{ \begin{matrix} l_1 & l_4 & l_7 \\ l_8 & l_9 & x \end{matrix} \right\} \left\{ \begin{matrix} l_2 & l_5 & l_8 \\ l_4 & x & l_6 \end{matrix} \right\} \left\{ \begin{matrix} l_3 & l_6 & l_9 \\ x & l_1 & l_2 \end{matrix} \right\}; \quad (\text{C.21})$$

hence, the triangle conditions are given by

$$\begin{aligned} & |l_1 - l_2| \leq l_3 \leq l_1 + l_2 , \quad |l_4 - l_5| \leq l_6 \leq l_4 + l_5 , \quad |l_7 - l_8| \leq l_9 \leq l_7 + l_8 , \\ & |l_1 - l_4| \leq l_7 \leq l_1 + l_4 , \quad |l_2 - l_5| \leq l_8 \leq l_2 + l_5 , \quad |l_3 - l_6| \leq l_9 \leq l_3 + l_6 . \end{aligned} \quad (\text{C.22})$$

The Wigner-9j symbol obeys 72 symmetries:

$$\begin{aligned} & \left\{ \begin{matrix} l_1 & l_2 & l_3 \\ l_4 & l_5 & l_6 \\ l_7 & l_8 & l_9 \end{matrix} \right\} = (-1)^{\sum_{i=1}^9 l_i} \left\{ \begin{matrix} l_2 & l_1 & l_3 \\ l_5 & l_4 & l_6 \\ l_8 & l_7 & l_9 \end{matrix} \right\} = (-1)^{\sum_{i=1}^9 l_i} \left\{ \begin{matrix} l_1 & l_2 & l_3 \\ l_7 & l_8 & l_9 \\ l_4 & l_5 & l_6 \end{matrix} \right\} \\ & \quad \text{(odd permutation of rows or columns)} \\ & = \left\{ \begin{matrix} l_2 & l_3 & l_1 \\ l_5 & l_6 & l_4 \\ l_8 & l_9 & l_7 \end{matrix} \right\} = \left\{ \begin{matrix} l_4 & l_5 & l_6 \\ l_7 & l_8 & l_9 \\ l_1 & l_2 & l_3 \end{matrix} \right\} \\ & \quad \text{(even permutation of rows or columns)} \\ & = \left\{ \begin{matrix} l_1 & l_4 & l_7 \\ l_2 & l_5 & l_8 \\ l_3 & l_6 & l_9 \end{matrix} \right\} = \left\{ \begin{matrix} l_9 & l_6 & l_3 \\ l_8 & l_5 & l_2 \\ l_7 & l_4 & l_1 \end{matrix} \right\} \\ & \quad \text{(reflection of the symbols)} . \end{aligned} \quad (\text{C.23})$$

C.4 Analytic expressions of the Wigner symbols

Here, we show some analytical formulas of the Wigner symbols.

The I symbols, which are defined as

$$I_{l_1 l_2 l_3}^{s_1 s_2 s_3} \equiv \sqrt{\frac{(2l_1 + 1)(2l_2 + 1)(2l_3 + 1)}{4\pi}} \begin{pmatrix} l_1 & l_2 & l_3 \\ s_1 & s_2 & s_3 \end{pmatrix}, \quad (\text{C.24})$$

are expressed as

$$\begin{aligned} I_{l_1 l_2 l_3}^{0 \ 0 \ 0} &= \sqrt{\frac{\prod_{i=1}^3 (2l_i + 1)}{4\pi}} (-1)^{\sum_{i=1}^3 \frac{-l_i}{2}} \\ &\times \frac{(\sum_{i=1}^3 \frac{l_i}{2})! \sqrt{(-l_1 + l_2 + l_3)!} \sqrt{(l_1 - l_2 + l_3)!} \sqrt{(l_1 + l_2 - l_3)!}}{(\frac{-l_1 + l_2 + l_3}{2})! (\frac{l_1 - l_2 + l_3}{2})! (\frac{l_1 + l_2 - l_3}{2})! \sqrt{(\sum_{i=1}^3 l_i + 1)!}} \\ &\quad (\text{for } l_1 + l_2 + l_3 = \text{even}) \\ &= 0 \quad (\text{for } l_1 + l_2 + l_3 = \text{odd}), \end{aligned} \quad (\text{C.25})$$

$$\begin{aligned} I_{l_1 \ l_2 \ l_3}^{0 \ 1 \ -1} &= \sqrt{\frac{5}{8\pi}} (-1)^{l_2 + 1} \sqrt{\frac{(l_2 - 1)(l_2 + 1)}{l_2 - 1/2}} \quad (\text{for } l_1 = l_2 - 2, l_3 = 2) \\ &= \sqrt{\frac{15}{16\pi}} (-1)^{l_2} \sqrt{\frac{l_2 + 1/2}{(l_2 - 1/2)(l_2 + 3/2)}} \quad (\text{for } l_1 = l_2, l_3 = 2) \\ &= \sqrt{\frac{5}{8\pi}} (-1)^{l_2} \sqrt{\frac{l_2(l_2 + 2)}{l_2 + 3/2}} \quad (\text{for } l_1 = l_2 + 2, l_3 = 2) \\ &= \sqrt{\frac{3}{8\pi}} (-1)^{l_3 + 1} \sqrt{l_3 + 1} \quad (\text{for } l_1 = l_3 - 1, l_2 = 1) \\ &= \sqrt{\frac{3}{4\pi}} (-1)^{l_3 + 1} \sqrt{l_3 + 1/2} \quad (\text{for } l_1 = l_3, l_2 = 1) \\ &= \sqrt{\frac{3}{8\pi}} (-1)^{l_3 + 1} \sqrt{l_3} \quad (\text{for } l_1 = l_3 + 1, l_2 = 1). \end{aligned} \quad (\text{C.26})$$

The Wigner-9j symbols are calculated as

$$\begin{aligned} \left\{ \begin{matrix} l_1 & l_2 & l_3 \\ l_4 & l_5 & l_6 \\ 1 & 1 & 2 \end{matrix} \right\} &= \sqrt{\frac{2(l_3 \pm 1) + 1}{5}} \left\{ \begin{matrix} l_1 & l_4 & 1 \\ l_3 \pm 2 & l_3 \pm 1 & l_5 \end{matrix} \right\} \left\{ \begin{matrix} l_2 & l_5 & 1 \\ l_3 \pm 1 & l_3 & l_1 \end{matrix} \right\} \quad (\text{for } l_6 = l_3 \pm 2) \\ &= \sqrt{\frac{(2l_3 - 1)(2l_3 + 2)(2l_3 + 3)}{30(2l_3)(2l_3 + 1)}} \left\{ \begin{matrix} l_1 & l_4 & 1 \\ l_3 & l_3 - 1 & l_5 \end{matrix} \right\} \left\{ \begin{matrix} l_2 & l_5 & 1 \\ l_3 - 1 & l_3 & l_1 \end{matrix} \right\} \\ &\quad + \sqrt{\frac{2(2l_3 - 1)(2l_3 + 1)(2l_3 + 3)}{15(2l_3)(2l_3 + 2)}} \left\{ \begin{matrix} l_1 & l_4 & 1 \\ l_3 & l_3 & l_5 \end{matrix} \right\} \left\{ \begin{matrix} l_2 & l_5 & 1 \\ l_3 & l_3 & l_1 \end{matrix} \right\} \\ &\quad + \sqrt{\frac{(2l_3 - 1)(2l_3)(2l_3 + 3)}{30(2l_3 + 1)(2l_3 + 2)}} \left\{ \begin{matrix} l_1 & l_4 & 1 \\ l_3 & l_3 + 1 & l_5 \end{matrix} \right\} \left\{ \begin{matrix} l_2 & l_5 & 1 \\ l_3 + 1 & l_3 & l_1 \end{matrix} \right\} \\ &\quad (\text{for } l_6 = l_3), \end{aligned} \quad (\text{C.27})$$

where these Wigner-6j symbols are analytically given by

$$\begin{aligned}
\left\{ \begin{array}{ccc} l_1 & l_2 & 1 \\ l_4 & l_5 & l_6 \end{array} \right\} &= (-1)^{l_1+l_4+l_6+1} \sqrt{\frac{l_1+l_4+l_6+2}{2l_4+3} \frac{P_2}{P_3} \frac{l_1+l_4-l_6+1}{2l_1+1} \frac{P_2}{P_3}} \quad (\text{for } l_2 = l_1 - 1, l_5 = l_4 + 1) \\
&= (-1)^{l_1+l_4+l_6+1} \sqrt{\frac{2(l_1+l_4+l_6+2)(l_1+l_4-l_6+1)}{2l_4+3} \frac{P_3}{P_3}} \\
&\quad \times \sqrt{\frac{(-l_1+l_4+l_6+1)(l_1-l_4+l_6)}{2l_1+2} \frac{P_3}{P_3}} \quad (\text{for } l_2 = l_1, l_5 = l_4 + 1) \\
&= (-1)^{l_1+l_4+l_6+1} \sqrt{\frac{-l_1+l_4+l_6+1}{2l_4+3} \frac{P_2}{P_3} \frac{l_1-l_4+l_6+1}{2l_1+3} \frac{P_2}{P_3}} \quad (\text{for } l_2 = l_1 + 1, l_5 = l_4 + 1) \\
&= (-1)^{l_1+l_4+l_6+1} [l_4(l_4+1) + l_1(l_1-1)(l_4+1) - l_6(l_6+1) - l_1(l_1+1)l_4] \\
&\quad \times \sqrt{\frac{2(l_1+l_4+l_6+1)(l_1+l_4-l_6)}{(-l_1+l_4+l_6+1)(l_1-l_4+l_6)2l_4+2} \frac{P_3}{P_3} \frac{P_3}{2l_1+1} \frac{P_3}{P_3}} \quad (\text{for } l_2 = l_1 - 1, l_5 = l_4) \\
&= 2(-1)^{l_1+l_4+l_6+1} \frac{l_4(l_4+1) + l_1(l_1+1)(l_4+1) - l_6(l_6+1) - l_1(l_1+1)l_4}{\sqrt{2l_4+2} \frac{P_3}{P_3} \frac{P_3}{2l_1+2} \frac{P_3}{P_3}} \\
&\quad (\text{for } l_2 = l_1, l_5 = l_4) \\
&= (-1)^{l_1+l_4+l_6+1} [l_4(l_4+1) + (l_1+1)(l_1+2)(l_4+1) - l_6(l_6+1) - l_1(l_1+1)l_4] \\
&\quad \times \sqrt{\frac{2(-l_1+l_4+l_6)(l_1-l_4+l_6+1)}{(l_1+l_4+l_6+2)(l_1+l_4-l_6+1)2l_4+2} \frac{P_3}{P_3} \frac{P_3}{2l_1+3} \frac{P_3}{P_3}} \quad (\text{for } l_2 = l_1 + 1, l_5 = l_4) .
\end{aligned} \tag{C.28}$$

Using these analytical formulas, one can reduce the time cost involved with calculating the CMB bispectrum from PMFs.

D Polarization vector and tensor

We summarize the relations and properties of a divergenceless polarization vector $\epsilon_a^{(\pm 1)}$ and a transverse and traceless polarization tensor $e_{ab}^{(\pm 2)}$ [6, 11] .

The polarization vector with respect to a unit vector $\hat{\mathbf{n}}$ is expressed using two unit vectors $\hat{\theta}$ and $\hat{\phi}$ perpendicular to $\hat{\mathbf{n}}$ as

$$\epsilon_a^{(\pm 1)}(\hat{\mathbf{n}}) = \frac{1}{\sqrt{2}}[\hat{\theta}_a(\hat{\mathbf{n}}) \pm i \hat{\phi}_a(\hat{\mathbf{n}})] . \quad (\text{D.1})$$

This satisfies the relations:

$$\begin{aligned} \hat{n}^a \epsilon_a^{(\pm 1)}(\hat{\mathbf{n}}) &= 0 , \\ \epsilon_a^{(\pm 1)*}(\hat{\mathbf{n}}) &= \epsilon_a^{(\mp 1)}(\hat{\mathbf{n}}) = \epsilon_a^{(\pm 1)}(-\hat{\mathbf{n}}) , \\ \epsilon_a^{(\lambda)}(\hat{\mathbf{n}}) \epsilon_a^{(\lambda')}(\hat{\mathbf{n}}) &= \delta_{\lambda, -\lambda'} \quad (\text{for } \lambda, \lambda' = \pm 1) . \end{aligned} \quad (\text{D.2})$$

By defining a rotational matrix, which transforms a unit vector parallel to the z axis, namely $\hat{\mathbf{z}}$, to $\hat{\mathbf{n}}$, as

$$S(\hat{\mathbf{n}}) \equiv \begin{pmatrix} \cos \theta_n \cos \phi_n & -\sin \phi_n & \sin \theta_n \cos \phi_n \\ \cos \theta_n \sin \phi_n & \cos \phi_n & \sin \theta_n \sin \phi_n \\ -\sin \theta_n & 0 & \cos \theta_n \end{pmatrix} , \quad (\text{D.3})$$

we specify $\hat{\theta}$ and $\hat{\phi}$ as

$$\hat{\theta}(\hat{\mathbf{n}}) = S(\hat{\mathbf{n}})\hat{\mathbf{x}} , \quad \hat{\phi}(\hat{\mathbf{n}}) = S(\hat{\mathbf{n}})\hat{\mathbf{y}} , \quad (\text{D.4})$$

where $\hat{\mathbf{x}}$ and $\hat{\mathbf{y}}$ are unit vectors parallel to x - and y -axes. By using Eq. (D.1), the polarization tensor is constructed as

$$e_{ab}^{(\pm 2)}(\hat{\mathbf{n}}) = \sqrt{2} \epsilon_a^{(\pm 1)}(\hat{\mathbf{n}}) \epsilon_b^{(\pm 1)}(\hat{\mathbf{n}}) . \quad (\text{D.5})$$

To utilize the polarization vector and tensor in the calculation of this thesis, we need to expand Eqs. (D.1) and (D.5) with spin spherical harmonics. An arbitrary unit vector is expanded with the spin-0 spherical harmonics as

$$\begin{aligned} \hat{r}_a &= \sum_m \alpha_a^m Y_{1m}(\hat{\mathbf{r}}) , \\ \alpha_a^m &\equiv \sqrt{\frac{2\pi}{3}} \begin{pmatrix} -m(\delta_{m,1} + \delta_{m,-1}) \\ i(\delta_{m,1} + \delta_{m,-1}) \\ \sqrt{2}\delta_{m,0} \end{pmatrix} . \end{aligned} \quad (\text{D.6})$$

Here, note that the repeat of the index implies the summation. The scalar product of α_a^m is calculated as

$$\alpha_a^m \alpha_a^{m'} = \frac{4\pi}{3} (-1)^m \delta_{m, -m'} , \quad \alpha_a^m \alpha_a^{m'*} = \frac{4\pi}{3} \delta_{m, m'} . \quad (\text{D.7})$$

Through the substitution of Eq. (D.4) into Eq. (D.6), $\hat{\theta}$ is expanded as

$$\hat{\theta}_a(\hat{\mathbf{n}}) = \sum_m \alpha_a^m Y_{1m}(\hat{\theta}(\hat{\mathbf{n}})) = \sum_m \alpha_a^m \sum_{m'} D_{mm'}^{(1)*}(S(\hat{\mathbf{n}})) Y_{1m'}(\hat{\mathbf{x}})$$

$$= -\frac{s}{\sqrt{2}}(\delta_{s,1} + \delta_{s,-1}) \sum_m \alpha_a^m s Y_{1m}(\hat{\mathbf{n}}) . \quad (\text{D.8})$$

Here, we use the properties of the Wigner D -matrix as described in Appendix B [3, 5, 6, 13]

$$\begin{aligned} Y_{\ell m}(S(\hat{\mathbf{n}})\hat{\mathbf{x}}) &= \sum_{m'} D_{mm'}^{(\ell)*}(S(\hat{\mathbf{n}})) Y_{\ell m'}(\hat{\mathbf{x}}) , \\ D_{ms}^{(\ell)}(S(\hat{\mathbf{n}})) &= \left[\frac{4\pi}{2\ell+1} \right]^{1/2} (-1)^s Y_{\ell m}^*(\hat{\mathbf{n}}) . \end{aligned} \quad (\text{D.9})$$

In the same manner, $\hat{\phi}$ is also calculated as

$$\hat{\phi}_a(\hat{\mathbf{n}}) = \frac{i}{\sqrt{2}}(\delta_{s,1} + \delta_{s,-1}) \sum_m \alpha_a^m s Y_{1m}(\hat{\mathbf{n}}) ; \quad (\text{D.10})$$

hence, the explicit form of Eq. (D.1) is calculated as

$$\epsilon_a^{(\pm 1)}(\hat{\mathbf{n}}) = \mp \sum_m \alpha_a^m {}_{\pm 1} Y_{1m}(\hat{\mathbf{n}}) . \quad (\text{D.11})$$

Substituting this into Eq. (D.5) and using the relations of Appendix C and $I_{2\ 1\ 1}^{\mp 2 \pm 1 \pm 1} = \frac{3}{2\sqrt{\pi}}$, the polarization tensor can also be expressed as

$$e_{ab}^{(\pm 2)}(\hat{\mathbf{n}}) = \frac{3}{\sqrt{2\pi}} \sum_{M m_a m_b} \mp 2 Y_{2M}^*(\hat{\mathbf{n}}) \alpha_a^{m_a} \alpha_b^{m_b} \begin{pmatrix} 2 & 1 & 1 \\ M & m_a & m_b \end{pmatrix} . \quad (\text{D.12})$$

This obeys the relations:

$$\begin{aligned} e_{aa}^{(\pm 2)}(\hat{\mathbf{n}}) &= \hat{n}_a e_{ab}^{(\pm 2)}(\hat{\mathbf{n}}) = 0 , \\ e_{ab}^{(\pm 2)*}(\hat{\mathbf{n}}) &= e_{ab}^{(\mp 2)}(\hat{\mathbf{n}}) = e_{ab}^{(\pm 2)}(-\hat{\mathbf{n}}) , \\ e_{ab}^{(\lambda)}(\hat{\mathbf{n}}) e_{ab}^{(\lambda')}(\hat{\mathbf{n}}) &= 2\delta_{\lambda, -\lambda'} \quad (\text{for } \lambda, \lambda' = \pm 2) . \end{aligned} \quad (\text{D.13})$$

Using the projection operators as

$$\begin{aligned} O_a^{(0)} e^{i\mathbf{k}\cdot\mathbf{x}} &\equiv k^{-1} \nabla_a e^{i\mathbf{k}\cdot\mathbf{x}} = i \hat{k}_a e^{i\mathbf{k}\cdot\mathbf{x}} , \\ O_{ab}^{(0)} e^{i\mathbf{k}\cdot\mathbf{x}} &\equiv \left(k^{-2} \nabla_a \nabla_b + \frac{\delta_{a,b}}{3} \right) e^{i\mathbf{k}\cdot\mathbf{x}} = \left(-\hat{k}_a \hat{k}_b + \frac{\delta_{a,b}}{3} \right) e^{i\mathbf{k}\cdot\mathbf{x}} , \\ O_a^{(\pm 1)} e^{i\mathbf{k}\cdot\mathbf{x}} &\equiv -i \epsilon_a^{(\pm 1)}(\hat{\mathbf{k}}) e^{i\mathbf{k}\cdot\mathbf{x}} , \\ O_{ab}^{(\pm 1)} e^{i\mathbf{k}\cdot\mathbf{x}} &\equiv k^{-1} \left(\nabla_a O_b^{(\pm 1)} + \nabla_b O_a^{(\pm 1)} \right) e^{i\mathbf{k}\cdot\mathbf{x}} = \left(\hat{k}_a \epsilon_b^{(\pm 1)}(\hat{\mathbf{k}}) + \hat{k}_b \epsilon_a^{(\pm 1)}(\hat{\mathbf{k}}) \right) e^{i\mathbf{k}\cdot\mathbf{x}} , \\ O_{ab}^{(\pm 2)} e^{i\mathbf{k}\cdot\mathbf{x}} &\equiv e_{ab}^{(\pm 2)}(\hat{\mathbf{k}}) e^{i\mathbf{k}\cdot\mathbf{x}} , \end{aligned} \quad (\text{D.14})$$

the arbitrary scalar, vector and tensor are decomposed into the helicity states as

$$\eta(\mathbf{k}) = \eta^{(0)}(\mathbf{k}) , \quad (\text{D.15})$$

$$\omega_a(\mathbf{k}) = \omega^{(0)}(\mathbf{k}) O_a^{(0)} + \sum_{\lambda=\pm 1} \omega^{(\lambda)}(\mathbf{k}) O_a^{(\lambda)} , \quad (\text{D.16})$$

$$\chi_{ab}(\mathbf{k}) = -\frac{1}{3}\chi_{\text{iso}}(\mathbf{k})\delta_{a,b} + \chi^{(0)}(\mathbf{k})O_{ab}^{(0)} + \sum_{\lambda=\pm 1}\chi^{(\lambda)}(\mathbf{k})O_{ab}^{(\lambda)} + \sum_{\lambda=\pm 2}\chi^{(\lambda)}(\mathbf{k})O_{ab}^{(\lambda)}. \quad (\text{D.17})$$

Then, using Eq. (D.2) and (D.13), we can find the inverse formulae as

$$\omega^{(0)}(\mathbf{k}) = -O_a^{(0)}\omega_a(\mathbf{k}), \quad (\text{D.18})$$

$$\omega^{(\pm 1)}(\mathbf{k}) = -O_a^{(\mp 1)}(\hat{\mathbf{k}})\omega_a(\mathbf{k}), \quad (\text{D.19})$$

$$\chi^{(0)}(\mathbf{k}) = \frac{3}{2}O_{ab}^{(0)}(\hat{\mathbf{k}})\chi_{ab}(\mathbf{k}), \quad (\text{D.20})$$

$$\chi^{(\pm 1)}(\mathbf{k}) = \frac{1}{2}O_{ab}^{(\mp 1)}(\hat{\mathbf{k}})\chi_{ab}(\mathbf{k}), \quad (\text{D.21})$$

$$\chi^{(\pm 2)}(\mathbf{k}) = \frac{1}{2}O_{ab}^{(\mp 2)}(\hat{\mathbf{k}})\chi_{ab}(\mathbf{k}). \quad (\text{D.22})$$

From these, we can derive the relations of several projection operators as

$$\begin{aligned} O_{ab}^{(0)}(\hat{\mathbf{k}}) &= -\hat{k}_a\hat{k}_b + \frac{1}{3}\delta_{ab} \\ &= -\sqrt{\frac{3}{2\pi}} \sum_{Mm_a m_b} Y_{2M}^*(\hat{\mathbf{k}})\alpha_a^{m_a}\alpha_b^{m_b} \begin{pmatrix} 2 & 1 & 1 \\ M & m_a & m_b \end{pmatrix}, \\ O_{ab}^{(\pm 1)}(\hat{\mathbf{k}}) &= \hat{k}_a\epsilon_b^{(\pm 1)}(\hat{\mathbf{k}}) + \hat{k}_b\epsilon_a^{(\pm 1)}(\hat{\mathbf{k}}) \\ &= \pm \frac{3}{\sqrt{2\pi}} \sum_{Mm_a m_b} \mp 1 Y_{2M}^*(\hat{\mathbf{k}})\alpha_a^{m_a}\alpha_b^{m_b} \begin{pmatrix} 2 & 1 & 1 \\ M & m_a & m_b \end{pmatrix}, \\ O_{ab}^{(\pm 2)}(\hat{\mathbf{k}}) &= e_{ab}^{(\pm 2)}(\hat{\mathbf{k}}) \\ &= \frac{3}{\sqrt{2\pi}} \sum_{Mm_a m_b} \mp 2 Y_{2M}^*(\hat{\mathbf{k}})\alpha_a^{m_a}\alpha_b^{m_b} \begin{pmatrix} 2 & 1 & 1 \\ M & m_a & m_b \end{pmatrix}, \\ P_{ab}(\hat{\mathbf{k}}) &\equiv \delta_{ab} - \hat{k}_a\hat{k}_b \\ &= -2 \sum_{L=0,2} I_{L11}^{01-1} \sum_{Mm_a m_b} Y_{LM}^*(\hat{\mathbf{k}})\alpha_a^{m_a}\alpha_b^{m_b} \begin{pmatrix} L & 1 & 1 \\ M & m_a & m_b \end{pmatrix}, \\ O_{ab}^{(0)}(\hat{\mathbf{k}})P_{bc}(\hat{\mathbf{k}}) &= \frac{1}{3}P_{ac}(\hat{\mathbf{k}}), \\ O_{ab}^{(\pm 1)}(\hat{\mathbf{k}})P_{bc}(\hat{\mathbf{k}}) &= \hat{k}_a\epsilon_c^{(\pm 1)}(\hat{\mathbf{k}}), \\ O_{ab}^{(\pm 2)}(\hat{\mathbf{k}})P_{bc}(\hat{\mathbf{k}}) &= e_{ac}^{(\pm 2)}(\hat{\mathbf{k}}), \\ \hat{k}_c &= i\eta^{abc}\epsilon_a^{(+1)}(\hat{\mathbf{k}})\epsilon_b^{(-1)}(\hat{\mathbf{k}}), \\ \eta^{abc}\hat{k}_a\epsilon_b^{(\pm 1)}(\hat{\mathbf{k}}) &= \mp i\epsilon_c^{(\pm 1)}(\hat{\mathbf{k}}). \end{aligned} \quad (\text{D.23})$$

E Calculation of $f_{W^3}^{(a)}$ and $f_{\widetilde{W}W^2}^{(a)}$

Here, we calculate each product between the wave number vectors and the polarization tensors of $f_{W^3}^{(a)}$ and $f_{\widetilde{W}W^2}^{(a)}$ mentioned in Sec. 8.2.1 [14].

Using the relations discussed in Appendix D, the all terms of $f_{W^3}^{(a)}$ are written as

$$\begin{aligned}
e_{ij}^{(-\lambda_1)} e_{jk}^{(-\lambda_2)} e_{ki}^{(-\lambda_3)} &= -(8\pi)^{3/2} \sum_{M,M',M''} \lambda_1 Y_{2M}^*(\hat{\mathbf{k}}_1)_{\lambda_2} Y_{2M'}^*(\hat{\mathbf{k}}_2)_{\lambda_3} Y_{2M''}^*(\hat{\mathbf{k}}_3) \\
&\quad \times \frac{1}{10} \sqrt{\frac{7}{3}} \begin{pmatrix} 2 & 2 & 2 \\ M & M' & M'' \end{pmatrix}, \\
e_{ij}^{(-\lambda_1)} e_{kl}^{(-\lambda_2)} e_{kl}^{(-\lambda_3)} \hat{k}_{2i} \hat{k}_{3j} &= -(8\pi)^{3/2} \sum_{L',L''=2,3} \sum_{M,M',M''} \lambda_1 Y_{2M}^*(\hat{\mathbf{k}}_1)_{\lambda_2} Y_{L'M'}^*(\hat{\mathbf{k}}_2)_{\lambda_3} Y_{L''M''}^*(\hat{\mathbf{k}}_3) \\
&\quad \times \frac{4\pi}{15} (-1)^{L'} I_{L'12}^{\lambda_2 0 - \lambda_2} I_{L''12}^{\lambda_3 0 - \lambda_3} \begin{pmatrix} 2 & L' & L'' \\ M & M' & M'' \end{pmatrix} \left\{ \begin{matrix} 2 & L' & L'' \\ 2 & 1 & 1 \end{matrix} \right\}, \\
e_{ij}^{(-\lambda_1)} e_{ki}^{(-\lambda_2)} e_{jl}^{(-\lambda_3)} \hat{k}_{2l} \hat{k}_{3k} &= -(8\pi)^{3/2} \sum_{L',L''=2,3} \sum_{M,M',M''} \lambda_1 Y_{2M}^*(\hat{\mathbf{k}}_1)_{\lambda_2} Y_{L'M'}^*(\hat{\mathbf{k}}_2)_{\lambda_3} Y_{L''M''}^*(\hat{\mathbf{k}}_3) \\
&\quad \times \frac{4\pi}{3} (-1)^{L'} I_{L'12}^{\lambda_2 0 - \lambda_2} I_{L''12}^{\lambda_3 0 - \lambda_3} \begin{pmatrix} 2 & L' & L'' \\ M & M' & M'' \end{pmatrix} \left\{ \begin{matrix} 2 & L' & L'' \\ 1 & 1 & 2 \\ 1 & 2 & 1 \end{matrix} \right\}, \\
e_{ij}^{(-\lambda_1)} e_{ik}^{(-\lambda_2)} e_{kl}^{(-\lambda_3)} \hat{k}_{2l} \hat{k}_{3j} &= -(8\pi)^{3/2} \sum_{L',L''=2,3} \sum_{M,M',M''} \lambda_1 Y_{2M}^*(\hat{\mathbf{k}}_1)_{\lambda_2} Y_{L'M'}^*(\hat{\mathbf{k}}_2)_{\lambda_3} Y_{L''M''}^*(\hat{\mathbf{k}}_3) \\
&\quad \times \frac{4\pi}{3} (-1)^{L'} I_{L'12}^{\lambda_2 0 - \lambda_2} I_{L''12}^{\lambda_3 0 - \lambda_3} \begin{pmatrix} 2 & L' & L'' \\ M & M' & M'' \end{pmatrix} \\
&\quad \times \left\{ \begin{matrix} 2 & 1 & L' \\ 2 & 1 & 1 \end{matrix} \right\} \left\{ \begin{matrix} 2 & L' & L'' \\ 2 & 1 & 1 \end{matrix} \right\}.
\end{aligned} \tag{E.1}$$

In the calculation of $f_{\widetilde{W}W^2}^{(a)}$, we also need to consider the dependence of the tensor contractions on η^{ijk} . Making use of the relation:

$$\eta^{abc} \alpha_a^{m_a} \alpha_b^{m_b} \alpha_c^{m_c} = -i \left(\frac{4\pi}{3} \right)^{3/2} \sqrt{6} \begin{pmatrix} 1 & 1 & 1 \\ m_a & m_b & m_c \end{pmatrix}, \tag{E.2}$$

the first two terms of $f_{\widetilde{W}W^2}^{(a)}$ reduce to

$$\begin{aligned}
i\eta^{ijk} e_{kq}^{(-\lambda_1)} e_{jm}^{(-\lambda_2)} e_{iq}^{(-\lambda_3)} \hat{k}_{3m} &= -(8\pi)^{3/2} \sum_{L''=2,3} \sum_{M,M',M''} \lambda_1 Y_{2M}^*(\hat{\mathbf{k}}_1)_{\lambda_2} Y_{2M'}^*(\hat{\mathbf{k}}_2)_{\lambda_3} Y_{L''M''}^*(\hat{\mathbf{k}}_3) \\
&\quad \times \sqrt{\frac{2\pi}{5}} (-1)^{L''} I_{L''12}^{\lambda_3 0 - \lambda_3} \begin{pmatrix} 2 & 2 & L'' \\ M & M' & M'' \end{pmatrix} \left\{ \begin{matrix} 2 & 2 & L'' \\ 1 & 2 & 1 \end{matrix} \right\}, \\
i\eta^{ijk} e_{kq}^{(-\lambda_1)} e_{mi}^{(-\lambda_2)} e_{mq}^{(-\lambda_3)} \hat{k}_{3j} &= -(8\pi)^{3/2} \sum_{L''=2,3} \sum_{M,M',M''} \lambda_1 Y_{2M}^*(\hat{\mathbf{k}}_1)_{\lambda_2} Y_{2M'}^*(\hat{\mathbf{k}}_2)_{\lambda_3} Y_{L''M''}^*(\hat{\mathbf{k}}_3) \\
&\quad \times 2\sqrt{2\pi} (-1)^{L''} I_{L''12}^{\lambda_3 0 - \lambda_3} \begin{pmatrix} 2 & 2 & L'' \\ M & M' & M'' \end{pmatrix} \left\{ \begin{matrix} 2 & 2 & L'' \\ 1 & 1 & 1 \\ 1 & 1 & 2 \end{matrix} \right\}.
\end{aligned} \tag{E.3}$$

For the other terms, by using the relation

$$\eta^{abc}\hat{k}_a e_{bd}^{(\lambda)}(\hat{\mathbf{k}}) = -\frac{\lambda}{2} i e_{cd}^{(\lambda)}(\hat{\mathbf{k}}) , \quad (\text{E.4})$$

we have

$$\begin{aligned} i\eta^{ijk} e_{pj}^{(-\lambda_1)} e_{pm}^{(-\lambda_2)} \hat{k}_{1k} \hat{k}_{2l} e_{il}^{(-\lambda_3)} \hat{k}_{3m} &= -\frac{\lambda_1}{2} (8\pi)^{3/2} \sum_{L', L''=2,3} \sum_{M, M', M''} \\ &\times \lambda_1 Y_{2M}^*(\hat{\mathbf{k}}_1)_{\lambda_2} Y_{L'M'}^*(\hat{\mathbf{k}}_2)_{\lambda_3} Y_{L''M''}^*(\hat{\mathbf{k}}_3) \\ &\times \frac{4\pi}{3} (-1)^{L''} I_{L'12}^{\lambda_2 0 - \lambda_2} I_{L''12}^{\lambda_3 0 - \lambda_3} \\ &\times \begin{pmatrix} 2 & L' & L'' \\ M & M' & M'' \end{pmatrix} \begin{Bmatrix} 2 & L' & L'' \\ 1 & 2 & 1 \\ 1 & 1 & 2 \end{Bmatrix} , \\ i\eta^{ijk} e_{pj}^{(-\lambda_1)} e_{pm}^{(-\lambda_2)} \hat{k}_{1k} \hat{k}_{2l} e_{im}^{(-\lambda_3)} \hat{k}_{3l} &= -\frac{\lambda_1}{2} (8\pi)^{3/2} \sum_{L', L''=2,3} \sum_{M, M', M''} \\ &\times \lambda_1 Y_{2M}^*(\hat{\mathbf{k}}_1)_{\lambda_2} Y_{L'M'}^*(\hat{\mathbf{k}}_2)_{\lambda_3} Y_{L''M''}^*(\hat{\mathbf{k}}_3) \\ &\times \frac{2\pi}{15} \sqrt{\frac{7}{3}} (-1)^{L''} I_{L'12}^{\lambda_2 0 - \lambda_2} I_{L''12}^{\lambda_3 0 - \lambda_3} \\ &\times \begin{pmatrix} 2 & L' & L'' \\ M & M' & M'' \end{pmatrix} \begin{Bmatrix} 2 & L' & L'' \\ 1 & 2 & 2 \end{Bmatrix} . \end{aligned} \quad (\text{E.5})$$

F Graviton non-Gaussianity from the Weyl cubic terms

Here, let us derive the bispectra of gravitons coming from the parity-even and parity-odd Weyl cubic terms, namely, Eqs. (8.16) and (8.17) [14]. For convenience, we decompose the interaction Hamiltonians of W^3 and $\widetilde{W}W^2$ (8.15) into

$$H_{int} = \sum_{n=1}^4 H_{int}^{(n)}. \quad (F.1)$$

Depending on this, we also split the graviton non-Gaussianity as

$$\left\langle \prod_{n=1}^3 \gamma^{(\lambda_n)}(\mathbf{k}_n) \right\rangle_{int} = \sum_{m=1}^4 \left\langle \prod_{n=1}^3 \gamma^{(\lambda_n)}(\mathbf{k}_n) \right\rangle_{int}^{(m)}. \quad (F.2)$$

In what follows, we shall show the computation of each fraction.

F.1 W^3

The bracket part of Eq. (8.12) in terms of $H_{W^3}^{(1)}$ is expanded as

$$\begin{aligned} & \left\langle 0 \left| \left[: H_{W^3}^{(1)}(\tau') :, \prod_{n=1}^3 \gamma^{(\lambda_n)}(\mathbf{k}_n, \tau) \right] \right| 0 \right\rangle \\ &= \left\langle 0 \left| : H_{W^3}^{(1)}(\tau') : \prod_{n=1}^3 \gamma^{(\lambda_n)}(\mathbf{k}_n, \tau) \right| 0 \right\rangle - \left\langle 0 \left| \left[\prod_{n=1}^3 \gamma^{(\lambda_n)}(\mathbf{k}_n, \tau) \right] : H_{W^3}^{(1)}(\tau') : \right| 0 \right\rangle \\ &= - \int d^3x' \Lambda^{-2} (H\tau')^2 \left(\frac{\tau'}{\tau_*} \right)^A \frac{1}{4} \left[\prod_{n=1}^3 \int \frac{d^3\mathbf{k}'_n}{(2\pi)^3} e^{i\mathbf{k}'_n \cdot \mathbf{x}'} \sum_{\lambda'_n=\pm 2} \right] e_{ij}^{(\lambda'_1)}(\hat{\mathbf{k}}'_1) e_{jk}^{(\lambda'_2)}(\hat{\mathbf{k}}'_2) e_{ki}^{(\lambda'_3)}(\hat{\mathbf{k}}'_3) \\ &\quad \times \left[: \left\langle 0 \left| \left\{ \prod_{n=1}^3 (\ddot{\gamma}_{dS} - k_n'^2 \gamma_{dS})(k'_n, \tau') a_{k'_n}^{(\lambda'_n)} \right\} \left\{ \prod_{m=1}^3 \gamma_{dS}^*(k_m, \tau) a_{-k_m}^{(\lambda_m)\dagger} \right\} \right| 0 \right\rangle : \right. \\ &\quad \left. - : \left\langle 0 \left| \left\{ \prod_{m=1}^3 \gamma_{dS}(k_m, \tau) a_{k_m}^{(\lambda_m)} \right\} \left\{ \prod_{n=1}^3 (\ddot{\gamma}_{dS}^* - k_n'^2 \gamma_{dS}^*)(k'_n, \tau') a_{-k'_n}^{(\lambda'_n)\dagger} \right\} \right| 0 \right\rangle : \right] \\ &= -\Lambda^{-2} (H\tau')^2 \left(\frac{\tau'}{\tau_*} \right)^A \frac{1}{4} (2\pi)^3 \delta \left(\sum_{n=1}^3 \mathbf{k}_n \right) e_{ij}^{(\lambda_1)}(-\hat{\mathbf{k}}_1) e_{jk}^{(\lambda_2)}(-\hat{\mathbf{k}}_2) e_{ki}^{(\lambda_3)}(-\hat{\mathbf{k}}_3) \\ &\quad \times 6 \left[\left\{ \prod_{n=1}^3 (\ddot{\gamma}_{dS} - k_n^2 \gamma_{dS})(k_n, \tau') \gamma_{dS}^*(k_n, \tau) \right\} - \left\{ \prod_{n=1}^3 \gamma_{dS}(k_n, \tau) (\ddot{\gamma}_{dS}^* - k_n^2 \gamma_{dS}^*)(k_n, \tau') \right\} \right] \\ &= -\frac{3}{2} \Lambda^{-2} (H\tau')^2 \left(\frac{\tau'}{\tau_*} \right)^A (2\pi)^3 \delta \left(\sum_{n=1}^3 \mathbf{k}_n \right) e_{ij}^{(-\lambda_1)}(\hat{\mathbf{k}}_1) e_{jk}^{(-\lambda_2)}(\hat{\mathbf{k}}_2) e_{ki}^{(-\lambda_3)}(\hat{\mathbf{k}}_3) \\ &\quad \times 2i \text{Im} \left[\prod_{n=1}^3 (\ddot{\gamma}_{dS} - k_n^2 \gamma_{dS})(k_n, \tau') \gamma_{dS}^*(k_n, \tau) \right]. \quad (F.3) \end{aligned}$$

Here, we use

$$\begin{aligned}
\left\langle 0 \left| : \prod_{n=1}^3 a_{\mathbf{k}'_n}^{(\lambda'_n)} a_{-\mathbf{k}_n}^{(\lambda_n)\dagger} : \right| 0 \right\rangle &= (2\pi)^9 \delta(\mathbf{k}_1 + \mathbf{k}_3) \delta_{\lambda_1, \lambda'_3} \delta(\mathbf{k}'_1 + \mathbf{k}_3) \delta_{\lambda'_1, \lambda_3} \delta(\mathbf{k}_2 + \mathbf{k}'_2) \delta_{\lambda_2, \lambda'_2} + 5 \text{ perms.} \\
&= \left\langle 0 \left| : \prod_{n=1}^3 a_{\mathbf{k}_n}^{(\lambda_n)} a_{-\mathbf{k}'_n}^{(\lambda'_n)\dagger} : \right| 0 \right\rangle \\
e_{ij}^{(-\lambda)}(\hat{\mathbf{k}}) &= e_{ij}^{(\lambda)}(-\hat{\mathbf{k}}) .
\end{aligned} \tag{F.4}$$

Furthermore, since

$$\begin{aligned}
\ddot{\gamma}_{dS} - k^2 \gamma_{dS} &= \frac{2H\tau'}{M_{\text{pl}}} k^{3/2} e^{-ik\tau'} , \\
\prod_{n=1}^3 \gamma_{dS}^*(k_n, \tau) &\xrightarrow{\tau \rightarrow 0} i \frac{H^3}{M_{\text{pl}}^3} (k_1 k_2 k_3)^{-3/2} ,
\end{aligned} \tag{F.5}$$

the time integral at $\tau \rightarrow 0$ is performed as

$$\begin{aligned}
&\text{Im} \left[\int_{-\infty}^{\tau} d\tau' (H\tau')^2 \left(\frac{\tau'}{\tau_*} \right)^A \prod_{n=1}^3 (\ddot{\gamma}_{dS} - k_n^2 \gamma_{dS})(k_n, \tau') \gamma_{dS}^*(k_n, \tau) \right] \\
&= \frac{8H^5}{M_{\text{pl}}^3} \sqrt{k_1^3 k_2^3 k_3^3} \text{Im} \left[\left(\prod_{n=1}^3 \gamma_{dS}^*(k_n, \tau) \right) \tau_*^{-A} \int_{-\infty}^{\tau} d\tau' \tau'^{5+A} e^{-ik_t \tau'} \right] \\
&\xrightarrow{\tau \rightarrow 0} \frac{8H^8}{M_{\text{pl}}^6} \text{Re} \left[\tau_*^{-A} \int_{-\infty}^0 d\tau' \tau'^{5+A} e^{-ik_t \tau'} \right] ,
\end{aligned} \tag{F.6}$$

where $k_t \equiv \sum_{n=1}^3 k_n$. Thus, the graviton non-Gaussianity in the late time limit arising from $H_{W^3}^{(1)}$ is

$$\begin{aligned}
\left\langle \prod_{n=1}^3 \gamma^{(\lambda_n)}(\mathbf{k}_n) \right\rangle_{W^3}^{(1)} &= (2\pi)^3 \delta \left(\sum_{n=1}^3 \mathbf{k}_n \right) 8 \left(\frac{H}{M_{\text{pl}}} \right)^6 \left(\frac{H}{\Lambda} \right)^2 \text{Re} \left[\tau_*^{-A} \int_{-\infty}^0 d\tau' \tau'^{5+A} e^{-ik_t \tau'} \right] \\
&\times 3e_{ij}^{(-\lambda_1)}(\hat{\mathbf{k}}_1) e_{jk}^{(-\lambda_2)}(\hat{\mathbf{k}}_2) e_{ki}^{(-\lambda_3)}(\hat{\mathbf{k}}_3) .
\end{aligned} \tag{F.7}$$

The bracket part in terms of $H_{W^3}^{(2)}$ is given by

$$\begin{aligned}
&\left\langle 0 \left| \left[: H_{W^3}^{(2)}(\tau') : , \prod_{n=1}^3 \gamma^{(\lambda_n)}(\mathbf{k}_n, \tau) \right] \right| 0 \right\rangle \\
&= \left\langle 0 \left| : H_{W^3}^{(2)}(\tau') : \prod_{n=1}^3 \gamma^{(\lambda_n)}(\mathbf{k}_n, \tau) \right| 0 \right\rangle - \left\langle 0 \left| \left[\prod_{n=1}^3 \gamma^{(\lambda_n)}(\mathbf{k}_n, \tau) \right] : H_{W^3}^{(2)}(\tau') : \right| 0 \right\rangle \\
&= \frac{3}{2} \Lambda^{-2} (H\tau')^2 \left(\frac{\tau'}{\tau_*} \right)^A k_2 k_3 (2\pi)^3 \delta \left(\sum_{n=1}^3 \mathbf{k}_n \right) \hat{k}_{2i} \hat{k}_{3j} e_{ij}^{(-\lambda_1)}(\hat{\mathbf{k}}_1) e_{kl}^{(-\lambda_2)}(\hat{\mathbf{k}}_2) e_{kl}^{(-\lambda_3)}(\hat{\mathbf{k}}_3) \\
&\times 2i \text{Im} \left[(\ddot{\gamma}_{dS} - k_1^2 \gamma_{dS})(k_1, \tau') \dot{\gamma}_{dS}(k_2, \tau') \dot{\gamma}_{dS}(k_3, \tau') \prod_{n=1}^3 \gamma_{dS}^*(k_n, \tau) \right] + 5 \text{ perms.} .
\end{aligned} \tag{F.8}$$

Using

$$\dot{\gamma}_{dS} = i \frac{H\tau}{M_{\text{pl}}} \sqrt{k} e^{-ik\tau'} , \quad (\text{F.9})$$

we can reduce the time integral to

$$\begin{aligned} \text{Im} \left[\int_{-\infty}^{\tau} d\tau' (H\tau')^2 \left(\frac{\tau'}{\tau_*} \right)^A k_2 k_3 (\ddot{\gamma}_{dS} - k_1^2 \gamma_{dS})(k_1, \tau') \dot{\gamma}_{dS}(k_2, \tau') \dot{\gamma}_{dS}(k_3, \tau') \prod_{n=1}^3 \gamma_{dS}^*(k_n, \tau) \right] \\ \xrightarrow{\tau \rightarrow 0} -\frac{2H^8}{M_{\text{pl}}^6} \text{Re} \left[\tau_*^{-A} \int_{-\infty}^0 d\tau' \tau'^{5+A} e^{-ik_t \tau'} \right] , \end{aligned} \quad (\text{F.10})$$

and obtain

$$\begin{aligned} \left\langle \prod_{n=1}^3 \gamma^{(\lambda_n)}(\mathbf{k}_n) \right\rangle_{W^3}^{(2)} &= (2\pi)^3 \delta \left(\sum_{n=1}^3 \mathbf{k}_n \right) 8 \left(\frac{H}{M_{\text{pl}}} \right)^6 \left(\frac{H}{\Lambda} \right)^2 \text{Re} \left[\tau_*^{-A} \int_{-\infty}^0 d\tau' \tau'^{5+A} e^{-ik_t \tau'} \right] \\ &\quad \times \frac{3}{4} \hat{k}_{2i} e_{ij}^{(-\lambda_1)}(\hat{\mathbf{k}}_1) \hat{k}_{3j} e_{kl}^{(-\lambda_2)}(\hat{\mathbf{k}}_2) e_{kl}^{(-\lambda_3)}(\hat{\mathbf{k}}_3) + 5 \text{ perms.} . \end{aligned} \quad (\text{F.11})$$

The graviton non-Gaussianities from $H_{W^3}^{(3)}$ and $H_{W^3}^{(4)}$ are derived in the same manner as that from $H_{W^3}^{(2)}$:

$$\begin{aligned} \sum_{m=3}^4 \left\langle \prod_{n=1}^3 \gamma^{(\lambda_n)}(\mathbf{k}_n) \right\rangle_{W^3}^{(m)} &= (2\pi)^3 \delta \left(\sum_{n=1}^3 \mathbf{k}_n \right) 8 \left(\frac{H}{M_{\text{pl}}} \right)^6 \left(\frac{H}{\Lambda} \right)^2 \text{Re} \left[\tau_*^{-A} \int_{-\infty}^0 d\tau' \tau'^{5+A} e^{-ik_t \tau'} \right] \\ &\quad \times \left[\frac{3}{4} \hat{k}_{3k} e_{ki}^{(-\lambda_2)}(\hat{\mathbf{k}}_2) e_{ij}^{(-\lambda_1)}(\hat{\mathbf{k}}_1) e_{jl}^{(-\lambda_3)}(\hat{\mathbf{k}}_3) \hat{k}_{2l} \right. \\ &\quad \left. - \frac{3}{2} \hat{k}_{3j} e_{ji}^{(-\lambda_1)}(\hat{\mathbf{k}}_1) e_{ik}^{(-\lambda_2)}(\hat{\mathbf{k}}_2) e_{kl}^{(-\lambda_3)}(\hat{\mathbf{k}}_3) \hat{k}_{2l} + 5 \text{ perms.} \right] . \end{aligned} \quad (\text{F.12})$$

F.2 $\widetilde{W}W^2$

At first, we shall focus on the contribution of $H_{\widetilde{W}W^2}^{(1)}$. The bracket part is computed as

$$\begin{aligned} &\left\langle 0 \left| \left[: H_{\widetilde{W}W^2}^{(1)}(\tau') : , \prod_{n=1}^3 \gamma^{(\lambda_n)}(\mathbf{k}_n, \tau) \right] \right| 0 \right\rangle \\ &= \left\langle 0 \left| : H_{\widetilde{W}W^2}^{(1)}(\tau') : \prod_{n=1}^3 \gamma^{(\lambda_n)}(\mathbf{k}_n, \tau) \right| 0 \right\rangle - \left\langle 0 \left| \left[\prod_{n=1}^3 \gamma^{(\lambda_n)}(\mathbf{k}_n, \tau) \right] : H_{\widetilde{W}W^2}^{(1)}(\tau') : \right| 0 \right\rangle \\ &= - \int d^3 x' \Lambda^{-2} (H\tau')^2 \left(\frac{\tau'}{\tau_*} \right)^A (-3) \left[\prod_{n=1}^3 \int \frac{d^3 \mathbf{k}'_n}{(2\pi)^3} e^{i\mathbf{k}'_n \cdot \mathbf{x}'} \sum_{\lambda'_n = \pm 2} \right] \\ &\quad \times \eta^{ijk} e_{kq}^{(\lambda'_1)}(\hat{\mathbf{k}}'_1) e_{jm}^{(\lambda'_2)}(\hat{\mathbf{k}}'_2) e_{iq}^{(\lambda'_3)}(\hat{\mathbf{k}}'_3) (ik'_{3m}) \\ &\quad \times [(\ddot{\gamma}_{dS} - k_1'^2 \gamma_{dS})(k'_1, \tau') (\ddot{\gamma}_{dS} - k_2'^2 \gamma_{dS})(k'_2, \tau') \dot{\gamma}_{dS}(k'_3, \tau') \\ &\quad \times : \left\langle 0 \left| \left\{ \prod_{m=1}^3 a_{k'_m}^{(\lambda'_m)} \right\} \left\{ \prod_{n=1}^3 \gamma_{dS}^*(k_n, \tau) a_{-k_n}^{(\lambda_n)\dagger} \right\} \right| 0 \right\rangle : \end{aligned}$$

$$\begin{aligned}
& - \left(\ddot{\gamma}_{dS}^* - k_1'^2 \gamma_{dS}^* \right) (k_1', \tau') \left(\ddot{\gamma}_{dS}^* - k_2'^2 \gamma_{dS}^* \right) (k_2', \tau') \dot{\gamma}_{dS}^*(k_3', \tau') \\
& \quad \times : \left\langle 0 \left| \left\{ \prod_{n=1}^3 \gamma_{dS}(k_n, \tau) a_{k_n}^{(\lambda_n)} \right\} \left\{ \prod_{m=1}^3 a_{-k_m'}^{(\lambda_m')\dagger} \right\} \right| 0 \right\rangle : \\
& = \Lambda^{-2} (H\tau')^2 \left(\frac{\tau'}{\tau_*} \right)^A 3(2\pi)^3 \delta \left(\sum_{n=1}^3 \mathbf{k}_n \right) \eta^{ijk} e_{kq}^{(\lambda_1)}(-\hat{\mathbf{k}}_1) e_{jm}^{(\lambda_2)}(-\hat{\mathbf{k}}_2) e_{iq}^{(\lambda_3)}(-\hat{\mathbf{k}}_3) (-ik_{3m}) \\
& \quad \times \left[\left(\ddot{\gamma}_{dS} - k_1^2 \gamma_{dS} \right) (k_1, \tau') \left(\ddot{\gamma}_{dS} - k_2^2 \gamma_{dS} \right) (k_2, \tau') \dot{\gamma}_{dS}(k_3, \tau') \left\{ \prod_{n=1}^3 \gamma_{dS}^*(k_n, \tau) \right\} \right. \\
& \quad \left. - \left(\ddot{\gamma}_{dS}^* - k_1'^2 \gamma_{dS}^* \right) (k_1, \tau') \left(\ddot{\gamma}_{dS}^* - k_2'^2 \gamma_{dS}^* \right) (k_2, \tau') \dot{\gamma}_{dS}^*(k_3, \tau') \left\{ \prod_{n=1}^3 \gamma_{dS}(k_n, \tau) \right\} \right] \\
& \quad + 5 \text{ perms.} \\
& = \Lambda^{-2} (H\tau')^2 \left(\frac{\tau'}{\tau_*} \right)^A (-3i) k_3 (2\pi)^3 \delta \left(\sum_{n=1}^3 \mathbf{k}_n \right) \eta^{ijk} e_{kq}^{(-\lambda_1)}(\hat{\mathbf{k}}_1) e_{jm}^{(-\lambda_2)}(\hat{\mathbf{k}}_2) e_{iq}^{(-\lambda_3)}(\hat{\mathbf{k}}_3) \hat{k}_{3m} \\
& \quad \times 2i \text{Im} \left[\left(\ddot{\gamma}_{dS} - k_1^2 \gamma_{dS} \right) (k_1, \tau') \left(\ddot{\gamma}_{dS} - k_2^2 \gamma_{dS} \right) (k_2, \tau') \dot{\gamma}_{dS}(k_3, \tau') \left\{ \prod_{n=1}^3 \gamma_{dS}^*(k_n, \tau) \right\} \right] \\
& \quad + 5 \text{ perms.} . \tag{F.13}
\end{aligned}$$

Via the time integral:

$$\begin{aligned}
& \text{Im} \left[\int_{-\infty}^{\tau} d\tau' (H\tau')^2 \left(\frac{\tau'}{\tau_*} \right)^A k_3 \left(\ddot{\gamma}_{dS} - k_1^2 \gamma_{dS} \right) (k_1, \tau') \left(\ddot{\gamma}_{dS} - k_2^2 \gamma_{dS} \right) (k_2, \tau') \right. \\
& \quad \left. \times \dot{\gamma}_{dS}(k_3, \tau') \left\{ \prod_{n=1}^3 \gamma_{dS}^*(k_n, \tau) \right\} \right] \\
& \xrightarrow{\tau \rightarrow 0} -\frac{4H^8}{M_{\text{pl}}^6} \text{Im} \left[\tau_*^{-A} \int_{-\infty}^0 d\tau' \tau'^{5+A} e^{-ik_t \tau'} \right] , \tag{F.14}
\end{aligned}$$

we have

$$\begin{aligned}
& \left\langle \prod_{n=1}^3 \gamma^{(\lambda_n)}(\mathbf{k}_n) \right\rangle_{\widetilde{W}W^2}^{(1)} = (2\pi)^3 \delta \left(\sum_{n=1}^3 \mathbf{k}_n \right) 8 \left(\frac{H}{M_{\text{pl}}} \right)^6 \left(\frac{H}{\Lambda} \right)^2 \text{Im} \left[\tau_*^{-A} \int_{-\infty}^0 d\tau' \tau'^{5+A} e^{-ik_t \tau'} \right] \\
& \quad \times (-3i) \left[\eta^{ijk} e_{kq}^{(-\lambda_1)}(\hat{\mathbf{k}}_1) e_{jm}^{(-\lambda_2)}(\hat{\mathbf{k}}_2) e_{iq}^{(-\lambda_3)}(\hat{\mathbf{k}}_3) \hat{k}_{3m} + 5 \text{ perms.} \right] . \tag{F.15}
\end{aligned}$$

Like this, we can gain the second counterpart:

$$\begin{aligned}
& \left\langle \prod_{n=1}^3 \gamma^{(\lambda_n)}(\mathbf{k}_n) \right\rangle_{\widetilde{W}W^2}^{(2)} = (2\pi)^3 \delta \left(\sum_{n=1}^3 \mathbf{k}_n \right) 8 \left(\frac{H}{M_{\text{pl}}} \right)^6 \left(\frac{H}{\Lambda} \right)^2 \text{Im} \left[\tau_*^{-A} \int_{-\infty}^0 d\tau' \tau'^{5+A} e^{-ik_t \tau'} \right] \\
& \quad \times i \left[\eta^{ijk} e_{kq}^{(-\lambda_1)}(\hat{\mathbf{k}}_1) e_{mi}^{(-\lambda_2)}(\hat{\mathbf{k}}_2) e_{mq}^{(-\lambda_3)}(\hat{\mathbf{k}}_3) \hat{k}_{3j} + 5 \text{ perms.} \right] . \tag{F.16}
\end{aligned}$$

The bracket part with respect to $H_{\widetilde{W}W^2}^{(3)}$ is

$$\left\langle 0 \left| \left[: H_{\widetilde{W}W^2}^{(3)}(\tau') :, \prod_{n=1}^3 \gamma^{(\lambda_n)}(\mathbf{k}_n, \tau) \right] \right| 0 \right\rangle$$

$$\begin{aligned}
&= \left\langle 0 \left| : H_{\widetilde{WW}^2}^{(3)}(\tau') : \prod_{n=1}^3 \gamma^{(\lambda_n)}(\mathbf{k}_n, \tau) \right| 0 \right\rangle - \left\langle 0 \left| \left[\prod_{n=1}^3 \gamma^{(\lambda_n)}(\mathbf{k}_n, \tau) \right] : H_{\widetilde{WW}^2}^{(3)}(\tau') : \right| 0 \right\rangle \\
&= - \int d^3x' \Lambda^{-2} (H\tau')^2 \left(\frac{\tau'}{\tau_*} \right)^A 4 \left[\prod_{n=1}^3 \int \frac{d^3\mathbf{k}'_n}{(2\pi)^3} e^{i\mathbf{k}'_n \cdot \mathbf{x}'} \sum_{\lambda'_n = \pm 2} \right] \\
&\quad \times \eta^{ijk} e_{pj}^{(\lambda'_1)}(\hat{\mathbf{k}}'_1) e_{pm}^{(\lambda'_2)}(\hat{\mathbf{k}}'_2) e_{il}^{(\lambda'_3)}(\hat{\mathbf{k}}'_3) (ik'_{1k})(ik'_{2l})(ik'_{3m}) \\
&\quad \times \left[: \left\langle 0 \left| \left\{ \prod_{n=1}^3 \dot{\gamma}_{dS}(k'_n, \tau') a_{k'_n}^{(\lambda'_n)} \right\} \left\{ \prod_{m=1}^3 \gamma_{dS}^*(k_m, \tau) a_{-k_m}^{(\lambda_m)\dagger} \right\} \right| 0 \right\rangle : \right. \\
&\quad \left. - : \left\langle 0 \left| \left\{ \prod_{m=1}^3 \gamma_{dS}(k_m, \tau) a_{k_m}^{(\lambda_m)} \right\} \left\{ \prod_{n=1}^3 \dot{\gamma}_{dS}^*(k'_n, \tau') a_{-k'_n}^{(\lambda'_n)\dagger} \right\} \right| 0 \right\rangle : \right] \\
&= \Lambda^{-2} (H\tau')^2 \left(\frac{\tau'}{\tau_*} \right)^A (-4)(2\pi)^3 \delta \left(\sum_{n=1}^3 \mathbf{k}_n \right) \\
&\quad \times \eta^{ijk} e_{pj}^{(\lambda_1)}(-\hat{\mathbf{k}}_1) e_{pm}^{(\lambda_2)}(-\hat{\mathbf{k}}_2) e_{il}^{(\lambda_3)}(-\hat{\mathbf{k}}_3) (-ik_{1k})(-ik_{2l})(-ik_{3m}) \\
&\quad \times \left[\left\{ \prod_{n=1}^3 \dot{\gamma}_{dS}(k_n, \tau') \gamma_{dS}^*(k_n, \tau) \right\} - \left\{ \prod_{n=1}^3 \dot{\gamma}_{dS}^*(k_n, \tau') \gamma_{dS}(k_n, \tau) \right\} \right] + 5 \text{ perms.} \\
&= \Lambda^{-2} (H\tau')^2 \left(\frac{\tau'}{\tau_*} \right)^A (-4)(-i)^3 k_1 k_2 k_3 (2\pi)^3 \delta \left(\sum_{n=1}^3 \mathbf{k}_n \right) \\
&\quad \times \eta^{ijk} e_{pj}^{(-\lambda_1)}(\hat{\mathbf{k}}_1) e_{pm}^{(-\lambda_2)}(\hat{\mathbf{k}}_2) e_{il}^{(-\lambda_3)}(\hat{\mathbf{k}}_3) \hat{k}_{1k} \hat{k}_{2l} \hat{k}_{3m} \\
&\quad \times 2i \text{Im} \left[\prod_{n=1}^3 \dot{\gamma}_{dS}(k_n, \tau') \gamma_{dS}^*(k_n, \tau) \right] + 5 \text{ perms.} . \tag{F.17}
\end{aligned}$$

The time integral is

$$\begin{aligned}
&\text{Im} \left[\int_{-\infty}^{\tau} d\tau' (H\tau')^2 \left(\frac{\tau'}{\tau_*} \right)^A \prod_{n=1}^3 k_n \dot{\gamma}_{dS}(k_n, \tau') \gamma_{dS}^*(k_n, \tau) \right] \\
&\xrightarrow{\tau \rightarrow 0} \frac{H^8}{M_{\text{pl}}^6} \text{Im} \left[\tau_*^{-A} \int_{-\infty}^0 d\tau' \tau'^{5+A} e^{-ik_t \tau'} \right] , \tag{F.18}
\end{aligned}$$

so that the bispectrum of gravitons becomes

$$\begin{aligned}
\left\langle \prod_{n=1}^3 \gamma^{(\lambda_n)}(\mathbf{k}_n) \right\rangle_{\widetilde{WW}^2}^{(3)} &= (2\pi)^3 \delta \left(\sum_{n=1}^3 \mathbf{k}_n \right) 8 \left(\frac{H}{M_{\text{pl}}} \right)^6 \left(\frac{H}{\Lambda} \right)^2 \text{Im} \left[\tau_*^{-A} \int_{-\infty}^0 d\tau' \tau'^{5+A} e^{-ik_t \tau'} \right] \\
&\quad \times i \left[\eta^{ijk} e_{pj}^{(-\lambda_1)}(\hat{\mathbf{k}}_1) e_{pm}^{(-\lambda_2)}(\hat{\mathbf{k}}_2) e_{il}^{(-\lambda_3)}(\hat{\mathbf{k}}_3) \hat{k}_{1k} \hat{k}_{2l} \hat{k}_{3m} + 5 \text{ perms.} \right] . \tag{F.19}
\end{aligned}$$

Through the same procedure, the bispectrum from $H_{\widetilde{WW}^2}^{(4)}$ is estimated as

$$\left\langle \prod_{n=1}^3 \gamma^{(\lambda_n)}(\mathbf{k}_n) \right\rangle_{\widetilde{WW}^2}^{(4)} = (2\pi)^3 \delta \left(\sum_{n=1}^3 \mathbf{k}_n \right) 8 \left(\frac{H}{M_{\text{pl}}} \right)^6 \left(\frac{H}{\Lambda} \right)^2 \text{Im} \left[\tau_*^{-A} \int_{-\infty}^0 d\tau' \tau'^{5+A} e^{-ik_t \tau'} \right]$$

$$\times (-i) \left[\eta^{ijk} e_{pj}^{(-\lambda_1)}(\hat{\mathbf{k}}_1) e_{pm}^{(-\lambda_2)}(\hat{\mathbf{k}}_2) e_{im}^{(-\lambda_3)}(\hat{\mathbf{k}}_3) \hat{k}_{1k} \hat{k}_{2l} \hat{k}_{3l} + 5 \text{ perms.} \right] . \quad (\text{F.20})$$

References

- [1] K. Thorne, *Multipole Expansions of Gravitational Radiation*, *Rev.Mod.Phys.* **52** (1980) 299–339.
- [2] E. T. Newman and R. Penrose, *Note on the Bondi-Metzner-Sachs group*, *J. Math. Phys.* **7** (1966) 863–870.
- [3] J. N. Goldberg, A. J. MacFarlane, E. T. Newman, F. Rohrlich, and E. C. G. Sudarshan, *Spin s spherical harmonics and edth*, *J. Math. Phys.* **8** (1967) 2155.
- [4] M. Zaldarriaga and U. Seljak, *An All-Sky Analysis of Polarization in the Microwave Background*, *Phys. Rev.* **D55** (1997) 1830–1840, [[astro-ph/9609170](#)].
- [5] T. Okamoto and W. Hu, *The Angular Trispectra of CMB Temperature and Polarization*, *Phys. Rev.* **D66** (2002) 063008, [[astro-ph/0206155](#)].
- [6] S. Weinberg, *Cosmology*, . Oxford, UK: Oxford Univ. Pr. (2008) 593 p.
- [7] R. Gurau, *The Ponzano-Regge asymptotic of the 6j symbol: an elementary proof*, *Annales Henri Poincare* **9** (2008) 1413–1424, [[arXiv:0808.3533](#)].
- [8] H. A. Jahn and J. Hope, *Symmetry properties of the wigner 9j symbol*, *Phys. Rev.* **93** (Jan, 1954) 318–321.
- [9] “The wolfram function site.” <http://functions.wolfram.com/>.
- [10] W. Hu, *Angular trispectrum of the cosmic microwave background*, *Phys. Rev.* **D64** (2001) 083005, [[astro-ph/0105117](#)].
- [11] M. Shiraishi, D. Nitta, S. Yokoyama, K. Ichiki, and K. Takahashi, *CMB Bispectrum from Primordial Scalar, Vector and Tensor non-Gaussianities*, *Prog. Theor. Phys.* **125** (2011) 795–813, [[arXiv:1012.1079](#)].
- [12] M. Shiraishi, D. Nitta, S. Yokoyama, K. Ichiki, and K. Takahashi, *Computation approach for CMB bispectrum from primordial magnetic fields*, *Phys. Rev.* **D83** (2011) 123523, [[arXiv:1101.5287](#)].
- [13] M. Shiraishi, S. Yokoyama, D. Nitta, K. Ichiki, and K. Takahashi, *Analytic formulae of the CMB bispectra generated from non- Gaussianity in the tensor and vector perturbations*, *Phys. Rev.* **D82** (2010) 103505, [[arXiv:1003.2096](#)].
- [14] M. Shiraishi, D. Nitta, and S. Yokoyama, *Parity Violation of Gravitons in the CMB Bispectrum*, *Prog.Theor.Phys.* **126** (2011) 937–959, [[arXiv:1108.0175](#)].